PHYLOGENOMIC ANALYSIS AND GENOMIC STRUCTURE OF HUMAN *RCAN* GENES. EFFECT OF *RCAN* OVEREXPRESSION ON LYMPHOCYTE DEVELOPMENT AND FUNCTION.

Eva Serrano Candelas

DOCTORAL THESIS UPF / 2012

THESIS DIRECTOR

Dra. Mercè Pérez Riba

Cancer and Molecular Genetics Department, Bellvitge Biomedical Research Institute (IDIBELL)

DEPARTMENT OF EXPERIMENTAL HEALTH SCIENCES

UNIVERSITAT POMPEU FABRA

“Humanity's first sin was faith; the first virtue was doubt”

“El primer pecado de la humanidad fue la fe, la primera virtud fue la duda”

Carl Sagan

AGRADECIMIENTOS

Conforme iba escribiendo, de pronto me acordaba de quién me dijo ese truquito para la PCR que hizo que por fin me saliera, de quién me dejó un pelín de ese anticuerpo que se me había acabado o de quién me dio esa palmadita cuando más lo necesitaba. Me he dado cuenta a cada paso de que hay tantas cosas que agradecer a tanta gente que es imposible agradeceros a todos/as. Seguro que me olvido de mucha gente, pero espero que, si es así, nadie se sienta ofendido/a.

A ti, Sergius, por enseñarme cositas, por soportarme mis estresses y por esas birras fuera del lab que siempre me han venido tan bien. A Alvarito, por toda la ayuda que me has dado, por acompañarme en las noches de experimentos y por los jolgorios y cuchufletas. A Sonia, porque siempre vas con una sonrisa y tienes esa constancia tan admirable, y también por hacer de madre adoptiva ratonil. A Mari, que me orientó desde un principio y me enseñó que con mimo las cosas salen mucho mejor. A todas las "nenas" que nos han ayudado, a Judith, Lidia, Claudia... y a especialmente a Neus, no pierdas los ánimos porque todos sabemos lo que vales. Y, bueno, a Itzi, hija adoptiva del grupo, por tu sonrisa permanente y tu envidiable ilusión por todo.

A Montserabid, por tu sapiencia, tu paciencia cuando "I blod my face" y por surtirme de enseres para la mudanza. Srta. Fontrodona, qué decir, tú me has enseñado que ser una freaky de la ciencia también puede ser chic. A Jone, por tener una energía inagotable, por los ratos de cultivos que hemos salvado contigo y por las chelitas. A Charls (Carlitos), que nunca debiste irte del lab. A Jorch, doctor, a sus pies, porque me has hecho saber que los de Castellón también pueden ser un encanto y a Sandrita, un sol de persona. A Juanjito, mi GPS particular, creo que con eso digo todo.

Al aprendiz de marinero, Eric, por estar siempre tan "in" que se contagia, a Jalil, que siempre me hace reír con sus motes locos, a Iris, a Cristina y las dos Laias, que siempre se interesan por como estoy y siempre me dan ánimos cuando me ven. A Andrea y Pablo, la pareja más divertida de Genética. Y a Julián, por hacer que nunca falte el tequila en las fiestas y una sonrisa en el trabajo.

Y especialmente a Mireiuskin, "mi alma gitana" como nadie, en todos los aspectos, por estar ahí en los bajones y en los subidones, por adoptarme en mis viajes a Barcelona y por mil millones de cosas más.

A Txelcius, porque no se puede ser más dulce, gracias por esas noches, esas birritas a escondidas, por las cenitas en casa... y a Martuken, porque sabes que mi

cDNA sin ti nunca hubiera sido posible, porque eres una luchadora nata y haces que se contagie. A las dos, gracias, por un montón de cosas.

A la vieja escuela, Fati, Bego y Naida, el trio ICO, que me ayudaron tantísimo en mis comienzos y a Vane y Montse, las "chicas de secuenciación" por alegrarte el día cuando les llevas una secuencia. Y también a los chicos de las otras partes del pasillo, Octavio, el Manchas, Raúl, Albert... porque el cafelito de después de comer nunca hubiera sido lo mismo...

A ti, Gloria, por acogerme en tu laboratorio y enseñarme tantísimas cosas, porque sin ti este trabajo no hubiera ni empezado, y también a German, ya no sólo por la ayuda en el trabajo, que es incalculable, sino también por el constante apoyo, por haberme acogido en tu tierra y porque eres un encanto y un currante. También gracias a tí, Domènec, por haber tenido tanta paciencia y haberme ayudado tantísimo con el tema del promotor.

Y no puedo dejar de agradecer a todos/as y cada uno/a de los mexicanos y los españoles exiliados allí, porque habéis hecho que nos sintamos como en casa, a todos los niveles. Sólo puedo decir una cosa: Osais Pandais.

A Ruth, por acogerme durante tres años y haberse convertido en una amiga, sabes que ya toca que bajes a Valencia, ¿no? Y, Laia, gracias por haber dado ese salto para venirte conmigo, porque hemos sufrido la CAM juntas y sólo tú y yo sabemos lo que es eso y lo que une...

A mis compis de la carrera, porque habéis hecho todo mucho más fácil y llevadero, pero especialmente a Raulete por tu ¡oh, mente pre-clara! que me ayudó tanto al principio y que no dejo de admirar.

A mis chicas, desperdigadas por ahí. A Izarne, porque siempre va hacia adelante y no tiene miedo de sacar la cresta a pasear si hace falta, a Mari, por ser un ejemplo a seguir en todo, a Teresa, por tu creatividad sin límites y tu capacidad para simplificar las cosas, a Vicky, por ser tan sincera... y a mis chicos... a Yusi, por tener siempre las cosas tan claras, al Pei, porque nunca te rindes y siempre ves el lado positivo a las cosas, a Antonio, por haber estado ahí durante tanto tiempo... pero, sobretodo, a Lau, porque estás ahí sí o sí y porque me enseñas cada día que aún se puede crecer un poquito más.

A Paquito, simplemente porque eres un sol, a Pauet, porque, pese a tu locura, ¡eres genial!, a los Sres. Señores porque un cafelín con vosotros es mucho más que un cafelín, y a los cuñaos, porque tienes razón, Cesc, no puedo dejar de

agradecer que me nutráis y me visitéis en la cueva. Y, cómo no, a I. M. Nevat Astaroth, por haberme hecho tanta compañía durante la escritura.

Gracias a Esther Castaño y a Eva Julià, del SCT, por haber tenido tanta paciencia conmigo y haberme enseñado tantas cosas. A Miguel López por ayudarnos con las UPL y, por extensión, a Virginia, a ambos por echarnos una mano cuando nos hacía falta. Quisiera también agradecer al Dr. Borràs por su inestimable ayuda con los experimentos de proliferación, aunque nunca hayan funcionado...

A tí Mercè, por confiar en mí, por proporcionarme la ocasión de poder hacer todo esto, por guiarme, por enseñarme y por darme la oportunidad de conocer esa persona que hay detrás de mi "jefa". Quiero darle las gracias también a toda tu familia por acogernos a los miembros del laboratorio como uno más. Infinitamente gracias, Mercè.

Pero en realidad nada de esto hubiera sido posible sin las personas más importantes en mi vida. A ti, "po", porque me has dejado trastear con todo desde que era chiqui y has despertado mi curiosidad por saber cosas. A ti, madre, porque siempre has sido un ejemplo a seguir y me has ayudado siempre a encontrar el camino. A ti, Patico, porque me has enseñado a no tirar la toalla y querer superarme a cada momento. Y a ti, Miquel. Espero que seas consciente de lo que me has ayudado y apoyado durante este tiempo, porque creo que nunca te lo podré agradecer lo suficiente.

A todos y cada uno, gracias.

SUMMARY

The protein phosphatase calcineurin (Cn), together with its substrates, the transcription factors NFATc, play an essential role in several physiological processes of vertebrates, such as the immune response, angiogenesis, morphogenesis of the heart valves and neural and muscle development. Concretely in the immune system, the Cn-NFATc signaling pathway is crucial in the generation of T cell repertory in the thymus and in several processes of mature T lymphocytes, as T cell activation and survival. The members of the Regulators of Calcineurin (RCAN) family interact with Cn and compete with NFATc transcription factors for binding to Cn. RCANs can act either promoting or suppressing Cn activity towards its substrates. Due to their capacity to negatively modulate Cn-NFATc signaling, RCAN proteins are considered as potential immunosuppressant proteins. The aim of the present work was to deepen in the physiological processes that regulate the expression of RCAN and to evaluate the effect of their overexpression in the immune system. To this end, we have analyzed the evolution of *RCAN* genes and the genomic structure of the three human members of the *RCAN* gene family and, more specifically, the regulation of *RCAN3* gene expression. Furthermore, we have evaluated the expression pattern of the different mouse *Rcan* genes in lymphoid tissues, and we have analyzed the *in vivo* relevance of *RCAN1* and *RCAN3* overexpression in T cell development and function. In this context, *RCAN1* and *RCAN3* overexpression enhances positive selection of thymocytes. Moreover, *RCAN1* overexpression increases the generation of nT_{regs} in thymus and seem to influence the effector/memory T cells proportion in homeostasis. Furthermore, RCAN proteins appear to modulate other TCR signaling pathways different than Cn-NFATc. Therefore, RCAN proteins are important players of *in vivo* T cell development, differentiation and activation.

RESUMEN

La fosfatasa calcineurina (Cn), junto con sus substratos, los factores de transcripción NFATc, juega un papel esencial en varios procesos fisiológicos de vertebrados, como la respuesta inmune, la angiogénesis, la morfogénesis de las válvulas cardíacas o el desarrollo neuronal y muscular. Concretamente en el sistema inmune, la vía de señalización celular Cn-NFATc es crucial en la generación del repertorio de células T en el timo y en varios procesos de la función de los linfocitos T maduros, como la activación y la supervivencia de las células T. Los miembros de la familia de Reguladores de Calcineurina (RCAN) interaccionan con Cn y compiten con los factores de transcripción NFATc por su unión a Cn. Las RCAN pueden actuar promoviendo o inhibiendo la vía de Cn sobre sus sustratos. Debido a esta capacidad de regular negativamente la vía de señalización Cn-NFATc, las proteínas RCAN son consideradas como proteínas potencialmente inmunosupresoras. El objetivo del presente trabajo ha sido profundizar en los procesos fisiológicos que regulan la expresión de los genes *RCAN* y evaluar el efecto de su sobrexpresión en el sistema inmune. Con este fin, hemos analizado la evolución de los genes *RCAN* y la estructura genómica de los tres miembros *RCAN* en humanos y, más específicamente, la regulación de la expresión génica de *RCAN3*. Asimismo, hemos examinado el patrón de expresión de los diferentes genes *Rcan* de ratón en tejidos linfoides y hemos analizado la relevancia *in vivo* de la sobrexpresión de *RCAN1* y *RCAN3* en el desarrollo y la función de las células T. En este contexto, la sobrexpresión de *RCAN1* y de *RCAN3* induce la selección positiva de timocitos. Además, la sobrexpresión de *RCAN1* aumenta la generación de células nT_{regs} en timo y parece influir en la proporción de células T efectoras/memoria en homeostasis. Asimismo, las proteínas RCAN parecen modular otras vías de señalización dependientes del TCR diferentes a la vía Cn-NFATc. Por tanto, las proteínas RCAN son agentes importantes en el desarrollo, la diferenciación y la activación de células T.

PREFACE

The concept of “supersystem” was firstly introduced by Tada in 1997 ({Tada, 1997 #1226}) to designate these highly integrated life systems that are able to be self-regulated and self-organized. Together with the nervous system or the process of embryogenesis, the immune system constitutes the clearest example of this kind of supersystems.

The immune system presents a well-established behavior that implies the orchestration of multiple cell types and very complex signaling pathways and, subsequently, requires of tight mechanisms of regulation. An excessive immune response can cause irreversible tissue damage and several pathologies such as asthma, lupus or other autoimmune diseases, whilst inefficient immune response leaves us unprotected from foreign invaders and can even favor tumor formation and/or growth.

An example of the importance of the well-balanced signaling requirements in the immune system is the deregulation of Cn/NFATc signaling or depletion of any of the Cn or NFATc members. Such alterations on this pathway cause drastic effects at several points of T cell development and function. Therefore, a fine-tune modulation of Cn/NFATc signaling will be essential in the proper regulation of immune system responses.

Among the endogenous modulators of calcineurin, RCAN proteins play a relevant role to ensure an accurate regulation of the Cn-NFATc signaling in vertebrate systems, which need to orchestrate a wide variety of complex signaling networks to produce many cellular responses, including the immune system development and functional responses.

TABLE OF CONTENTS

AGRADECIMIENTOS ..... **v**

SUMMARY ..... **ix**

RESUMEN ..... **xii**

PREFACE ..... **xiii**

TABLE OF CONTENTS ..... **xv**

LIST OF FIGURES AND TABLES ..... **xxi**
List of figures ..... **xxi**
List of tables ..... **xxiii**

ABREVIATIONS AND UNITS ..... **xxv**
Abreviations ..... **xxv**
Units ..... **xxx**

INTRODUCTION **33**
1.- T lymphocytes **36**
2.- T cell receptor (TCR) **38**
2.1.- TCR structure 38
2.2.- TCR signaling 39
2.3.- TCR co-stimulation 41
3.- T cell development and mature function **42**
3.1.- Early developmental stages and the β-selection checkpoint 43
3.2.- Positive and negative selection of thymocytes 43
3.3.- Mature T cell activation and function 45
4.- TCR-activated signaling pathways involved in development of T lymphocytes **47**
4.1.- TCR proximal events 47
4.2.- MAPK pathways 48
4.3.- Ca^{2+}-dependent signaling 49
4.4.- Other molecules 49
5.- Signaling pathways involved in mature peripheral function of T lymphocytes **50**
5.1.- Clonal expansion and differentiation 50
5.2.- Effector function 50
5.3.- Cell homeostasis 51
6.- The Calcineurin-NFATc signaling pathway **51**
6.1.- Calcineurin 51
6.2.- Nuclear Factor of Activated T cells (NFAT) 53
6.3.- Cn/NFATc signaling in T cell development and function 55
6.4.- Modulators of calcineurin activity 58
7.- Regulators of Calcineurin (RCAN) **59**
7.1.- RCAN transcripts, isoforms and regulation of transcription 60

RCAN1 61
RCAN2 62
RCAN3 63
7.2.- Structure of RCAN proteins and regulation of RCAN function 63
7.2.a.-The RRM domain 64
7.2.b.-The SP domain 64
The LXXP and the ExxP motifs 64
The FLISSP motif 64
7.2.c.-The TXXP motif 65
7.2.d.-The PXIXIT-like motif 65
7.3.- Regulation of RCAN signaling by interacting proteins and RCAN involvement in signaling pathways other than Cn-NFATc 67
7.4.- Functions of RCAN proteins 69
7.5.- RCAN proteins in immune system 73

OBJECTIVES 77
RESULTS 81
1. RCAN genes: evolution, structure and regulation. 83
ABSTRACT 84
INTRODUCTION 85
MATERIAL AND METHODS 87
Genomic sequences retrieval 87
Sequence alignments and analysis 87
Evolutionary trees 87
Searching for paralogous genes 88
Comparative analysis of genome sequences 88
Luciferase reporter gene assay 89
RESULTS 89
RCAN genes evolution 89
RCAN gene structure comparison 93
Natural antisense transcripts in RCAN genes 96
Analysis of RCAN gene promoter 98
DISCUSSION 99
ACKNOWLEDGMENTS 103
FOOTNOTES 103
REFERENCES 103
FIGURES 112
ANNEX TO ARTICLE 138
2.- RCAN proteins as modulators of calcineurin-dependent processes in T cell development and activation 141
ABSTRACT 142
INTRODUCTION 143
MATERIAL AND METHODS 146
Mice 146
Real time quantitative PCR analysis for mouse Rcan transcripts 147
Genotyping TghRCAN1 mice 147
Antibody generation 148
Generation of retroviral vectors and particles 149

Isolation and transduction of bone marrow progenitor cells 149
Reconstitution of mice with transduced bone marrow cells 150
Surface and intracellular staining 150
Pull-down and coimmunoprecipitation assays 151
RESULTS 151
Rcan genes are expressed in adult and embryonic lymphoid tissues 151
The human RCAN1 transgenic mice (TghRCAN1) overexpresses hRCAN1 in lymphoid tissues 152
TgRCAN1 increases the proportion of positively selected thymocytes in heterozygous female animals. 153
hRCAN1 overexpression increases peripheral $CD3^+$ cells and decreases the effector/memory peripheral T cell population in heterozygous females animals. 155
Natural T_{reg} cells are increased in thymus and iT_{regs} are decreased in spleen in TgRCAN1 heterozygous female animals. 156
Efficient hRCAN3 overexpression in murine lymphoid organs after adoptive transfer of retrovirally transduced BM progenitors. 157
RCAN3 overexpression increases thymic positive selection and decreases $CD4^+$ and $CD8^+$ cells in peripheral lymphoid organs. 158
DISCUSSION 159
ACKNOWLEDGMENTS 165
FOOTNOTES 165
REFERENCES 165
FIGURES 174
ANNEX TO ARTICLE 201

CONCLUDING REMARKS 203
Evolution, gene structure and regulation of *RCAN* gene expression 205
***In vivo* functional role of RCAN proteins in the immune system 210**
TghRCAN1 mouse and animals reconstituted with BM progenitors that overexpress *RCAN3* gene as models to study T cell development and function 211
Effects of overexpression of *hRCAN1* and *hRCAN3* in murine lymphoid organs 213
Effects of *RCAN* overexpression in thymus 213
Effects of *RCAN* overexpression in peripheral lymphoid organs 216

CONCLUSIONS 221

MATERIAL AND METHODS 227
I.- GENERAL PROTOCOLS IN DNA MANIPULATION AND ANALYSIS 229
I.1.- Polymerase chain reaction (PCR) 229
I.1.a.- PCR amplification for cloning 230
I.1.b- PCR screening 230
I.1.c- PCR Sequencing 231
I.1.d.- PCR for mycoplasma detection 231
I.1.f.- Semiquantitative PCR for determination of mRNA levels 232
I.1.g.- Real-time quantitative PCR for determination of mRNA levels 232
I.2.- DNA gel electrophoresis 234
I.2.a.- DNA electrophoresis in agarose gels 235
I.2.b.- DNA electrophoresis in polyacrylamide gels 235

I.3.- DNA quantification 236
I.4.- Plasmids 236
II.- GENERAL PROTOCOLS IN PROTEIN ANALYSIS 237
II.1.- Preparation of total soluble protein lysates 237
II.1.a.- Preparation of soluble protein cell lysates from mammalian cells 237
II.1.a.- Preparation of soluble protein cell lysates from mammalian tissue 238
II.2.- Protein quantification 238
II.2.a.- Quantification of proteins by spectrophotometry 238
II.2.b.-Bicinchoninic Acid Assaycolorimetric assay for protein quantification 239
II.3.- Discontinuos polyacrilamide gel electrophoresis (SDS-PAGE) of proteins 239
II.4.- Detection of proteins in polyacrylamide gels by Coomassie Blue staining 240
II.5.- Protein transfer of gel proteins to membranes (Western blot -electroblotting) 240
II.6.- Detection of proteins in a membrane 241
II.6.a.- Detection of proteins by Ponceau-S staining 241
II.6.b- Immunodetection of proteins 241
II.7.- Antibodies for immunodetection of proteins in a membrane and anti-RCAN1 Monoclonal antibody generation 242
III.- GENERAL PROTOCOLS IN BACTERIA MANIPULATION 243
III.1.- Bacterial Strains 243
XL1-Blue 243
DH10B 243
Rosetta (Rosetta2(DE3)pLysS) 243
III.2.- Preparation of Competent Bacteria 244
III.2.a.- Preparation of XL1-Blue Chemi-competent (Heat-shock) cells 244
III.2.b.- Preparation of Rosetta Chemi-competent (Heat-shock) cells 244
III.3.- Transformation of Competent Bacterial Cells 245
III.3.a.-Transformation of XL1-Blue and Rosetta Chemi-Competent (Heat-shock) cells 245
III.3.b.- Transformation of DH10B Electro-competent Cells 246
III.4.- Glycerol stocks from bacterial transformed cells. 246
IV.- RECOMBINANT DNA TECHNOLOGY (DNA CLONING) 247
IV.1.- DNA Ligation 248
IV.1.a.- DNA Ligation in pGEM®-T vector 248
IV.1.b.-DNA ligation of purified DNA fragment and the plasmid of destination 248
IV.2.- White/blue colony screening for insert cloning 249
IV.3.- Amplification and purification of plasmid DNA 249
IV.4.- Restriction enzyme digestion 249
IV.5.- Shrimp Alkaline Phosphatase (SAP) Treatment 250
IV.6.- In-gel purification of DNA 250
IV.7.- Bacterial culture to perform PCR screening 251
V. PRODUCTION OF HETEROLOGOUS PROTEINS IN BACTERIAL CELLS 251
V.1.- Screening of clones for protein expression 252
V.2.- High-scale production of recombinant proteins 252
V.3.- Purification of GST-fusion proteins 253
VI. GENERAL PROTOCOLS IN MAMMALIAN CELLS MANIPULATION 254
VI.1.- Mammalian cell lines 254
VI.2.- Maintenance of mammalian cells 254
VI.3.- Mycoplasma test 255
VI.4.- Mammalian cell DNA transfection 255

VI.4.a.- Mammalian cell DNA transfection by calcium phosphate method 256
VI.4.b.- Mammalian cell DNA transfection by PEI method 256
VI.5.- Cryopreservation of Mammalian Cells 257
VI.6- Production of IL-3 from WEHI cells 257
VI.7- Production of SCF from BHK/MKL cells 258
VII.- PROTOCOLS FOR ANALYSIS OF PROTEIN-PROTEIN INTERACTION 258
VII.1.- GST Pull down 258
VII.2.- Immunoprecipitation 259
VIII.- DETERMINATION OF mRNA LEVELS IN MAMMALIAN CELLS AND TISSUES 260
VIII.1.- RNA extraction 260
VIII.2.- DNAse treatment of RNA samples 260
VIII.3.- Reverse transcription of total RNA: cDNA synthesis 260
IX.- LUCIFERASE REPORTER GENE ASSAY 261
X.- GENERAL PROTOCOLS IN ANIMAL MANIPULATION 263
X.1- DNA purification from animal tail for genotyping 263
XI.- BONE MARROW RECONSTITUTION WITH RETROVIRAL TRANSDUCED HEMATOPOIETIC PROGENITORS 263
Day 1 263
Day 5 264
Day 6 265
Day 7 266
Day 8 266
Day 9 267
XI.- CYTOMETRIC ANALYSIS OF CELLULAR LYMPHOID SUBPOPULATIONS 268
XI.1.- Isolation of lymphocytes cells from lymphoid tissues 268
XI.2.- Analysis of lymphocyte populations by surface and intracelular markers staining 270
XI.4.- Stimulation of cells and analysis of intracellular phosphoproteins 270
XII.- COMMON LABORATORY SOLUTIONS AND BUFFERS 271
XII.1- General buffers 271
PBS (Phosphate Buffered Saline) 271
TBS (Tris Buffered Saline) 271
XII.2.- Solutions for bacterial manipulation 271
LB (Luria Bertani) medium and LB-agar plates 271
SOB (Super Optimal Broth) medium 271
SOC medium 272
2xYP medium 272
$CaCl_2$ solution for preparation of XL1-Blue competent bacteria 272
FSB (Frozen Storage Buffer) solution for preparation of Rosetta2 competent bacteria 272
Potassium acetate solution 273
IPTG solution 273
X-Gal 273
Antibiotics 273
XII.3.- Solutions for mammalian cells manipulation 274
Erythrocytes Lysis Buffer 274
HeBBS buffer for mammalian cells transfection 274
4% PFA (Paraformaldehid) solution 274
FACs buffer 275
XII.4.- Solutions for DNA analysis 275

DNA loading buffer 275
TBE (Tris/Boric Acid/EDTA) Buffer 275
XII.5.-Solutions for protein analysis 275
Bacterial Lysis Buffer 275
RIPA-like lysis buffer for mammalian cells 276
IGEPAL-based lysis buffer for mammalian cells 276
Protein loading buffer – Laemmli buffer 276
4xTris-HCl/SDS, pH 6.8 solution 277
4xTris-HCl/SDS, pH 8.8 solution 277
Electrophoresis running buffer 277
Transfer buffer 277
Coomassie Blue Staining Solution 278
Coomassie Blue Destaining Solution 278
Ponceau-S Staining Solution 278
TBS-T (Tris Buffered Saline-Tween) 0.1% 278
Blocking Solution 278
Luminol solution 279
Luminol Stock-Solution 279
Enhancer Solution 279

AUXILIARY BIBLIOGRAPHY 281

ANNEX 307

LIST OF FIGURES AND TABLES

LIST OF FIGURES

INTRODUCTION

Figure 0.1. Schematic representation of hematopoiesis of lymphoid and myeloid cells... 35
Figure 2.1. Signaling cascades triggered by TCR-MHC-peptide interaction. 39
Figure 3.1. T lymphocyte maturation 42
Figure 3.2. Selection of T cell repertoire depending on TCR interaction for MHC-peptide complex in the thymus..... 44
Figure 3.3. Expression pattern of different surface cell markers during thymocyte differentiation. 44
Figure 3.4. Representation of the different phases of adaptive immunity..... 45
Figure 3.5. Two-color flow cytometry analysis of CD44 and CD62L populations among periheral cells. 46
Figure 6.1. Cartoon of crystal structure of CnA anb CnB heterodimer..... 52
Figure 6.2. Squematic representation of CaM- dependent activation of CnA. 53
Figure 6.3. Schematic representation of NFATc protein structure based on NFATc1..... 55
Figure 7.1. Schematic representation of RCAN protein structure. 63
Figure 7.3. Different proteins involved in TCR signaling interact with RCAN proteins..... 74

RESULTS - Article 1

Figure 1. RCAN gene family evolution. 113
Figure 2. Large-scale segmental duplication between chromosome 1 and chromosome 6 is determined by the presence of paralogous genes..... 115
Figure 3. Gene structure comparison of the human RCAN family members. 117
Figure 4. Human RCAN3 gene structure, alternative splicing, and protein isoforms..... 119
Figure 5. Phylogenetic analysis of the RCAN3 exons in vertebrates. 121
Figure 6. Transcriptional activity and in silico prediction of Transcription Factors Binding Sites (TFBS) along the 5' region of the RCAN3 gene..... 123
Figure S1. Phylogenetic analysis of CLIC proteins 124
Figure S2. Comparative genomic sequence analysis of RCAN genes. 128
Figure S3 A and B. Alignment of human RCAN proteins. 129
Figure S3 C. Alignment of human RCAN proteins. 131
Figure S4. Multi-species alignment of human RCAN1, RCAN2 and RCAN3 natural antisense transcripts: RCAN1AS, RCAN2AS and RCAN3AS..... 133
Figure S5. Comparative analysis of RCAN3-associated CpG island sequence conservation between mammals and in silico prediction of TFBS in this region. 135
Figure A1. Species tree. Adapted from From Genomicus; 139

RESULTS - Article 2

Figure 1A and B. Mouse Rcan mRNAs are expressed in adult and embryonic mouse lymphoid tissues. 174
Figure 1C. Mouse Rcan mRNAs are expressed in adult and embryonic mouse lymphoid tissues. 175
Figure 2. Human RCAN1 isoforms are overexpressed in transgenic hRCAN1 mouse lymphoid tissues. 177
Figure 3A. Overexpression hRCAN1 gene increases positive selection and pERK signaling of thymocytes in TghRCAN1 female animals. 179
Figure 4A. Overexpression of hRCAN1 increases the proportion of peripheral T cells with a reduced activation state phenotype. 181
Figure 4B and C. Overexpression of hRCAN1 increases the proportion of peripheral T cells with a reduced activation state phenotype. 183
Figure 5. FoxP3+ (Tregs) cell population increases in thymus (nTreg), but decreases in spleen (pTreg) of the TghRCAN1 transgenic mice. 185
Figure 6A, B and C. Bone marrow reconstitution with hematopoietic progenitor cells overexpressing HA-hRCAN3 protein. 186
Figure 6D. Bone marrow reconstitution with hematopoietic progenitor cells overexpressing HA-hRCAN3 protein. 187
Figure 6E. Bone marrow reconstitution with hematopoietic progenitor cells overexpressing HA-hRCAN3 protein. 188
Figure 7A. hRCAN3 overexpression increases positive-selection in the thymus and decreases CD4+ and CD8+ cells in peripheral lymphoid organs. 189
Figure 7 B and C. hRCAN3 overexpression increases positive-selection in the thymus and decreases CD4+ and CD8+ cells in peripheral lymphoid organs. 191
Figure S1. Ly75 expression in embryonic samples. 192
Figure S2. Analysis of DN immature subsets in hRCAN1 transgenic mice. 193
Figure. S3. RCAN interacts with CRAF and Cn in a non-mutually exclusive manner. 194
Figure. S4. Overexpression of hRCAN1 increased the TCR expression in SP thymocytes. 195
Figure. S5. Alignment of human RCAN and mouse Rcan proteins. 197
Figure A1. Correct length of amplicons in the real time quantitative PCR analysis of mouse Rcan mRNA forms 201

MATERIAL AND METHODS

Figure XI.1. Mouse lymphoid organs dissection. 269

LIST OF TABLES

INTRODUCTION

Table 1.1. Th, Tc and T_{regs} subpopulations. 37
Table 6.1. Modulatory proteins of Cn. 59
Table 7.1 Functions of RCAN proteins. 70
Table 7.1 Function of RCAN proteins 71
Table 7.1 Function of RCAN proteins 72

RESULTS - Article 1

Table S1. Paralogous genes located in cromosome 1 (1p32-p36.3) and 6 (6p12-p21.2/q12-q22.1). 136
Table S1. Paralogous genes located in cromosome 1 (1p32-p36.3) and 6 (6p12-p21.2/q12-q22.1). 137
Table S2. Different nomenclature for RCAN3 mRNA transcripts and protein isoforms used in bibliography, compared with our proposal 138

RESULTS - Article 2

Supplementary Table 1A- DNA primers and probes for real time quantitative PCR analysis of mouse Rcan mRNA forms 198
Supplementary Table 1B- Primers for genotyping and mRNA quantification in TghRCAN1 mice 199
Supplementary Table 2A – Antibodies used for flow cytometry analysis and for T cell stimulation. 200
Table I.1. Primers used for mycoplasma detection 231

MATERIAL AND METHODS

Table I.2. Amplification program used for real-time quantitative PCR 234
Table II.1. Monoclonal antibodies used for protein immunodetection in membranes 242
Table IX.1. Primers used for *RCAN3* 5' flanking regions contructs 262
Table XI. Transfection conditions used for production of retroviral particles in HEK 293T cells 265
Table XII.2. Antibiotics used for bacterial cell culture 273

ANNEX

Table A1. Surface and intracelular T lymphocyte markers. 309

ABREVIATIONS AND UNITS

ABREVIATIONS

-/-	Heterozygous
+/-	Wild Type
+/+	Homozygous
∞	Infinite
A238L	African swine fever virus; IκB-like protein
aa	amino acid
AD	Activation domain
AICD	Antigen induced cell death
AID	Autoinhibitory domain
AKAP79	A kinase anchor protein 79
AP1	Activator protein 1
APC	Antigen presenting cell
APC	Allophycocyanin (fluorochrome)
BBH	CnB-binding helical domain
Bcl10	B Cell CLL/lymphoma-10
BM	Bone marrow
BSA	Bovine serum albumin
Ca^{2+}	Calcium
Cabin1	Calcineurin binding protein 1
CALP	Calcipressin, former name of RCAN
CaM	Calmodulin
CaMKIV	Ca^{2+}/CaM-dependent kinase type IV
cAMP	Cyclic adenosine monophosphate
CAPRI	Ca^{2+}-promoted Ras inactivator
Carma1	Caspase Recruitment Domain [CARD], member 11
CBM	carma1-Bcl10-MALT1 complex
CD	Cluster of differentiation
cDNA	Complementary deoxyribonucleic acid
CIC	Calcineurin-inhibitor CALP (calcipressin, former name of RCAN)
Cn	Calcineurin; PPP3
CnA	Calcineurin A, catalytic subunit
CnB	Calcineurin B, regulatory subunit
Co-IP	Co-immunoprecipitation
COX-2	Cyclooxygenase 2
CRAC	Ca^{2+}-release-activated Ca^{2+}

CREB	cAMP response element-binding
CsA	Cyclosporin A
CSP1	Calcipressin, former name of RCAN
cTEC	Cortical Thymic Endothelial Cell
CTL	Cytotoxic T lymphocytes, Tc
CypA	Cyclophilin A
CHP	Calcineurin B homologous protein
DAG	Diacylglycerol
DMSO	Dimethyl sulfoxide
DN	Double negative stage in T cell development, $CD4^-CD8^-$
DNA	Deoxyribonucleic acid
dNTP	Deoxynucleotide triphosphate
DP	Double positive stage of T cell development, $CD4^+CD8^+$
DSCR	Down syndrome critical region
DSCR1	Down syndrome candidate region 1; former name of RCAN1
DSCR1L1	Down syndrome candidate region 1 like 1; former name of RCAN2
DSCR1L2	Down syndrome candidate region 1 like 2; former name of RCAN3
DTT	Dithiothreitol
EC	Endothelial cell
Elk-1	Ets-like transcription factor-1
ER	Endoplasmic reticulum
ERK	Extracellular signal-regulated kinases
EST	Expressed sequence tag
EtBr	ethidium bromide
EtOH	Ethanol
FACS	Fluorescence activated cell sorting
FasL	Fas Ligand
FasR	Fas Ligand receptor
FCS	Fetal calf serum
FITC	Fluorescein isothiocyanate
FKBP12	FK506 binding protein 1A, 12 kDa
FKBP38	FK506 binding protein 8, 38 kDa
FoxP3	Forkhead box P3
FTOC	Fetal thymus organ culture
Gads	Grb2 like adaptor protein
GAP	GTPase-activating protein
GAPDH	Glyceraldehyde 3-phosphate dehydrogenase
Gasp	Grb2-associating protein; Themis protein
GATA3/4	GATA-binding protein 3 and 4

GEF	Guanine exchange factor
GFP	Green fluorescent protein
Grb2	Growth factor receptor bound protein2
GSK3β	Glycogen synthase kinase-3 β
GST	Glutathione S-transferase
HA	Hemagglutinin
HPRT1	Hypoxanthine phosphoribosyltransferase 1
HSA	Homo Sapiens
HSC	Hematopoietic stem cell
HUVEC	Human Umbilical Vein Endothelial Cells
IFN-γ	Interferon gamma
Ig	Immunoglobulin
IKK	IκB Kinases
IL	Interleukin
IL-R	Interleukin receptor
INCA	Inhibitor of NFAT-calcineurin interaction
Io	Ionomycin, sodium salt
IP	Immunoprecipitation
IP_3	Inositol-1,4,5-triphosphate
IP_3R	IP_3 receptor
IRAK-1	IL-1β receptor (IL-1R)-associated kinase 1
ITAM	Immunoreceptor tyrosine-based activation motif
IκB	Inhibitor of NF-κB
Jak	Janus kinase
KSR2	kinase suppressor of ras 2
LAT	Linker Activator for T Cells
Lck	Lymphocyte-specific protein tyrosine kinase
mAb	Monoclonal antibody
MALT1	Mucosa Associated Lymphoid Tissue Lymphoma Translocation Gene-1
MAPK	Mitogen-activated protein kinase
MCIP	Modulatory calcineurin-interacting protein (another former name of RCAN)
MCP-1	Monocyte chemotactic protein-1
MEF2	Myocyte enhancer factor 2
MEK	MAPK/ERK kinase
MEKK	MEK kinase
MeOH	Methanol
MHC	Major Histocompatibility Complex

MIF	Mean intensity of fluorescence
MKK	Mitogen activated protein kinase kinase
mRNA	Messenger ribonucleic acid
MSCV	Murine Stem Cell Virus
mTEC	medullary Thymic Endothelial Cell
mTOR	Mammalian target of rapamycin
MU	Monitor units
NATs	Natural antisense transcripts
NFAT	Nuclear Factor of Activated T cells
NFATc	cytosolic Nuclear Factor of Activated T cells
NFATn	nuclear Nuclear Factor of Activated T cells
NF-κB	Nuclear Factor-κB
NHR	NFAT homology region
NIK	NF-κB-inducing kinase
NK and KN-T	Natural Killer cell and Natural Killer T cell
NLS	Nuclear localization signal
NMR	Nuclear Magnetic Resonance
OD	Optical density
PAGE	Polyacrylamide gel electrophoresis
PBS	Phosphate buffered saline
PCR	Polymerase chain reaction
PE	Phycoerythrin
PerCP	Peridinin-chlorophyll complex
PFA	Paraformaldehyde
PI_3K	PI_3 kinase
PIP_2	Phosphatidylinositol-4,5-bisphosphate
PKA	cAMP-dependent protein kinase
PKB	Protein kinase B
PKCθ	Protein Kinase C Theta
PLCg	Phospholipase C gamma 1
PMA	Phorbol 12-myristate 13-acetate
PMSF	Phenylmethylsulfonyl fluoride
PPP3	Protein phosphatase 3, (formerly PP2B); Cn
PTK	Protein Tyrosine Kinases
RAC	Ras-related C3 botulinum toxin substrate
RAF	rapidly accelerated fibrosarcoma
RAG1 and 2	Recombination Activating Gene 1 and 2
Ras	Rat sarcoma
RASGRP1	RAS guanyl releasing protein 1

RCAN	Regulator of calcineurin
RHD or RHR	Rel-homology domain or region
ROS	Reactive oxygen species
RT	Room temperature
RXR	Retinoid X receptor
SAP/JNK	Stress-Activated Protein Kinase/c-Jun N-terminal Kinase
SD	Standard deviation
SSC	Side SCatter
SDS	Sodium dodecyl sulfate
SEM	Standard error of the mean
SLP-76	Src homology 2 (SH2) domain-containing leukocyte protein of 76 kDa
SOS	Son of sevenless
SP	Single positive thymocytes ($CD4^+$ or $CD8^+$)
SP region/repeat	Serine-Proline rich region/repeat
SPF	Specific pathogen free
Sra	Sarah (former name of Rcan in *D. melanogaster*)
Src	Sarcoma protein kinase
SRR	Serine-rich regions
STAT	Signal Transducer and Activator of Transcription
Syk	Spleen tyrosine kinase
TAB1 and 2	TAK-1 binding protein 1 and 2
TAK1	TGF-β activated kinase 1
TBS	Tris-Buffered Saline
Tc	cytotoxic T cell
T_{CM}	central memory T cell
TCR	T cell receptor
TCRα-cpm	TCR α-chain connecting peptide motif
T_{EM}	effector memory cell T cell
TEMED	N,N,N',N'-Tetramethylethylenediamine
TF	Tissue factor
TFBS	Transcription factor binding site
TGF-β	Transforming growth factor β
TGF-βR	TGF-β receptor
Th	helper T cell
TLR2/4	Toll-like receptor 2 and 4
T_m	Melting temperature
T_M	memory T cell

TNF-α	Tumor necrosis factor alpha
TNNI3	cardiac troponin I
Tollip	Toll-interacting protein
TRAF2 and 6	TNF receptor-associated Factor 2 and 6
T_{reg}	regulatory T cell
Tαβ and Tγδ	TCRαβ and TCRγδ
VEGF	Vascular endothelial growth factor
WB	Western blot
WT	Wild Type
ZAP-70	Zeta-associated protein, 70 kD

UNITS

°C	Celsius degree
A, mA	Ampere, milliAmpere
bp	base pair (s)
fmol	femptomol
g	gravity acceleration unit
g, mg, µg, ng	gram, milligram, microgram, nanogram
h	hour
h	hours
kb	kilobase pairs
kd	kilodalton
l, ml, µl	liter, milliliter, microliter
M, mM, µM, nM	molar, millimolar, micromolar, nanomolar
min	minute
rad	rads
s	seconds
V	volt
v/v	volume/volume
w/v	weight/volume

Introduction

The immune system is a highly complex system that protects the organism from foreign invaders and mediates the removal of infected cells or cells displaying tumor antigens. The immune response is composed by innate (or non-specific) and adaptive (or specific) components, the latter specific of vertebrates systems, and it is characterized to be tolerant against self-antigens (self-tolerant), in order to prevent autoimmunity.

Immune system is composed of many different cell types, each of them with different functions. All these cell types became from hematopoietic stem cells (HSC) precursors generated in the bone marrow (BM). In embryonic mice, fetal liver serves as reservoir for HSCs until birth, before they migrate to BM (Dzierzak, 2005). HSC have self-renewal capability and pluripotent ability to differentiate in cells from all hematopoietic lineages, including lymphoid and myeloid lineages (Quesenberry and Levitt, 1979; Kondo *et al.*, 2003) (Fig. 0.1). Among all lymphoid populations, T lymphocytes mediate adaptive cellular immunity against intracellular pathogens, while B lymphocytes mediate the adaptive humoral immunity, which is the most important response against extracellular pathogens and is mediated by antibodies.

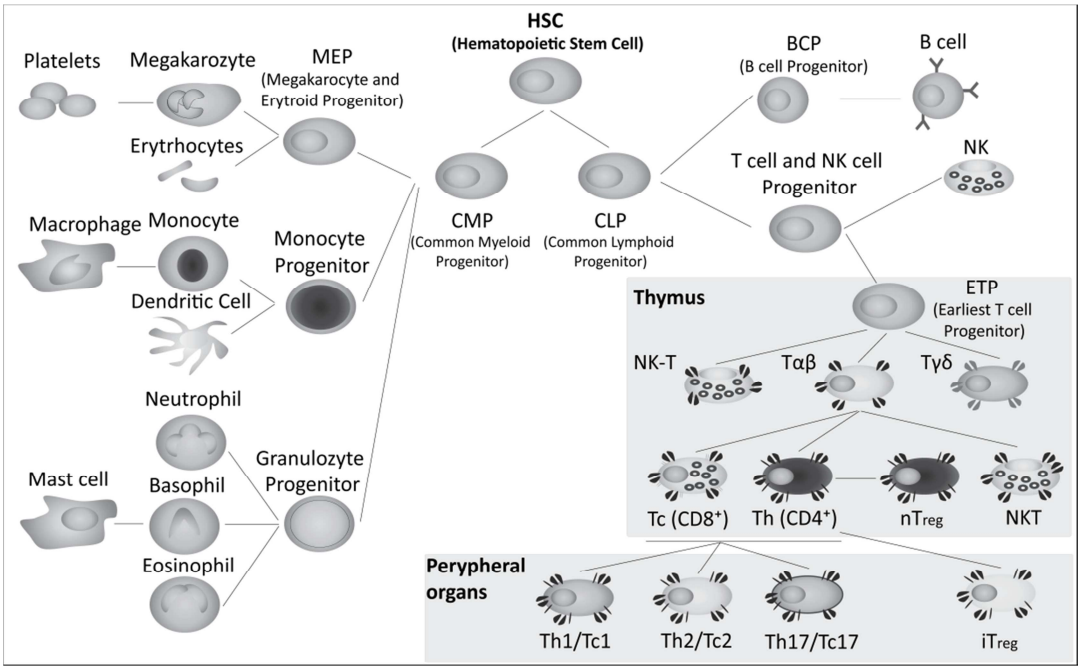

Figure 0.1. Schematic representation of hematopoiesis of lymphoid and myeloid cells.

1.- T LYMPHOCYTES

T lymphocytes or T cells ("T" stands from thymus) are highly specialized cells that recognize foreign and self-peptides presented by the Major Histocompatibility Complex (MHC; class I or class II) of the Antigen Presenting Cells or APCs (dendritic cells, macrophages and thymic epithelial cells, among others). This antigen-MHC complex recognition is mediated by the T cell receptor (TCR) complex in the T cell membrane. Depending on the TCR structure, we can subdivide T cells into TCRαβ (or Tαβ) and TCRγδ (or Tγδ, about 5% of TCR cells) cells. Although TCRγδ cells share many of the characteristics with the TCRαβ cells, they have a restricted tissue distribution and present a more limited TCR repertory (reviewed in Bluestone *et al.*, 1995).

Among Tαβ lymphocytes, several distinct populations can be found. The conventional T cells provide clonal antigen specific responses. They include the cytotoxic lineage (Tc, CTL or CD8+), that recognize antigens bound to MHC class I, and the helper lineage (Th or CD4+ cells), that recognize antigens bound to MHC class II. Once activated, Th/Tc cells can differentiate into two major subsets named Th1/Tc1 and Th2/Tc2, or in other minority subsets, as Th17/Tc17 or Th9/Tc9, depending on their function and the production of specific cytokines (Table 1.1).

Among other unconventional TCRαβ cells types, there are the regulatory T cells or T_{reg} that work as immunosuppressants of the immune response and are essential for maintaining self-tolerance. T_{regs} can be subdivided into two subpopulations, the natural occurring T_{regs} (nT_{regs}; $CD4^+CD25^+$) that are generated in the thymus and the induced T_{regs} (iT_{regs}; $CD4^+CD25^-$), generated in periphery. Other unconventional TCRαβ cells are the Natural Killer T cells (NK-T) cells. NK-T cells participate in several processes of the innate and adaptive immune response, including tissue destruction, antitumor responses, host defense and regulation of inflammation and autoimmunity; and can be distinguished from the NK cells because they express TCRαβ in the membrane (Niemeyer *et al.*, 2008; Biron and Brossay, 2001).

Table 1.1.A- Th SUBSETS					
NAME	**CYTOKINE STIMULUS**	**TF**	**EFFECTOR CYTOKINES**	**CHEMOKINE RECEPTORS**	**EFFECTOR FUNCTION**
Th0/Tc0	mixed between Th1/Tc1 and Th2/Tc2	-	mixed between Th1/Tc1 and Th2/Tc2	mixed between Th1/Tc1 and Th2/Tc2	Differentiate to Th1/Tc1 or Th2/Tc2
Th1/Tc1	IL2, TNF-α, IL12, IL23, INF-γ	T-bet STAT4 STAT1	IL2, IL12, INF-γ, IL27, TNF-α, GM-SCF	CCR5, CCR1	**Th1**: Promote cellular immunity (Tc cells, NK...).Promotes B cells Th1-like isotype switching (IgG2a, IgG2b, IgG3) **Tc1:** Mediate cellular immunity (Granzyme, perforin). Promotes Th1 differentiation.
Th2/Tc2	IL4, IL25	GATA3 STAT6 MAF	IL3, IL4, IL5, IL6, IL9, IL10, IL13	CCR3, CCR4, CrTh2	**Th2:** Promote humoral immunity (B cell).Promotes B cells Th2-like isotype switching (IgG1, IgE, IgA) **Tc2:** Mediate cellular immunity (Granzyme, perforin). Promotes Th2 differentiation.
Th17/Tc17	IL1β, IL6, IL21, IL23 (TGF-β controversial)	RORγt RORα Runx1 STAT3	IL17A, IL17F, IL21 ,IL22, IL26, TNFα	CCR4, CCR5, CCR6, CXCR3, CXCR6	Inflammation. Autoimmunity. Memory
Th9	IL4; TGFβ	PU.1	IL9, IL10		Inflammation. . Mucus production
Th22/Tc22		RORγt AHR	IL13, IL2		Inflammation. . Autoimmunity.
TFh	IL12, IL6, IL21, IL-23, IL-27	Bcl-6	IL6, IL21	CXCR5	T cell helper for B cells
Treg	TGFβ, IL2 (only iTregs)	FoxP3 STAT5	TGFβ or IL10 (see table 1b)	CCR8, CCR4	Regulation and tolerance

Table 1.1.B.- Treg SUBSETS				
NAME	**GENERATION**	**CITOKINES STIMULUS**	**SURFACE MARKERS**	**EFFECTOR CITOKINES**
nTreg	Thymus	TCR/CD28, IL-2	$CD4^+CD25^+CD127^{low}$	TGF-β
iTreg - Tr1	Periphery	CD3, IL10, Retinoid acid	$CD4^+CD25^-$	IL10
iTreg-Th3	Periphery	CD3, TGF-β	$CD4^+CD25^+$	TGF-β
ITreg- CD8 Tregs	Periphery	TGF-β	$CD8^+CD122^+$	TGF-β, IL10

Table 1.1. Th, Tc and T_{regs} subpopulations. TF, transcription factors.

2.- T CELL RECEPTOR (TCR)

2.1.- TCR structure

T cell antigen receptor (TCRαβ) is an heterodimer composed by two disulfide bond-linked transmembrane chains αβ and, together with six non covalently linked CD3 subunits (two zeta (ζ) chains, two epsilon (ε) chains, one delta (δ) chain and one gamma (γ) chain) forms the TCR-CD3 complex, also called TCR complex*. The Tγδ or TCRγδ cells present a different TCR heterodimer composed by γ- and δ-chains. From now, we will refer only to the TCRαβ as TCR. The TCR heterodimer recognize peptide–MHC complex by their variable region and the CD3 subunits serve as a transducing complex.

The variable regions of TCRα and β chains are generated by recombination of variable (V), diversity (D) and joining (J) segments of the TCR loci, mediated by the transposase-related Recombination Activating Gene 1 and 2 (RAG1 and RAG2) proteins (proposed by Sakano *et al.*, 1979 and reviewed elsewhere, Wagner_2007, Lewis and Wu, 1997; Ramsden *et al.*, 2010; Genolet *et al.*, 2012). This variable region confers to the TCR unique antigen specific recognition capacity.

The CD3 subunits are non-polymorphic and contain a total of ten Immunoreceptor Tyrosine-based Activation Motifs (ITAMs). The presence of ten ITAM motifs has shown to be essential for signal amplification, in order to respond to a very low concentration of antigen (Irving *et al.*, 1993), and also can confer specific binding to the different downstream Protein Tyrosine Kinases (PTKs) (Osman *et al.*, 1996).

TCR activation, in coordination with other membrane receptors and cytokines, mediates the different checkpoints in T cell development as well as the activation, function and survival of mature peripheral lymphocytes.

*some authors consider ζ chains, (also known as p23) as TCR subunits (Wange and Samelson, 1996), while other consider them as CD3 subunits (Cantrell, 2002) or independent subunits (Abbas *et al.*, 2007). We will refer them as a part of the CD3 complex.

2.2.- TCR signaling

Figure 2.1 shows a schematic view of the different signaling pathways that are activated after TCR-MHC-peptide interaction, including different members of the MAPK family (mitogen-activated protein kinase), Ca^{2+}-dependent signals and participation of several transcription factors.

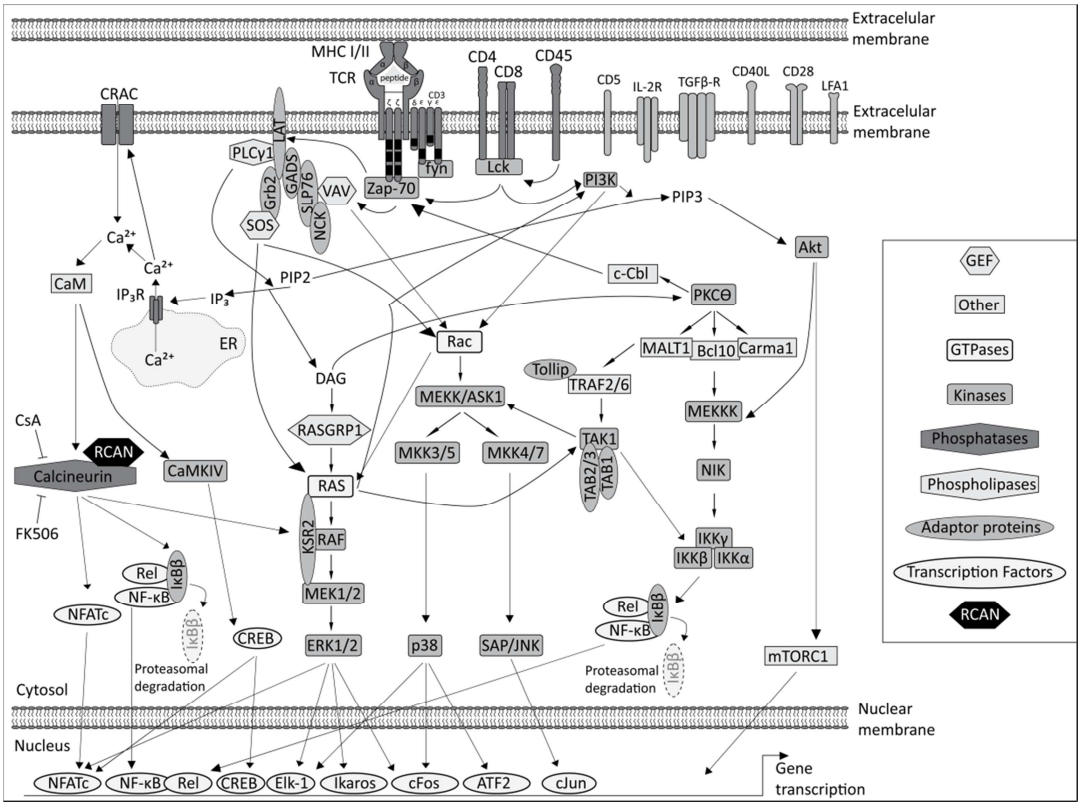

Figure 2.1. Signaling cascades triggered by TCR-MHC-peptide interaction.

TCR binding to MHC-peptide complex triggers CD3 activation, which will transmit this signal to downstream intracellular molecules. Several models have been proposed to explain this early event in TCR activation, as a clustering of TCR molecules (Purtic *et al.*, 2005), immune synapse formation (Bromley *et al.*, 2001) recruitment of TCR to membrane lipid rafts (Dykstra *et al.*, 2003) or TCR-CD3 conformational change (Reiser *et al.*, 2002) (reviewed in Smith-Garvin *et al.*, 2009). Probably, combination of all these events can act in order to activate initial TCR complex triggering.

After TCR triggering, ITAM motifs at the cytoplasmic regions of CD3 chains are phosphorylated and activated by Src family kinases (Lck/Fyn), which are activated by CD4/CD8 and CD45 co-receptors interaction with the MHC complex. Once

phosphorylated, ITAMs of CD3ζ recruit ZAP-70 and promote its activation by phosphorylation. ZAP-70 activation induces phosphorylation of VAV (a Guanine Nucleotide Exchange Factor, GEF) and the adaptor molecules SLP-76 (Src homology 2 (SH2) domain-containing leukocyte protein of 76 kDa) and LAT (Linker Activator for T Cells) (Zhang *et al.*, 1998). These adaptor molecules act as platforms for signaling, inducing the recruitment and activation of Phospholipase C gamma 1 (PLCγ1) and other molecules, as Growth factor receptor bound protein 2 (Grb2) and the GEF protein, Son of sevenless (SOS) (Rudd, 1999; Samelson, 2002). PLCγ1 mediates the hydrolysis of phosphatidylinositol-4,5-bisphosphate (PIP_2) to inositol-1,4,5-triphosphate (IP_3) and diacylglycerol (DAG). DAG activates PKCθ (Protein Kinase C Theta) and the GEF specific for RAS (rat sarcoma oncogene homolog), the RASGRP1 protein, while IP_3 binding to IP_3R (IP_3 receptor) in the endoplasmic reticulum (ER) triggers the Ca^{2+} release from intracellular storages (Cantrell, 2002).

PKCθ activation regulates the CBM complex (formed by Carma1 (Caspase Recruitment Domain [CARD], member 11), Bcl10 (B-Cell CLL/lymphoma-10) and the paracaspase MALT1 (Mucosa Associated Lymphoid Tissue Lymphoma Translocation Gene-1) proteins) (Thome and Weil, 2007). This complex activates, via NIK (NF-κB-inducing kinase), the phosphorylation of IκBβ (Inhibitor of NF-κB), which leads it to proteasomal-mediated degradation, the activation of the IKK (IκB kinases) heterotrimeric complex and the subsequent NF-κB (Nuclear Factor-κB) activation. CBM complex also recruits TRAF2 and 6 (Tumor Necrosis Factor [TNF] Receptor-Associated Factor 2 and 6) molecules, that activate TAK1 (Transforming growth factor β [TGF-β] activated kinase 1). TAK1 cooperates in NF-κB activation (Sun *et al.*, 2004) and, together with the VAV-dependent activation of the GTPase RAC (RAS-related C3 botulinum toxin substrate), triggers MKK3/5 (Mitogen activated kinase kinase 3 and 5)-p38 and MKK4/7-SAP/JNK (Stress-Activated Protein Kinase/c-Jun N-terminal Kinase) pathways (Wan *et al.*, 2006) and the consequent activation of cFos and cJun transcription factors.

RASGRP1 activation, in cooperation with SOS, leads to the activation of RAF-MEK-ERK pathways with subsequent activation of several transcription factors, such as Elk-1 (Quilliam *et al.*, 2002).

Ca^{2+} flux release from intracellular stores activates CRAC (Ca^{2+}-release-activated Ca^{2+}) and others channels, that contributes to increase even more the intracellular Ca^{2+} concentration. This intracellular Ca^{2+} increase will lead to the activation of the Ca^{2+}- and calmodulin (CaM)-dependent serine-threonine protein phosphatase Calcineurin (Cn or PPP3, formerly PP2B), which is then able to dephosphorylate and activate its substrates, including the NFATc transcription factors (cytosolic

Nuclear Factor of Activated T cells). Calcineurin also mediates IκBβ proteasomal degradation and has been involved in activation of RAF-MEK-ERK pathway by activation of the KSR2 scaffold molecule (Dougherty *et al.*, 2009). Likewise, CaM activates CaMKIV (Ca^{2+}/CaM -dependent kinase type IV), which phosphorylates and activates the transcription factor CREB (cyclic adenosine monophosphate (cAMP) response element-binding).

LCK (lymphocyte-specific protein tyrosine kinase) mediated activation of PI3K (Phosphoinositide-3 kinase) will mediate the production of phosphatidylinositol-3,4,5-triphosphate (PIP_3) and subsequent activation of AKT-mTOR (Akt or PKB, protein kinase B; mTOR, mammalian target of rapamycin) pathway, that leads to the activation of several downstream molecules that regulate gene transcription at different points.

Therefore, different signaling pathways activated after TCR-MHC-peptide interaction will cooperate to properly activate the processes involved in the generation of immune response.

2.3.- TCR co-stimulation

Cooperation of different co-stimulatory molecules in the plasma membrane is fine-tuning T cell stimulation and promoting the activation of different pathways, in order to modulate TCR-dependent pathways (Anderton and Wraith, 2002; Smith-Garvin *et al.*, 2009).

One example of co-stimulatory molecule is the Interleukin 2 (IL2). After IL2 binding to its receptor, IL2R, induces activation of JAK (Janus kinase) and downstream activation of STAT (Signal Transducer and Activator of Transcription) transcription factors (Zorn *et al.*, 2006) that, in cooperation with other costimulatory signals, as TGF-βR (TGF-β receptor) and CD28, stimulates *FoxP3* (Forkhead box P3) gene expression and promotes the acquisition of a T_{reg} lineage (Wang *et al.*, 2006; Chen *et al.*, 2003).

Other co-stimulatory molecule is CD5, which induces additional stimulation of Ca^{2+}-dependent pathways, PI_3K activity and tyrosine phosphorylation that activates RAC and VAV proteins (June *et al.*, 1987; Gringhuis *et al.*, 1998). Coordination of all these different molecules confers to CD5 the ability to fine-tuning TCR signaling (Azzam *et al.*, 2001).

Other co-stimulatory molecules are CD45, CD9, CD2 or CD80, among others.

3.- T CELL DEVELOPMENT AND MATURE FUNCTION

Immature lymphoid progenitors enter the thymus through endothelial venules in the thymic medulla and undergo different stages of development before they become mature thymocytes. Figure 3.1 shows a schematic representation of T cell maturation.

A

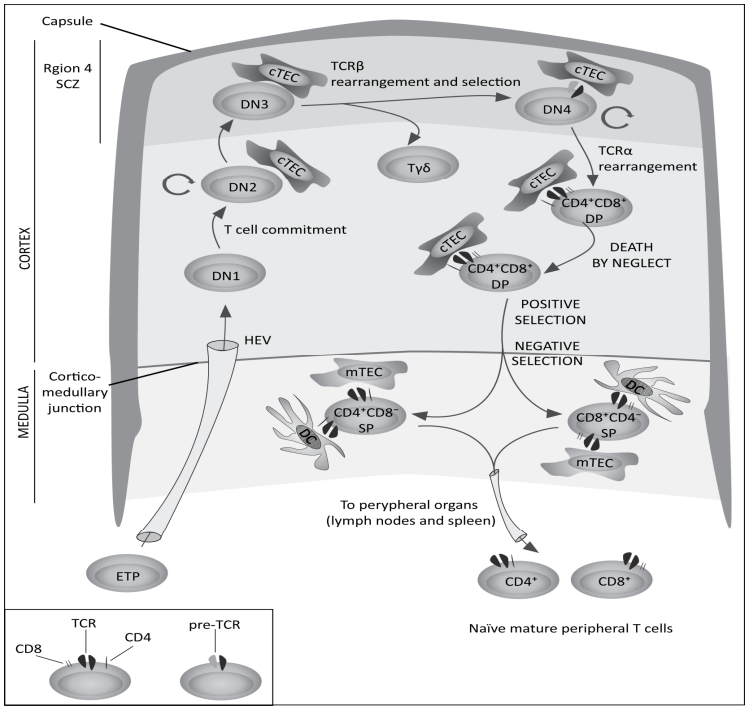

B

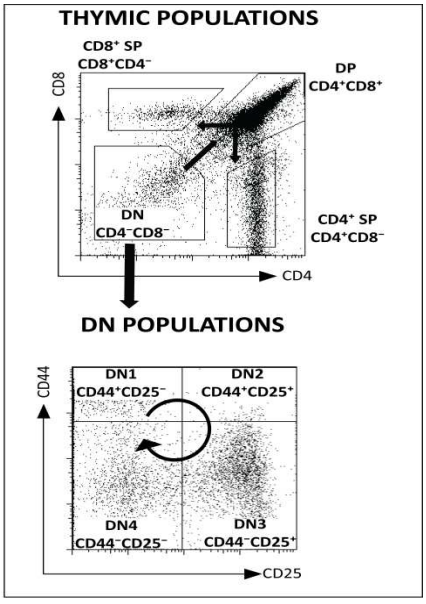

Figure 3.1. T lymphocyte maturation. A) Diagram of T cell maturation in thymus. Adapted from Blackburn and Manley, 2004 and Weerkamp, 2005. cTEC, cortical Thymic Endothelial Cell; DC, Denditric cell; DN, Double negative; DP, Double positive; ETP, Earliest T cell progenitor; HEV, High Endothelial Venule;; mTEC, medullary Thymic Endothelial Cell; SCZ, Sub-capsullar zone; SP, Single positive. B) Two-color flow cytometry analysis of different thymic subpopulations.

3.1.- Early developmental stages and the β-selection checkpoint

T cells maturate in the thymus from the Earliest T cell Progenitor (ETP), a partially T cell lineage committed HSC population, as they maintain some multipotent capability (Shortman and Wu, 1996 and reviewed in Weerkamp, 2005; Bell and Bhandoola, 2008; Wada *et al.*, 2008). These partially committed HSC precursors from fetal liver or bone marrow enter thymus and are named as double negative (DN) thymocytes, since they do not express CD4 or CD8 molecules.

DN population can be further subdivided into four phenotypically and functional subsets that can be differentiated by the surface expression of CD25 (Interleukin 2 receptor; IL2-R) and CD44 (hyaluronan receptor) molecules: CD44+CD25- (DN1), CD44+CD25+ (DN2), CD44-CD25+ (DN3) and CD44-CD25- (DN4) (Ma *et al.*, 2011) (Fig. 3.1B). In human, T cells also express the hematopoietic progenitor marker CD34 (Galy *et al.*, 1993). The commitment to the T cell lineage takes place in the DN1 to DN2 transition and is imposed by the Notch signaling pathway (Yuan *et al.*, 2010). DN3 cells, in a cell autonomous manner and with participation of several molecules (reviewed in Michie and Zuniga-Pflucker, 2002), will test the correct assembly of the pre-T cell receptor (pre-TCR), composed by pre-TCRα chain with a recently recombined TCRβ chain, in the "β-selection" checkpoint, before progressing to DN4 stage. This critical control point rescue cells from apoptosis, promotes cessation of TCRβ rearrangement to ensure allelic exclusion, and initiates the expression of the TCRα chain and the CD4 and CD8 co-receptors. Afterwards, DN4 cells undergo several rounds of cell division, and finally differentiate into $CD4^+CD8^+$ double positive cells (DP) (Yamasaki and Saito, 2007).

3.2.- Positive and negative selection of thymocytes

To ensure an immunocompetent and self-tolerant TCR repertoire, DP thymocytes test their ability to recognize endogenous peptides presented by molecules of the MHC exposed by thymic stromal cells (Anderson and Jenkinson, 2001). The affinity and avidity of this interaction will determine the survival of the thymocyte. Thus, inefficient interaction with MHC-peptide complex eliminates non-functional cells ("death by neglect"), weak interactions allow maturation to the single-positive stage ("positive selection") and strong interactions drive cells to apoptosis ("negative selection") (Fig. 3.2). Interestingly, non-functional cells and also hyperactive cells can be rescued from apoptosis by rearranging their TCR-α chain (receptor editing process) (review in Labrecque *et al.*, 2011 and Starr *et al.*, 2003).

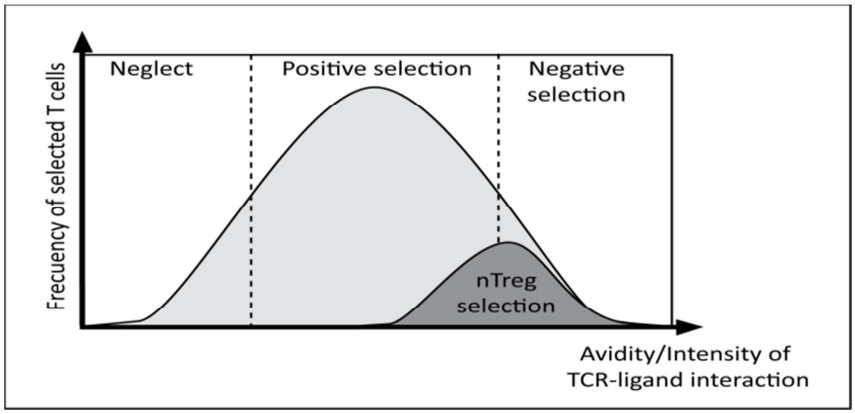

Figure 3.2. Selection of T cell repertoire depending on TCR interaction for MHC-peptide complex in the thymus. Adapted from Fehervari and Sakaguchi, 2004.

Positively selected cells differentially upregulate the expression of several molecules in the plasma membrane, such as CD3, TCR, CD69 and CD5 (Fig. 3.3). Afterwards, they will develop into mature single positive (SP) cells: $CD4^+CD8^-$ SP ($CD4^+$) or $CD8^+CD4^-$ SP cells ($CD8^+$). These mature cells are naïve cells (Th0), characterized by the expression of CD62L (L-selectin), as they have not interacted with activating peptides. Naïve cells egress from the thymus to the blood stream to reach peripheral organs (spleen and lymph nodes).

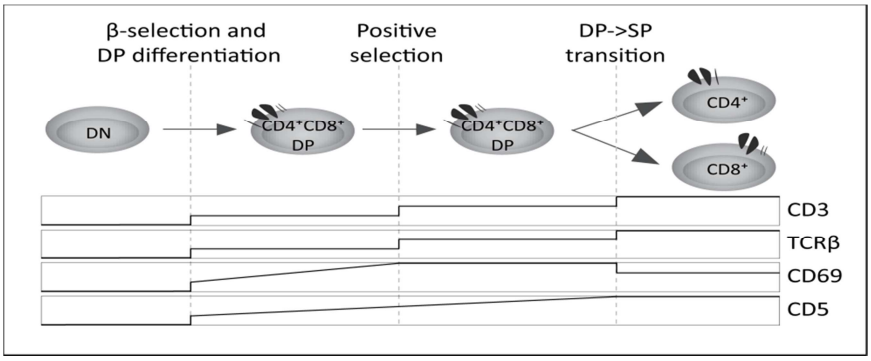

Figure 3.3. Expression pattern of different surface cell markers during thymocyte differentiation. Adapted from Williams *et al.*, 2004 and Gurney and Uittenbogaart, 2006.

Importantly, generation of the nT_{reg} population among the $CD4^+$ cells occurs in a TCR activation strength that is near to negative selection process (Fig. 3.2). It is regulated by the participation of several molecules different to those that promote the generation of conventional $CD4^+$ cells, among them, the cytokines IL2 and, in a lesser extent, IL7 and IL15, the costimulatory molecules CD28 and CD80

and the transcription factors Foxo1, STAT5 and, of course, FoxP3 (Josefowicz *et al.*, 2012; Hsieh *et al.*, 2012).

Every step on thymocyte development takes place in different thymic structures (Figure 3.1A). HSC progenitors enter to the cortical-medullary junction and they migrate to the outer cortex. Cells move to the inner cortex as they became DP cells and are the cortical thymic epithelial cells (cTEC) which mediate the positive selection process. In contrast, negative selection is mediated by dendritic cells (DC) and medullary thymic epithelial cells (mTEC) and takes place the cortical-medullary junction (reviewed in Ritter and Boyd, 1993; Gallegos and Bevan, 2004). All these migratory processes and also cell egression from the thymus are regulated by different chemokines, mainly CXCL12, CCL19, CCL21 and CCL25 (Soldevila, 2003; Takahama, 2006).

3.3.- Mature T cell activation and function

Once naïve peripheral T cells encounter an antigen presented by APC cells and became activated, they proliferate (clonal expansion) and reprogram their transcriptional activity to differentiate into different lineage of effector cells (Fig. 3.4). Moreover, in absence of co-stimulation, cells can become anergic, which are unable to proliferate and to produce effector cytokines. This process (anergy) is very important to avoid autoimmune responses.

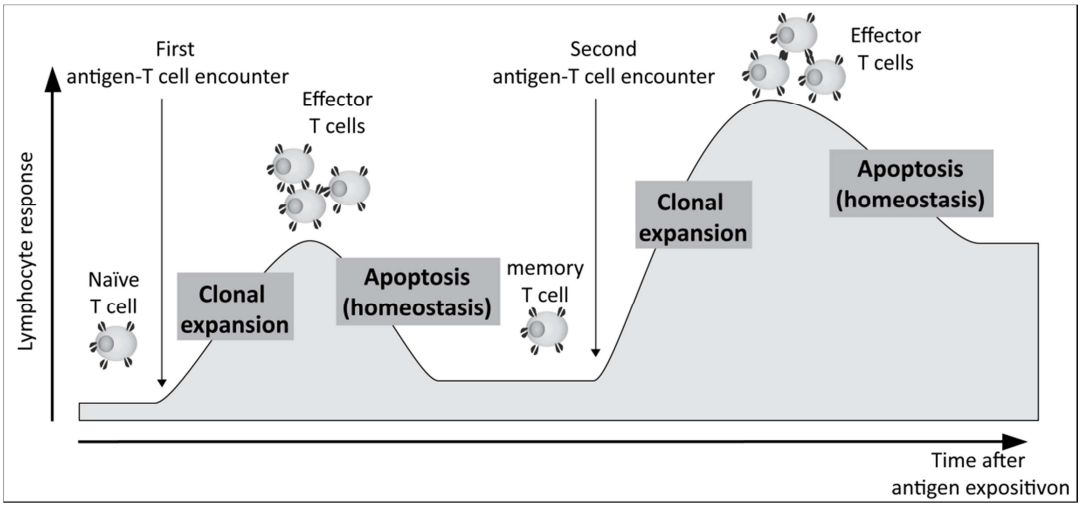

Figure 3.4. Representation of the different phases of adaptive immunity.

Activation of mature cells by TCR recognition of MHC-peptide complex triggers the expression of specific molecules in the plasma membrane of the T cells, as the very early activation markers CD69 and CD25 and the late activation marker CD44

(Budd *et al.*, 1987; Biselli *et al.*, 1992), while loss the expression of the lymph node homing receptor CD62L (L-selectin) (Hamann *et al.*, 1997). After effector response and pathogen clearance, the vast majority of cells will die, but a little number of cells will survive and persist as memory T cells (T_M) (Chandok and Farber, 2004). Memory cells will generate an earlier and stronger response when reencounter with specific pathogens and are more resistant to apoptosis (reviewed in Sprent and Surh, 2002). These memory cells are characterized by the expression of CD44 marker in the plasma membrane and can be subdivided in two major subsets, the lymphoid-homing central memory T cells (T_{CM}; $CD44^{hi}CD62L^{+}$) and the circulating and tissue-homing effector memory T cells (T_{EM}; $CD44^{hi}CD62L^{-}$) (Sallusto *et al.*, 2004). T_{CM} cells present incremented expansion potential, the presence of some specific lymphoid nodes homing receptors (such as CD62L and CCR7) and reduced sensitivity to apoptosis, in comparison with T_{EM} cells.

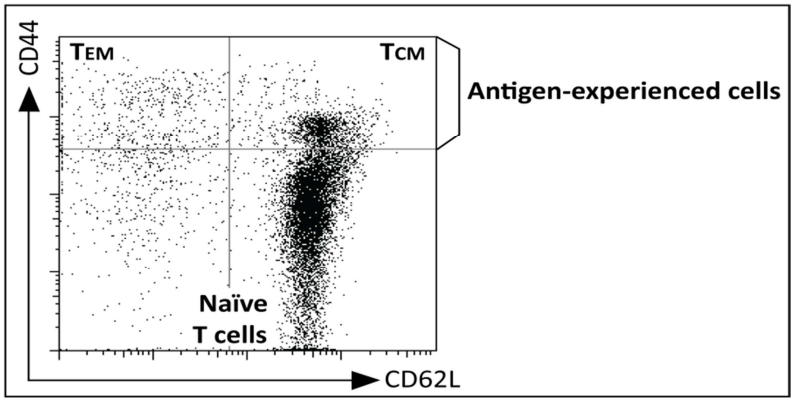

Figure 3.5. Two-color flow cytometry analysis of CD44 and CD62L populations among periheral cells. Naïve cells are $CD44^{lo}$ cells, while cells that have been exposed to antigen (antigen experienced cells) are $CD44^{hi}$ cells. T_{CM} population ($CD44^{hi}CD62L^{+}$) is composed by resting cells, while T_{EM} population ($CD44^{hi}CD62L^{-}$) comprises these cells that are in an activated status, from naïve or from T_{CM} cells.

All these thymocyte development selection processes (β-selection, positive and negative selection of DP thymocytes), and also peripheral processes on mature lymphocytes depend of TCR-mediated activation of different stimulatory and inhibitory signaling cascades that will result in different outcomes, due to the promotion of different transcriptional programs and orchestration of the production of different cytokines, chemokines and growth factors.

4.- TCR-ACTIVATED SIGNALING PATHWAYS INVOLVED IN DEVELOPMENT OF T LYMPHOCYTES

Two models have been proposed to explain the molecular mechanisms that allow thymocytes to discriminate between positive and negative selecting signals through the activation of the same TCR/CD3 complex (reviewed in Sebzda *et al.*, 1999; Chao *et al.*, 2005). The Qualitative/Affinity model predicts that mutually exclusive peptides with different individual affinities for the TCR will promote positive (low affinity) and negative (high affinity) selection by activating unique signals (Page *et al.*, 1994; Hogquist *et al.*, 1994; Jameson *et al.*, 1995). Conversely, the Quantitative/Avidity model of selection suggests that the total avidity of the TCR (the total strength) for specific peptides governs final cell fate decisions. Accordingly with this model, low concentrations of a high affinity ligand can promote positive selection, whilst high concentrations of the same peptide will promote clonal deletion (Ashton-Rickardt and Tonegawa, 1994).

Collectively, experiments with TCR altered peptide ligands and different TCR-signaling related mice models agree with the avidity model in the assumption that different strength in the activation of the TCR activates differentially the kinetics and the amount of downstream molecules (reviewed in Anderton and Wraith, 2002 and Labrecque *et al.*, 2011). Also, different cellular compartments participate in the regulation of the final T cell fate (Daniels *et al.*, 2006).

4.1.- TCR proximal events

Experiments with Fetal Thymic Organ Culture (FTOC) showed that negative-selecting peptides induced more CD3ζ chain and ZAP-70 phosphorylation than positive-selecting peptides (Daniels *et al.*, 2006). Also, the adaptor protein LAT presented different kinetic of activation (phosphorylation of LAT, p-LAT): negative selectors induced a strong and transient early peak, whereas positive selectors induced a weaker and sustained p-LAT and its translocation to lipid rafts after 30 min of stimulation (Daniels *et al.*, 2006; Werlen *et al.*, 2000).

An immediate consequence of LAT activation is the recruitment and activation of PLCγ, which leads to the production of DAG and IP_3 and the consequent increment of intracellular Ca^{2+} concentration by IP_3R stimulation at the endoplasmic reticulum (ER) (Fig. 2.1). Weakly activation of LAT by low-avidity ligands promotes slower induction of Ca^{2+} flux, whereas strong activation of LAT by high-avidity peptides promotes a rapid Ca^{2+} flux (Daniels *et al.*, 2006). Also, subcellular compartmentalization of DAG downstream molecules occurs. Positive-selecting peptides trigger RASGRP1 to the Golgi apparatus, while negative-selecting peptides recruit RASGRP1 to the plasma membrane. Besides, Grb2-SOS complex,

which has dual activity for RAS and RAC, is recruited to the plasma membrane upon LAT activation by strong peptides, but not by low-avidity ligands.

4.2.- MAPK pathways

Positive-selecting signals will lead to weak activation in the Golgi of the GTPase RAS, the downstream effector or RASGRP1, and, consequently, the activation of the ERK pathway in the Golgi (Daniels *et al.*, 2006; Rincon *et al.*, 2000a; Fischer *et al.*, 2005). Conversely, negative-selecting signals, through activation of RAC, will activate p38 and SAP/JNK kinases (Tang *et al.*, 1999; Gong *et al.*, 2001) and, in cooperation with RAS, will activate RAS/ERK in the plasma membrane, where is able to respond to lower signals (Daniels *et al.*, 2006).

These results are in agreement with previous experiments with FTOC (McNeil *et al.*, 2005) that revealed that positive selecting peptides induced two phases in ERK phosphorylation, a first phase, that is slow and transient, and a second one, which was sustained for 96 h. Negative selecting peptides, however, induced a unique initial strong activation of ERK (McNeil *et al.*, 2005). It has also been reported the ERK kinase involvement only in positive selection, but not in negative selection (Rincon *et al.*, 2000b; Fischer *et al.*, 2005). This effect is supported by experiments with FTOC using PD98059, a Mek1/2 inhibitor (Alberola-Ila *et al.*, 1995), and posterior experiments by using dominant negative forms of Mek1/2 (Sugawara *et al.*, 1998) and double mutant mice for Erk1 and Erk2 proteins (McGargill *et al.*, 2009). However, the functional consequence of the strong and transient activation of ERK upon negative-selecting peptides remains unclear.

In the other hand, it is assumed that p38 and SAP/JNK activation is essential for thymocyte negative selection, but not for positive selection (Rincon *et al.*, 1998b; Sugawara *et al.*, 1998). However, in 2003, Hsu *et al*., by using dominant negative forms of MEKK3 and MEKK6 (MAP/ERK kinase (MEK) kinase 3 and 6) it was suggested a possible role of p38 also in positive selection (Hsu *et al.*, 2003). Posteriorly, it has been described that Grb2-SOS activation upon positive-selecting conditions, although it is not recruited to the plasma membrane (Daniels *et al.*, 2006), it can act as a positive general regulator of TCR proximal molecules, as CD3ζ chain, PLCγ1 or LAT (Jang *et al.*, 2010). By using deficient mice in Grb2 in T cells, the authors elucidated that Grb2 controls the activation of p38 and pJNK also upon low-avidity ligands stimulation, suggesting a possible role of both proteins also in this process. Nonetheless, ectopic deletion of Grb2 did not cause deficiency in positive selection, when comparing heterozygous wild type (WT) control littermates (Gong *et al.*, 2001).

4.3.- Ca^{2+}-dependent signaling

Increment of intracellular Ca^{2+} concentration in the cell serves to integrate different pathways, by the activation of several Ca^{2+}-sensitive sensors, essential in development and function of T cells (reviewed in Oh-hora, 2009). As discussed above (section 4.1), Ca^{2+} flux is different upon activation of positive and negative selecting peptides. However, no functional studies have been performed to unravel the direct consequence of these differences of Ca^{2+} flux in downstream effector Ca^{2+}-dependent molecules. It has been only reported that Ca^{2+} activates the protein CAPRI (Ca^{2+}-promoted RAS inactivator) in the plasma membrane, considered as a GTPase-activating protein (GAP), which negatively regulates RAS and RAC activity (Lockyer *et al.*, 2001; Dai *et al.*, 2011). This activation of CAPRI could explain the transient activation of RAS/MEK/ERK pathway that is observed upon negative selecting peptides and the weaker and restricted to Golgi activation of RAS/MEK/ERK pathway upon positive selecting peptides. .

Ca^{2+} is crucial in the activation of CaM and consequent activation of Ca^{2+}/CaM-dependent kinase type IV (CaMKIV) and downstream effector substrates such as CREB. By using CREB deficient mice, it was seen that this molecule is dispensable in thymocyte selection processes but not for mature proliferation (Barton *et al.*, 1996). CaM also regulates the activity of Cn, that also binds Ca^{2+} and plays an essential role in thymocytes selection and also in mature peripheral function (see Section 6.3). In this context, strength and sustaining of activated Cn has been reported to be essential, together with ERK, in the CD4/CD8 lineage commitment (Adachi and Iwata, 2002).

4.4.- Other molecules

Other signaling molecules have been described to be required in deletion of autoreactive thymocytes (negative selection) but not for positive selection. Among them, the proapoptotic Bim constitutes the effector protein in programed cell death of thymocytes (Bouillet *et al.*, 2002; Cante-Barrett *et al.*, 2006). Other molecules are the phosphatase PTEN (Suzuki *et al.*, 2001), the kinase MINK (McCarty *et al.*, 2005) and the proapoptotic transcription factor Nur77 (Zhou *et al.*, 1996; Calnan *et al.*, 1995). In contrast, positive selection requires different molecules, as the TCR α-chain connecting peptide motif (TCRα-cpm) (Werlen *et al.*, 2000), the Grb2-associating protein (Gasp; also called Themis) (Johnson *et al.*, 2009; Fu *et al.*, 2009) and the VAV protein (Fischer *et al.*, 1995). Other molecules, as c-Cbl (Naramura *et al.*, 1998), Src-like adaptor protein (SLAP) (Sosinowski *et al.*, 2001) and the COOH-terminal Src kinase (Csk) (Schmedt and Tarakhovsky, 2001)

negatively modulate the process of positive selection, without affecting negative selection process.

5.- SIGNALING PATHWAYS INVOLVED IN MATURE PERIPHERAL FUNCTION OF T LYMPHOCYTES

Mature T lymphocytes synchronize different signals provided by different cytokines, chemokines and growth factors that activate different signaling pathways. The final balance of them will promote the transduction of cytokine genes that will coordinate the cellular processes involved in immune response; as clonal expansion, differentiation, effector function, survival and homeostasis (see Figure 3.4) (Crabtree and Clipstone, 1994; Khaled and Durum, 2002; Veillette *et al.*, 2002).

5.1.- Clonal expansion and differentiation

After TCR interaction with MHC-peptide complex, and in cooperation with different costimulatory molecules, including CD28 or CD2; naïve (CD62L-) Th ($CD4^+$) and Tc ($CD8^+$) cells proliferate (clonal expansion) and differentiate into specific effector cell lineages. Both processes are tightly related and regulated by the balance between MAPK, PKC and Cn/NFATc signaling pathways, but in some cases these two processes can be independently regulated (Laouar and Crispe, 2000). In this context, PKC promotes differentiation into Th2 and Tc2 and negatively regulates the differentiation into Th1 or Tc1 lineages. In contrast, Ca^{2+} and Cn signaling, in coordination with ERK pathway, have the opposite effects (Noble *et al.*, 2000; Noble *et al.*, 2001). The differential role of the NFATc family members in Th differentiation will be further discussed (Section 6.3). The analysis of null mice in p38 and JNK2 MAPK revealed that p38 and JNK2 positively regulate Th1 differentiation, but inhibits IL2 production by $CD8^+$ cells (Tc1-like response), while JNK1 negatively regulates Th2 differentiation, without affecting Th1 responses, but promotes Tc1-like phenotype (expression of IL2-R) (Rincon *et al.*, 1998a; Rincon *et al.*, 1998b; Dong *et al.*, 1998 and reviewed in Rincon *et al.*, 2000b and Rincon and Pedraza-Alva, 2003).

5.2.- Effector function

Th and Tc lineage-committed cells will differentially secrete effector cytokines that will mediate specific immune responses (see table 1.1; reviewed in Noble *et al.*, 2001; Woodland and Dutton, 2003). In this context, production of IL2 effector cytokine requires cooperation of ERK, JNK and Cn pathways to activate cFos, cJun and NFATc transcription factors. NFATc transcription factors also cooperate with GATA (GATA-binding protein) transcription factor in IL4 and IL5 production, with

NF-κB and cJun in TNFα production and with other transcription factors to promote the gene expression of different cytokines (reviewed Macian *et al.*, 2001).

5.3.- Cell homeostasis

After pathogen clearance, the majority of activated cells will die in order to reestablish homeostasis and to maintain peripheral tolerance to self-antigens. For the same reason, naïve cells that fail to interact with MHC-peptide complex will also die over time by a lack of survival signals mediated by cytokines.

One of the mechanisms that regulate homeostasis of activated T cells is known as Antigen Induced Cell Death (AICD). Unlikely thymocytes, where programed cell death in the negative selection process is mediated by Bim protein (Cante-Barrett *et al.*, 2006), in mature lymphocytes apoptosis is driven by engagement of death receptors of the TNF family, such as Fas receptor (FasR , also known as CD95) or TNF-αR, or mediated by reactive oxygen species (ROS). Interestingly, the same IL2-mediated signaling that promotes proliferation and survival by activation of AKT and Bcl-2 expression sensitizes the cells to FasL-mediated AICD (Refaeli *et al.*, 1998). Finally, all the death signals will lead to the activation of caspases by different mechanisms and to final cell death (Khaled and Durum, 2002).

In lymphoid peripheral tissues it has been also described that P38 promotes $CD8^+$, but not $CD4^+$, cell death (reviewed in Rincon and Pedraza-Alva, 2003). Also, as described in section 6.3, Cn and the different members of the NFATc family can modulate survival of mature T cells.

6.- THE CALCINEURIN-NFATc SIGNALING PATHWAY

6.1.- Calcineurin

Cn or serine-threonine protein phosphatase 3 (PPP3) is the only serine/threonine phosphatase regulated by Ca^{2+} and CaM (reviewed in Aramburu *et al.*, 2000). This enzyme is a key mediator of the cellular signalling that couples the intracellular Ca^{2+} signals to different cellular responses through dephosphorylation of their substrates (reviewed in Li *et al.*, 2011). Cn is controlling normal cell cycle progression and salt stress adaptation in lower eukaryotes and plants, while in mammals it is involved in several processes, including development and function of the immune and nervous system, angiogenesis, morphogenesis of the heart valves and muscle development, among others (reviewed in Rusnak and Mertz, 2000; Aramburu *et al.*, 2004).

The structure of Cn is highly conserved from yeast to humans. Cn is a heterodimer formed by the catalytic subunit A (CnA) of 58-64 kDa, and the regulatory subunit (CnB) of 19 kDa (Fig. 7) (Rusnak and Mertz, 2000; Ke and Huai, 2003) . In mammals, CnA has three isoforms: α, β and γ; and CnB has two, CnB1 and CnB2. Cn shows ubiquitous expression in all mammalian tissues, but isoform CnB2 is restricted to testis and CnAγ to testis and brain (Aramburu *et al.*, 2000; Medyouf and Ghysdael, 2008).

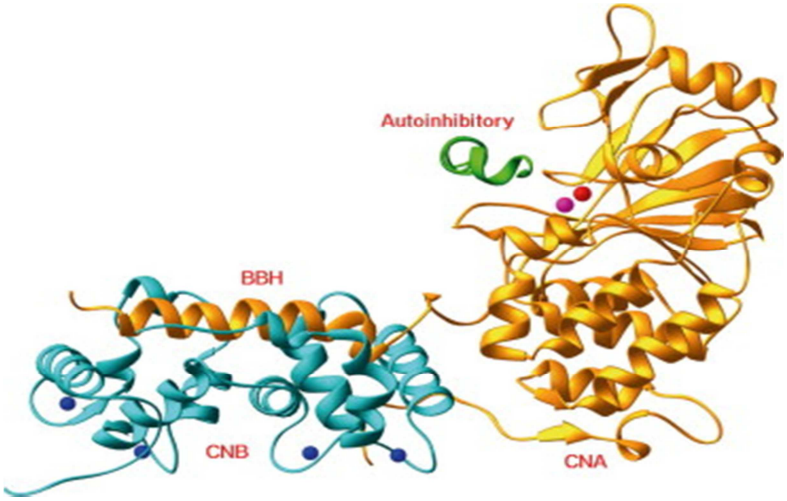

Figure 6.1. Cartoon of crystal structure of CnA anb CnB heterodimer. Calcineurin subunits are represented as follows: gold, CnA subunit (CNA); cyan, CnB subunit (CNB). The catalitic ions are represented as follows, red, Zn^{2+}; pink, Fe^{3+} and blue balls, Ca^{2+}. BBH, CnB-binding helical domain. In green is indicated the autoinhibitory domain (AID) of CnA subunit. Adapted from (Ke and Huai, 2003).

Cn activity is regulated by Ca^{2+} concentration. CnB contains four EF-hand motifs and each of them bind one Ca^{2+} molecule, two with high affinity (Kd= 0.3 µM and 0.9 µM range) and two with low affinity (Kd= 11 µM and 36 µM) (Feng and Stemmer, 1999). The high affinity EF-hand motifs in CnB molecule are considered as structural sites, as they are required for a stable CnB binding to the N-terminal region of CnA. The binding of Ca^{2+} to the low affinity sites in CnB serves as Ca^{2+} sensor and promotes a conformational change in the CaM binding region of CnA subunit that will allow CaM binding and the consequent AID (Autoinhibitory Domain) release from the active site on the catalytic subunit (Yang and Klee, 2000) (Fig. 6.2). CaM binding to CnA is dependent on Ca^{2+} binding to the EF-motif in CaM. This motif is a low affinity motif and finelly regulates CnA activity and will allow fully activation of Cn only in presence of high intracellular Ca^{2+} concentration (reviewed in Li *et al.*, 2011).

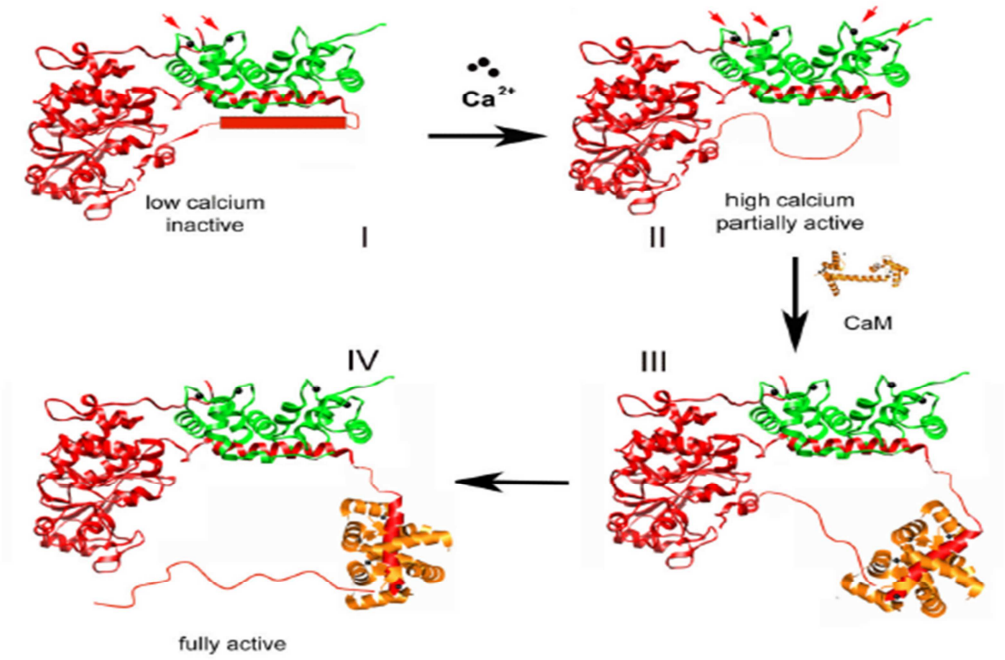

Figure 6.2. Squematic representation of CaM- dependent activation of CnA. Adapted from Li *et al.*, 2011.

Among the substrates of Cn, , the family of transcription factors NFATc integrates the calcium signals, via Cn, with other signaling pathways, as MAPK, by cooperation with other transcription factors to induce gene expression. The NFATc proteins constitute the basis for vertebrate morphogenesis and organogenesis (Wu *et al.*, 2007) and plays an essential role in other several cellular programmes (Crabtree and Olson, 2002), including the lymphocyte activation and tolerance (Macián et al, 2002, Hogan et al, 2003). Other Cn physiological substrates are the IκBβ protein (Biswas *et al.*, 2003), the enzyme NO synthase 2 (NOS2) (Dawson *et al.*, 1993), the microtubule-associated protein 2 (MAP2) and tau factor (Goto *et al.*, 1985; Murthy *et al.*, 1985; Yu *et al.*, 2008), the heat shock protein HSP25 (Gaestel *et al.*, 1992), the Bcl-2 family member BAD (Wang *et al.*, 1999), several members of dephosphins family, as dynamin I or amphiphysin 1 (Bauerfeind *et al.*, 1997; Cousin and Robinson, 2001), the IP_3R (Cameron *et al.*, 1995) or the transcription factors Elk-1 (Tian and Karin, 1999) and MEF2 (Wu *et al.*, 2001), among others.

6.2.- Nuclear Factor of Activated T cells (NFAT)

The Nuclear Factor of Activated T cells (NFAT) are a family of proteins related to the Rel family of transcription factors present in all eukariotes, and are restricted to vertebrates (Wu *et al.*, 2007). The NFAT family consists in five members in

vertebrates: NFATc1 (formerly, NFAT2 or NFATc), NFATc2 (formerly, NFAT1 or NFATp), NFATc3 (formerly, NFAT4 or NFATx), NFATc4 (formerly, NFAT3) and NFAT5 (formerly, NFATL1 or TonEBP), each of them with several isoforms as product of alternative splicing variants (reviewed in Macian, 2005).

Unlike all the other transcription factors containing Rel domains, NFATc1 to 4 activity is regulated by Cn-dependent dephosphorylation in response to Ca^{2+}, that promotes their rapid translocation from the cytoplasm to the nucleus and, in cooperation with other transcription factors (commonly named NFATn, but all of them NFAT unrelated proteins), as AP1, GATA4, MEF2 (Myocyte enhancer factor 2) and FoxP3 (Macian *et al.*, 2001; Crabtree and Olson, 2002; Bettelli *et al.*, 2005) triggers the expression of several genes.

Concerning NFAT5 protein, it does not contain any Cn binding site, so it is not regulated by Ca^{2+} and Cn-dependent dephosphorylation. Instead, the activity of this protein is regulated by hypertonic responses (Dahl *et al.*, 2001). However, it has been described that *NFAT5* gene transcription is regulated by Cn (Trama *et al.*, 2000).

NFATc proteins are ubiquitously expressed in animal tissues, but only NFATc1, NFATc2, NFATc3 and NFAT5 are expressed in the immune cells (Macian, 2005; (Trama *et al.*, 2000). NFATc3 has preferential expression in thymocytes and NFATc1, NFATc2 are mainly expressed in peripheral T cells (Oukka *et al.*, 1998; Amasaki *et al.*, 2000).

NFATc proteins (we will use NFATc proteins to refer to NFATc1 to NFATc4 proteins) contain four domains: N-terminal transactivation domain (AD), regulatory domain (also known as NFAT homology region or NHR), DNA-binding domain (Rel-homology domain/region or RHD/R) and C-terminal domain (Fig. 6.3). NFAT5 mantain the RHD and the C-terminal region, but bears a shorter NHR that lacks the Cn-binding site (reviewed in Macian, 2005). The regulatory domain contains multiple serine-rich regions (SRR motifs and SP repeats), which are the target of Cn dephosphorylation (Hogan *et al.*, 2003), a nuclear localization signal (NLS) and other motifs involved in NFATc regulation. The RHD contains the sites of interaction with other transcription factors, such as cJun or cFos.

NFATc bind to calcineurin by two conserved domains: The PXIXIT sequence and the LXVP motif, both higly conserved among the different human NFATc proteins (Martinez-Martinez *et al.*, 2006; Li *et al.*, 2011).

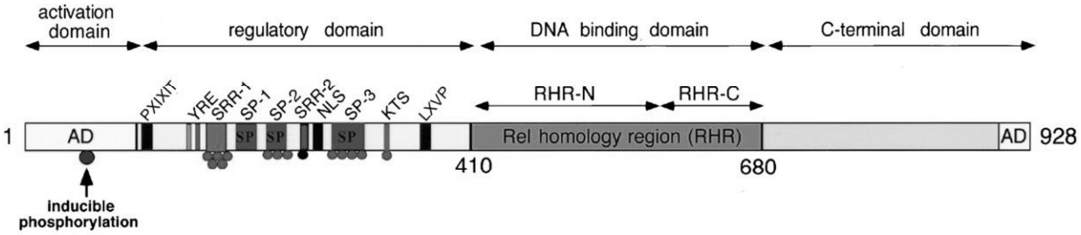

Figure 6.3. Schematic representation of NFATc protein structure based on NFATc1. Phosphorylation sites are indicated as circles. Figure adapted from Hogan *et al.*, 2003.

6.3.- Cn/NFATc signaling in T cell development and function

The role of Cn has been reported to be critical in development of thymocytes and function of mature T lymphocytes. *In vivo* treatment of mice with the Cn inhibitor Cyclosporin A (CsA) impaired the generation of T_{regs} (Mantel *et al.*, 2006). Also, CsA treatment compromised the development of single positive (SP) thymocytes but also impeded the deletion of self-reactive cells, affecting both positive and negative selection of thymocytes (Gao *et al.*, 1988; Jenkins *et al.*, 1988). However, other authors observed no effect of CsA and FK506 (Tacrolimus; other Cn inhibitor) in negative selection (Wang *et al.*, 1995). Nonetheless, as the administration of these drugs has other Cn-independent effects (as MHC downregulation) and affects thymus architecture (Beschorner *et al.*, 1987; Kanariou *et al.*, 1989; Nalesnik *et al.*, 1987; Pugh-Humphreys *et al.*, 1990; Thomson *et al.*, 1991), the role of Cn in negative selection remains controversial. In mature T cells, CsA or FK506 block the gene expression of numerous cytokines (*IL2*, *IL4*, *IL10*, *TNF-α*, among others) with the unique exception of *TGF*-β (reviewed in Rao *et al.*, 1997).

Experiments with CnAα-deficient mice showed normal populations and proliferation upon mitogen (ionomycin plus phorbol 12-myristate 13-acetate (PMA) stimulation, however, antigen-specific T cell response was reduced (less IL2, IL4 and IFN-γ secretion) (Zhang *et al.*, 1996). In contrast, $CnA\beta^{-/-}$ presented deficient T cell development (less SP cells in thymus and periphery) and impaired mature cell proliferation and IL2 production upon ionomycin/PMA activation, due to impaired expression of the pro-survival Bcl-2 protein, that caused an incremented apoptosis of SP cells in thymus and periphery (Bueno *et al.*, 2002; Manicassamy *et al.*, 2008). This data suggests a preferential role of CnAβ in survival of naïve cells. Recently, $CnA\beta^{-/-}$ mice has also been described to produce less $FoxP3^{+}$ cells in periphery, but increased amounts of pro-inflammatory cytokines (IL4, IL6 and IFN-γ), probably by an insufficient regulation mediated by T_{regs} (Doetschman *et al.*, 2011). Moreover, $CnA\beta^{-/-}$ mice presented increased proportion of $CD44^{hi}CD62L^{-}$ cells (T_{EM} subpopulation) among the $CD4^{+}$ T cells

(Doetschman *et al.*, 2011). On the contrary, CnB seems to play a preferential role in thymocyte development. In this context, CnB-deficient mice showed less total cellularity and less SP cells, in percentage and absolute numbers, in both, in thymus and periphery, with increased cell death (Neilson *et al.*, 2004). These mice presented a partial block in DN3 population and absolutely reflected an impaired DP to SP progression due to a defect in positive selection (decreased $CD5^{hi}$ and $CD69^{hi}$ populations in DP). Posteriorly, the same authors described that Cn regulates the ability of ERK to be phosphorylated after recognition of low avidity ligands, an essential process to accomplish positive selection (Neilson *et al.*, 2004). In contrast, transgenic mice bearing a constitutively active form of CnA displayed less general cellularity in the thymus and reduced levels of DP thymocytes (Hayden-Martinez *et al.*, 2000). This decrease in DP thymocytes was due to a partial block in DN3 stage, but enhanced negative selection was discarded, because these mice showed increased levels of CD69 and CD3 in DP cells and increased SP cells in thymus and periphery, as a result of enhanced positive selection (Hayden-Martinez *et al.*, 2000). All these data indicates that Cn is crucial in the discrimination and the modulation of the signal that is transduced trough the TCR during the development of thymocytes, and, therefore, is essential in the selection of T cell repertory.

Regarding NFATc transcription factors, they are involved in several processes of immune response by the regulation of several genes, as *IL2*, *IL4* and *TNFα*, among others (Rao *et al.*, 1997; Crabtree and Clipstone, 1994; Muller and Rao, 2010). Experiments with null mice and gain of function mutants for the different NFATc members demonstrated non-overlapping NFATc roles in thymocyte development and function.

$NFATc1^{-/-}$ and $RAG1^{-/-}$ mice and $NFATc1^{-/-}$ and $RAG2^{-/-}$ mice showed reduced proliferation (in an IL2 independent manner) and impaired Th2 responses (reduced IL4 and IL6 production) (Yoshida *et al.*, 1998; Ranger *et al.*, 1998a). Also presented reduced DN1 and increased DN4 populations in thymus (in $RAG1^{-/-}$ mice). B cells showed a slight increase in IgM (produced before isotype switching) and IgG2a production and reduced IgG1 (in $RAG1^{-/-}$ mice) and IgE (in $RAG2^{-/-}$ mice) production.

In contrast, $NFATc2^{-/-}$ mice displayed decreased Th1 responses and enhanced Th2 responses (Viola *et al.*, 1998; Erb *et al.*, 2003). Also, it presented accumulation of peripheral lymphocytes with "preactivated" phenotype (increased expression of CD69 and CD44 activation markers) and impaired deletion of alloreactive T cells ($CD4^{+}$ $V\beta11^{+}$ cells), but not due to alterations in FasL-mediated AICD (Schuh *et al.*, 1998).

NFATc3$^{-/-}$ mice showed normal gene expression of cytokines but reduced proportions of mature SP cells in thymus, due to increased cell death (Oukka *et al.*, 1998; Cante-Barrett *et al.*, 2007). Oukka *et al*. described an increased sensitivity to TCR-mediated signaling that drives cells to negative selection and produces a hyperactivated phenotype of peripheral cells, due to altered expression of several genes: reduced levels of Bcl-2 (anti-apoptotic) in DP and SP thymic populations, and increased levels of FasL (pro-apoptotic) in splenocytes. In contrast, Canté-Barrett et al. (Cante-Barrett *et al.*, 2007) did not detect changes in intracellular expression of Bcl-2 and Bim and described an increased "death by neglect", due to a defect in positive selection process, confirmed by reduced levels of CD69^{hi} and TCRβ^{hi} populations among DP thymocytes. On the contrary, constitutively nuclear form of NFATc3 induced differentiation of DP mainly to CD4 cells, probably by regulating expression of CD4 and CD8 co-receptors (Amasaki *et al.*, 2002).

NFATc1/c2 double deficient mice presented normal T cell populations, but deficient Th1 and Th2 effector functions (Peng *et al.*, 2001). Also, both proteins resulted essential in B cell homeostasis, yet the double deficient mice presented a hyperactivated Th2-like phenotype of B cells (increased IgG1 and IgE secretion).

NFATc2-c3 double deficient mice presented lymphadenopathy, splenomegaly and increased proportion of peripheral T cells with activated phenotype, showing a spontaneous Th2 response (increased IL-4, IL-5, IL-6, and IL-10 secretion) in a costimulatory-independent manner. Also, thymocytes presented a partial block in DN3 and, also, peripheral T cells are more resistant to AICD (Ranger *et al.*, 1998b). All that results suggest an inhibitory function of these proteins in Th2 responses. Also, these mice show an early mortality at 8-10 weeks due to the resistance of CD4^{+} T cells to T_{regs}-mediated suppression (Bopp *et al.*, 2005). More recently, it has been described a defect on positive selection similar to CnB$^{-/-}$ mice (Gallo *et al.*, 2007).

NFATc proteins also cooperate with SMAD proteins in the induction of FoxP3 expression (Mantel *et al.*, 2006; Tone *et al.*, 2008). Moreover, FoxP3 cooperates with NFATc in the induction of T_{reg}-mediated peripheral tolerance (Bettelli *et al.*, 2005; Rudensky *et al.*, 2006).

Collectively, all these results demonstrate direct implication of Cn and differential function of NFATc members at different points of thymocytes development and mature T cell function.

6.4.- Modulators of calcineurin activity

Inhibition of Cn by the immunosuppressive drugs CsA and FK506 is the basis of current immunosuppressive therapy (reviewed in Martinez-Martinez and Redondo, 2004). Unfortunately, life-span time treatment with these anti-calcineurininc drugs entails severe secondary effects, like nephrotoxicity, neurotoxicity, hypertension, diabetes, and increased cancer risk (Martinez-Martinez and Redondo, 2004). Both drugs bind cytosolic immunophilins (Cyclophilin A (CypA) and FKBP12, respectively) prior to interact with Cn. The toxicity of these drug-immunophilin complexes is mainly due to the fact inhibit Cn phosphatase activity against all Cn substrates. Therefore, the study for more specific inhibitors of the Cn-NFATc signaling pathway is a challenge in the immunosuppressive therapy field.

Searching for specific immunosupressor drugs that disrupts Cn-NFATc interaction has been focused in the PXIXIT sequence of NFATs, SPRIEIT for NFATc1, NFATc2 and NFATc4, and SPSIQIT for NFATc3. SPRIEIT peptide was shown to inhibit NFATc activation and signaling (Aramburu *et al.*, 1998). Afterwards, a synthetic optimized version of this amino acid sequence, the VIVIT peptide, resulted in more efficient displacement of Cn-NFATc interaction and increased inhibition (Aramburu *et al.*, 1999; Choi *et al.*, 2012). This sequence resulted also in a useful tool for developing more specific immunosupresive drugs, such as Inhibitor of NFAT-calcineurin interaction (INCA) compounds (Roehrl *et al.*, 2004). The INCA compounds were shown to interact with a novel allosteric site in Cn that impedes Cn-NFATc interaction, without affecting Cn phosphatase activity (Kang *et al.*, 2005), however, due to their structural similarity with quinones, resulted to bear a high toxicity.

Moreover, several proteins have been proposed as negative modulators of the Cn-NFATc signaling (Table 6.1), among them, the RCAN family of proteins.

Table 6.1.- REGULATORY PROTEINS OF CALCINEURIN		
PROTEIN	**REFERENCES**	**PxIxIT sequence**
A-kinase anchoring protein 79 (AKAP79)	Coghlan et al., 1995; Kashishian et al., 1998; Dell'Acqua et al., 2002; Li et al., 2012; Zhang et al., 2008	PIAIIIT
Calcineurin Homologous Protein 1 (CHP1) or p22	Lin et al., 1999; Di Sole et al., 2012	-
Cabin1/Cain	Lai et al., 1998; Sun et al., 1998; Esau et al., 2001; Jang et al., 2007; Rodriguez et al., 2005; Martinez-Martinez et al., 2009; Hammond and Udvadia, 2010	PEITVT (Cabin1)
Carabin	Pan et al., 2007	-
mitochondrial FK506 binding protein 38 (FKBP38)	Shirane and Nakayama, 2003; Weiwad et al., 2005	-
african swine fever virus protein A238L	Miskin et al., 1998; Miskin et al., 2000; Granja et al., 2004; Silk et al., 2007; Abrams et al., 2008	PKIIIT
Calsarcin family members	Frey et al., 2000; Frey et al., 2004; Frank et al., 2007; Frey et al., 2008	-
Regulators of Calcineurin (RCAN). Also known as DSCR, MCIP, CSP or CALP	Fuentes et al., 2000; Gorlach et al., 2000; Rothermel et al., 2000	PSVVVH

Table 6.1. Modulatory proteins of Cn.

7.- REGULATORS OF CALCINEURIN (RCAN)

The family of proteins Regulator of Calcineurin (RCAN) proteins is conserved in eukaryotes. All of them bear several conserved motifs: FLISPP and LXXP. Except some punctual exceptions, three paralogous genes are found only in vertebrates whilst there is only one member in the rest of Eukarya. In vertebrates, the RCAN family is formed by RCAN1 (also known as DSCR1, calcipressin-1 (CSP1 or CALP1), MCIP1 or Adapt78), RCAN2 (formerly known as DSCR1L1, calcipressin-2 (CALP2 or CSP2), MCIP2 or ZAKI-4) and RCAN3 (previously known as DSCR1L2, calcipressin-3 (CALP3 or CSP3) or MCIP3). Each of them codify for several transcripts (see section 7.1 and article 1 in results chapter).

RCAN1 was the first family member to be identified (Fuentes *et al.*, 1995). It was denominated DSCR1 from Down Syndrome Critical Region 1 (later on known as Down Syndrome Candidate 1), because it was firstly identified as EST (expressed sequence tag) from human chromosome 21, as a possible candidate susceptible to be involved in Down's syndrome. In 1996 the human RCAN2 member (formerly, ZAKI-4 and posteriorly known as DSCR1L1 and RCAN2) was described as a thyroid hormone-responsive gene (Miyazaki *et al.*, 1996), but it was in 2000 when it was described as a RCAN1 homologous protein, based in its capacity to inhibit Cn signaling (Strippoli *et al.*, 2000; Fuentes *et al.*, 2000; Rothermel *et al.*, 2000). Was in the same year when human RCAN3 (formerly known as DSCR1L2) was also identified (Strippoli *et al.*, 2000). Thanks to the discovery of RCAN orthologs in other organisms (*D. melanogaster*, *C. elegans*, mouse, hamster, *S. Pombe*, *S. cerevisae*) the three proteins were defined as a conserved family of proteins in Eukarya based on the FLISPP motif conservation. Mulero *et al*. extended their study of RCAN orthologs performing an exhaustive comparative genomic analysis that allowed them to define the RCAN proteins as a novel functional subfamily in vertebrates into the Eukarya (Mulero *et al.*, 2007). This subfamily was characterized by the presence of two different motifs highly conserved in vertebrates (FLISPP, CIC) while only the FLISPP motif was reported to be present in invertebrates, fungi and some protozoa (Mulero *et al.*, 2007). Posteriorly, the CIC motif was found to contain the functional PXIXIT-like motif. Moreover, the LXXP, TXXP and the EXXP motif were also described to be conserved among Eukarya (Mehta *et al.*, 2009). In addition, a novel nomenclature for the different exons, transcript forms and protein isoforms has been proposed for the scientific community (Davies *et al.*, 2007), based on the exon composition of the different RCAN members, in order to facilitate their study and nomenclature of possible new identified members. This nomenclature will be described in detail in the article 1 in results chapter.

Several *in vivo* studies attribute a dual role of RCAN proteins as facilitators or inhibitors of Cn signaling. This dual capability has been ascribed to the participation of different RCAN motifs, their phosphorylation status, the different affinity for Cn and the amount of RCAN proteins (Vega *et al.*, 2002; Vega *et al.*, 2003; Shin *et al.*, 2006; Mehta *et al.*, 2009; Shin *et al.*, 2011). This dual role of RCAN proteins will be detailed in the results and discussion chapter (see also section 7.4.).

7.1.- RCAN transcripts, isoforms and regulation of transcription

Additional information about gene expression can be obtained from several databases. The Gene Expression Database (GXD), implemented in the Mouse

Genome Informatics (MGI) (http://www.informatics.jax.org/expression.shtml; Finger *et al.*, 2011), and the e-Mouse Atlas Project (http://www.emouseatlas.org; Richardson *et al.*, 2010) integrate very useful information of gene expression in different mouse tissues at different stages of development. Also, the Comparative Toxicogenomics Database (http://ctdbase.org; Davis *et al.*, 2011) collects information of different chemical compounds that can affect gene expression.

A very exhaustive study of mouse *Rcan* mRNA forms and protein isoforms has been performed in adult brain, showing differential pattern of distribution in brain, suggesting that they could play differential roles (Porta *et al.*, 2007a). However, the analysis of the expression pattern of mouse *Rcan* genes in the immune system has not been described.

RCAN1

Human *RCAN1* gene (ADAPT78, DSCR1, MCIP1 or Calcipressin 1; HSA 21q22.12) (corresponding to *Rcan1* in mouse) is transcribed in two majoritarian mRNA forms, *RCAN1-1* and *RCAN1-4* (corresponding to *Rcan1-1* and *Rcan1-2* in mouse, respectively), which are translated into RCAN1-1 and RCAN1-4 protein products, respectively (corresponding to Rcan1-1 and Rcan1-2 in mouse) (see Figure 3 upper panel in article 1 in results chapter). Both isoforms are transcribed in adult human heart and skeletal muscle, but none of them were detected in lung by Northern blot analysis (Fuentes *et al.*, 1997). RCAN1-1, highly detected in fetal human brain, was not detected in adult human kidney and placenta; while RCAN1-4 was not detected in human brain. It is important to note that mouse Rcan1-2 is sometimes referred as Rcan1-4 isoform. Northern blot analysis and *in situ* hybridization with expression probes against a common region for both murine *Rcan1* mRNA forms (*Rcan1-1* and *Rcan1-2*) revealed that Rcan1 is expressed in the early stages of development, mainly in brain and heart, while in adult tissues present similar tissue distribution to that found for human *RCAN1* (Casas *et al.*, 2001).

In humans, also *RCAN1-2* and *RCAN1-3* mRNA products have been described at mRNA levels by Rapid Amplification of cDNA 5' Ends (RACE 5') analysis, but not at protein level (Fuentes *et al.*, 1997). Exon 2 lacks a methionine start site and exon 3 encodes only for 3 amino acids. *RCAN1-2* is mainly transcribed in fetal brain and liver.

RCAN1-1 form is constitutively expressed, but can be positively regulated by glucocorticoids (human; U *et al.*, 2004; Hirakawa *et al.*, 2009, Sun *et al.*, 2011a) and vascular endothelial growth factor (VEGF) (human; Qin *et al.*, 2006) and negatively regulated by Notch signaling pathway (mouse; Mammucari *et al.*, 2005).

RCAN1-4 is an inducible form which expression can be induced by several mitogens and inflammatory cytokines: VEGF and thrombin (human; Hesser *et al.*, 2004; Minami *et al.*, 2004; Qin *et al.*, 2006; Holmes *et al.*, 2010); IL-1β and TNF-α (mouse; Cho *et al.*, 2008; Jang *et al.*, 2011), angiotensin II (human and mouse; Lin *et al.*, 2003; Esteban *et al.*, 2011), estrogen hormones (Pedram *et al.*, 2008; Gurgen *et al.*, 2011) and various osmotic stress agents, including Ca^{2+} (human, hamster and mouse; Lin *et al.*, 2003; Crawford *et al.*, 1997; Leahy *et al.*, 1999; Yang *et al.*, 2000; Michtalik *et al.*, 2004). *Rcan1-4* mRNA form was also induced in brain, heart, lung and kidney of mice treated with LPS (Minami *et al.*, 2009). Moreover, *Rcan1-4* was induced after IgE-mediated stimulation of bone marrow–derived mast cells (BMMCs), and it requires Egr1 binding to *Rcan1* promoter (Yang *et al.*, 2009b). Specifically in Jurkat cell line and primary human T lymphocytes, crosslinking with anti-CD3 plus anti-CD28 also triggered the expression of *RCAN1-4* mRNA form (Narayan *et al.*, 2005; Aubareda *et al.*, 2006).

Finally, in THP-1 human mononuclear cells, increased *RCAN1* gene expression was detected when they are co-cultured with *C. albicans* (Barker *et al.*, 2005).

RCAN2

Human *RCAN2* gene (formerly DSCR1L1, MCIP2, ZAKI-4 or Calcipressin 2, HSA 6p12.3) encodes for three mRNA forms, *RCAN2-1*, *RCAN2-2* and *RCAN2-4* (Cao *et al.*, 2002) (see Figure 3 middle panel in article 1 in results chapter). *RCAN2-1* (also known as *RCAN2*-β*1*) and *RCAN2-2* (also known as *RCAN2*-β*2*) will be translated using the ATG located in exon 3 and will rise to the same protein isoform; RCAN2-3 (or RCAN2-β; corresponding to Rcan2-1 in mouse). Both transcripts were mainly detected in human brain, heart, skeletal muscle, kidney, liver and placenta. *RCAN2-4* transcript (also known as *RCAN2-α*; corresponding to *Rcan2-3* in mouse) will be translated in RCAN2-4 (or RCAN2-α; corresponding to Rcan2-3 in mouse) protein, by using the ATG located in exon 4. This transcript is nearly exclusively transcribed in human brain (Cao *et al.*, 2002). RCAN2 is also expressed in embryonic (E15.5) brains (Oeschger *et al.*, 2012).

In mouse, only *Rcan2-1* and *Rcan2-3* (known as *Rcan2*-β and *Rcan2-α*, respectively) have been described, corresponding to human *RCAN2-1* and *RCAN2-4* transcripts, respectively. They will encode for two different protein isoforms, Rcan2-1 (isoform α) and Rcan2-3 (isoform β), corresponding to human RCAN2-3 and RCAN2-4 proteins, respectively (Mizuno *et al.*, 2004). *Rcan2-1* was detected in brain, heart and skeletal muscle, but *Rcan2-3* was only detected in brain.

Interestingly, all human and mouse *RCAN2* transcripts can be detected as two mRNA species (3.4 and 1.4 kb), probably generated by alternative polyadenylation

sites, and only the specie of 3.4 kb from the *RCAN2-4* transcript has been seen to be positively regulated by thyroid hormone in human skin fibroblasts (Miyazaki *et al.*, 1996; Cao *et al.*, 2002), mouse brain (Mizuno *et al.*, 2004), mouse heart and mouse skeletal muscle (Yang *et al.*, 2000). This up-regulation by thyroid hormone seems to be promoted via PI3K-AKT/PKB-mTOR signaling (Cao *et al.*, 2005).

RCAN3

Human *RCAN3* gene (formerly DSCR1L2, MCIP3 or Calcipressin 3, HSA 1p35.3-p33) has been described to present a complex transcription with numerous mRNA forms (Strippoli *et al.*, 2000; Canaider *et al.*, 2006; Facchin *et al.*, 2008; Facchin *et al.*, 2011). *RCAN3* transcripts are ubiquitously expressed, with increased expression in human heart, skeletal muscles, liver, kidney, and peripheral blood leukocytes (Strippoli *et al.*, 2000) and in human endothelial cells (Facchin *et al.*, 2011).

Little is known about *RCAN3* regulation of expression. It is known that AGN194204 (Retinoid X receptor (RXR) agonist) triggers the expression of *Rcan3* in murine naïve T lymphocytes (Rasooly *et al.*, 2005).

7.2.- Structure of RCAN proteins and regulation of RCAN function

RCAN proteins bear different conserved motifs that are conserved among all the canonical RCAN Eukarya proteins (Fig. 7.1): a putative RNA-recognition motif (RRM domain), that spans the first common exon and several amino acids located in the variable first exon, the serine-proline rich region (SP region), located in the second common exon, and the PXIXIT and the TXXP motifs, both located in the last exon. The SP region contains three important motifs: the LXXP, the FLISPP and the EXXP. The PXIXIT and LXXP motifs of RCAN are involved in Cn-RCAN interaction (Aubareda *et al.*, 2006; Mehta *et al.*, 2009; Rodriguez *et al.*, 2009).

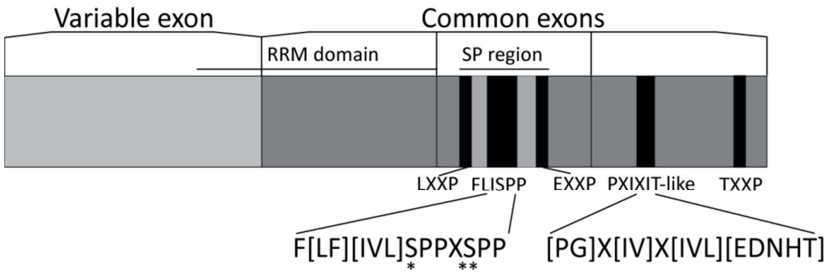

Figure 7.1. Schematic representation of RCAN protein structure. The last three are common to all RCAN isoforms and all different RCAN transcripts are generated by alternative splicing.

GSK3β (*) and MAPK, BMK1 or DYRK1A (**) phosphorylation sites within the FLISPP motif and consensus sequences for all canonical eukaryotic RCAN motifs are indicated.

7.2.a.-The RRM domain

As shown in Figure 7.1, the more terminal domain in RCAN proteins is the RRM-domain (RNA recognition motif). By sequence homology with other RRM it has been determined to spans the first common exon of RCAN proteins, but also includes several amino acids of the RCAN N-terminal variable exon (Strippoli *et al.*, 2000). This type of motifs usually binds RNA or single-stranded DNA (Interpro ID: IPR000504). The 3D structure of the RRM domain of mouse Rcan1-4 was analyzed by nuclear magnetic resonance (NMR) (PDB ID: 1WEY). The RRM motif of RCAN proteins has been hypothesized that could be involved in stabilizing the protein, but their functional relevance has not been described (Genesca *et al.*, 2003; Mehta *et al.*, 2009).

7.2.b.-The SP domain

The LXXP and the ExxP motifs

The LXXP is an RCAN motif conserved in Eukarya that resembles the LXVP Cn binding site in NFATc proteins. As LXVP of NFATc, the overexpression of LXXP motif of yeast Rcn1 and human RCAN1 was reported to inhibit phosphatase activity of Cn over all Cn substrates, and also to be important for Cn stimulation at physiological levels, in yeast (Mehta *et al.*, 2009; Rodriguez *et al.*, 2009).

Concerning the EXXP motif, mutation of all their residues to alanine in yeast Rcn1 demonstrated that it is required for its stimulatory function on Cn activity (Mehta *et al.*, 2009).

It has been postulated that LXXP and EXXP motifs, together with TXXP motif, may be required for GSK3β dependent phosphorylation of yeast Rcn1 within the FLISPP motif (Fig. 7.1) and subsequent ubiquitination and proteasomal degradation of yeast Rcn1 mediated by SCF^{Cdc4} (Kishi *et al.*, 2007). However, Mehta and colleagues did not obtain differences in protein degradation and/or ubiquitination in yeast Rcn1 mutants lacking the three motifs when compared to wt proteins (Mehta *et al.*, 2009).

The FLISSP motif

This motif has been considered until recently as the signature of the family. The two serine residues within the FLISSP motif have been shown to be phosphorylated by several kinases (see Figure 7.1). At least in human RCAN1-4

(NP_981963) and mouse Rcan1-2 (NP_062339), ERK, BMK1 (Big MAP kinase 1), DYRK1A (Dual specificity tyrosine-phosphorylation-Regulated Kinase 1A) and P38 are able to phosphorylate the 112 serine residue, S112, (** in Fig. 7.1) (Vega et al., 2002; Abbasi et al., 2006; Jung et al., 2011; Ma *et al.*, 2012) and it serves as a priming site for further phosphorylation of the 108 serine residue, S108 (* in Fig. 7.1) by GSK3β (Vega et al., 2002; Genesca et al., 2003). Remarkably, GSK3β-mediated phosphorylation of the RCAN1 ortholog in Drosophila, the Sarah (Sra) protein, is essential for completion of meiosis (Takeo *et al.*, 2012).

Mutation of both serine residues at the FLISPP motif of RCAN1-1 and RCAN1-4 isoforms in mammary cells did not affected Cn binding, but reduced the inhibitory capability of RCAN1 towards Cn-NFATc signaling, and also prevented proteasomal-mediated degradation of RCAN1 (Genesca *et al.*, 2003). In addition, it was described that 14-3-3 protein binds to RCAN1 when it is phosphorylated at both S108 and S112 residues and drives it to proteasomal degradation (Abbasi *et al.*, 2006). Conversely, this phosphorylation event resulted to be essential to achieve optimal Cn activity in yeast (Hilioti *et al.*, 2004; Kishi *et al.*, 2007; Mehta *et al.*, 2009) and in vertebrates (Abbasi *et al.*, 2006).

Therefore, the RCAN FLISPP motif can modulate either positively or negatively calcineurin activity, depending in cell context and/or experimental conditions.

7.2.c.-The TXXP motif

The elimination of TXXP abolished the ability of yeast Rcn1 to activate, but not to inhibit, Cn (Mehta *et al.*, 2009). In the same work, the authors demonstrated that the TXXP motif and the GSK3β-dependent phosphorylation of the FLISPP motif on yeast Rcn1 and human RCAN1 would act together in the stimulation but not the inhibition of Cn activity.

7.2.d.-The PXIXIT-like motif

Initially, the PKIIQT motifs of RCAN1 that precedes and overlaps with the TXXP motif (PKIIQTXXP in RCAN1 and RCAN2, and QKIAQTXXP in RCAN3) was thought to be a PXIXIT motif similar to the PXIXIT motif on NFATc proteins (Chan *et al.*, 2005; Rothermel *et al.*, 2000). However, Aubareda *et al*. observed that this sequence does not bind Cn nor inhibits NFAT signaling (Aubareda *et al.*, 2006). In the same work, it was reported that the sequence responsible in RCAN protein for Cn binding and NFATc signaling inhibition was located at the same exon 7 of RCAN1, prior the PKIIQT sequence. This sequence was named as calcineurin-inhibitor CALP1 (renamed as RCAN1) (CIC) motif. The mammal consensus sequence is LGPGEKYELHA[GA]T[DE][ST]TPSVVVHVC[ED]S. One year after, Mulero et al.

(Mulero *et al.*, 2007) described a CIC motif also in RCAN3 and, in 2009, described the minimal 18 amino acid residues (RCAN1$^{198-218}$ and RCAN3$^{183-203}$) important for CIC inhibitory function (Mulero *et al.*, 2009). Importantly, this sequence competes with the NFATc PXIXIT motif for binding to Cn. Remarkably; this interaction does not affect the phosphatase activity of Cn toward other substrates than NFATc. Recently, it has been characterized the PSVVVH sequence among the CIC peptide as the PXIXIT-like motif of RCAN proteins (Mulero et al, 2009; Mehta *et al.*, 2009; Martinez-Martinez *et al.*, 2009) (Figure 7.1).

Mutation of the core hydrophobic residues in yeast Rcan1 PIXIT-like motif (GAITID) reduced the stimulatory action of Rcn1, indicating that this motif can also be involved in the stimulatory function of RCAN over calcineurin activity at physiological levels (Mehta *et al.*, 2009). Recently, our group has demonstrated that RCAN proteins are phosphorylated at the last serine residue of the CIC motif and this modification increases the affinity of this peptide for Cn and the inhibition of Cn-NFAT signaling in Jurkat cells (Martinez-Høyer et al, personal communication).

By using the CIC peptide of RCAN1, our group developed a low throughput screening assay to identify molecules that mimic the RCAN capability to displace NFATc from the Cn-NFATc interaction (Mulero *et al.*, 2009; Mulero *et al.*, 2010). One of the molecules identified was dipyridamole, which efficiently inhibited the nuclear import of NFATc, the activation of NFATc-dependent luciferase reporter gene and partially inhibited NFATc-dependent cytokine gene expression in Jurkat T cell lines (Mulero *et al.*, 2009). It was also demonstrated to present immunosuppressive properties *in vivo* (Weyrich *et al.*, 2005).

Additional phosphorylation of RCAN1 by PKA has been recently described, but the precise phosphoacceptor residue has not yet been determined (Kim *et al.*, 2012). This post-translational modification seems to increase the half-life of RCAN1 and enhances its inhibitory function towards Cn.

In summary, the TXXP and the EXXP motifs are involved in Cn stimulation, while the LXXP, the PXIXIT and the FLISPP motifs seem to participate in both stimulatory and inhibitory function of RCAN.

The knowledge of the function of the different motifs of RCAN proteins and the consequences of their post-translational modification would help us to understand the dual role of RCAN proteins towards Cn signaling in different cell types and processes. Furthermore, molecules that mimic the interaction of RCAN proteins with Cn and disrupt Cn-NFATc interaction could help us to understand the *in vivo* effects of RCAN in Cn-NFATc signaling. Also, these mimetic molecules

could be of invaluable use in the development of new immunosuppressive compounds that specifically inhibit Cn-NFATc, to be used with therapeutic purposes as an alternative to the current drugs, CsA and FK506, to avoid their severe side effects.

7.3.- Regulation of RCAN signaling by interacting proteins and RCAN involvement in signaling pathways other than Cn-NFATc

In addition to the well characterized interaction of RCAN with Cn through the PXIXIT and LXXP motifs (Aubareda *et al.*, 2006; Mehta *et al.*, 2009; Rodriguez *et al.*, 2009), several proteins have been identified as RCAN interacting proteins.

Integrin αVβ3 was coimmunoprecipitated with human RCAN1 protein in Human Umbilical Vein Endothelial Cells (HUVEC) (Iizuka *et al.*, 2004). This study relates RCAN1 proteins with angiogenesis by means of regulating cell migration and cell adhesion by connecting directly VEGF responses to integrin αvβ3 in a Cn independent-manner.

RCAN1-4 isoform was reported to interact with Toll-interacting protein (Tollip) (Lee *et al.*, 2009). In resting conditions Tollip forms a complex with IRAK-1 (IL-1β receptor (IL-1R)-associated kinase 1) protein kinase and inhibits its activity. IRAK-1 is associated with the intracitoplasmatic tail complex of the Toll-like receptors 2 and 4 (TLR2 and TLR4). When interleukin 1 (IL1), bind to TLRs, IRAK-1 associates to these receptors and activate several downstream signaling cascades. One of these proteins activated is TRAF6 (TNF receptor-associated Factor 6). In resting conditions also Tollip is recruiting TRAF6, but under IL-1 stimulus, TRAF6 is released and recruits a complex called TRIKA2, formed by TGF-β-activated kinase 1 (TAK1) and TAK-1 binding protein 1 and 2 (TAB1 and TAB2). This association of TRAF6 to the TRIKA2 complex activates TAK1 and upregulates downstream pro-inflammatory genes, as IL-8. Presence of RCAN1-4 recruits Tollip from complexes with IRAK-1 and TRAF-6, thus, acting as facilitator for IL-1R-dependent signaling via IRAK-1/TRAF6 complex formation.

RCAN1 protein was also found to directly interact with TAK-1 binding protein 2 (TAB2) (component of the TRIKA2 complex) by yeast two-hybrid assays (Liu *et al.*, 2009). *In vitro* and *in vivo* assays demonstrated that this interaction recruits the TRIKA2 complex to Cn to form a macromolecular complex that enhances Cn-NFATc signaling by direct phosphorylation of RCAN1 by TAK1. Moreover, this phosphorylation can be autoregulated by a Cn-dependent dephosphorylation and inactivation of TAK1 and TAB1. It is known that the components of the TRIKA2 complex can function as a signaling orchestrator for several pathways as the

MKK(3/6)-p38, the MKK4-SAP/JNK and NF-κB (Ninomiya-Tsuji *et al.*, 1999, Wang *et al.*, 2001) signaling pathways.

By yeast two-hybrid assay, the NF-κB-inducing kinase (NIK) (Lee *et al.*, 2008) was described to interact with the C-terminal (90-197 aa) region of the human RCAN1-4 protein. This interaction occurs only in wild type NIK but not in kinase dead mutants. The NIK-dependent phosphorylation of RCAN1 increments RCAN1 stability by altering RCAN1 solubility and by blocking its targeting to degradation by the proteasome. Also, it has been related with Alzheimer disease and Down's Syndrome, because NIK-mediated phosphorylation of RCAN1 leads to Tau-like aggregates formation in neuronal cells, fact that could explain Alzheimer disease- and Down's Syndrome-associated neurological anomalies.

β-transducin repeat containing E3 ubiquitin protein ligase 1 (ß-TrCP1) and 2 (ß-TrCP2) ($SCF^{ß\text{-}TrCP1/2}$), two members of the F-box protein family, (a component of the SCF E3 ubiquitin ligase complex) were coimmunoprecipitated with human RCAN1-1 and, in response to H_2O_2, RCAN1-1 is poly-ubiquitinated and degraded. Moreover, SCF^{FBW4} was coimmunoprecipitated with human RCAN1-1 and also caused its poly-ubiquitination, but in a H_2O_2 independent manner (Asada *et al.*, 2008). In this context, Rcn1, the human RCAN1 homolog in yeast, has been shown to be triggered to proteasomal degradation by SCF^{CDC4} E3 ubiquitin ligase complex (Kishi *et al.*, 2007). In addition, it has been reported that CREB and STAT2 activate proteasomal degradation of human RCAN1 protein, probably through the activation of different E3 ubiquitin ligase (Seo and Chung, 2008). More recently, it has been described that also SCF^{FBW7}, enhanced by STAT2, mediates the proteasomal degradation of RCAN1 (Lee *et al.*, 2012). Thus, different SCF protein ligases, modulated by different pathways, as CREB or STAT2, modulate the proper level of RCAN1 via proteasome, depending on cell context and in response to different stimulus.

BMK1, a downstream effector of MEKK3 (also known as ASK1), is able to phosphorylate RCAN1 protein (Abbasi *et al.*, 2005). This phosphorylation is induced by angiotensin II on the BMK1, MEK5 and MEKK3 protein complex. Once phosphorylated, RCAN1 dissociates from Cn and associates to 14-3-3 protein, diminishing RCAN1 inhibitory effect on Cn activity and releasing NFATc from its binding to 14-3-3, which can then interact with Cn and become activated (Abbasi *et al.*, 2006). These results explain the activating effect of angiotensin II-mediated activation of Cn-NFATc pathway via RCAN1 phosphorylation.

Fragile X mental retardation protein (FMRP) is involved in mental retardation in Fragile X syndrome patients. Phosphorylated FMRP co-immunoprecipitates with

RCAN1 and this interaction is necessary for protein synthesis in dendritic spines (Wang *et al.*, 2012). Authors postulate that altered amount or dysfunction of RCAN1 protein may have consequences in long-term memory and may be involved in Fragile X syndrome-associated mental anomalies.

It has been described that RCAN3 interact with human cardiac troponin I (TNNI3) (Canaider *et al.*, 2006; Facchin *et al.*, 2008; Facchin *et al.*, 2011). This interaction was firstly described by yeast two-hybrid assay and further confirmed by GST-pull down assay. RCAN3 interact with TNNI3 through its non-common exon (exon 2) and, for that reason, it would be specific for RCAN3. TNNI3 protein is involved in cardiac contraction in the absence of calcium and troponin C (Cummins and Perry, 1978) and has been associated with hypertrophic cardiomyopathy (Kostareva *et al.*, 2009; Garcia-Pavia *et al.*, 2011; van den Wijngaard *et al.*, 2011). This interaction suggests a novel Cn-independent role of RCAN3 protein in cardiac hypertrophy and function.

Finally, GST-pull down and coimmunoprecipitation assays demonstrated that the v-raf (rapidly accelerated fibrosarcoma)-1 murine leukemia viral oncogene homolog 1 (CRAF or Raf-1) interacts with human RCAN1-4 (Cho *et al.*, 2005). CRAF is a member of the serine/threonine RAF protein kinase family together with ARAF and BRAF. RAF proteins participate in the RAS-RAF-MEK-ERK signaling cascade, involved in proliferation, migration and apoptosis, among others processes. In T lymphocytes ERK activation is essential in positive selection of thymocytes (section 4.2). RAF activation is regulated by the interaction with the GTPase RAS and by several phosphorylation and dephosphorylation events, and also requires the formation of homo- or heterodimers, but the three members are differentially regulated (Matallanas *et al.*, 2011; Roskoski, 2010). BRAF presents the higher basal kinase activity, followed by CRAF, and requires less phosphorylated sites to achieve its fully activation. The interaction of RCAN1-4 with CRAF described by Cho *et al*. takes place through two regions: a primary binding site in the N-terminus of RCAN1-4 (residues 1–6) and a potential binding motif in the central region of RCAN1-4 (residues 85–121) that is common to all RCAN proteins (Cho *et al.*, 2005). However, no functional effect of this interaction has been described.

7.4.- Functions of RCAN proteins

As mentioned above, RCAN proteins present a dual role either facilitating or suppressing Cn activity. Moreover, RCAN proteins are involved in other signaling pathways different to Cn-NFATc. Table 7.1 and section 7.5 summarizes the most important phenotypes associated with RCAN overexpression or ablation in several biological processes, inferred from different reported *in vitro* and *in vivo* studies.

Moreover, the role of RCAN proteins in Cn-NFATc-dependent pathways involved in neural system has been extensively studied, due to their importance in Down's Syndrome patients and in Alzheimer disease (reviewed in Keating *et al.*, 2006; de la Luna and Estivill, 2006; Park *et al.*, 2009; Ermak *et al.*, 2011).

Table 7.1.- FUNCTIONS OF RCAN PROTEINS

Biological process	References	model	RCAN physiological role	RCAN function over Cn activity
Cardiac and skeletal muscle formation and cardiac hypertrophy	Rothermel *et al.*, 2001	TghRCAN1 mice	Inhibition of cardiac hypertrophy in β-adrenergic and in CnA c.a.	Reduced activity of NFATc-dependent *IL2* promoter
	Vega *et al.*, 2003	Rcan1$^{-/-}$ mice	Increment of cardiac hypertrophic phenotype of a CnA c.a. Protection from cardiac hypertrophy under TAC and adrenergic stimulation	Depending on the stimulus
	Hill *et al.*, 2002	TghRCAN1 mice	Inhibition of cardiac hypertrophy under pressure overload by TAB	N/D
	Sanna *et al.*,2006	Rcan1$^{-/-}$, Rcan2$^{-/-}$ and Rcan1/Rcan2$^{-/-}$ mice	Protection from cardiac hypertrophy under pressure overload. Increment of slow oxidative fiber-type program in muscle.	Enhancement of Cn activity in MEFs under thapsigargin stimulation.
Food intake and diabetic processes	Jang *et al.*,2011	db/db and STZ-induced diabetic mice models	Increased expression of *Rcan1-4* gene	N/D
		Mes-13 cells stably transfected with mouse Rcan1-4	Induction of ACE, collagens type I, type III, type IV, and MMP-9 and reduction of AGT	N/D, but the phenotype was not altered by CsA administration
	Sun *et al.*, 2011b	Rcan2$^{-/-}$ mice	Reduced body weight. Amelioration of high-fat diet-induced obesity. Reduced food intake.	Not detected changes in Cn activity in hypothalamus
	Peiris *et al.*, 2012	TghRCAN1-1 mice	Several synthoms associated with β-cell dysfunction observed in diabetes (age-associated hyperglycemia, reduced glucose tolerance, hypoinsulinemia, loss of β-cells, reduced β-cell insulin secretion, aberrant mitochondrial ROS production)	N/D

Table 7.1 Functions of RCAN proteins. Abbreviations used: AAA, abdominal aortic aneurysm; ACE, angiotensin converting enzyme; AD, Alzheimer disease; AGT, angiotensinogen; c.a., constitutively active; db, diabetic; DS, Down's Syndrome; EC, endothelial cells; HD, Huntington disease; LTP, long-term potentiation; L-LTP; late-phase long-term potentiation; MEFs, Mouse Embryonic Fibroblasts; MMP-9, matrix metalloprotease 9; N/D, non-determined; PPF, paired-pulse facilitation; STZ, Streptozotocin; TAB, transverse aortic banding; TAC, transverse aortic constriction; VSMC, Vascular Smooth Muscle Cell.

Table 7.1.- FUNCTIONS OF RCAN PROTEINS				
Biological process	**References**	**model**	**RCAN physiological role**	**RCAN function over Cn activity**
Neuronal system	Sanna *et al.*,2006	Rcan1$^{-/-}$, Rcan2$^{-/-}$ and Rcan1/Rcan2-/- mice	Impairment of working memory acquisition	N/D in brain, but the phenotype is not reverted in Rcan1$^{-/-}$/Rcan2$^{-/-}$/CnA$^{+/-}$ mice
	Ermak *et al.*,2001	Post-mortem human brain samples of AD patients	Increased levels of RCAN1-1 protein, concretely in the cerebral cortex and the hippocampus, the most affected regions in these patients	N/D
	Ermak *et al.*,2002	HA-1 cells stably transfected with entire *hRCAN1* gene	Protection against oxidative (H_2O_2) and calcium stress.	N/D
		PC-12 cells stably transfected with doxycycline (Dox)-regulable *hRCAN1-1* in presence or absence of siRCAN1-1	Increased cell number in absence of Dox treatment, and reduced cell number in presence of Dox and siRCAN1, in basal conditions and under oxidative and calcium stress.	N/D
	Lin *et al.*,2011	Blood samples of AD patients	Several polimorfisms of *RCAN1* gene associated to AD	N/D
	Fuentes *et al.*,2000	Fetal brain samples of DS patients	Increased levels of RCAN1-1 protein	N/D
	Hoeffer *et al.*,2007	Rcan1$^{-/-}$ mice	Impaired spatial learning and memory. Impaired L-LTP and PPF	Increased Cn activity and protection of Cn from calpain cleavage in nuclei and mitochondria
	Porta *et al.*,2007b	Primary neurons from Rcan1$^{-/-}$ mice	Decreased cell death under H_2O_2 stimulation	N/D
		Primary neurons from Rcan1$^{-/-}$ and WT mice transduced with Rcan1-4	Increased cell death under H_2O_2 stimulation	N/D
	Dierssen *et al.*, 2011	TghRCAN1-4 mice	Deficiencies in working (short-term) memory (under visual-spatial learning task). Defects in hippocampus	N/D
	Keating *et al.*,2008	TghRCAN1-1 mice	Reduction of chromaffin cell exocytosis. Accelerated fusion pore kinetics. The initial fusion pore is more short-lived.	N/D
		Rcan1$^{-/-}$ mice	Reduction of chromaffin cell exocytosis. Slowed fusion pore kinetics. The initial fusion pore is longer lasting.	N/D
	Sun *et al.*, 2011a	Fetal brain samples of DS patients and post-mortem brain samples of AD patients	Elevated *RCAN1-1* gene expression	N/D
		Primary murine neurons transduced with RCAN1-1	Increase of neuronal apoptosis by activation of caspase-9 and -3	N/D
	Martin *et al.*,2012	TghRCAN1 (entire gen)	Decreased adult neurogenesis and differentiation. Causes LTP defects.	Not detected changes in Cn activity in brain
	Ermak *et al.*,2009	Post-mortem brain samples of HD patients	Reduced levels of RCAN1-1 protein	N/D
		Differentiated and non-differentiated neural progenitor cell line (ST14A) with normal huntingtin (Q15) or mutant huntingtin (Q120) transduced with hRCAN1-1	Rescue of toxicity of mutant huntingtin	Reduced Cn activity, mostly in differentiated cells

Table 7.1 Function of RCAN proteins. Abbreviations used: AAA, abdominal aortic aneurysm; ACE, angiotensin converting enzyme; AD, Alzheimer disease; AGT, angiotensinogen; c.a., constitutively active; db, diabetic; DS, Down's Syndrome; EC, endothelial cells; HD, Huntington disease; LTP, long-term potentiation; L-LTP; late-phase long-term potentiation; MEFs, Mouse Embryonic Fibroblasts; MMP-9, matrix metalloprotease 9; N/D, non-determined; PPF, paired-pulse facilitation; STZ, Streptozotocin; TAB, transverse aortic banding; TAC, transverse aortic constriction; VSMC, Vascular Smooth Muscle Cell.

Table 7.1.- FUNCTIONS OF RCAN PROTEINS				
Biological process	**References**	**model**	**RCAN physiological role**	**RCAN function over Cn activity**
Angiogenesis, tumor growth and metastasis	Qin *et al.*,2006	HUVEC and PT67 transduced with hRCAN1-1	Increased basal and VEGF-induced proliferation of HUVEC cells. Induction of DSCR1-4 expression in HUVEC cells. Stimulation of basal and VEGF-induced angiogenesis (PT67 cells injected *in vivo*)	Increased basal and VEGF-induced NFATc activation.
		HUVEC and PT67 transduced with hRCAN1-4	Decreased VEGF-induced proliferation without affecting basal proliferation of HUVEC cells. Inhibition of VEGF-induced angiogenesis (PT67 cells injected *in vivo*) without affecting basal angiogenesis	Decreased basal and VEGF-induced NFAT activation in HUVEC cells.
		HUVEC and PT67-transduced with si-hRCAN1-1	Decreased VEGF-induced proliferation without affecting basal proliferation of HUVEC cells. Decreased angiogenesis *in vivo* (injected PT67 cells)	Decreased VEGF-induced NFAT activation without affecting basal NFATc activation in HUVEC cells.
		HUVEC and PT67-transduced with si-hRCAN1-4	Increased basal and VEGF-induced proliferation of HUVEC cells. Angiogenesis (T67 cells injected *in vivo*) was not affected	Increased basal and VEGF-induced NFAT activation in HUVEC cells.
	Minami *et al.*,2004	HUVEC transduced with hRCAN1	Attenuation of VEGF- and trombin-induced cell proliferation and tube formation	N/D
		Injection of adenovirus encoding hRCAN1 in mice with implanted tumor	Reduction of neo-vascularization and tumor-progression	N/D
	Iizuka *et al.*,2004	knock down of *Rcan1* in HUVEC	Reduced migration and cell spreading	N/D
		knock down of *Rcan1* in mice	Inhibition of angiogenesis in vivo	N/D
	Ryeom *et al.*,2008	Rcan1$^{-/-}$ mice	Decreased tumor growth and angiogenesis due to increased apoptosis of epithelial cells	Hyperactivated NFATc1 translocation and NFATc dependent genes (Cox-2)
	Baek *et al.*,2009	Ts65Dn DS mouse model	Decreased tumor growth and angiogenesis due to reduced proliferation of epithelial cells	Decreased NFATc1 translocation and NFATc dependent genes (Cox-2)
	Esteban *et al.*,2011	Rcan1-/- mice	Reduced Angiotensin II-induced VSMC migration, neointima formation and AAA	Not detected changes in Cn activity in VSMCs or aortic tissues
	Stathatos *et al.*, 2005	GPR54-expressing NPA cells (thyroid cancer cell line) stimulated with metastin	Induction of *Rcan1-4* gene expression	Reduction of Cn activity
		Human thyroid papillary cancers samples	Presence of RCAN1-4 in primary tumors, but absence of RCAN1-4 in metastatic samples and in primary tumor regions similar to the metastasis	N/D
	Gollogly *et al.*, 2007	HUVEC transduced with RCAN1	Reduced VEGF-induced proliferation, migration and endothelial cell tube formation	N/D
		HUVEC transduced with RCAN2α	Reduced VEGF-induced proliferation, migration and endothelial cell tube formation	N/D

Table 7.1 Function of RCAN proteins. Abbreviations used: AAA, abdominal aortic aneurysm; ACE, angiotensin converting enzyme; AD, Alzheimer disease; AGT, angiotensinogen; c.a., constitutively active; db, diabetic; DS, Down's Syndrome; EC, endothelial cells; HD, Huntington disease; LTP, long-term potentiation; L-LTP; late-phase long-term potentiation; MEFs, Mouse Embryonic Fibroblasts; MMP-9, matrix metalloprotease 9; N/D, non-determined; PPF, paired-pulse facilitation; STZ, Streptozotocin; TAB, transverse aortic banding; TAC, transverse aortic constriction; VSMC, Vascular Smooth Muscle Cell.

7.5.- RCAN proteins in immune system

Regarding the function of RCAN proteins in the immune system, RCAN proteins have demonstrated their immunosuppressive effect in stimulated Jurkat T cells, inhibiting, when overexpressed, NFATc translocation to the nucleus, NFATc activation and NFATc-dependent cytokines gene expression such as *IL2*, *IL3*, *IL13*, *GM-SCF*, *IFN-γ* and *TNF-α* (Aubareda *et al.*, 2006; Mulero *et al.*, 2007, Mulero *et al.*, 2009).

Also, overexpression of human RCAN1-4 was shown to inhibit gene expression of several genes associated with cell adhesion or inflammation, such as *Cox-2* (*Cyclooxygenase 2*), *E-selectin*, and *TF* (tissue factor) in VEGF-stimulated endothelial cells (Hesser *et al.*, 2004) and *Cox-2, TNF-α* and *IL-1β* in PMA-stimulated U87MG glioblastoma cell line by stabilizing IκBα protein, in a Cn-independent manner (Kim *et al.*, 2006).

The *in vivo* role of Rcan proteins in adaptive immunity has been further demonstrated in several studies by using *Rcan* deficient mice. *In vivo* experiments with deficient mice in *Rcan1* gene for both *Rcan1-1* and *Rcan1-2* transcripts revealed that an early expression of FasL that leads to a defect in naïve $CD4^+$ proliferation and in Th1 response, due to premature cell death upon stimulation, suggesting an inhibitory role of Rcan1 protein in Cn-NFATc signaling (Ryeom *et al.*, 2003). Conversely, experiments with triple knockout mice for *Rcan1*, *Rcan2* and *CnA*β ascribed a facilitating role for Rcan in Cn-NFATc signaling, because Cn absence did not rescue the *Rcan1*$^{-/-}$ and *Rcan2*$^{-/-}$ phenotype (Sanna *et al.*, 2006).

Rcan1 has also been described to be involved in mast cell function. Mast cells are specialized immune cells that play an essential role in inflammation and protection against pathogens (reviewed in Abraham and St John, 2010). They are activated by IgG or IgE binding to the high affinity IgE receptor (FcεRI) on their surface, and they return to their basal resting condition by several negative signals (Molfetta *et al.*, 2007). In this context, *Rcan1*$^{-/-}$ mice has been described to present increased IgE-dependent activation of NFATc and NF-κB pathways, but no changes in the activation of P38, JNK, AKT or Syk were detected (Yang *et al.*, 2009b). Moreover, Rcan1 deficiency promoted a prolonged expression of *IL6*, *IL13* and *TNF*, consistent to an incremented protein production of these cytokines. Moreover, this effect was reverted when *Rcan1* was overexpressed. Finally, *Rcan1*$^{-/-}$ mice presented increased mast cell activation, degranulation and late-phase passive cutaneous anaphylaxis *in vivo*. All this data suggests that Rcan1 would be a negative regulator of FcεRI-triggered signals.

The analysis of *Rcan1*$^{-/-}$ mice also suggested a role of *Rcan1* in macrophage and the innate immune response. LPS-treated *Rcan1*$^{-/-}$ mice presented increased expression of the pro-inflammatory cytokines as IL6 and inflammation markers, as *E-selectin*, vascular cell adhesion molecule 1 (VCAM-1) and endothelial cell adhesion molecule 1 (ECAM-1) (Minami *et al.*, 2009). Also, these mice presented increased mortality, while overexpression of *Rcan1-4* protected against LPS-induced death. Moreover, *Rcan1*$^{-/-}$ mice infected with *Fransicella tularensis* presented enhanced production of the pro-inflammatory cytokines MCP-1 (monocyte chemotactic protein-1), IL6, IFN-γ and TNF-α in the lung and spleen 7 days after infection (Bhoiwala *et al.*, 2011). These results suggest an important role of Rcan1 in the modulation of inflammation and innate immune responses.

Finally, the interaction of RCAN proteins with different proteins involved in TCR signaling cascade (see section 7.3 and Figure 7.3) suggest the involvement of RCAN proteins in different points of TCR activation.

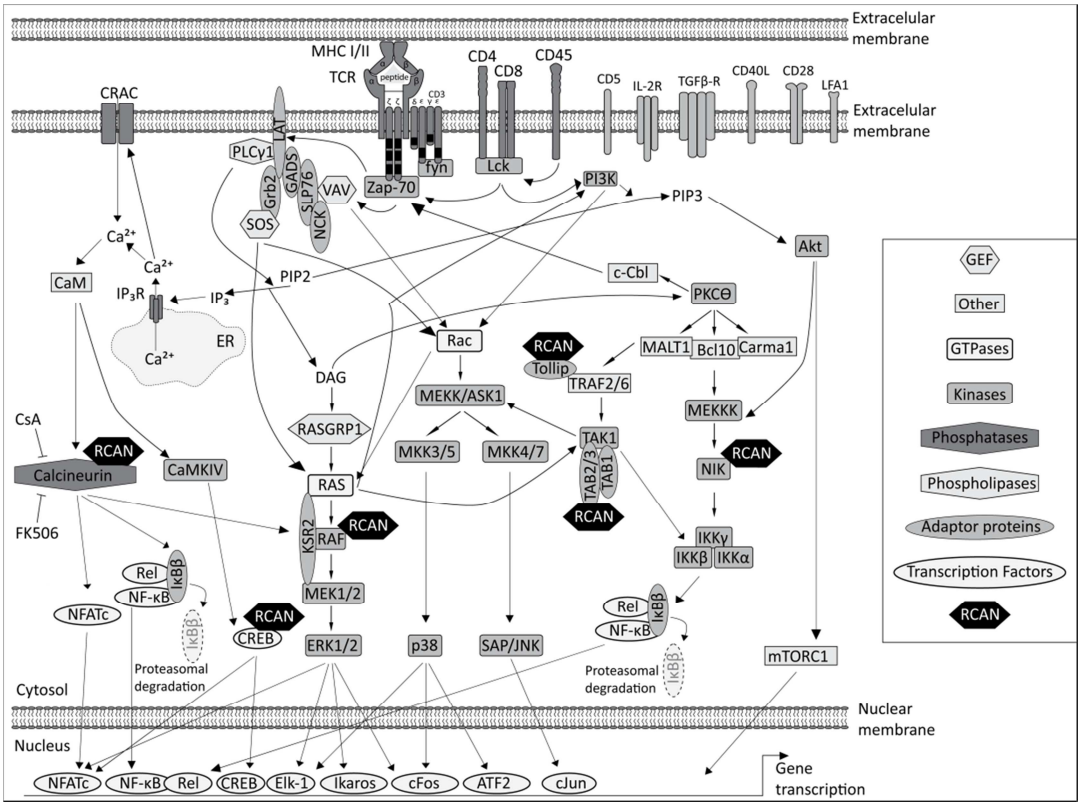

Figure 7.3. Different proteins involved in TCR signaling interact with RCAN proteins.

Taking together, all these data suggest that RCAN proteins can modulate diverse TCR-dependent events, including the modulation of the Cn-NFATc signaling pathway, and point out the functional relevance of RCAN proteins in adaptive immune system. Moreover, RCAN proteins are involved in the modulation of inflammation and innate immune responses. Further experiments must be performed to better understand the exact role of RCAN proteins in this complex signaling pathway that constitute the essence of the immune response.

OBJECTIVES

The main objectives of this thesis work are:

1. To analyze the genomic evolution of *RCAN* genes in vertebrates

2. To deepen in the structure of the human *RCAN* genes and the *RCAN* gene expression regulation

3. To characterize the functional role of RCAN proteins overexpression in thymocyte development and T cell function *in vivo*.

RESULTS

1. RCAN GENES: EVOLUTION, STRUCTURE AND REGULATION.

Eva Serrano-Candelas, Domènec Farré, Álvaro Aranguren-Ibáñez, Mercè Pérez-Riba

My contribution to this article has been: Searching and manual annotation of *RCAN* paralogous genes, phylogenetic analysis of *CLIC* genes, the analysis of the structure of *RCAN* genes, multispecies alignments of NATs, searching for retrotransposons elements inside the *RCANs* and contributed, together with Dr. Farré, to the evolution analysis shown in Figure 1, multispecies alignment and TFBS prediction in *RCAN3* promoter. I have also participated in the general design and conception of the experiments, figures preparation and manuscript writing.

A. Aranguren have prepared *RCAN3* promoter constructs and performed NFATc-reporter luciferase assays. Dr. Farré performed phylogenetic trees in Figure 5, contributed to the evolution analysis, multispecies alignments and TFBS prediction and to discussion and writing of the manuscript. Dr. M. Pérez contributed to the general design and conception of the experiments and manuscript writing.

RCAN genes: evolution, structure and regulation.

Eva Serrano-Candelas[1], Domènec Farré[2], Álvaro Aranguren-Ibáñez[1], Mercè Pérez-Riba[1]

[1]Human Molecular Genetics Department, Bellvitge Biomedical Research Institute – IDIBELL. L'Hospitalet de Llobregat, Barcelona 08908, Spain
[2]Institut d'Investigacions Biomèdiques August Pi i Sunyer - IDIBAPS, Barcelona 08036, Spain

To whom correspondence should be addressed: Mercè Pérez-Riba, Human Molecular Genetics Group, Bellvitge Biomedical Research Institute – IDIBELL. L'Hospitalet de Llobregat, Barcelona 08908, Spain. Tel: +34 932607427. FAX: +34 932607414. mpr@idibell.cat.

ABSTRACT

The Regulators of Calcineurin (RCAN) proteins are endogenous regulators of the calcineurin-NFATc signaling pathway. This family of proteins has been described to be involved in several biological processes such as cardiac hypertrophic responses, muscle fibers remodeling after exercise, acquisition of working (short-term) memory, neuronal degeneration, T cell activation and immune response, among others. It has been described that in most vertebrates they form a functional subfamily of three members RCAN1, RCAN2 and RCAN3 whereas only one RCAN is present in most of the rest of Eukarya. Here, we have characterized several vertebrate organims that have lost or gain some *RCAN* gene. Vertebrates *RCAN*s genes co-localize with *RUNX* and *CLIC* genes in the ACD clusters (ACD21, ACD6 and ACD1), which generation and evolution is still unknown. Here, we propose that vertebrate genes within the ACD clusters have evolved from single copy genes present in invertebrates and lower eukaryotes through two rounds of whole genome duplication, followed by a segmental duplication, differently than previously thought. We also deepen in the *RCAN* gene structure and we describe the existence of antisense transcripts associated with the three human *RCAN* genes supporting that, at least *RCAN2* and *RCAN3* promoters could act as bidirectional promoters. In addition, all three *RCAN* promoter regions include CpG islands. Regarding the human *RCAN3* gene, we performed a phylogenetic analysis of *RCAN3* exons and analyzed the transcriptional activity of the CpG island associated with the *RCAN3* promoter, demonstrating that this CpG island is transcriptionally active and could constitute the promoter region that drives the expression of *RCAN3* gene. The knowledge of *RCAN* gene evolution, structure and gene expression regulation provides novel insights in the RCAN gene family members that could be relevant to deal with future therapeutic approaches.

INTRODUCTION

The Regulator of Calcineurin (RCAN, formerly known as DSCR and calcipressin, among others) proteins are endogenous modulators of the Ca^{2+} and calmodulin-dependent serine-threonine phosphatase calcineurin (Cn; also known as PPP3, formerly PP2B). This enzyme has many important physiological substrates including the transcription factors cytosolic Nuclear Factors of Activated T cells (NFATc). The Cn-NFATc signaling pathway is a key element on several biological processes such as lymphocyte activation, angiogenesis, morphogenesis of the heart valves, and neural and muscle development (reviewed in Aramburu *et al.*, 2004). It is noteworthy that NFATc proteins are restricted to vertebrates (reviewed in Wu *et al.*, 2007b).

RCAN proteins bind to Cn in a similar manner than NFATc transcription factors do. The most important anchoring site of NFATc and RCAN proteins to Cn is the PXIXIT motif (Garcia-Cozar *et al.*, 1998; Aramburu *et al.*, 1998; Mehta *et al.*, 2009) which, in NFATc proteins is responsible for NFATc activation and induction of NFATc-mediated gene expression and signaling (Aubareda *et al.*, 2006; Martinez-Martinez *et al.*, 2009 Mulero *et al.*, 2009). Both RCAN and NFATc proteins also contain an additional LXXP Cn-binding motif, that at least in yeast *Rcan1*, has been reported to be functional (Rodriguez *et al.*, 2009). Recently, it has been described a dual facilitative or inhibitory role of the members of the RCAN family towards Cn-NFATc signaling in mammals based on the amount of protein, the affinity of the different binding motifs to Cn and the participation of other additional RCAN motifs (Vega *et al.*, 2003; Shin *et al.*, 2006; Mehta *et al.*, 2009) .

There are three members of the RCAN protein family in most of vertebrates: RCAN1, RCAN2 and RCAN3, each of them coding for several transcripts and protein isoforms (reviewed in Davies *et al.*, 2007); whereas only one member can be found in most of invertebrates, fungi and protozoa (Mulero *et al.*, 2007). In vertebrates, the RCAN proteins share a highly amino acid sequence identity at the central and C-terminal regions but a different amino-terminal region. The FLISPP motif, highly conserved in all the Eukarya, has been considered the signature of this family. Recently, it has been described additional motifs present in all eukaryotic organims that could be involved in Cn signaling, the EXXP and the TXXP. It is important to note that all these motifs, and also the PXIXIT and the LXXP motif, are restrained to the last two coding exons of RCAN (Mehta *et al.*, 2009). Due to their high amino acid identity of the three RCAN proteins and the conserved regulatory function towards Cn-NFATc signaling, these proteins in vertebrates constitute a functional subfamily among the eukaryotic RCAN family (Mulero *et al.*, 2007).

Vertebrate *RCAN* genes have been described to map within ACD clusters (for *AML* (renamed as *RUNX*), *CLIC* and *DSCR* (renamed as *RCAN*) genes) (Strippoli *et al.*, 2002). Concretely, human *RCAN1* is located in chromosome 21 (ACD21 cluster), human *RCAN2* in chromosome 6 (ACD6 cluster) and human *RCAN3* in chromosome 1 (ACD1 cluster). It has been postulated that they have evolved from successive gene duplications during the two rounds of whole genome duplication (1R-WGD and 2R-WGD) (Strippoli *et al.*, 2002) that has been claimed as the origin of vertebrates, the 2R hypothesis (proposed by Ohno, 1970 and reviewed in Hokamp *et al.*, 2003). This hypothesis implies the existence of four vertebrate orthologs for each gene in invertebrates, known as the "one-to-four rule" (Meyer and Schartl, 1999; Ohno, 1999). Since not all genes fit within this rule, this 2R hypothesis theory still remains controversial (McLysaght *et al.*, 2002; Hokamp *et al.*, 2003). It is considered that the original invertebrate genome suffered one first round of whole genome duplication that gave rise to the emergence of two groups of vertebrates, agnathans (jawless vertebrates) and gnathostomes (jawed vertebrates), that split approximately 652 million years ago (Mya), after the 1R-WGD (Blair and Hedges, 2005). Gnathostomes, but not agnathans, underwent a second round of whole genome duplication. Several time estimations for both WGD and the split of agnatha-gnasthostomata have been proposed (Vienne *et al.*, 2003, Hedges, 2009; Blair and Hedges, 2005 Skrabanek and Wolfe, 1998), depending on the genes analyzed and the phylogenetic analysis used for the study.

Concerning *RCAN* gene expression, little is known about how they are regulated. It has been described that *RCAN1-1* transcription is mainly regulated by glucocorticoids, *RCAN1-4* is activated by the calcium dependent NFATc and C/EBPβ transcription factors, osmotic stress and steroid hormones, among others, whereas *RCAN2-4* is triggered by thyroid hormone (Gurgen *et al.*, 2011 and reviewed in Davies *et al.*, 2007). Regarding *RCAN3* gene, there are no functional studies about its gene expression regulation. Recently, it has been described that *RCAN3* gives rise to 21 different putative transcripts based on RT-PCR analysis. In addition, this gene bears a putative bidirectional promoter that could control the expression of three different *RCAN3* natural antisense transcripts (NATs), named *RCAN3AS*, that are formed by combinations of three different exons, the first and the third common to all of them (Facchin *et al.*, 2011). However, neither protein detection nor functional effect has been reported up to now for these NATs.

Here, we describe for the first time the evolution of the three *RCAN* genes present in almost all jawed vertebrates and, in particular, it is described the structure conservation of human *RCAN* genes. Moreover, we suggest the existence of several associated NATs in all *RCAN* gens and the presence of conserved

retrotransposon sequences in these regions. In addition, all three *RCAN* genes promoter regions include CpG islands, being at least the *RCAN3*-associated CpG island functional.

MATERIAL AND METHODS

Genomic sequences retrieval

Ensembl database (http://www.ensembl.org and http://metazoa.ensembl.org; Birney *et al.*, 2004; Spudich *et al.*, 2007; release 68), Biomart tool implemented in Ensembl (www.biomart.org; Smedley *et al.*, 2009), UCSC database (http://genome.ucsc.edu/; Dreszer *et al.*, 2012), NCBI Reference Sequence (RefSeq) database (http://www.ncbi.nlm.nih.gov/RefSeq/; Pruitt *et al.*, 2007; Wheeler *et al.*, 2008; Boratyn *et al.*, 2012), and BLAST (http://blast.ncbi.nlm.nih.gov/; Altschul *et al.*, 1990; Johnson *et al.*, 2008) were used for sequence searching and retrieval of the different genomic and protein sequences.

Sequence alignments and analysis

Alignments in Figure S3 and Figure S5 were performed using MAFFT v.6 online version (http://mafft.cbrc.jp/alignment/software/; Katoh *et al.*, 2009) with the following parameters: FFT-NS-I method, scoring matrix BLOSUM62, Gap opening penalty=3, and offset value=1. These alignments were subsequently edited using GeneDoc software (http://www.nrbsc.org/gfx/genedoc/; Nicholas, 1997). Alignments and pip-type graphs of antisense transcripts (Figure S4) were achieved using multi-zPicture (http://zpicture.dcode.org/multiz.php; Ovcharenko *et al.*, 2004) applying an ECR criteria of ≥ 10pb; ≥ 50% ID. Transposable element sequences were identified using Censor tool implemented in Repbase database (http://www.girinst.org/censor/index.php; Jurka *et al.*, 2005). Transcription factor binding sites were predicted using PROMO software v.3 (http://alggen.lsi.upc.es/cgi-bin/promo_v3/promo/promoinit.cgi?dirDB=TF_8.3; Messeguer *et al.*, 2002; Farre *et al.*, 2003) selecting *Homo sapiens* or eutherian weight matrices, a maximum matrix dissimilarity rate = 5%, and binding site length ≥ 6nt.

Evolutionary trees

Phylogenic trees were inferred using the Minimum Evolution (ME) method (Rzhetsky, 1992). The percentage of replicate trees in which the associated taxa clustered together in the bootstrap test (100 replicates) is shown next to the branches (Felsenstein, 1985). The evolutionary distances were computed using

the Poisson correction method (Zuckerkandl, 1965) for proteins (Figure S1) and the Maximum Composite Likelihood method (Tamura, 2004) for genomic sequences (Figure 5) and are in the units of the number of amino acid/base substitutions per site. Trees are drawn to scale, with branch lengths in the same units as those of the evolutionary distances. The ME tree was searched using the Close-Neighbor-Interchange (CNI) algorithm (Nei, 2000) at a search level of 0. The Neighbor-joining algorithm (Saitou, 1987) was used to generate the initial tree. All positions containing gaps and missing data were eliminated in the protein analysis and all ambiguous positions were removed for each sequence pair in the genomic analysis. Evolutionary analyses were conducted in MEGA5 (Tamura, 2011). Alignments used for phylogenetic analysis were performed by Muscle software (http://www.ebi.ac.uk/Tools/msa/muscle/; Edgar, 2004) implemented in MEGA5 with the following parameters: UPGMB clustering method, Gap opening penalty= -400, and iterations= 10.

Searching for paralogous genes

Ideograms of chromosome 1 and 6 at 850-band resolution level in Figure 2 were obtained from NCBI Genome Decoration Page (http://www.ncbi.nlm.nih.gov/genome/tools/gdp/; GRCh37/hg18) and were used to locate the chromosome 1 and 6 duplicated segment by adding RefSeq genes locations as a custom track retrieved from UCSC Table Browser utility (http://genome.ucsc.edu/cgi-bin/hgTables) as gene transfer format (GFT). Paralogous genes were identified using "Paralogons in the Human Genome" v.5.28 database (http://wolfe.gen.tcd.ie/dup/; McLysaght *et al.*, 2002), as a preliminary approach, and subsequently corroborated as current functional paralogous and complemented with data from Ensembl (http://www.ensembl.org) using GRCh37/hg19 genome version assembly. The identified paralgous were manually represented in a non-scaled bar.

Comparative analysis of genome sequences

VISTA tool (http://pipeline.lbl.gov; Frazer *et al.*, 2004) implemented in UCSC genome browser (http://genome.ucsc.edu; Birney *et al.*, 2004) was used for multiple alignment comparing with human sequence. Two version of the human genome were used to perform the multiple comparative genome analysis: Hg19 (GCRh37) human genome version was used for alignments with mouse (Shuffle-LAGAN (SLAGAN) alignment version) and primate sequences, while, due to incompleteness of Hg19 version alignment data, Hg18 (NCBI36) human genome version was used for alignments with mouse sequence (PROLAGAN alignment version) and sequences of the other studied vertebrates.

Luciferase reporter gene assay

Constructs were obtained by PCR with specific primers (-4775Kb_TSS_hRCAN3_Fw (CCAACTGATCCACCCACCTTGG); -1999Kb_Fw (CCACTTGTATCATTTTCATA); 699pb_Fw (ATCTCATTTGATGTGAAAACTC); -281pb_Fw (GGAGTAAGAGGAGGAGGGAG); +550pb_Rv (CGCCAGAGGTCCTGTTTTC)), using the BAC clone RP4-633K13 obtained from Children's Hospital Oakland Research Institute (CHORI) (http://www.chori.org/) as template and posterior cloning into pGL3-luc Basic reporter vector (Promega, Madison, USA). HEK 293T cells were seeded at 50000 cells/well in 24-well plates. 24 h later, each well was transfected with 30 fmol of each construct and 1 ng of pRLNull vector (Promega) as an internal transfection control. Empty pGL3 vector was included in the analysis as control. The total amount of plasmid DNA was kept constant in every condition using empty pCDNA3.1 vector (Invitrogen Corporation, Carlsbad, USA). 48h after transfection, cells were lysed and analyzed using the Dual Luciferase Reporter Assay (Promega) following manufacturer's protocol on a multiplate luminometer (FLUOstar Optima, BMG). Luciferase units were normalized to Renilla luciferase values.

RESULTS

RCAN genes evolution

We have previously described that *RCAN* family consists of three genes in jawed vertebrates (hereafter referred as vertebrates unless otherwise specified), except for *Tetraodon nigroviridis* (tetraodon) and *Takifugu rubripens* (fugu), and form a functional subfamily, while only one gene and protein is found in the rest of Eukarya (Mulero *et al.*, 2007). In vertebrates, Strippoli and colleagues mapped *RCAN* genes within the ACD clusters (Strippoli *et al.*, 2002). As for the *RCAN* gene family, the *RUNX* and *CLIC* gene families also include several genes. In spite of some punctual exceptions, as mouse, pig and fishes, in vertebrates there are six *CLIC* genes (*CLIC1-6*) whereas there are three *RUNX* genes (*RUNX1-3*).

To deepen in *RCAN* genome evolution, we performed an exhaustive search for *RUNX*, *CLIC* and *RCAN* orthologs in Chordata by using the blastp option of the BLAST search tool (Johnson *et al.*, 2008). Among the invertebrates, *Ciona intestinalis (Sea squirt),* as Urochordata representative specie, present one orthologous gene for each of the three human ACD members. The ortholog of the human *RCAN* (*CiRCAN*; ENSCING00000013221) maps at chromosome 8 and both *RUNX* (*CiRUNX*; ENSCING00000001322) and *CLIC* (*CiCLIC*; ENSCING00000004649) orthologs map at chromosome 12, but they are separated by 1Mb. In addition,

the search in *Branchiostoma floridae* (Amphioxus), as representative of the invertebrate Cephalochordata, identified one *RCAN* (Gene ID: 7217844), one *RUNX* (Gene ID: 7214657), and one *CLIC* (Gene ID: 7206331) orthologs, all of them located in different scaffolds (this genome is still incompletely assembled). Therefore, these results from invertebrate species suggest that, before vertebrate generation, each of the three genes of the ACD cluster is positioned in independent locations.

When searching in ancient jawless vertebrates (agnathans), *Myxine glutinosa* (hagfish) and *Petromyzon marinus* (lamprey), for ACD orthologous genes, we found that both, hagfish and lamprey, have two copies for *Runx* genes, called *RunxA* and *RunxB* (Hecht *et al.*, 2008; Cattell *et al.*, 2011). We also found that lamprey possesses three copies of the *Clic* gene (*LpClic1*; ENSPMAG00000002107 and *LpClic5*; ENSPMAG00000000089 and *nLpClic6* (ENSPMAG00000002003), an incomplete annotated sequence), whereas neither hagfish nor lamprey contain any human *RCAN* ortholog. A more detailed phylogenetic analysis of the *CLIC* genes than the one previously described (Rand, 2003) suggests that the ancestors of *LpClic1* and *LpClic5* genes diverged at the very early stages in vertebrate evolution (Supplemental Figure S1).

Here we proposed that the first round of whole genome duplication (1R-WGD) was likely the origin of the two *Runx* copies in jawless vertebrates, and the *Clic* genes present in lamprey (Figure 1), although the *Clic* genes were lost in hagfish and the ancient *Rcan* genes disappeared in both organisms.

Concerning the two copies of *Clic, Runx* and *Rcan* genes generated after the 1R-WGD, our hypothesis suggests that one of each of the *Runx* and *Rcan* copies have been lost in jawed vertebrates. In the early predecessor of gnathostomes, before the second round of whole-genome duplication (2R-WGD), an ancient ACD cluster precursor (*Runx1/2/3-Clic4/5/6-Rcan1/2/3*) was formed. The 2R-WGD, around 532 Mya, occasioned the split of the current ACD21 cluster (*Runx1-Clic6-Rcan1*; HSA 21q22.12) from the ACD1/6 cluster precursor and the divergence of the current *Clic3* (HSA 9q34.3) and *Clic1* (HSA 6p21.3) genes (Figure 1).

Subsequently, a large-scale segmental duplication and translocation between the two ancestral chromosomes corresponding to human chromosome 1 and 6 resulted in the appearance of the current human clusters ACD6 (*Runx2-Clic5-Rcan2*; HSA 6p13.3) and ACD1 (*Runx3-Clic4-Rcan3*; HSA 1p35.3). This segmental duplication event seems to already happened in the early jawed vertebrates, considering that the three ACD clusters are present in *Latimeria chalumnae* (coelacanth), a big marine fish, representative of Sarcopterygii, that split from the

rest of fishes more than 400 Mya (between 416 to 450 Mya) (Inoue *et al.*, 2005; Benton and Donoghue, 2007) and from the rest of sarcopterygians 410-415 Mya (Johanson *et al.*, 2006).

Our ACD genome evolution hypothesis is in line with previously reported vertebrate phylogenetic studies on human ACD members that indicate that the members of the ACD21 cluster are most ancestral than the ACD6 and ACD1 members, which are regarded as contemporary members (Rennert *et al.*, 2003; Mulero *et al.*, 2007, Strippoli *et al.*, 2002; Rand, 2003).

Taking also into account that Ensembl database (Birney *et al.*, 2004; Spudich *et al.*, 2007) links the protein coded by *nLpClic6* gene with human CLIC2 protein, we propose that the origin of human *CLIC2* and *nLpClic6* genes is a single gene duplication event after the 1R-WGD (Fig. 1, *ancClic''*). Our phylogenetic analysis points out that the human and mouse *CLIC2* genes have more sequence similarity to the *Clic* genes located within the ACD cluster (*Clic4*, *Clic5* and *Clic6*) than to the rest of *Clic* genes. Therefore, *Clic2* ancestral gene (Fig. 1, *ancClic''*) could appear from gene duplication of the *Clic4/5/6* precursor (Fig.1 *ancClic'*). However, we also consider that this *Clic2* ancestral gene (*ancClic2*) could emerge from gene duplication of the *Clic1/3* precursor (*ancClic*) (see discussion).

To reinforce the idea that segmental duplication happened between ancestral chromosomes corresponding to human 1 and 6, as there is no previous data available, we decided to look for paralogous genes surrounding this two ACD1 and ACD6 clusters (Figure 2). By using the "Paralogons in the Human Genome v.5.28" tool (McLysaght *et al.*, 2002) to find sets of chromosome regions with a common origin, and manual searching of paralogous genes in the Ensembl database (Birney *et al.*, 2004), we were able to delimitate a large segment of chromosome 1 (1p32-p36.3; > 18Mb) that contains functional paralogs in chromosome 6 (6p12-p21.2/q12-q22.1; > 75Mb). Figure 2 shows a view of the duplicated region that includes around 35 pairs of paralogous genes. Supplementary Table 1 summarizes exact location and gene information of the different paralogous genes of human chromosomes 1 and 6. Therefore, our phylogenetic studies points out that ACD clusters have evolved by two rounds of whole genome duplication and one segmental duplication event and that they have been maintained together because they probably collaborate in many signaling pathways of vertebrate biological processes. In fact, the three ACD clustered genes have been described to participate in immune responses (Honda and Taniguchi, 2006; He *et al.*, 2011; Hesser *et al.*, 2004; Minami *et al.*, 2009; Lee *et al.*, 2009; Narayan *et al.*, 2005 (Estecha *et al.*, 2012; Levanon and Groner, 2004; Puig-Kroger and Corbi, 2006; Djuretic *et al.*, 2009; Ryeom *et al.*, 2003; Sanna *et al.*, 2006) and in bone formation

(Lian and Stein, 2003; Lian *et al.*, 2004; Bassett *et al.*, 2012; Yang *et al.*, 2009). Therefore, it could be interesting to analyze their cooperation in these processes.

Although there are three *Rcan* genes in almost all vertebrates and only one gene in most of the rest of Eukarya, we have found some punctual exceptions. For *Sorex araneus* (common shrew), *Taeniopygia guttata* (zebra finch) *Procavia capensis* (hyrax), *Felis catus* (cat) and *Vicugna pacos* (alpaca), no corresponding human *RCAN1* ortholog has been described. All of them are novel genomic sequence versions that are not totally assembled and contain numerous sequence gaps. By means of genomic comparative analysis, we have been able to locate a putative *RCAN1* coding sequence for all of them (scaffold 232239, chromosome 1B random, scaffold 13048, scaffold 3164 and scaffold 2225, respectively).

In *Dario rerio* (zebrafish) we also found the presence of one additional *Rcan* gene (ENSDARG00000003109; called *RCAN1*). The origin of this gene can be explained by a recombination of *RCAN1* and *RCAN3* genes. This is supported by the presence of the *srrm1* paralogous gene (*si:dkey-67c22.2*) and the *KCNE1* gene surrounding this additional *RCAN1*. *SRRM1* and *KCNE1* are usual neighbors of *RCAN3* and *RCAN1* genes, respectively. Moreover, the comparative genomic analysis links this region in zebrafish with *RCAN3* and *RCAN1* region in human genomic sequences. Therefore this vertebrate organism bears four *RCAN* genes.

Other exceptions for the *RCAN* gene family in vertebrates is present in fishes other than zebrafish and coelacanth: *Orizias latipes* (medaka), *Tetraodon nigroviridis* (tetraodon), *Takifugu rubripens* (fugu), *Gadus morhua* (cod), *Gasterosteus aculeatus* (stickleback) and *Oreochromis niloticus* (tilapia). In all of them only *RCAN1* and *RCAN3* can be found. Interestingly, in all them, and also in zebrafish, *RCAN3* is located near *NIPAL3*, but separated from *CLIC4* and *RUNX3*, while the *RUNX1-CLIC6-RCAN1* cluster is conserved. Moreover, all of them contain at least two copies of *CLIC5*. These characteristics suggest some reorganization events that take place exclusively in fishes, but posteriorly to zebrafish divergence, that caused the appearance of additional *CLIC* genes and the loss of *RCAN2* gene. By means of genomic alignments using zebrafish *RCAN2* sequence, we were not able to find homology with any region on the other fishes, except for medaka. In this organism, a 57 bp length sequence with homology with *RCAN2* can be found in the scaffold 4515 and may constitute a residual *RCAN2* sequence.

Also *Anolis carolinensis* (anole lizard) lacks *RCAN2* and even its neighbor partner gene *ENPP5*. Since all ACD clusters are present in another sauria, such as *Pelodiscus sinensis* (Chinese softshell turtle), we used its *RCAN2-ENPP5* region for comparative analysis against lizard sequence, to find any possible putative *RCAN2*

gene in any unassembled contig, but we did not found any result, suggesting a posterior event that gave rise to *RCAN2* and *ENNP5* genes loss in this organism.

Also in the primate *Callithrix jacchus* (marmoset) we can found three additional *RCAN* paralogous genes (ENSCJAG00000010396, ENSCJAG00000034792 and ENSCJAG00000033745). The first one (ENSCJAG00000010396) is located in the chromosome 6, in a syntenic region to human chromosome 2. In the Ensembl database (Birney *et al.*, 2004; Spudich *et al.*, 2007), this gene has been named as *RCAN2*. However, we propose that the original *RCAN2* is the gene named *LOC100412694* (ENSCJAG00000012084), because it is located in chromosome 4 of marmoset, in a syntenic region to human chromosome 6 and together with *RUNX2* and *CLIC5*. As a consequence, this ENSCJAG00000010396 gene would be an additional "*RCAN2*" gene. Regarding the two other additional *RCAN* genes in marmoset (ENSCJAG00000034792 and ENSCJAG00000033745), they are located in non-assembled scaffolds. By means of BLAST search using the megablast option (Morgulis *et al.*, 2008), we were able to found a non-annotated region in marmoset chromosome 1 were these two scaffolds would be located. These two sequences would constitute two splicing mRNA forms of the same gene. The origin of these novel additional *RCAN* (conserved as genes or pseudogenes) in this organism may be a recent gene duplication.

Finally, in 2009, Mehta and colleagues described a new yeast *Rcan* gene (*Rcan2*) that emerged as a result of a novel duplication in an ancestor of yeast and contains a highly degenerated sequence (Mehta *et al.*, 2009).

In summary, additional rearrangements and duplications events would gave rise to additional copies and/or loss of RCAN gens in some vertebrates and lower eukaryotes.

RCAN gene structure comparison

In spite of differences at the amino-terminal, vertebrate RCAN proteins are well conserved at their central and C-terminal regions. Gene structure also shows remarkably similar features (Figure 3).

The human *RCAN1* is located at human chromosome 21 (HSA, 21q22.12). This gene contains 7 exons, the first four being alternative and mutually exclusive first exons, whereas exons 5, 6 and 7 are common to all transcript forms (Figure 3, top panel). Four transcript forms have been identified for human *RCAN1* by 5'RACE (Fuentes *et al.*, 1997), three of them are annotated in RefSeq database (Pruitt *et al.*, 2007; Wheeler *et al.*, 2008) and all of them are included in the UCSC database (Dreszer *et al.*, 2012). Among these RCAN1 transcripts, *RCAN1-1* (exons 1,5,6,7)

and *RCAN1-4* (exons 4,5,6,7) are the predominant expressed forms. These two transcripts encode protein isoforms RCAN1-1 and RCAN1-4, respectively. RCAN1-1 isoform is constitutively expressed but subjected to up-regulation by glucocorticoids, among others, (U *et al.*, 2004; Hirakawa *et al.*, 2009) and down-regulation by the Notch signaling pathway (Mammucari *et al.*, 2005). *RCAN1-4* transcription is induced by increase of intracellular calcium concentration, due to the presence of several NFATc and C/EBPβ binding sites in its promoter, and by estrogen hormone, among others stimuli (Yang *et al.*, 2000; Wu *et al.*, 2007a; Harris *et al.*, 2005). RCAN1-1 and RCAN1-4 isoforms are ubiquitously expressed, with abundant expression in adult heart, while RCAN1-1 is also expressed at high levels in fetal brain (Fuentes *et al.*, 1995 Fuentes *et al.*, 1997). By means of comparative analysis, we found that vertebrate *RCAN1* shows highly conservation of coding *RCAN1* regions and moderate conservation of the 5'-untranslated region (UTR) and 3'-UTR regions (Figure S2A).

RCAN2 maps at the human chromosome 6 (HSA6, 6p12.3). This gene has 7 exons being exons 5, 6 and 7 common to all transcripts forms. Similarly to *RCAN1* gene, exons 1, 2 and 4 are mutually exclusive first exons. Three mRNA forms and two protein isoforms have been described in humans (Figure 3, middle panel). Exon 3 is present in both RCAN2-1 (E1,3,5,6,7) and RCAN2-2 (E2,3,5,6,7) transcripts. RCAN2-3 (formerly RCAN2-β) protein is produced by two different transcripts, both containing a 5'-UTR first exon: *RCAN2-1* (exons 1,3,5,6,7; formerly β1) and *RCAN2-2* (exons 2,3,5,6,7; previously known as β2). RCAN2-4 (formerly RCAN2-α) protein is encoded by *RCAN2-4* (exons 4,5,6,7). Transcripts *RCAN2-1* and *RCAN2-2* coding for RCAN2-3 protein have been ubiquitously detected in basal conditions, with abundant mRNA levels in brain, heart, skeletal muscle and liver, while *RCAN2-4* has only been detected in brain (Cao *et al.*, 2002). *RCAN2-4* gene transcription is upregulated by thyroid hormone in skeletal muscle (Cao *et al.*, 2002). *RCAN2* gene coding regions are highly conserved in vertebrates (Figure S2B), and the 5' UTR of exon 4 is only annotated for mammals and chicken. Our comparative analysis of vertebrate *RCAN2* shows that while exons 1, 2 and 3 shows DNA sequence conservation in mammals, they are only annotated in primates and the SLAGAN version of human-mouse alignment. The *RCAN2* 3'-UTR is neither annotated nor conserved in chicken, zebrafish and frog (Figure S2B).

Concerning the human *RCAN3*, located at the chromosome 1 (HSA, 1p35.3-p33), it also includes 7 exons being the last four coding exons mainly common to all known transcript forms. The three first exons are mutually exclusive and non-coding (Figure 3, bottom panel). Up to 21 alternative transcripts of human *RCAN3* have been described (Strippoli *et al.*, 2000a, Strippoli *et al.*, 2000b, Canaider *et al.*, 2006, Facchin *et al.*, 2008, Facchin *et al.*, 2011), but only ten of them have been

accepted as complete mRNA at the NCBI RefSeq database (Pruitt *et al.*, 2007; Wheeler *et al.*, 2008). To avoid the complex naming of the different transcripts we propose a novel nomenclature of the *RCAN3* exons and of the different *RCAN3* accepted transcripts in the RefSeq database, according to exons being used (Davies *et al.*, 2007) (Figure 4 and Table S2) (hereafter exons and transcripts will be referred following the novel nomenclature proposed).

Human *RCAN3* transcript forms 1, 2, 2a and 3 give rise to the RCAN3-4 protein isoform (RefSeq: NP_038469; UniProt: Q9UKA8-1; 241 amino acid (aa)), the only RCAN3 protein detected so far for human and mice (Mulero Roig *et al.*, 2009, and Martínez-Hφyer *et al*, 2012, unpublished results Porta *et al.*, 2007). Transcripts not containing exon 5 or/and 6 modify the open reading frame and therefore encode a protein different to the other protein isoforms and with no amino acid identity at the common RCAN central and C-terminal regions. *RCAN3* gene is constitutively and ubiquitously expressed, predominantly in heart, brain, small intestine, lung, testis, prostate and peripheral blood leukocytes (PBLs) (Strippoli *et al.*, 2000a, Strippoli *et al.*, 2000b, Canaider *et al.*, 2006, Facchin *et al.*, 2008, Facchin *et al.*, 2011).

Our whole genome comparative analysis of *RCAN3* (Figure S2C) revealed that the coding region of exon 4 is not conserved or annotated in *Xenopus laevis*. The *RCAN3* 5'-UTR exons (exons 1, 2 and 3) are annotated and conserved in primates, but they are not conserved in the other mammals. However, manual genomic alignments of exon 2 revealed that exon 2 is annotated in primates as previously reported (Facchin *et al.*, 2011), but it is also annotated for *Bos Taurus* and *Mus musculus* (data not shown).

In order to deepen in the understanding of the origin and conservation of the 5' UTR exons (exons 1, 2, 3 and part of exon 4) and 3' UTR (part of exon 7) of the RCAN3 gene along the evolution, we performed an alignment and a subsequent phylogenetic study of the genomic regions corresponding to each exon in several mammal organisms (Figure 5). Results indicate that, in these regions, rodents (ratNor, musMus and cavPor) are more divergent with respect to the rest of mammals being analyzed, except for exon 3 and 5' UTR region of exon 4. In addition, these regions are very similar between primates, as they appear strongly clustered in the phylogenetic tree. Moreover, non-coding exons (exons 1, 2/2a and 3), 5' UTR of exon 4 and 3' UTR of exon 7 show higher sequence divergence than coding region (as the length of the branches indicates), but all of them behave in a similar manner. Interestingly, analysis of the exon 3 and the 5'-UTR of exon 4 associate the rodent *Cavia porcellus* with primates, however, the confidence of this association (bootstrap number) is low. As mouse annotated

exon 2 spans more upstream than human, we used this mouse exon sequence to delimitate this exon, whereas human exon annotation was used as a reference for the rest of exons (Fig. 5).

Therefore, *RCAN3* multispecies comparison suggests a parallel evolution between coding exons and non-coding exons indicating that 5' UTR exons are not a new product that only exists in primates. Its existence in other organims should be explored in more detail in order to understand *RCAN3* structure and regulation.

After analyzing the *RCAN* gene structure we can conclude that all the genes of this family have 7 exons, being exons 5 to 7 common to all transcripts and sharing high amino acid identity in their encoded proteins (Figure S3). Exons 1 to 4 of *RCAN1*, exons 1, 2 and 4 of *RCAN2,* and exons 1 to 3 of *RCAN3* are mutually exclusive first exons. This scenario with multiple genes and transcripts forms with independent 5' UTR first exons suggests that each of these genes carry several specific promoters tightly regulating gene expression in response to different stimuli under different environmental conditions.

Natural antisense transcripts in RCAN genes

Recently, four natural antisense transcripts (NATs) have been described that partially overlap the *RCAN3* gene (*RCAN3AS 1-3*) (Facchin *et al.*, 2011). These three transcripts are encoded by the same gene, which includes three exons and two introns, and are generated by alternative splicing. We decided to search for similar NATs in both *RCAN1* and *RCAN2* genes and we found one gene (*BC042616*) overlapping exon 1 on *RCAN2* and one EST (*DA403464*) located at the 5' region of the TSS of exon 1 on *RCAN1,* both with similar characteristics to *RCAN3AS* transcripts. They both are located upstream of the corresponding *RCAN* gene (partially overlapping exon 1 in case of *RCAN2*) and transcribed in the opposite sense (Figure 3 and Figure S4). Therefore, we suggest renaming these genes following the same nomenclature proposed by Canaider for *RCAN3AS* and design them as *RCAN2* antisense (*RCAN2AS*) and *RCAN1* antisense (*RCAN1AS*) transcripts.

As Figure 3 shows in more detail, it is not difficult to draw parallels between *RCAN3AS* and *RCAN2AS* transcripts, both including two introns, three exons and the first exon that partially overlaps with the exon 1 of the *RCAN2* gene (10nt in *RCAN3* and 16nt in *RCAN2*). The exons from the *RCAN2AS* transcripts are named as *RCAN2AS-E1*, *RCAN2AS-E2* and *RCAN2AS-E3* (Figure 3). Regarding *RCAN1AS,* the scenario slightly differs from the previously described *RCAN*-associated NATs. It has been described one antisense EST for the *RCAN1* gene (GenBank ID: *DA403464*, from human thalamus) that it is not included in the RefSeq database

(Pruitt *et al.*, 2007; Wheeler *et al.*, 2008). The transcript corresponding to this EST seems probably to be encoded by a gene that would contain at least two exons and one intron, however it is likely that an additional exon can be found overlapping exon 1 of *RCAN1* gene, but it has not been yet identified. It is noteworthy that this NAT has been described as capable of regulate *RCAN1* expression and as a putative agent for the treatment of Down's syndrome (patent WO/2010/151674 A2). Due to this functional effect, we suggest that the *DA403464* EST as *RCAN1AS* transcript and we propose to name their two exons as *RCAN1AS-E1* and *RCAN1AS-E2* (Figure 3).

As Supplemental Figure S2 shows, *RCAN1AS* and *RCAN2AS* are not annotated as transcribed mRNA for any of the analyzed organisms, whereas *RCAN3AS* it is only annotated for primate alignments with human sequences and only the third exon is annotated in the SLAGAN alignment between human and mouse. Manual alignment of the corresponding genomic sequences of several organisms with respect to the human *RCANAS* transcripts was performed (Figure S4). The results indicate that all species which do not contain sequencing gaps in these regions share more than 50% of nucleotide sequence identity with human transcripts, being almost identical in primates. In addition, by means of BLAST search using the blastn option (Johnson *et al.*, 2008) with these three *RCANAS* against the EST database, we found different ESTs from several organisms with high homology to the *RCAN2AS-E3,* but poor sequence identity with *RCAN1AS* and *RCAN3AS* transcripts and only 10-15% of query coverage.

In order to deepen within the origin and the nature of the antisense transcripts, we compared the *RCAN* NATs with the sequences available in the Repbase database of repetitive DNA elements by using the Censor web server tool (Jurka *et al.*, 1996; Jurka *et al.*, 2005). Our results indicate that the *RCAN3AS* nucleotide sequence presents more than 85% sequence homology with the LTR-retrotransposons MLT1J and LTR33, and *RCAN2AS* with LINE-1 retrotransposons and, remarkably, with the *LOC340211* gene (similar to LINE-1 reverse transcriptase homolog at human chromosome 22; NM_001012976) (Fig. 3) suggesting a retrotransposon nature origin of these transcripts. Nevertheless, for the *RCAN1AS* nucleotide sequence analysis we did not retrieve any result.

When analyzing the presence of repetitive elements within the *RCAN* genes by using the Repbase Database and the Censor web server tool, we also detected the presence of DNA sequences from the Tigger DNA-retrotransposon inside intron 3 of the three *RCAN* genes (Figure 3). In particular, Tigger1A sequence located in the *RCAN3* intron 3, is found intact and conserves its three ORFs (Kines and Belancio, 2012) while in *RCAN2* only the longest and central ORF, that codes for a

retrotransposase, is conserved. In *RCAN1* the Tigger sequence is highly degenerated and only few fragments are conserved. Interestingly, Tigger sequences in *RCAN1* and *RCAN2* are highly conserved in primates, but are not present in other mammals (data not shown).

Therefore, all human *RCAN* genes seem to have associated NATs transcribed in the opposite sense and that partially overlaps with the corresponding *RCAN* gene in case of *RCAN2* and *RCAN3*. Genomic sequences that code for these NATs are conserved among mammals. Moreover, analysis for repetitive sequences in *RCAN* genes revealed a possible retrotransposon nature of these NATs and the presence of Tigger sequences in the intron 3 of the three human *RCAN* genes.

Analysis of RCAN gene promoter

As mentioned before, *RCAN1* and *RCAN2* gene expression regulation has been studied to some extent, but functional regulation of the *RCAN3* gene is unknown. *In silico* analysis predicted that the *RCAN3* transcripts that bear exon 1, 2 or 2a as the first exon are driven by TATA-less promoters, while transcripts starting with exon 3 are regulated by a promoter containing a TATA box (Strippoli *et al.*, 2000a, Facchin *et al.*, 2011). The TSS of several *RCAN* transcripts (TSS in exon 2 of the three *RCAN* genes and in exon 1 of *RCAN1*) are located within a CpG island. Thus, these transcripts are likely under the regulation of a promoter susceptible of being methylated.

In this context, we explored the methylation status of the *RCAN*-associated CpG islands by using the data on the "Infinium HumanMethylation450 BeadChip (Illumina)" methylation array (data not shown). All the probes mapping to CpG islands associated with *RCAN1* and *RCAN3* (Figure 3) presented an unmethylated status in several normal and cancer human cell lines (data not shown), suggesting that these regions may be transcriptionally active. Unfortunately, none of the probes included on the array mapped to the CpG island associated to *RCAN2* and, for this reason, its methylation state and expression activity remains unknown.

Assuming that this unmethylated conformation of the *RCAN3*-associated CpG could confer the ability of active transcription, we decided to test this hypothesis at the experimental level. After having cloned different DNA regions 5' flanking the TSS of exon 2 of *RCAN3* and including the entire CpG island , (Figure 3 and 6A) we analyzed their transcriptional activity by using luciferase gene reporter assays (Figure 6A). The highest transcriptional activity was obtained with the construct harboring the fragment of CpG island that contains exon 2 but not exon 1 (-281 to +550 nt, where +1 correspond to the TSS of exon 2). The additional presence of *RCAN3* exon 1 or more upstream sequences in the construct reduced

transcriptional activity. These results suggest the presence of transcription factor binding sites (TFBS) or DNA conformational changes on exon 1 and upstream sequences that may act as transcriptional repressors of *RCAN3* transcripts starting at exon 2 or 2a.

To predict the presence of putative TFBS in this human *RCAN3* proximal promoter, we performed an *in silico* analysis using the PROMO software (Messeguer *et al.*, 2002; Farre *et al.*, 2003) with *Homo sapiens* weight matrices. The analysis along the CpG island (-521 to +492 nt) predicted many TFBS for SP1, TP53, and PAX5 (Figure 6B). TFBS for some additional transcription factors (NFAT, MAZ, E2F-1, VDR and ETF) were predicted in the region spanning exon 1 and more upstream sequences (-699 to -280), but not in the region -281 to + 550, that includes only exon 2 and corresponds to the construct with highest activity.

We also performed a multispecies prediction of TFBS along the *RCAN3*-associated CpG island on the DNA sequence of 18 eutherian mammals using eutherian weight matrices for the prediction. Supplemental Figure S5 shows some TFBS highly conserved among all the analyzed organisms. This TFBS conservation along the evolution reinforces the likelihood of a functional role of the CpG island region in the modulation of *RCAN3* gene expression.

Our results suggest that the genomic structure and regulation of the *RCAN* gene family is conserved along mammal evolution. Furthermore, we have shown that the *RCAN3*- associated CpG island, where exon 1 and 2/2a are located, is transcriptionally active and may be involved in regulating *RCAN3* transcriptional activation in different cellular conditions. Further studies should be performed to understand how *RCAN3* gene expression is regulated.

DISCUSSION

In this article, we propose a new hypothesis to explain the evolution of the *RCAN* gene family with a special emphasis on the three genes of this family existing in humans. In jawed vertebrates, RCAN genes form part of what has been named ACD clusters, together with *RUNX* and *CLIC* genes. Stripolli *et al*. speculated that the current ACD clusters originated as a result of successive segmental duplications and rearrangements during the two rounds of whole genome duplication (Strippoli *et al.*, 2002). In this context, we decide to go one step further to deepen in the three gene families evolution in order to advance on our knowledge about *RCAN* genes.

Results of searching for human *RUNX, CLIC* and *RCAN* orthologs in Urochordata (*Ciona intestinalis;* Sea squirt) and Cephalochordata (*Branchiostoma floridae*)

representative organisms confirmed the presence of a unique copy for these genes in the early Chordata. As reported previously, the two living representative organism of agnathans, hagfish (*Myxine glutinosa*) and lamprey (Petromyzon marinus), have two orthologs of *RUNX,* named *RunxA* and *RunxB* (Hecht *et al.*, 2008; Cattell *et al.*, 2011). It has been proposed that the ancestral chordate runt domain (RD), the precursor of human *RUNX* genes, underwent a primary duplication generating *Runt* and the ancestral *Runx* gene, followed by a posterior triplication of *Runx* that originated *Runx1, Runx2* and *Runx3*, present in all the jawed vertebrates. *RUNT* probably lost functionality during evolution and disappeared except in pufferfishes (*Takifugu rubripes* and *Tetraodon nigroviridis*) (Glusman *et al.*, 2004). This hypothesis is concordant with ours, which goes one step further and sets the triplication proposed by Glusman *et al.* as the 2R-WGD followed by one segmental duplication event as the origin of the actual three vertebrate *Runx* genes (Figure 1).

Even though our exhaustive searching process did not obtain any ortholog for the human *CLIC* in hagfish, we found three annotated *Clic* genes in lamprey: *LpCLic1*, *LpCLic5,* and a novel form of *Clic6* (that we have called *nLpClic6* or *nClic6* in figure 1). Phylogenetic analysis of the different known *CLIC* genes for different species (Figure S1) suggests that *LpClic5* differs from *LpClic1* in the same way than human, mouse and rat *CLIC1* and *CLIC3* genes differ from *CLIC4*, *CLIC5* and *CLIC6* genes. Orthologs annotated in the Ensembl database (Birney *et al.*, 2004; Spudich *et al.*, 2007) link *LpClic1* with human *CLIC1* and *CLIC3*, and *LpClic5* with human *CLIC5*. Search for LpClic homologous proteins in humans by using the BLAST search tool with the DELTA-BLAST option (Boratyn *et al.*, 2012) corroborated that both LpClic1 and LpClic5 proteins present major amino acid similarity with human CLIC1 and CLIC5 proteins, respectively. These results suggest a divergence at the very early stages in vertebrate evolution between *LpClic1*/*Clic1*/*Clic3* and *LpClic5*/*Clic4*/*Clic5*/*Clic6* ancestors and, as lamprey is considered a "living fossil" (Gess *et al.*, 2006), *LpClic1* and *LpClic5* (Fig. 1, *CLic1* and *CLic5*, respectively*)* are the most representative of these ancestor genes.

Regarding lamprey *nClic6* gene, the protein sequence is linked with human CLIC2 in the Ensembl database (Birney *et al.*, 2004; Spudich *et al.*, 2007) in the "supporting evidences" section. However, orthologs of *nClic6* annotated in the Ensembl database are human *CLIC4*, *CLIC5*, and *CLIC6*. Search for *nLpClic6* homologous human proteins by using the BLAST search tool with the DELTA-BLAST option (Boratyn *et al.*, 2012) resulted in similarity with different human CLIC proteins, being the major similarity with CLIC2. Detailed analysis revealed that annotation for *nLpClic6* sequence is incomplete as only two exons are annotated although there are evidences of the existence of more exons. For that

reason, it is difficult to determine exactly the origin of *nLpClic6*, but it seems to be linked to *CLIC2*. As phylogenetic analysis by using protein sequences shows that CLIC2 occupies an intermediate position between CLIC1/CLIC3 and CLIC4/CLIC5/CLIC6 (Figure S1), we hypothesize that the ancestor of *nLpClic6* and vertebrates *CLIC2* (Fig. 1, see *ancClic*'') appeared as a consequence of a single gene duplication event after the 1R-WGD and before the separation of agnathans and gnathostomes either from the *Clic1*/*3* ancestor (*ancClic*), or from the *Clic4*/*5*/*6* ancestor (*ancClic'*) (Figure 1). After the 2R-WGD, the other copy of *CLIC2* (*Clic2'*) in jawed vertebrates likely lost functionality and disappeared.

Our attempt for finding RCAN orthologs members in several databases using human RCANs or *Caenorhabditis elegans Rcn-1* sequences as templates did not report any homologous protein or gene in agnathans. Hence, we suggest that both copies of the ancestral *RCAN* originated after the first round of whole genome duplication were likely lost in agnathans.

Considering all this available data, a new hypothesis emerged as a plausible explanation of the evolution of *Clic*, *Runx*, and *Rcan* genes, different to that previously proposed where evolution of ACD clusters were originated by successive segmental duplications and rearrangements during the two rounds of whole genome duplication (Strippoli *et al.*, 2002). This novel hypothesis is graphically described in Figure 1. Briefly, one first round of genome duplication (1R-WGD) originated an additional copy for *Clic*, *Runx*, and *Rcan* genes. While hagfishes lost both *Clic* copies, lamprey conserves them. One of *Runx* genes (*ancRunx*) was lost only in jawed vertebrates, while jawless vertebrates still conserve both copies. One *Rcan* ancestral gene (*ancRcan*) would have been lost in both jawless and jawed vertebrates and, additionally, hagfish also lost the other ancestral *Rcan* gene (*ancRcan'*). After agnatha-gnasthostomata divergence, one copy of *Clic* gene (*ancClic'*, the ancestor of the current human *CLIC4*, *CLIC5*, and *CLIC6*) was somehow clustered with *Runx* and *Rcan*. Posteriorly, gnasthostomes underwent an additional round of whole genome duplication (2R-WGD) that originated *Clic1* and *Clic3* at the time that gave rise to the ACD21 cluster and the precursor of ACD1 and ACD6 clusters. Subsequent segmental duplication between chromosome 1 and 6 likely originated the definitive ACD1 and ACD6 clusters. The presence of up to 35 genes located around ACD1 and ACD6 clusters reinforces the idea of a segmental duplication among these chromosomal regions (Figure 2 and Table S1). Moreover, some additional reorganization events in vertebrates would cause the loss of some *Rcan* gene in some organims, as in the majority of fishes, or caused the appearance of additional copies of *Rcan* genes in other organims, as in the case or marmoset or zebrafish.

Actually, we cannot absolutely conclude that ACD cluster formation occurred after 1R-WGD, because hagfish and lamprey genomes are not yet assembled. However, as the respective *Clic* and *Runx* genes are located in different scaffolds, our suggestion that the clustering process occurred after the first round of WGD is the most plausible possibility.

Comparison among vertebrates served us to identify the presence of antisense transcripts upstream *RCAN1* and *RCAN2* genes that have similar characteristics for those that were previously described for *RCAN3* (Figure 3 and Figure S2). Interestingly, those *RCAN* antisense transcripts showed high identity among mammals (Figure S4) and they probably have a functional role in *RCAN* transcriptional regulation. This has been demonstrated that *RCAN1AS* regulates *RCAN1* gene transcription (patent WO/2010/151674 A2). This high NAT sequence conservation among the different mammal organisms, together with the presence of retroviral sequences at least in *RCAN2AS* and *RCAN3AS*, suggests the idea of ancient retroviral transposition in an ancient predecessor of the three *RCAN* genes (before the 2R-WGD) that was maintained along the posterior duplications with some degree of divergence. Retroviral transposition in the *RCANs* ancestor may be also the possible origin of the retroviral Tigger sequences found in intron 3 of the three *RCANs*. Tigger sequences have possibly been maintained nearly intact in primates for *RCAN2* and *RCAN3* because they can confer some essential characteristics for their regulation and/or function.

The recent description of novel *RCAN3* exons (Facchin *et al.*, 2011) makes necessary to rename again *RCAN3* exons, forms and isoforms in order to be more consistent with the nomenclature used for *RCAN1* and *RCAN2*. Therefore, as an effort to continue with the attempt of Davies (Davies *et al.*, 2007) to create a rational nomenclature system to designate the three human *RCAN* family members, we propose a novel nomenclature for the *RCAN3* exons, mRNA isoforms and proteins that have been described so far (Figure 4 and Table S2).

As it is reflected in Figure 4, at least three 5' non-coding exons exist for *RCAN3* and they are mutually exclusive. In an attempt to gain information about *RCAN3* evolution and to explore the possibility of its existence in other organisms, we performed a phylogenetic study using the corresponding genomic sequence of these exons in other organisms. As a result, we obtained two interesting conclusions. First, not only primate sequences are very close, but also rodent sequences corresponding to 5' non-coding exons seemed to be the most divergent sequences (Figure 5). Secondly, if we compare the phylogenic tree of these non-coding exons with the phylogenic tree of the coding exons, it could be hypothesized that these exons may be present in the primordial form of *RCAN3*,

originated after segmental duplication event (Figure 1, see SD) and they may be, more than an invention of primates, an invention of all the mammals. This idea can also be inferred from the genomic comparison of 5' UTR exons of *RCAN1* and *RCAN2* presented in Figure S2.

The experimental approach to study the 5' flanking region of *RCAN3* as a putative promoter, which includes a CpG island, brought some clues about the regulation of *RCAN3* transcription. In one side, it is observed an unmethylated status of the CpG island associated to *RCAN3* that suggests its potential for transcriptional activation. Unmethylated status of CpG islands has been associated with an opened status of the chromatin (Fan *et al.*, 2008), allowing binding of transcription factors for transcriptional regulation. In the other hand, we were able to prove that this CpG island associated to *RCAN3* has transcriptional activity by itself (Figure 6a). *In silico* analysis of TFBS (Figure 6b and S5) serves us as a guide for more exhaustive experiments in the future in order to untangle the transcriptional regulation of *RCAN3*. Finally, the knowledge of the molecular mechanisms involved in RCAN protein production may provide the possibility to modify the amount of protein needed to modulate a particular cellular function depending on the desired outcome.

ACKNOWLEDGMENTS

This work has been supported by grants SAF2009-08216, from MICINN and 2009SGR1490 from G.C. E.S.-C. was supported from SAF009-08216 and A.A-I. is a recipient of an FI fellowship from G.C.

FOOTNOTES

Abbreviations used were: Cn, calcineurin; HSA, Homo Sapiens; NAT, Natural antisense transcript; NFATc, Nuclear Factor of Activated T-cells, cytosolic; RCAN, Regulator of Calcineurin; SD, Segmental Duplication; TFBS, transcription Factors Binding Sites; TSS, transcription start site; UTR, Untranslated Region; WGD, Whole Genome Duplication.

REFERENCES

Altschul, S.F., Gish, W., Miller, W., Myers, E.W. and Lipman, D.J. **Basic local alignment search tool**. (1990) *J Mol Biol* 215 pp. 403-10.

Aramburu, J., Garcia-Cozar, F., Raghavan, A., Okamura, H., Rao, A. and Hogan, P.G. **Selective inhibition of NFAT activation by a peptide spanning the calcineurin targeting site of NFAT**. (1998) *Mol Cell* 1 pp. 627-37.

Aramburu, J., Heitman, J. and Crabtree, G.R. **Calcineurin: a central controller of signalling in eukaryotes**. (2004) *EMBO Rep* 5 pp. 343-8.

Aubareda, A., Mulero, M.C. and Perez-Riba, M. **Functional characterization of the calcipressin 1 motif that suppresses calcineurin-mediated NFAT-dependent cytokine gene expression in human T cells**. (2006) *Cell Signal* 18 pp. 1430-8.

Bassett, J.H., Logan, J.G., Boyde, A., Cheung, M.S., Evans, H., Croucher, P., Sun, X.Y., Xu, S., Murata, Y. and Williams, G.R. **Mice lacking the calcineurin inhibitor Rcan2 have an isolated defect of osteoblast function**. (2012) *Endocrinology* 153 pp. 3537-48.

Benton, M.J. and Donoghue, P.C. **Paleontological evidence to date the tree of life**. (2007) *Mol Biol Evol* 24 pp. 26-53.

Birney, E., Andrews, T.D., Bevan, P., Caccamo, M., Chen, Y., Clarke, L., Coates, G., Cuff, J., Curwen, V., Cutts, T., Down, T., Eyras, E., Fernandez-Suarez, X.M., Gane, P., Gibbins, B., Gilbert, J., Hammond, M., Hotz, H.R., Iyer, V., Jekosch, K., Kahari, A., Kasprzyk, A., Keefe, D., Keenan, S., Lehvaslaiho, H., McVicker, G., Melsopp, C., Meidl, P., Mongin, E., Pettett, R., Potter, S., Proctor, G., Rae, M., Searle, S., Slater, G., Smedley, D., Smith, J., Spooner, W., Stabenau, A., Stalker, J., Storey, R., Ureta-Vidal, A., Woodwark, K.C., Cameron, G., Durbin, R., Cox, A., Hubbard, T. and Clamp, M. **An overview of Ensembl**. (2004) *Genome Res* 14 pp. 925-8.

Blair, J.E. and Hedges, S.B. **Molecular phylogeny and divergence times of deuterostome animals**. (2005) *Mol Biol Evol* 22 pp. 2275-84.

Boratyn, G.M., Schaffer, A.A., Agarwala, R., Altschul, S.F., Lipman, D.J. and Madden, T.L. **Domain enhanced lookup time accelerated BLAST**. (2012) *Biol Direct* 7 p. 12.

Canaider, S., Facchin, F., Griffoni, C., Casadei, R., Vitale, L., Lenzi, L., Frabetti, F., D'Addabbo, P., Carinci, P., Zannotti, M. and Strippoli, P. **Proteins encoded by human Down syndrome critical region gene 1-like 2 (DSCR1L2) mRNA and by a novel DSCR1L2 mRNA isoform interact with cardiac troponin I (TNNI3)**. (2006) *Gene* 372 pp. 128-36.

Cao, X., Kambe, F., Miyazaki, T., Sarkar, D., Ohmori, S. and Seo, H. **Novel human ZAKI-4 isoforms: hormonal and tissue-specific regulation and function as calcineurin inhibitors**. (2002) *Biochem J* 367 pp. 459-66.

Cattell, M., Lai, S., Cerny, R. and Medeiros, D.M. **A new mechanistic scenario for the origin and evolution of vertebrate cartilage**. (2011) *PLoS One* 6 p. e22474.

Davies, K.J., Ermak, G., Rothermel, B.A., Pritchard, M., Heitman, J., Ahnn, J., Henrique-Silva, F., Crawford, D., Canaider, S., Strippoli, P., Carinci, P., Min, K.T., Fox, D.S., Cunningham, K.W., Bassel-Duby, R., Olson, E.N., Zhang, Z., Williams, R.S., Gerber, H.P., Perez-Riba, M., Seo, H., Cao, X., Klee, C.B., Redondo, J.M., Maltais, L.J., Bruford, E.A., Povey, S., Molkentin, J.D., McKeon, F.D., Duh, E.J., Crabtree, G.R., Cyert, M.S., de la Luna, S. and Estivill, X. **Renaming the DSCR1/Adapt78 gene family as RCAN: regulators of calcineurin**. (2007) *FASEB J* 21 pp. 3023-8.

Djuretic, I.M., Cruz-Guilloty, F. and Rao, A. **Regulation of gene expression in peripheral T cells by Runx transcription factors**. (2009) *Adv Immunol* 104 pp. 1-23.

Dreszer, T.R., Karolchik, D., Zweig, A.S., Hinrichs, A.S., Raney, B.J., Kuhn, R.M., Meyer, L.R., Wong, M., Sloan, C.A., Rosenbloom, K.R., Roe, G., Rhead, B., Pohl, A., Malladi, V.S., Li, C.H., Learned, K., Kirkup, V., Hsu, F., Harte, R.A., Guruvadoo, L., Goldman, M., Giardine, B.M., Fujita, P.A., Diekhans, M., Cline, M.S., Clawson, H., Barber,

G.P., Haussler, D. and James Kent, W. **The UCSC Genome Browser database: extensions and updates 2011**. (2012) *Nucleic Acids Res* 40 pp. D918-23.

Edgar, R.C. **MUSCLE: multiple sequence alignment with high accuracy and high throughput**. (2004) *Nucleic Acids Res* 32 pp. 1792-7.

Estecha, A., Aguilera-Montilla, N., Sanchez-Mateos, P. and Puig-Kroger, A. **RUNX3 regulates intercellular adhesion molecule 3 (ICAM-3) expression during macrophage differentiation and monocyte extravasation**. (2012) *PLoS One* 7 p. e33313.

Facchin, F., Canaider, S., Vitale, L., Frabetti, F., Griffoni, C., Lenzi, L., Casadei, R. and Strippoli, P. **Identification and analysis of human RCAN3 (DSCR1L2) mRNA and protein isoforms**. (2008) *Gene* 407 pp. 159-68.

Facchin, F., Vitale, L., Bianconi, E., Piva, F., Frabetti, F., Strippoli, P., Casadei, R., Pelleri, M.C., Piovesan, A. and Canaider, S. **Complexity of bidirectional transcription and alternative splicing at human RCAN3 locus**. (2011) *PLoS One* 6 p. e24508.

Fan, S., Zhang, M.Q. and Zhang, X. **Histone methylation marks play important roles in predicting the methylation status of CpG islands**. (2008) *Biochem Biophys Res Commun* 374 pp. 559-64.

Farre, D., Roset, R., Huerta, M., Adsuara, J.E., Rosello, L., Alba, M.M. and Messeguer, X. **Identification of patterns in biological sequences at the ALGGEN server: PROMO and MALGEN**. (2003) *Nucleic Acids Res* 31 pp. 3651-3.

Felsenstein, J. **Confidence limits on phylogenies: An approach using the bootstrap**. (1985) *Evolution* 39 pp. 783-791.

Frazer, K.A., Pachter, L., Poliakov, A., Rubin, E.M. and Dubchak, I. **VISTA: computational tools for comparative genomics**. (2004) *Nucleic Acids Res* 32 pp. W273-9.

Fuentes, J.J., Pritchard, M.A. and Estivill, X. **Genomic organization, alternative splicing, and expression patterns of the DSCR1 (Down syndrome candidate region 1) gene**. (1997) *Genomics* 44 pp. 358-61.

Fuentes, J.J., Pritchard, M.A., Planas, A.M., Bosch, A., Ferrer, I. and Estivill, X. **A new human gene from the Down syndrome critical region encodes a proline-rich protein highly expressed in fetal brain and heart**. (1995) *Hum Mol Genet* 4 pp. 1935-44.

Garcia-Cozar, F.J., Okamura, H., Aramburu, J.F., Shaw, K.T., Pelletier, L., Showalter, R., Villafranca, E. and Rao, A. **Two-site interaction of nuclear factor of activated T cells with activated calcineurin**. (1998) *J Biol Chem* 273 pp. 23877-83.

Gess, R.W., Coates, M.I. and Rubidge, B.S. **A lamprey from the Devonian period of South Africa**. (2006) *Nature* 443 pp. 981-4.

Glusman, G., Kaur, A., Hood, L. and Rowen, L. **An enigmatic fourth runt domain gene in the fugu genome: ancestral gene loss versus accelerated evolution**. (2004) *BMC Evol Biol* 4 p. 43.

Gurgen, D., Hegner, B., Kusch, A., Catar, R., Chaykovska, L., Hoff, U., Gross, V., Slowinski, T., da Costa Goncalves, A.C., Kintscher, U., Gustafsson, J.A., Luft, F.C. and Dragun, D. **Estrogen receptor-beta signals left ventricular hypertrophy sex differences in normotensive deoxycorticosterone acetate-salt mice**. (2011) *Hypertension* 57 pp. 648-54.

Harris, C.D., Ermak, G. and Davies, K.J. **Multiple roles of the DSCR1 (Adapt78 or RCAN1) gene and its protein product calcipressin 1 (or RCAN1) in disease**. (2005) *Cell Mol Life Sci* 62 pp. 2477-86.

He, G., Ma, Y., Chou, S.Y., Li, H., Yang, C., Chuang, J.Z., Sung, C.H. and Ding, A. **Role of CLIC4 in the host innate responses to bacterial lipopolysaccharide**. (2011) *Eur J Immunol* 41 pp. 1221-30.

Hecht, J., Stricker, S., Wiecha, U., Stiege, A., Panopoulou, G., Podsiadlowski, L., Poustka, A.J., Dieterich, C., Ehrich, S., Suvorova, J., Mundlos, S. and Seitz, V. **Evolution of a core gene network for skeletogenesis in chordates**. (2008) *PLoS Genet* 4 p. e1000025.

Hedges, S.B.K., S. **Chap. Vertebrates. The timetree of life** (2009),

Hesser, B.A., Liang, X.H., Camenisch, G., Yang, S., Lewin, D.A., Scheller, R., Ferrara, N. and Gerber, H.P. **Down syndrome critical region protein 1 (DSCR1), a novel VEGF target gene that regulates expression of inflammatory markers on activated endothelial cells**. (2004) *Blood* 104 pp. 149-58.

Hirakawa, Y., Nary, L.J. and Medh, R.D. **Glucocorticoid evoked upregulation of RCAN1-1 in human leukemic CEM cells susceptible to apoptosis**. (2009) *J Mol Signal* 4 p. 6.

Hokamp, K., McLysaght, A. and Wolfe, K.H. **The 2R hypothesis and the human genome sequence**. (2003) *J Struct Funct Genomics* 3 pp. 95-110.

Honda, K. and Taniguchi, T. **IRFs: master regulators of signalling by Toll-like receptors and cytosolic pattern-recognition receptors**. (2006) *Nat Rev Immunol* 6 pp. 644-58.

Inoue, J.G., Miya, M., Venkatesh, B. and Nishida, M. **The mitochondrial genome of Indonesian coelacanth Latimeria menadoensis (Sarcopterygii: Coelacanthiformes) and divergence time estimation between the two coelacanths**. (2005) *Gene* 349 pp. 227-35.

Johanson, Z., Long, J.A., Talent, J.A., Janvier, P. and Warren, J.W. **Oldest coelacanth, from the Early Devonian of Australia**. (2006) *Biol Lett* 2 pp. 443-6.

Johnson, M., Zaretskaya, I., Raytselis, Y., Merezhuk, Y., McGinnis, S. and Madden, T.L. **NCBI BLAST: a better web interface**. (2008) *Nucleic Acids Res* 36 pp. W5-9.

Jurka, J., Kapitonov, V.V., Pavlicek, A., Klonowski, P., Kohany, O. and Walichiewicz, J. **Repbase Update, a database of eukaryotic repetitive elements**. (2005) *Cytogenet Genome Res* 110 pp. 462-7.

Jurka, J., Klonowski, P., Dagman, V. and Pelton, P. **CENSOR--a program for identification and elimination of repetitive elements from DNA sequences**. (1996) *Comput Chem* 20 pp. 119-21.

Katoh, K., Asimenos, G. and Toh, H. **Multiple alignment of DNA sequences with MAFFT**. (2009) *Methods Mol Biol* 537 pp. 39-64.

Kines, K.J. and Belancio, V.P. **Expressing genes do not forget their LINEs: transposable elements and gene expression**. (2012) *Front Biosci* 17 pp. 1329-44.

Lee, J.Y., Lee, H.J., Lee, E.J., Jang, S.H., Kim, H., Yoon, J.H. and Chung, K.C. **Down syndrome candidate region-1 protein interacts with Tollip and positively modulates interleukin-1 receptor-mediated signaling**. (2009) *Biochim Biophys Acta* 1790 pp. 1673-80.

Levanon, D. and Groner, Y. **Structure and regulated expression of mammalian RUNX genes**. (2004) *Oncogene* 23 pp. 4211-9.

Lian, J.B., Javed, A., Zaidi, S.K., Lengner, C., Montecino, M., van Wijnen, A.J., Stein, J.L. and Stein, G.S. **Regulatory controls for osteoblast growth and differentiation: role of Runx/Cbfa/AML factors**. (2004) *Crit Rev Eukaryot Gene Expr* 14 pp. 1-41.

Lian, J.B. and Stein, G.S. **Runx2/Cbfa1: a multifunctional regulator of bone formation**. (2003) *Curr Pharm Des* 9 pp. 2677-85.

Mammucari, C., Tommasi di Vignano, A., Sharov, A.A., Neilson, J., Havrda, M.C., Roop, D.R., Botchkarev, V.A., Crabtree, G.R. and Dotto, G.P. **Integration of Notch 1 and calcineurin/NFAT signaling pathways in keratinocyte growth and differentiation control**. (2005) *Dev Cell* 8 pp. 665-76.

Martinez-Martinez, S., Genesca, L., Rodriguez, A., Raya, A., Salichs, E., Were, F., Lopez-Maderuelo, M.D., Redondo, J.M. and de la Luna, S. **The RCAN carboxyl end mediates calcineurin docking-dependent inhibition via a site that dictates binding to substrates and regulators**. (2009) *Proc Natl Acad Sci U S A* 106 pp. 6117-22.

McLysaght, A., Hokamp, K. and Wolfe, K.H. **Extensive genomic duplication during early chordate evolution**. (2002) *Nat Genet* 31 pp. 200-4.

Mehta, S., Li, H., Hogan, P.G. and Cunningham, K.W. **Domain architecture of the regulators of calcineurin (RCANs) and identification of a divergent RCAN in yeast**. (2009) *Mol Cell Biol* 29 pp. 2777-93.

Messeguer, X., Escudero, R., Farre, D., Nunez, O., Martinez, J. and Alba, M.M. **PROMO: detection of known transcription regulatory elements using species-tailored searches**. (2002) *Bioinformatics* 18 pp. 333-4.

Meyer, A. and Schartl, M. **Gene and genome duplications in vertebrates: the one-to-four (-to-eight in fish) rule and the evolution of novel gene functions**. (1999) *Curr Opin Cell Biol* 11 pp. 699-704.

Minami, T., Yano, K., Miura, M., Kobayashi, M., Suehiro, J., Reid, P.C., Hamakubo, T., Ryeom, S., Aird, W.C. and Kodama, T. **The Down syndrome critical region gene 1 short variant promoters direct vascular bed-specific gene expression during inflammation in mice**. (2009) *J Clin Invest* 119 pp. 2257-70.

Morgulis, A., Coulouris, G., Raytselis, Y., Madden, T.L., Agarwala, R. and Schaffer, A.A. **Database indexing for production MegaBLAST searches**. (2008) *Bioinformatics* 24 pp. 1757-64.

Mulero, M.C., Aubareda, A., Orzaez, M., Messeguer, J., Serrano-Candelas, E., Martinez-Hoyer, S., Messeguer, A., Perez-Paya, E. and Perez-Riba, M. **Inhibiting the calcineurin-NFAT (nuclear factor of activated T cells) signaling pathway with a regulator of calcineurin-derived peptide without affecting general calcineurin phosphatase activity**. (2009) *J Biol Chem* 284 pp. 9394-401.

Mulero, M.C., Aubareda, A., Schluter, A. and Perez-Riba, M. **RCAN3, a novel calcineurin inhibitor that down-regulates NFAT-dependent cytokine gene expression**. (2007) *Biochim Biophys Acta* 1773 pp. 330-41.

Mulero Roig, M.C., Pérez Riba, M. and Celada Cotarelo, A. **Estudi de la funció de les proteïnes RCAN en l'activació limfocitària aplicació en la cerca de nous fàrmacs**

immunosupressors (2009), Universitat de Barcelona,, Barcelona http://www.tdx.cat/TDX-0210109-085418/

Narayan, A.V., Stadel, R., Hahn, A.B., Bhoiwala, D.L., Cornielle, G., Sarazin, E., Koleilat, I. and Crawford, D.R. **Redox response of the endogenous calcineurin inhibitor Adapt 78**. (2005) *Free Radic Biol Med* 39 pp. 719-27.

Nei, M.K., S. **Molecular Evolution and Phylogenetics.** (2000), Oxford University Press New York

Nicholas, K.B.N.H.B.J.D., D.W. II **GeneDoc: Analysis and Visualization of Genetic Variation**. (1997) *EMBNEW. NEWS* 4.

Ohno, S. **Evolution by gene duplication** (1970), Springer-Verlag, Berlin,

Ohno, S. **Gene duplication and the uniqueness of vertebrate genomes circa 1970-1999**. (1999) *Semin Cell Dev Biol* 10 pp. 517-22.

Ovcharenko, I., Loots, G.G., Hardison, R.C., Miller, W. and Stubbs, L. **zPicture: dynamic alignment and visualization tool for analyzing conservation profiles**. (2004) *Genome Res* 14 pp. 472-7.

Porta, S., Marti, E., de la Luna, S. and Arbones, M.L. **Differential expression of members of the RCAN family of calcineurin regulators suggests selective functions for these proteins in the brain**. (2007) *Eur J Neurosci* 26 pp. 1213-26.

Pruitt, K.D., Tatusova, T. and Maglott, D.R. **NCBI reference sequences (RefSeq): a curated non-redundant sequence database of genomes, transcripts and proteins**. (2007) *Nucleic Acids Res* 35 pp. D61-5.

Puig-Kroger, A. and Corbi, A. **RUNX3: a new player in myeloid gene expression and immune response**. (2006) *J Cell Biochem* 98 pp. 744-56.

Rand, V. **Genome evolution: a study of MHC paralogous genes in the human genome.** (2003), Ph.D. Thesis. University of Cambridge. http://www.sanger.ac.uk/Info/theses/

Rennert, J., Coffman, J.A., Mushegian, A.R. and Robertson, A.J. **The evolution of Runx genes I. A comparative study of sequences from phylogenetically diverse model organisms**. (2003) *BMC Evol Biol* 3 p. 4.

Rodriguez, A., Roy, J., Martinez-Martinez, S., Lopez-Maderuelo, M.D., Nino-Moreno, P., Orti, L., Pantoja-Uceda, D., Pineda-Lucena, A., Cyert, M.S. and Redondo, J.M. **A conserved docking surface on calcineurin mediates interaction with substrates and immunosuppressants**. (2009) *Mol Cell* 33 pp. 616-26.

Ryeom, S., Greenwald, R.J., Sharpe, A.H. and McKeon, F. **The threshold pattern of calcineurin-dependent gene expression is altered by loss of the endogenous inhibitor calcipressin**. (2003) *Nat Immunol* 4 pp. 874-81.

Rzhetsky, A.N., M **A simple method for estimating and testing minimum evolution trees**. (1992) *Molecular Biology and Evolution* 9 pp. 945-967.

Saitou, N.N., M. **The neighbor-joining method: A new method for reconstructing phylogenetic trees**. (1987) *Molecular Biology and Evolution* 4 pp. 406-425.

Sanna, B., Brandt, E.B., Kaiser, R.A., Pfluger, P., Witt, S.A., Kimball, T.R., van Rooij, E., De Windt, L.J., Rothenberg, M.E., Tschop, M.H., Benoit, S.C. and Molkentin, J.D. **Modulatory calcineurin-interacting proteins 1 and 2 function as calcineurin facilitators in vivo**. (2006) *Proc Natl Acad Sci U S A* 103 pp. 7327-32.

Shin, S.Y., Choo, S.M., Kim, D., Baek, S.J., Wolkenhauer, O. and Cho, K.H. **Switching feedback mechanisms realize the dual role of MCIP in the regulation of calcineurin activity**. (2006) *FEBS Lett* 580 pp. 5965-73.

Skrabanek, L. and Wolfe, K.H. **Eukaryote genome duplication - where's the evidence?** (1998) *Curr Opin Genet Dev* 8 pp. 694-700.

Smedley, D., Haider, S., Ballester, B., Holland, R., London, D., Thorisson, G. and Kasprzyk, A. **BioMart--biological queries made easy**. (2009) *BMC Genomics* 10 p. 22.

Spudich, G., Fernandez-Suarez, X.M. and Birney, E. **Genome browsing with Ensembl: a practical overview**. (2007) *Brief Funct Genomic Proteomic* 6 pp. 202-19.

Strippoli, P., D'Addabbo, P., Lenzi, L., Giannone, S., Canaider, S., Casadei, R., Vitale, L., Carinci, P. and Zannotti, M. **Segmental paralogy in the human genome: a large-scale triplication on 1p, 6p, and 21q**. (2002) *Mamm Genome* 13 pp. 456-62.

Strippoli, P., Lenzi, L., Petrini, M., Carinci, P. and Zannotti, M. **A new gene family including DSCR1 (Down Syndrome Candidate Region 1) and ZAKI-4: characterization from yeast to human and identification of DSCR1-like 2, a novel human member (DSCR1L2)**. (2000a) *Genomics* 64 pp. 252-63.

Strippoli, P., Petrini, M., Lenzi, L., Carinci, P. and Zannotti, M. **The murine DSCR1-like (Down syndrome candidate region 1) gene family: conserved synteny with the human orthologous genes**. (2000b) *Gene* 257 pp. 223-32.

Tamura, K.N., M.; Kumar, S. **Prospects for inferring very large phylogenies by using the neighbor-joining method**. (2004) *Proceedings of the National Academy of Sciences (USA)* 101 pp. 11030-11035.

Tamura, K.P., D.; Peterson, N.; Stecher, G.; Nei, M.; Kumar, S. **MEGA5: Molecular Evolutionary Genetics Analysis using Maximum Likelihood, Evolutionary Distance, and Maximum Parsimony Methods**. (2011) *Molecular Biology and Evolution; unpublished results*.

U, M., Shen, L., Oshida, T., Miyauchi, J., Yamada, M. and Miyashita, T. **Identification of novel direct transcriptional targets of glucocorticoid receptor**. (2004) *Leukemia* 18 pp. 1850-6.

Vega, R.B., Rothermel, B.A., Weinheimer, C.J., Kovacs, A., Naseem, R.H., Bassel-Duby, R., Williams, R.S. and Olson, E.N. **Dual roles of modulatory calcineurin-interacting protein 1 in cardiac hypertrophy**. (2003) *Proc Natl Acad Sci U S A* 100 pp. 669-74.

Vienne, A., Rasmussen, J., Abi-Rached, L., Pontarotti, P. and Gilles, A. **Systematic phylogenomic evidence of en bloc duplication of the ancestral 8p11.21-8p21.3-like region**. (2003) *Mol Biol Evol* 20 pp. 1290-8.

Wheeler, D.L., Barrett, T., Benson, D.A., Bryant, S.H., Canese, K., Chetvernin, V., Church, D.M., Dicuccio, M., Edgar, R., Federhen, S., Feolo, M., Geer, L.Y., Helmberg, W., Kapustin, Y., Khovayko, O., Landsman, D., Lipman, D.J., Madden, T.L., Maglott, D.R., Miller, V., Ostell, J., Pruitt, K.D., Schuler, G.D., Shumway, M., Sequeira, E., Sherry, S.T., Sirotkin, K., Souvorov, A., Starchenko, G., Tatusov, R.L., Tatusova, T.A., Wagner, L. and Yaschenko, E. **Database resources of the National Center for Biotechnology Information**. (2008) *Nucleic Acids Res* 36 pp. D13-21.

Wu, H., Kao, S.C., Barrientos, T., Baldwin, S.H., Olson, E.N., Crabtree, G.R., Zhou, B. and Chang, C.P. **Down syndrome critical region-1 is a transcriptional target of**

nuclear factor of activated T cells-c1 within the endocardium during heart development. (2007a) *J Biol Chem* 282 pp. 30673-9.

Wu, H., Peisley, A., Graef, I.A. and Crabtree, G.R. **NFAT signaling and the invention of vertebrates**. (2007b) *Trends Cell Biol* 17 pp. 251-60.

Yang, J., Rothermel, B., Vega, R.B., Frey, N., McKinsey, T.A., Olson, E.N., Bassel-Duby, R. and Williams, R.S. **Independent signals control expression of the calcineurin inhibitory proteins MCIP1 and MCIP2 in striated muscles**. (2000) *Circ Res* 87 pp. E61-8.

Yang, J.Y., Jung, J.Y., Cho, S.W., Choi, H.J., Kim, S.W., Kim, S.Y., Kim, H.J., Jang, C.H., Lee, M.G., Han, J. and Shin, C.S. **Chloride intracellular channel 1 regulates osteoblast differentiation**. (2009) *Bone* 45 pp. 1175-85.

Zuckerkandl, E.P., L. **Evolutionary divergence and convergence in proteins in Evolving Genes and Proteins** (1965), Academic Press, New York.

FIGURES AND TABLES

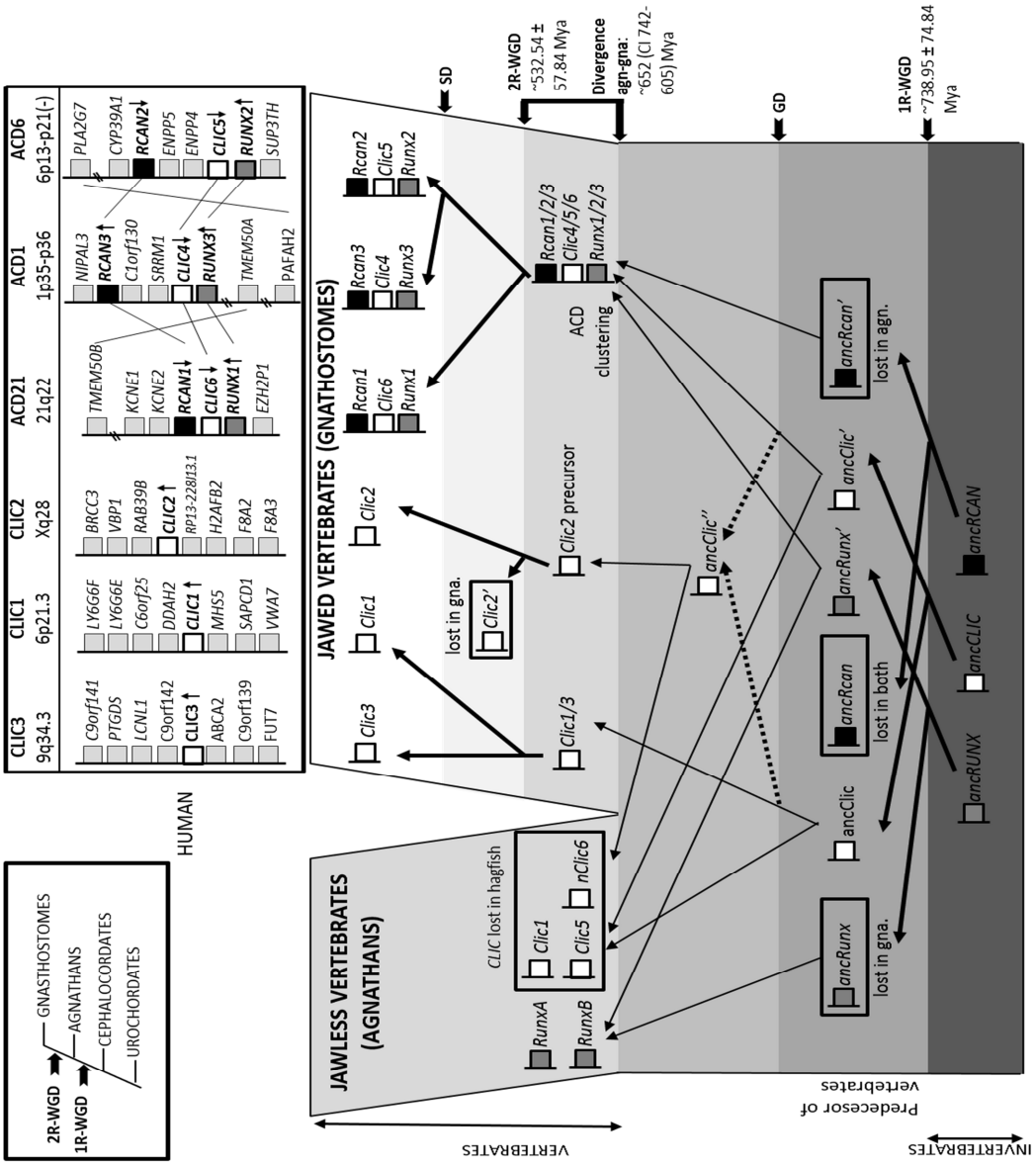

Figure 1. RCAN gene family evolution. Left upper panel summarizes phylogenetic relationship of chordates and the two rounds of whole-genome duplication (1R-WGD and 2R-WGD) postulated at the origin of vertebrates. Invertebrates have a single copy of *Rcan*, *Clic* and *Runx* genes, while in jawed vertebrates they diverged into multigenic families. Living agnathan organisms (jawless vertebrates; hagfish and lamprey) have two copies of Runx genes and only lamprey has three functional *Clic* genes, but no *RCAN* orthologs have been found in these species. In jawed vertebrates, all members of *Runx* and *Rcan* families and three members of the *Clic* family are located in ACD clusters. The two rounds of whole-genome duplication (1R-WGD and2R-WGD), occasioned the appearance of *Clic3*, *Clic1*, ACD21 cluster, and ACD1/6 cluster precursor. A posterior segmental duplication may be the origin of ACD1 and ACD6 clusters. ACD6 cluster is represented in inverted direction (-). *Clic2* (dot line) may be originated by gene duplication, before the 2R-WGD from either *Clic1/3* or *Clic4/5/6* precursor. Human genes and their chromosomal context are indicated in the right upper panel. *CLIC*, *RUNX* and *RCAN* ACD cluster members are represented in white, dark grey and black boxes, respectively, while other human genes are represented in light grey. The thicker arrows indicate gene duplication events. Abbreviations: anc: ancestral; GD: hypothesized single Gene Duplication; SD= Segmental Duplication; WGD= Whole Genome Duplication; Mya = Million Years Ago; agn= agnathans; gna= gnathostomes; CI= confidence interval. All chromosome locations are referred to human. Estimated times of 1R-WGD, 2R-WGD and divergence agn-gna were obtained from Vienne *et al.*, 2003 and Blair and Hedges, 2005, respectively. In the right upper panel (HUMAN), double transversal lines indicate that some genes where omitted in the representation for simplicity, arrows indicate the direction of the gene transcription and connecting lines link paralogous genes.

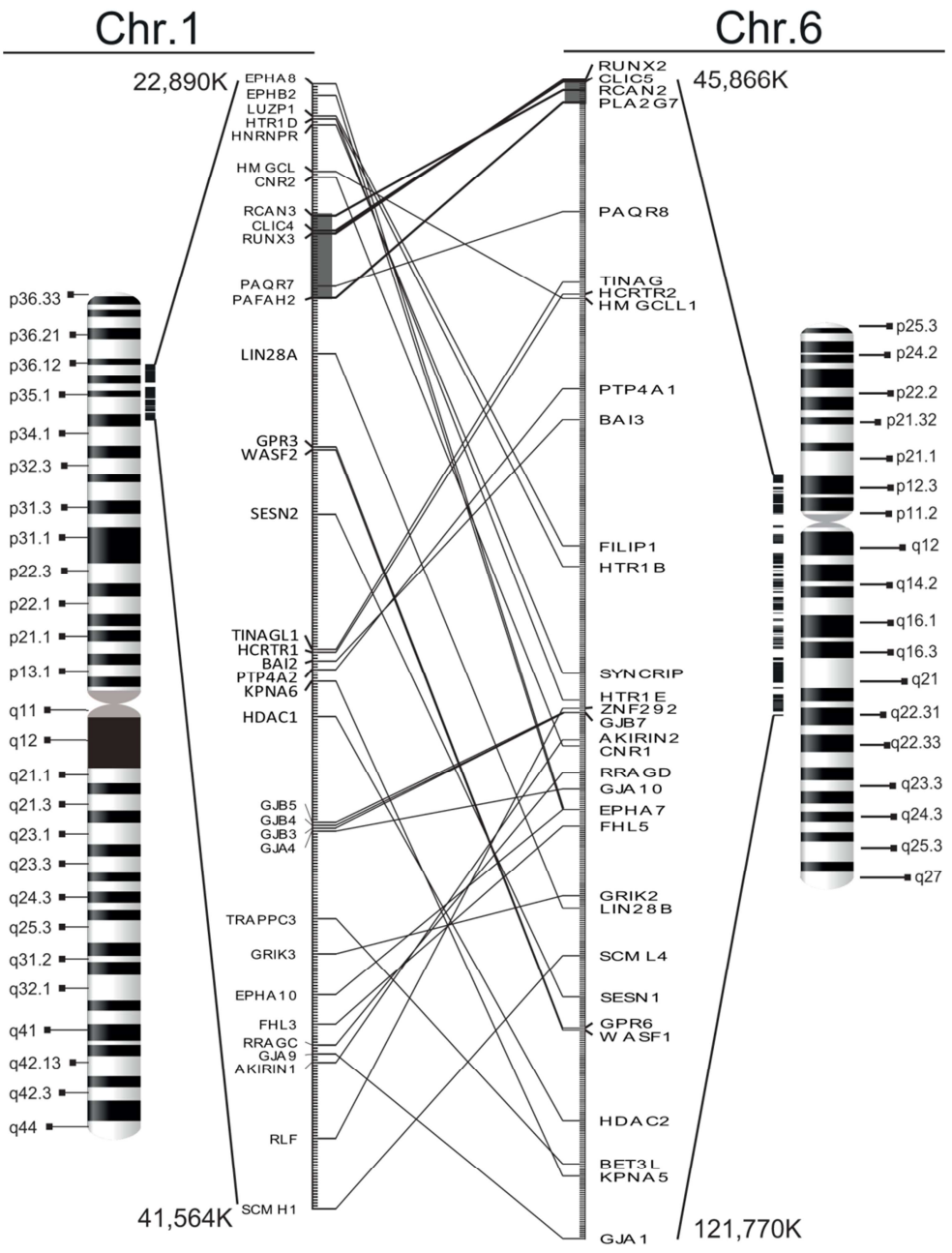
Chr.1
Chr.6
22,890K
41,564K
45,866K
121,770K
EPHA8
EPHB2
LUZP1
HTR1D
HNRNPR
HMGCL
CNR2
RCAN3
CLIC4
RUNX3
PAQR7
PAFAH2
LIN28A
GPR3
WASF2
SESN2
TINAGL1
HCRTR1
BAI2
PTP4A2
KPNA6
HDAC1
GJB5
GJB4
GJB3
GJA4
TRAPPC3
GRIK3
EPHA10
FHL3
RRAGC
GJA9
AKIRIN1
RLF
SCMH1
RUNX2
CLIC5
RCAN2
PLA2G7
PAQR8
TINAG
HCRTR2
HMGCLL1
PTP4A1
BAI3
FILIP1
HTR1B
SYNCRIP
HTR1E
ZNF292
GJB7
AKIRIN2
CNR1
RRAGD
GJA10
EPHA7
FHL5
GRIK2
LIN28B
SCML4
SESN1
GPR6
WASF1
HDAC2
BET3L
KPNA5
GJA1
p36.33
p36.21
p36.12
p35.1
p34.1
p32.3
p31.3
p31.1
p22.3
p22.1
p21.1
p13.1
q11
q12
q21.1
q21.3
q23.1
q23.3
q24.3
q25.3
q31.2
q32.1
q41
q42.13
q42.3
q44
p25.3
p24.2
p22.2
p21.32
p21.1
p12.3
p11.2
q12
q14.2
q16.1
q16.3
q21
q22.31
q22.33
q23.3
q24.3
q25.3
q27

Figure 2. Large-scale segmental duplication between chromosome 1 and chromosome 6 is determined by the presence of paralogous genes. The existence of more than 30 paralogous genes located within the flanking regions of the ACD1 and ACD6 clusters (marked in grey) suggests a large-scale (>18 Mb) segmental duplication among chromosome 1 (HSA1, p-arm) and chromosome 6 (HSA6, p- and q-arms). Each line connects two paralogous genes. Ideograms of both chromosomes are displayed, where dark and white bands represent G and R bands, respectively, as well as chromosome coordinates serve as a guide to positioning the duplicated segment.

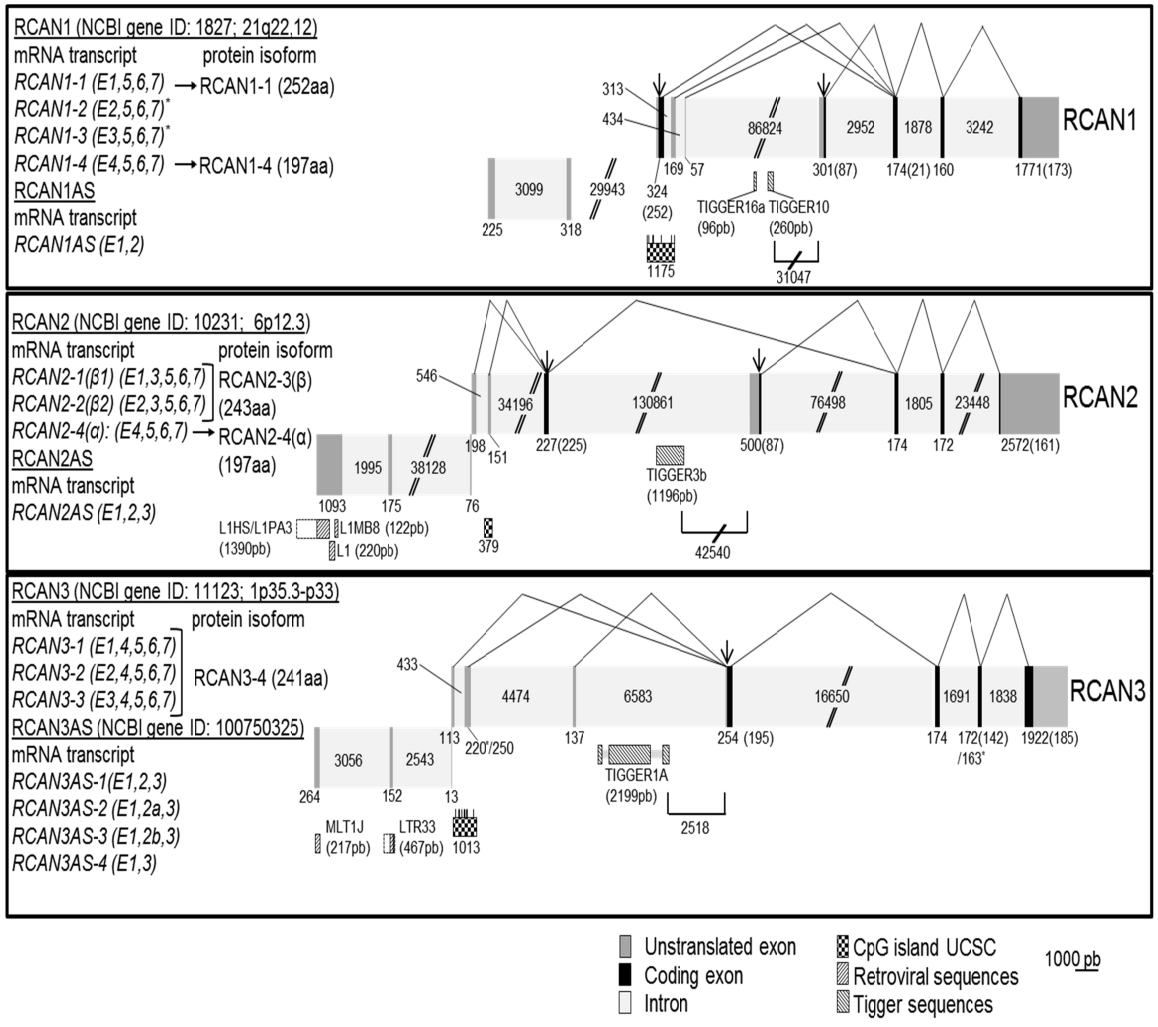
RCAN1 (NCBI gene ID: 1827; 21q22.12)
mRNA transcript
protein isoform
RCAN1-1 (E1,5,6,7) → RCAN1-1 (252aa)
RCAN1-2 (E2,5,6,7)*
RCAN1-3 (E3,5,6,7)*
RCAN1-4 (E4,5,6,7) → RCAN1-4 (197aa)
RCAN1AS
mRNA transcript
RCAN1AS (E1,2)
313
434
86824
2952
1878
3242
RCAN1
169
57
301(87)
174(21)
160
1771(173)
3099
29943
324
(252)
225
318
TIGGER16a
(96pb)
TIGGER10
(260pb)
1175
31047
RCAN2 (NCBI gene ID: 10231; 6p12.3)
mRNA transcript
protein isoform
RCAN2-1(β1) (E1,3,5,6,7)
RCAN2-2(β2) (E2,3,5,6,7)
RCAN2-3(β)
(243aa)
RCAN2-4(α): (E4,5,6,7) → RCAN2-4(α)
(197aa)
RCAN2AS
mRNA transcript
RCAN2AS (E1,2,3)
546
34196
130861
76498
1805
23448
RCAN2
198
151
227(225)
500(87)
174
172
2572(161)
1995
38128
1093
175
76
TIGGER3b
(1196pb)
42540
L1HS/L1PA3
(1390pb)
L1MB8 (122pb)
L1 (220pb)
379
RCAN3 (NCBI gene ID: 11123; 1p35.3-p33)
mRNA transcript
protein isoform
RCAN3-1 (E1,4,5,6,7)
RCAN3-2 (E2,4,5,6,7)
RCAN3-3 (E3,4,5,6,7)
RCAN3-4 (241aa)
RCAN3AS (NCBI gene ID: 100750325)
mRNA transcript
RCAN3AS-1(E1,2,3)
RCAN3AS-2 (E1,2a,3)
RCAN3AS-3 (E1,2b,3)
RCAN3AS-4 (E1,3)
433
4474
6583
16650
1691
1838
RCAN3
113
220*/250
137
254 (195)
174
172(142)
/163*
1922(185)
3056
2543
264
152
13
TIGGER1A
(2199pb)
2518
MLT1J
(217pb)
LTR33
(467pb)
1013
Unstranslated exon
Coding exon
Intron
CpG island UCSC
Retroviral sequences
Tigger sequences
1000 pb

Figure 3. Gene structure comparison of the human RCAN family members. The three members of the human *RCAN* gene family include seven exons, being the last three exons coding exons of which the encoded amino acid sequence is highly conserved between the three paralogous proteins (see Figure S3). Alternative transcripts arise mainly from alternative splicing of the first exons in each mRNA form. Arrows indicate translation start sites. Lines connecting exons indicate splicing forms of each *RCAN* gene. Double lines in intron regions refer to non-scaled intron length. Numbers indicate intron and exon sizes. Numbers in parenthesis indicate coding nucleotides within exons containing untranslated and translated regions. Vertical bars above CpG island associated to *RCAN1* and *RCAN3* correspond to the exactly positions of the metilation probes included in the methylation array. Asterisks in *RCAN1* mRNA forms (*) indicate that these transcripts have not been detected at protein level. Note that *RCAN3* exon numbering follows the new nomenclature outlined in Figure 4 and only the *RCAN3* mRNA transcripts that code for RCAN3-4 protein isoform are represented. Natural antisense transcripts (NATs) related with each *RCAN* gene and regions with homology with retroviruses (in NATs and intron 3) are also shown.

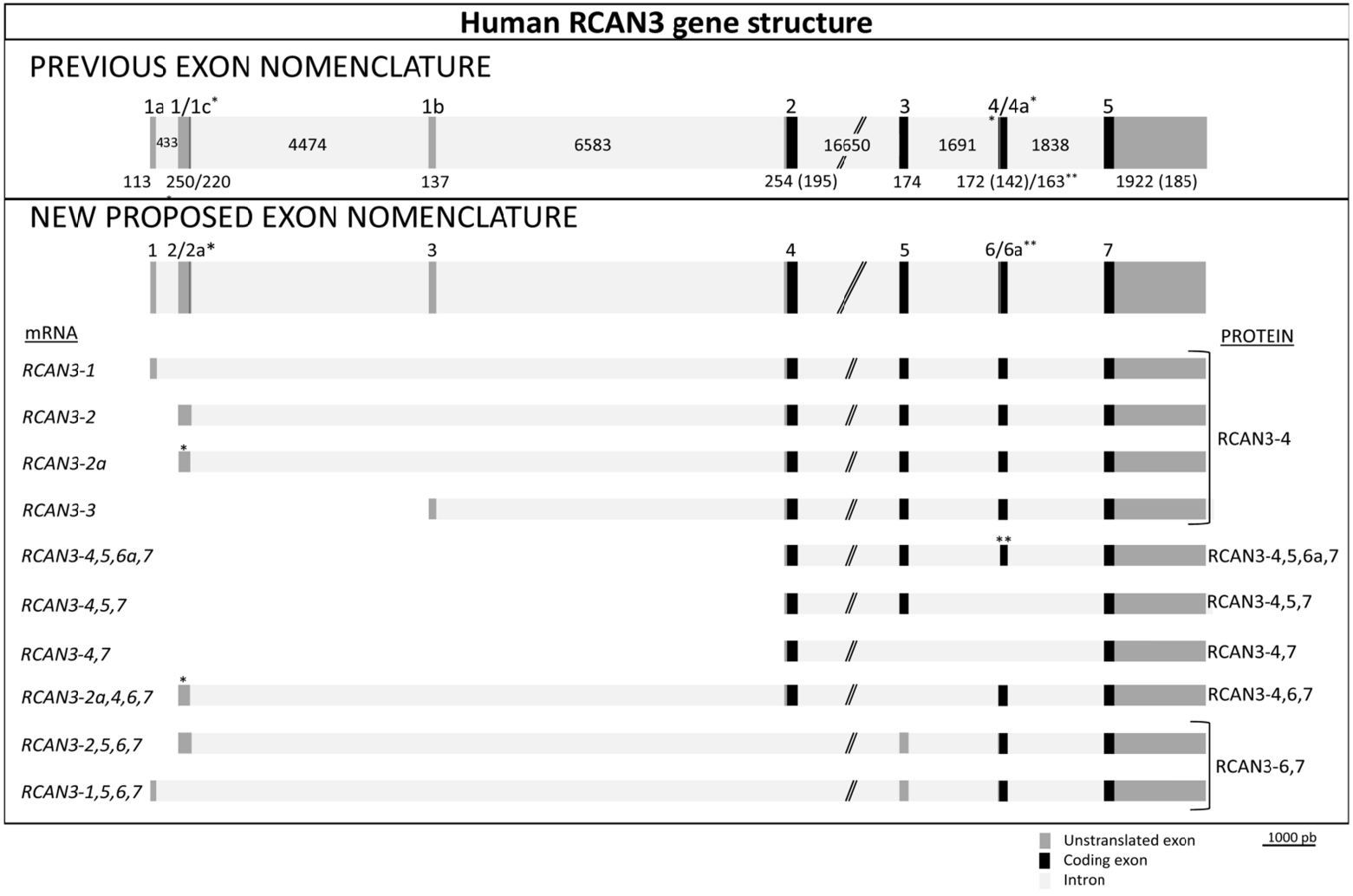
Human RCAN3 gene structure
PREVIOUS EXON NOMENCLATURE
1a
1/1c*
1b
2
3
4/4a*
5
433
4474
6583
16650
1691
1838
113
250/220
137
254 (195)
174
172 (142)/163**
1922 (185)
NEW PROPOSED EXON NOMENCLATURE
1
2/2a*
3
4
5
6/6a**
7
mRNA
PROTEIN
RCAN3-1
RCAN3-2
RCAN3-2a
RCAN3-3
RCAN3-4
RCAN3-4,5,6a,7
RCAN3-4,5,6a,7
RCAN3-4,5,7
RCAN3-4,5,7
RCAN3-4,7
RCAN3-4,7
RCAN3-2a,4,6,7
RCAN3-4,6,7
RCAN3-2,5,6,7
RCAN3-1,5,6,7
RCAN3-6,7
Unstranslated exon
Coding exon
Intron
1000 pb

Figure 4. Human RCAN3 gene structure, alternative splicing, and protein isoforms. The scheme shows the new proposed exon nomenclature in comparison to the previously established (reviewed in Davies et al, 2007) taking into account the recently described new exons (Facchin *et al.*, 2011) and those transcripts accepted in the RefSeq database (Pruitt *et al.*, 2007; Wheeler *et al.*, 2008). Black rectangles correspond to coding exons, dark grey rectangles to non-coding exons (5' and 3' UTR) and light grey rectangles correspond to intron regions. All intron and exon sizes (in bp) are indicated and represented in scale, except for intron 4. In parenthesis, size of the coding sequence in those exons that contain untranslated and translated regions. Exon 1 transcription start site (TSS) is the unique that has been demonstrated by 5' RACE. *RCAN3-1*, *RCAN3-2*, *RCAN3-2a* and *RCAN3-3* mRNA forms, all including coding exons 4, 5, 6 and 7, are translated into the same protein, named RCAN3-4, the longest known isoform for RCAN3 (241 amino acids) and the only one detected at the endogenous level. Asterisks indicate presence of a particular exon in specific transcripts: *RCAN3-2a* and *RCAN3-2a,4,6,7* transcripts include the non-coding exon 2a, an in-frame shorter variant of exon 2, and *RCAN3-4,5,6a,7* transcript includes the coding exon 6a that lacks an in-frame 30 nt length segment of exon 6.

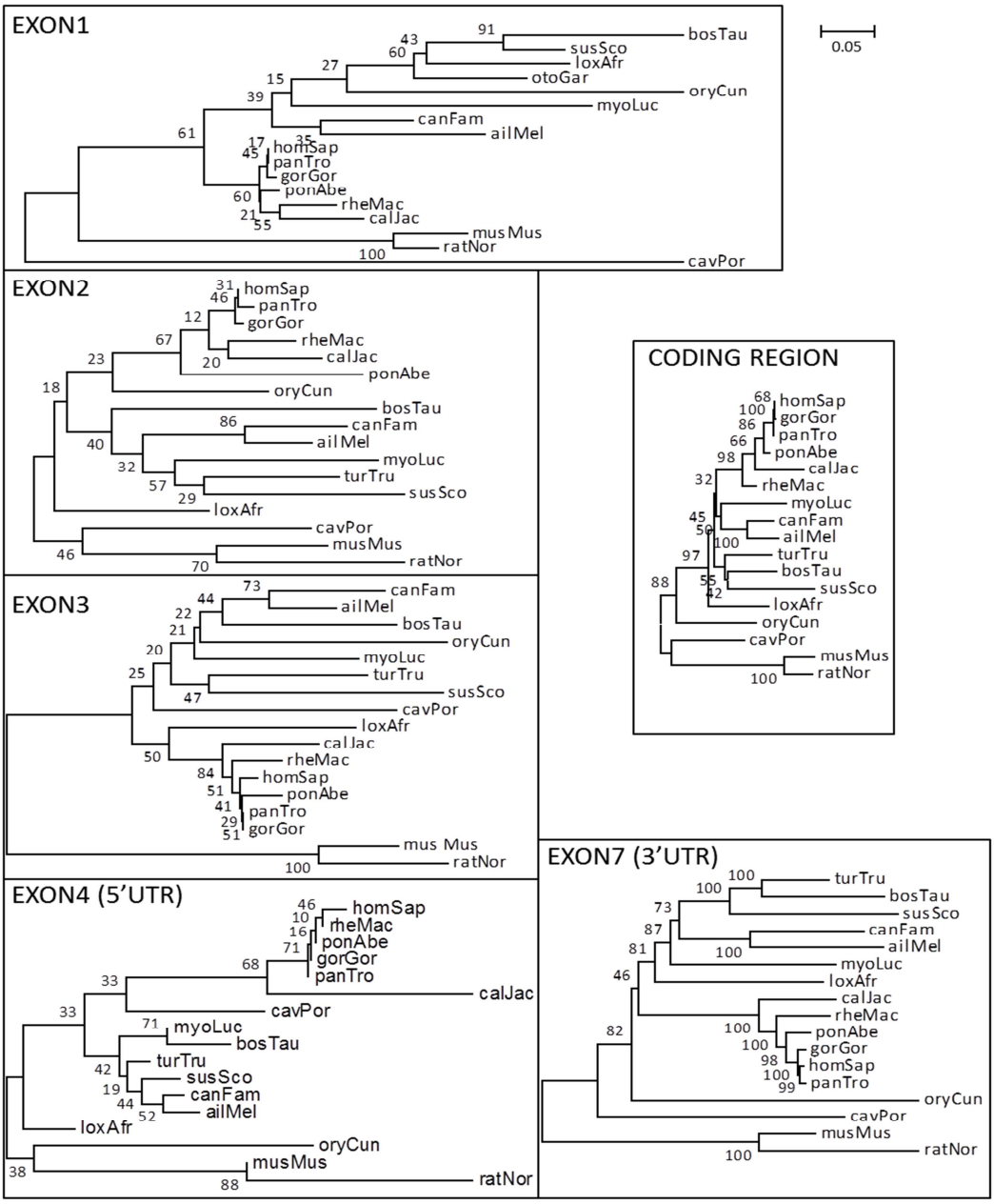
EXON1
0.05
bosTau
susSco
loxAfr
otoGar
oryCun
myoLuc
canFam
ailMel
homSap
panTro
gorGor
ponAbe
rheMac
calJac
musMus
ratNor
cavPor
EXON2
homSap
panTro
gorGor
rheMac
calJac
ponAbe
oryCun
bosTau
canFam
ailMel
myoLuc
turTru
susSco
loxAfr
cavPor
musMus
ratNor
CODING REGION
homSap
gorGor
panTro
ponAbe
calJac
rheMac
myoLuc
canFam
ailMel
turTru
bosTau
susSco
loxAfr
oryCun
cavPor
musMus
ratNor
EXON3
canFam
ailMel
bosTau
oryCun
myoLuc
turTru
susSco
cavPor
loxAfr
calJac
rheMac
homSap
ponAbe
panTro
gorGor
mus Mus
ratNor
EXON4 (5'UTR)
homSap
rheMac
ponAbe
gorGor
panTro
calJac
cavPor
myoLuc
bosTau
turTru
susSco
canFam
ailMel
loxAfr
oryCun
musMus
ratNor
EXON7 (3'UTR)
turTru
bosTau
susSco
canFam
ailMel
myoLuc
loxAfr
calJac
rheMac
ponAbe
gorGor
homSap
panTro
oryCun
cavPor
musMus
ratNor

Figure 5. Phylogenetic analysis of the RCAN3 exons in vertebrates. Human *RCAN3* genomic sequence corresponding to first exons (exon 1, 2 and 3) and to exon 4 untranslated regions (5' UTR), coding region (exon 4, 5, 6 and 7) and exon 7 untranslated region (3' UTR) were compared with the sequences of several vertebrate *RCAN3* orthologs. DNA sequences for the different species were retrieved from Ensembl database (Birney *et al.*, 2004) and used for subsequent phylogenetic analysis, as described in Material and Methods section. All primate genomic sequences appear as very closely related sequences, while rodent sequences (*Mus musculus*, *Rattus norvegicus* and *Cavia porcellus*) are the more divergent among all the mammals in all cases, except for exon 3 and the short 5'UTR sequence on exon 4. Studied species and genome sequence versions used were: *Homo sapiens* (v.GRCh37.p7 Feb 2009), *Pan troglodites* (panTro, Chimpanzee; v.2.1.4 Feb 2011), *Gorilla gorilla* (gorGor, v.3.1 Dec 2009), *Pongo abelii* (ponAbe, Orangutan; v.2 Sep 2007), *Macaca mulatta* (rheMac; v.1.0 Feb 2006), *Callithrix jacchus* (calJac, Marmoset; v.3.2.1 Jan 2010), *Cavia porcellus* (cavPor, Guinea Pig; v.3 Mar 2008), *Sus scorfa* (susSco, Pig; v. 10.2_Aug 2011), *Mus musculus* (musMus, Mouse; v.37 Apr 2007), *Rattus norvegicus* (rarNor, Rat; v.3.4 Dec 2004), *Oryctolagus cuniculus* (oryCun, Rabbit; v.2 Nov 2009), *Ailuropoda melanoleuca* (ailMel, Panda; v.1 Jul 2009), *Canis lupus familiaris* (canFam, Dog; v.2.0 May 2006), *Bos taurus* (bosTau, Cow; v.3.1 Nov 2009), *Tursiops truncates* (turTru, Dolphin; v.1 Jul 2008), *Loxodonta africana* (loxAfr, Elephant; v.3.0 Jul 2009), *Myotis lucifugus* (myoLuc, Microbat; v.2.0 Sep 2010).

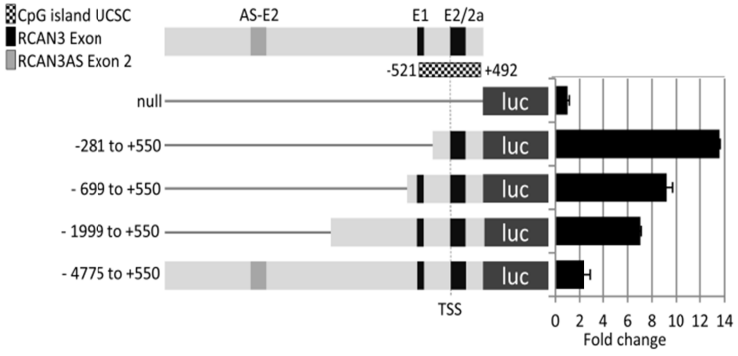
CpG island UCSC
RCAN3 Exon
RCAN3AS Exon 2
AS-E2
E1
E2/2a
-521
+492
null
-281 to +550
- 699 to +550
- 1999 to +550
- 4775 to +550
luc
TSS
0 2 4 6 8 10 12 14
Fold change

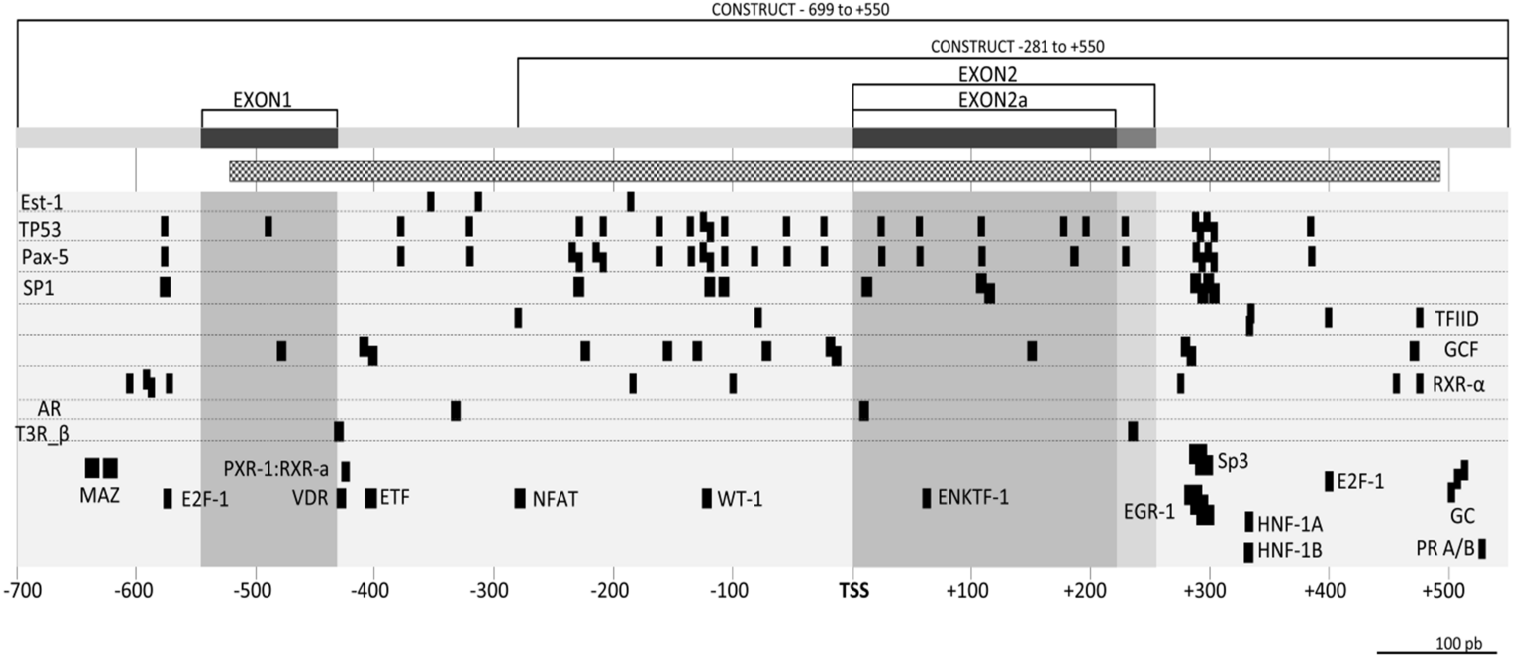
CONSTRUCT - 699 to +550
CONSTRUCT -281 to +550
EXON1
EXON2
EXON2a
Est-1
TP53
Pax-5
SP1
TFIID
GCF
RXR-α
AR
T3R_β
MAZ
E2F-1
PXR-1:RXR-a
VDR
ETF
NFAT
WT-1
ENKTF-1
Sp3
EGR-1
E2F-1
HNF-1A
HNF-1B
GC
PR A/B
-700
-600
-500
-400
-300
-200
-100
TSS
+100
+200
+300
+400
+500
100 pb

Figure 6. Transcriptional activity and in silico prediction of Transcription Factors Binding Sites (TFBS) along the 5' region of the RCAN3 gene. A) Left, schematic representation of serial DNA regions 5' flanking the TSS of the *RCAN3-2/2a* transcripts cloned into a pGL3-luc promoterless reporter vector (see details in Materials and Methods). The 5' flanking region of each construct is shown in bp referred to the TSS of exon 2. TSS (+1) is indicated with a vertical dashed line. Black boxes correspond to *RCAN3* non-coding exons 1 (E1) and 2/2a (E2/2a), and the dark grey box corresponds to exon 2 of RCAN3AS (E2AS). Squared box indicates the CpG island located surounding 2/2a exon. Right, luciferase reporter assays in HEK 293T cells transfected with 30 fmol of each construct. Results are presented as a fold-change relative to the activity of the empty vector. The graph shows the mean ± SD of three independent experiments performed in triplicate. B) *In silico* prediction of human TFBS in -700 to +550 region respect to the TSS of exon 2 using PROMO software (Messeguer *et al.*, 2002; Farre *et al.*, 2003). Exons 1 and 2/2a relative position are indicated above as dark grey boxes and the CpG island as a squared box. Guide number below indicates distances respect TSS of *RCAN3-2/2a* transcripts. Predicted TFBS are indicated as dark boxes with the name of the transcription factor next to the boxes or left or right at the same level when multiple predictions for the same factor.

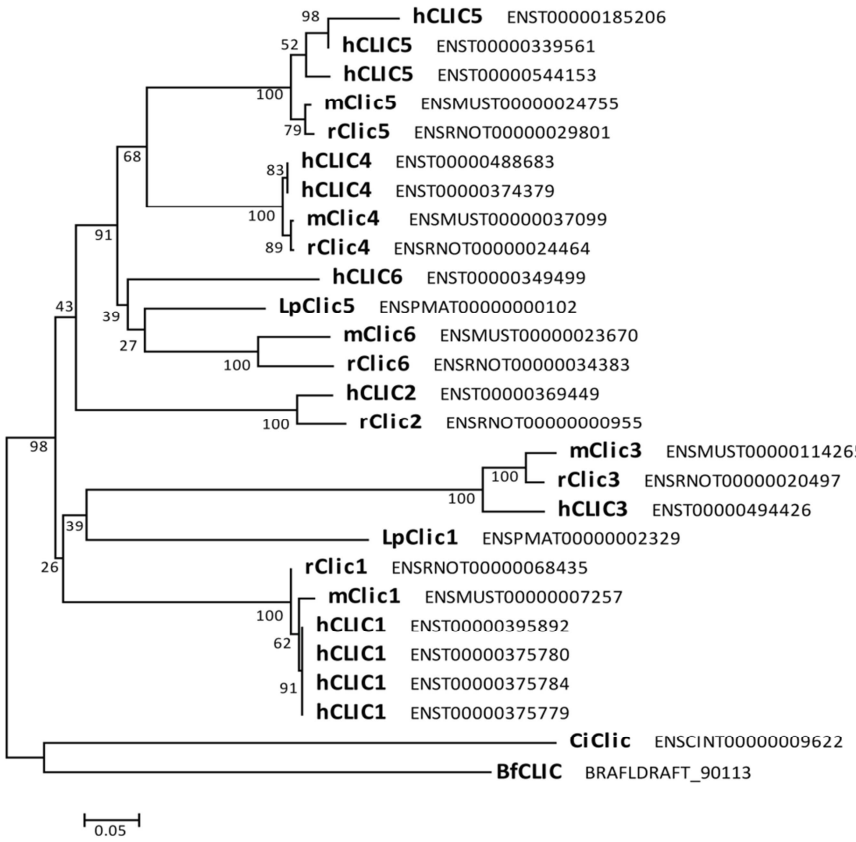

Figure S1. Phylogenetic analysis of CLIC proteins. Sequences of the known functional Lamprey Clic proteins (named LpClic1 and LpClic5) were retrieved from Ensembl database (Birney *et al.*, 2004) and used for subsequent phylogenetic analysis, as described in Material and Methods section, together with all human, mouse and rat CLIC protein isoforms (hCLIC, mClic and rClic; respectively). Note that Ensembl database contains three lamprey CLIC genes: *LpClic1*, *LpClic5* and *LpClic6*.). Since *nLpClic6* sequence it is incomplete, it has been excluded from the analysis. The obtained evolutionary tree shown here relates LpClic1 with human and rodent CLIC1/3 and LpClic5 with human and rodent CLIC4/5/6. Ensembl names for each transcript and Uniprot reference for *Branchiostoma floridae* protein are indicated.

A

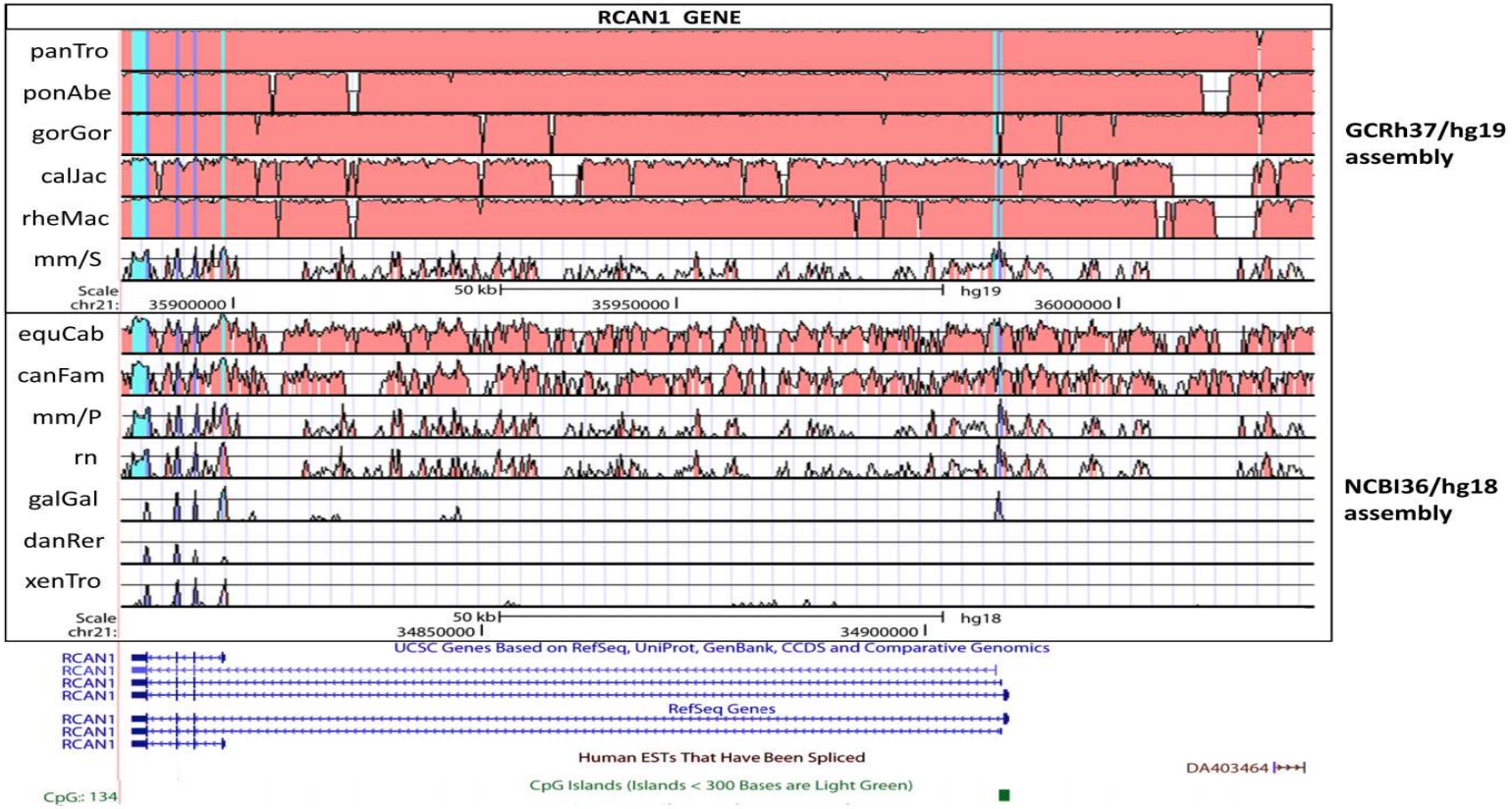

Figure S2A. Comparative genomic sequence analysis of *RCAN* genes

B

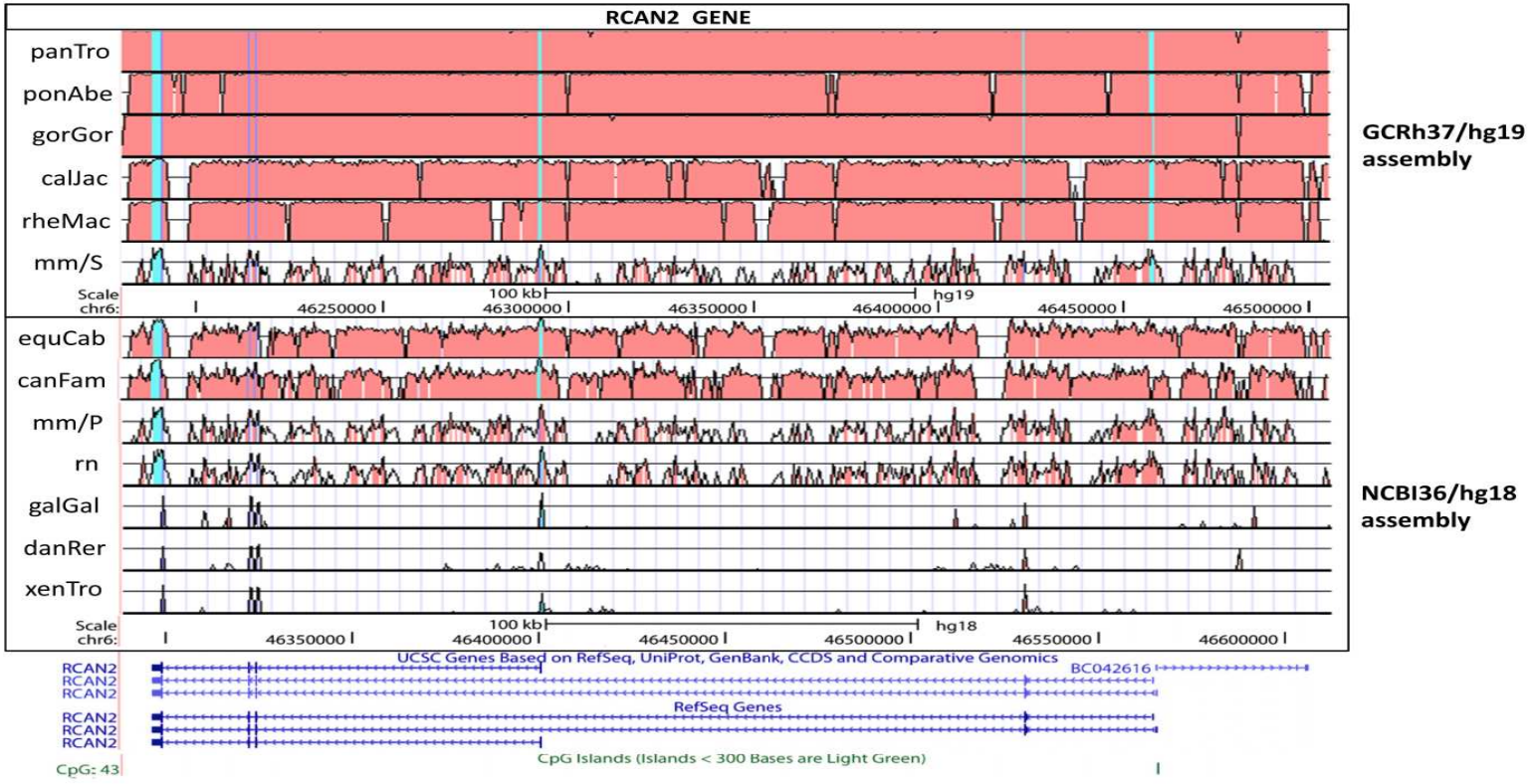

Figure S2B. Comparative genomic sequence analysis of *RCAN* genes

C

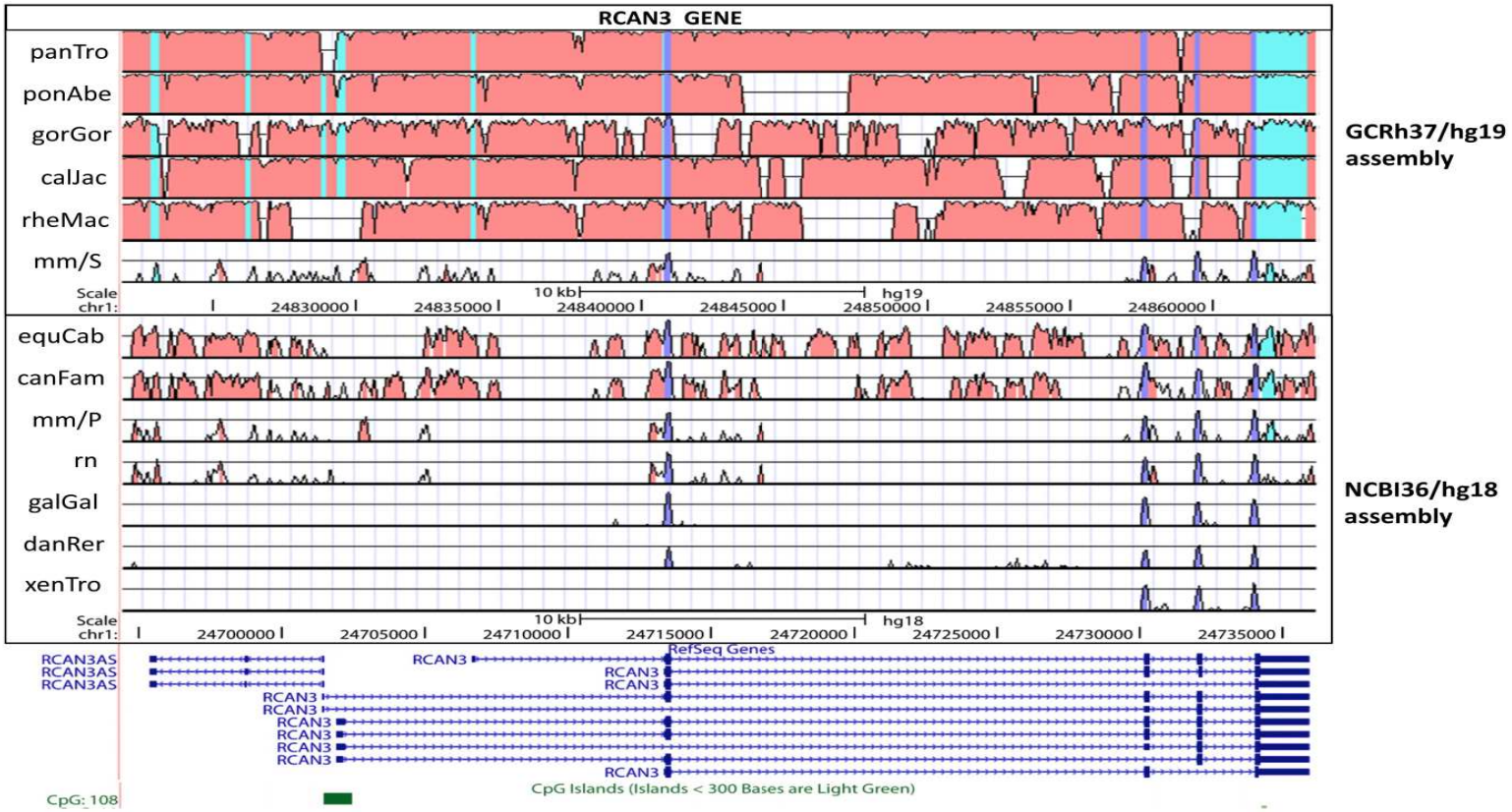

Figure S2C. Comparative genomic sequence analysis of *RCAN* genes

Figure S2. Comparative genomic sequence analysis of RCAN genes. Alignment plots of *RCAN1* (A)*, RCAN2* (B) and *RCAN3* (C) orthologs against human *RCAN* genes created by the VISTA tool of UCSC browser (Frazer *et al.*, 2004; Birney *et al.*, 2004) using Feb.2009-GRCh37/hg19 genome version for primates and mouse (SLAGAN alignment) and Mar.2006-NCBI36/hg18 for the rest of organism. Chromosomal scale and base pairs position guide are represented below the global comparative alignment in each assembly. All alignments are PROLAGAN alignments except if it is specified otherwise. The vertebrate genomes used in the alignments against human sequences were: *Pan troglodites* (panTro, Chimpanzee; Mar 2006), *Pongo abelii* (ponAbe, Orangutan; Jul 2007), *Gorilla gorilla* (gorGor; Dec 2009; SLAGAN alignment), *Callithrix jacchus* (calJac, Marmoset; Jun 2007), *Macaca mulatta* (rheMac; Jan 2006), *Mus musculus* (musMus/S; Jul 2007; SLAGAN alignment), *Equus caballus* (equCab, Horse; Jan 2007), *Canis lupus familiaris* (canFam, Dog; May 2005 v.80), *Mus musculus* (musMus/P; Jul 2007), *Rattus norvegicus* (ratNor, Rat; Nov 2004), *Gallus gallus* (galGal, Chicken; May 2006 v.55), *Danio rerio* (danRer, Zebrafish; Mar 2006; SLAGAN alignment), and *Xenopus tropicalis* (xenTro, Frog; Aug 2005; SLAGAN alignment). In plots, darker blue indicates coding regions; lighter blue, unstranslated regions (UTR) and pink, non-coding DNA sequence. 5' UTR and 3' UTR regions are conserved in primates and, in a lesser extent, in other mammals, although they are not always annotated. *RCAN* RefSeq transcripts are shown below the alignment. Arrows in transcripts indicate the sense of gene transcription and, therefore, the order of the exons (darker blue boxes). UCSC registered CpG islands are indicated below in green. A) Comparative genomic analysis of vertebrate *RCAN1* genes relative to the human gene (NCBI gene ID: 1827). The natural antisense transcript (NAT) *DA403464* is registered as human UCSC EST. B) Comparative genomic analysis of vertebrate *RCAN2* genes relative to the human gene (NCBI gene ID: 10231). *BC042616* gene (*RCAN2AS*) is registered as UCSC gene. C) Comparative analysis of the vertebrate *RCAN3* genes relative to the human gene (NCBI gene ID: 11123). *RCAN3* transcripts and *RCAN3AS* NATs, accepted as RefSeq genes, are shown.

A

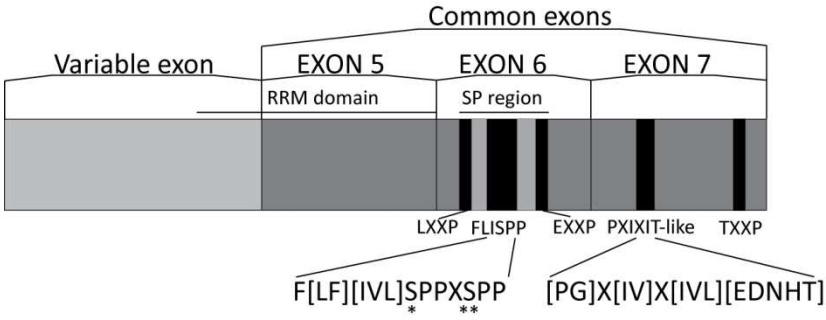

B

	hRCAN1-1	hRCAN1-4	hRCAN2-3	hRCAN2-4	hRCAN3
hRCAN1-1	100%	-	-	-	-
hRCAN1-4	100%	100%	-	-	-
hRCAN2-3	65%	65%	100%	-	-
hRCAN2-4	65%	65%	100%	100%	-
hRCAN3	60%	60%	68%	68%	100%

Figure S3 A and B. Alignment of human RCAN proteins. A) Schematic representation of RCAN protein structure. The last three exons (exon 5, 6 and 7 in RCAN1 and RCAN2; exon 3, 4 and 5 in RCAN3) are common to all RCAN isoforms; and the variable exon results from alternative splicing. GSK3β (*) and MAPK, BMK1 or DYRK1A (**) phosphorylation sites within the FLISPP motif, important in RCAN regulation, are indicated. B) Table indicates percentage of amino acid conservation among the C-terminal region of all human proteins.

C

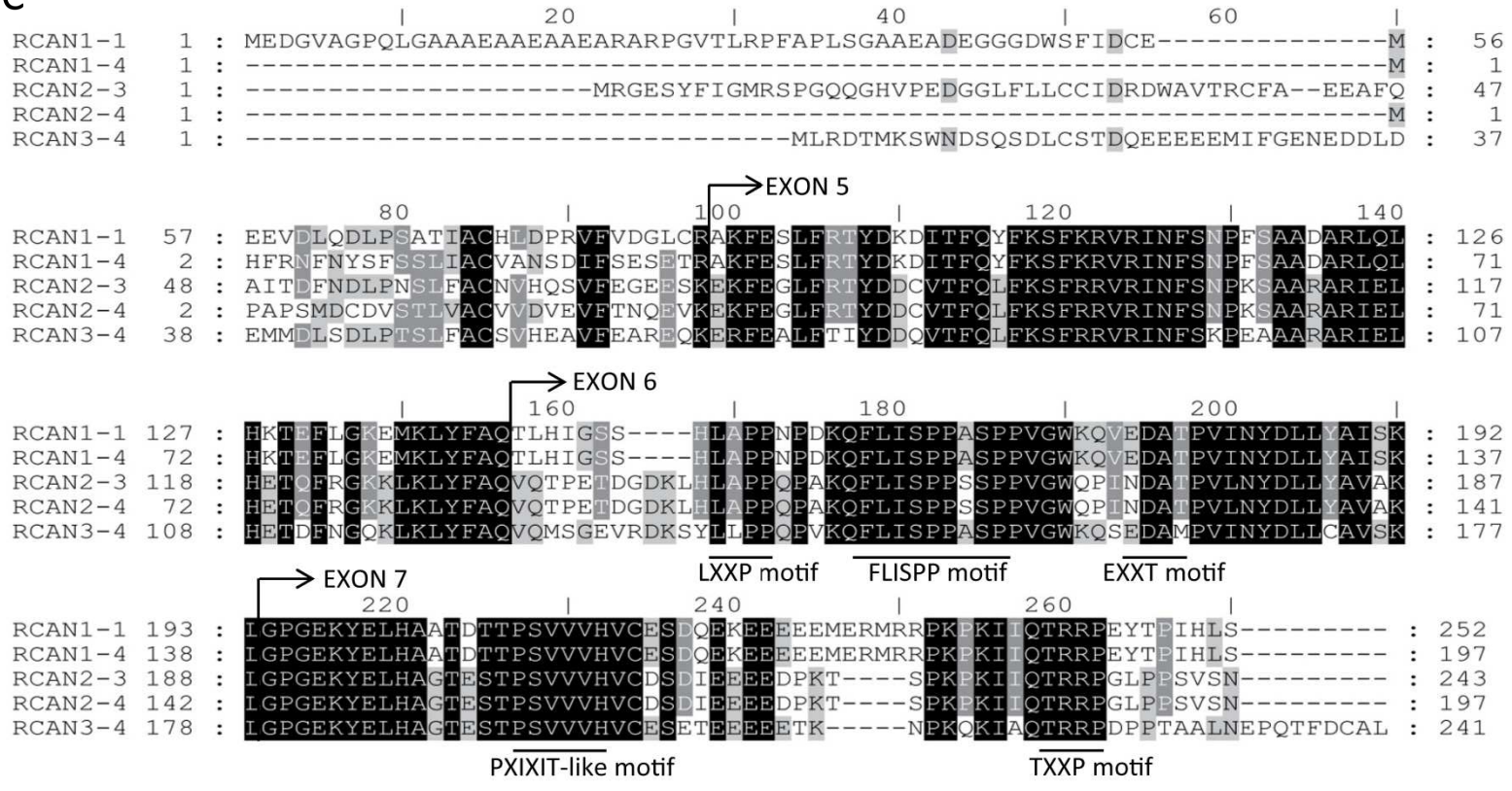
EXON 5
EXON 6
EXON 7
LXXP motif
FLISPP motif
EXXT motif
PXIXIT-like motif
TXXP motif

Figure S3 C. Alignment of human RCAN proteins. C) Protein sequence alignment among the different protein isoforms encoded by human RCAN genes [protein RefSeq acc. number: RCAN1-1, NP_004405.3 (252 aa); RCAN1-4, NP_981963.1 (197 aa); RCAN2α, NP_005813.2 (197 aa); RCAN2β, NP_001238902.1 / NP_001238903.1 (243 aa); RCAN3-4, NP_038469.1 / NP_001238906.1 / NP_001238907.1 / NP_001238908.1 (241 aa)]. All of them share exons 5 to 7, according to the new proposed nomenclature. The first exon of each protein has some conserved residues that may be important for its functional activity and/or regulation. Grey intensity shade increases with sequence conservation (50, 80 or 100% of amino acid conservation). Numbers correspond to amino acid positions for each protein. Conserved motifs are indicated.

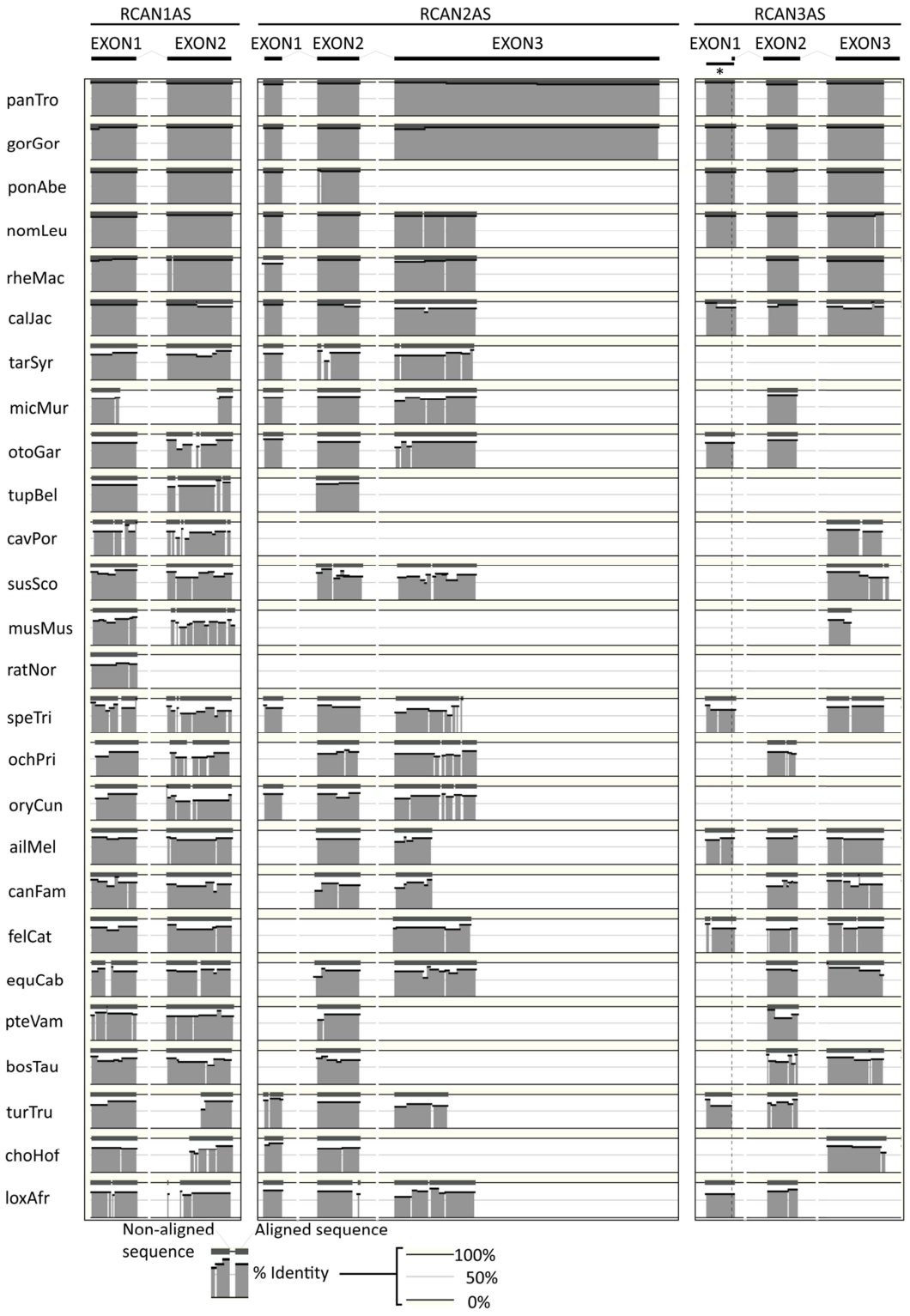
RCAN1AS
RCAN2AS
RCAN3AS
EXON1
EXON2
EXON1
EXON2
EXON3
EXON1
EXON2
EXON3
*
panTro
gorGor
ponAbe
nomLeu
rheMac
calJac
tarSyr
micMur
otoGar
tupBel
cavPor
susSco
musMus
ratNor
speTri
ochPri
oryCun
ailMel
canFam
felCat
equCab
pteVam
bosTau
turTru
choHof
loxAfr
Non-aligned sequence
Aligned sequence
% Identity
100%
50%
0%

Figure S4. Multi-species alignment of human RCAN1, RCAN2 and RCAN3 natural antisense transcripts: RCAN1AS, RCAN2AS and RCAN3AS. Pip-type graph conservation profile of human *RCAN1AS* (*DA403464* EST), *RCAN2AS* (*BC042616* gene) and *RCAN3AS* (NCBI gene ID: 100750325; Facchin *et al.*, 2011) in several eutherian mammals. Sequences were obtained using the genomic comparison tool of the Ensembl database (Birney *et al.*, 2004) and alignments were generated and visualized by zPicture software (Ovcharenko *et al.*, 2004). Asterisk (*) indicates the region of exon 1 of *RCAN3-1* transcript that was manually included to the alignment due to the impossibility to align sequences shorter than 19 nt (*RCAN3AS* exon 1 length is only 13 nt). Non-aligned regions correspond to gaps in the genome sequence. Species and genomes assemblies used for the analysis were: *Homo sapiens* (v.GRCh37.p7 Feb 2009), *Pan troglodites* (panTro, Chimpanzee; v.2.1.4 Feb 2011), *Gorilla gorilla* (gorGor, v.3.1 Dec 2009), *Pongo abelii* (ponAbe, Orangutan; v.2 Sep 2007), *Nomascus leucogenys* (nomLeu1.0, Gibbon; v. Jan 2010), *Macaca mulatta* (rheMac; v.1.0 Feb 2006), *Callithrix jacchus* (calJac, Marmoset; v.3.2.1 Jan 2010), *Tarsius syrichta* (tarSyr, Tarsier; v.1 Jul 2008), *Microcebus murin*us (micMur, Gray Mouse Lemur; v.1 Jun 2007), *Otolemur Garnettii* (otoGar, Bushbaby; v.3 Mar 2011), *Tupaia belangeri* (tupBel, Northern Treeshrew; v.1 Jun 2006), *Cavia porcellus* (cavPor, Guinea Pig; v.3 Mar 2008), *Sus Scorfa* (susSco, Pig; v.10.2 Aug 2011), *Mus musculus* (musMus, Mouse; v.37 Apr 2007), *Rattus norvegicus* (rarNor, Rat; v.3.4 Dec 2004), *Spermophilus tridecemlineatus* (speTri, Squirrel; v.2 Nov 2011), *Ochotona princeps* (ochPri, Pika; v.2.0 Jun 2007), *Oryctolagus cuniculus* (oryCun, Rabbit; v.2 Nov 2009), *Ailuropoda melanoleuca* (ailMel, Panda; v.1 Jul 2009), *Canis lupus familiaris* (canFam, Dog; v.2.0 May 2006), *Felis catus* (felCat, Cat; Mar 2006), *Equus caballus* (equCab, Horse; v.2 Sep 2007), *Pteropus vampyrus* (pteVam, Megabat; v.1 Jul 2008), *Bos Taurus* (bosTau, Cow; v.3.1 Nov 2009), *Tursiops truncates* (turTru, Dolphin; v.1 Jul 2008), *Choloepus hoffmanni* (choHof, Sloth; v.1 Sep 2008), *Loxodonta Africana* (loxAfr, Elephant; v.3.0 Jul 2009).

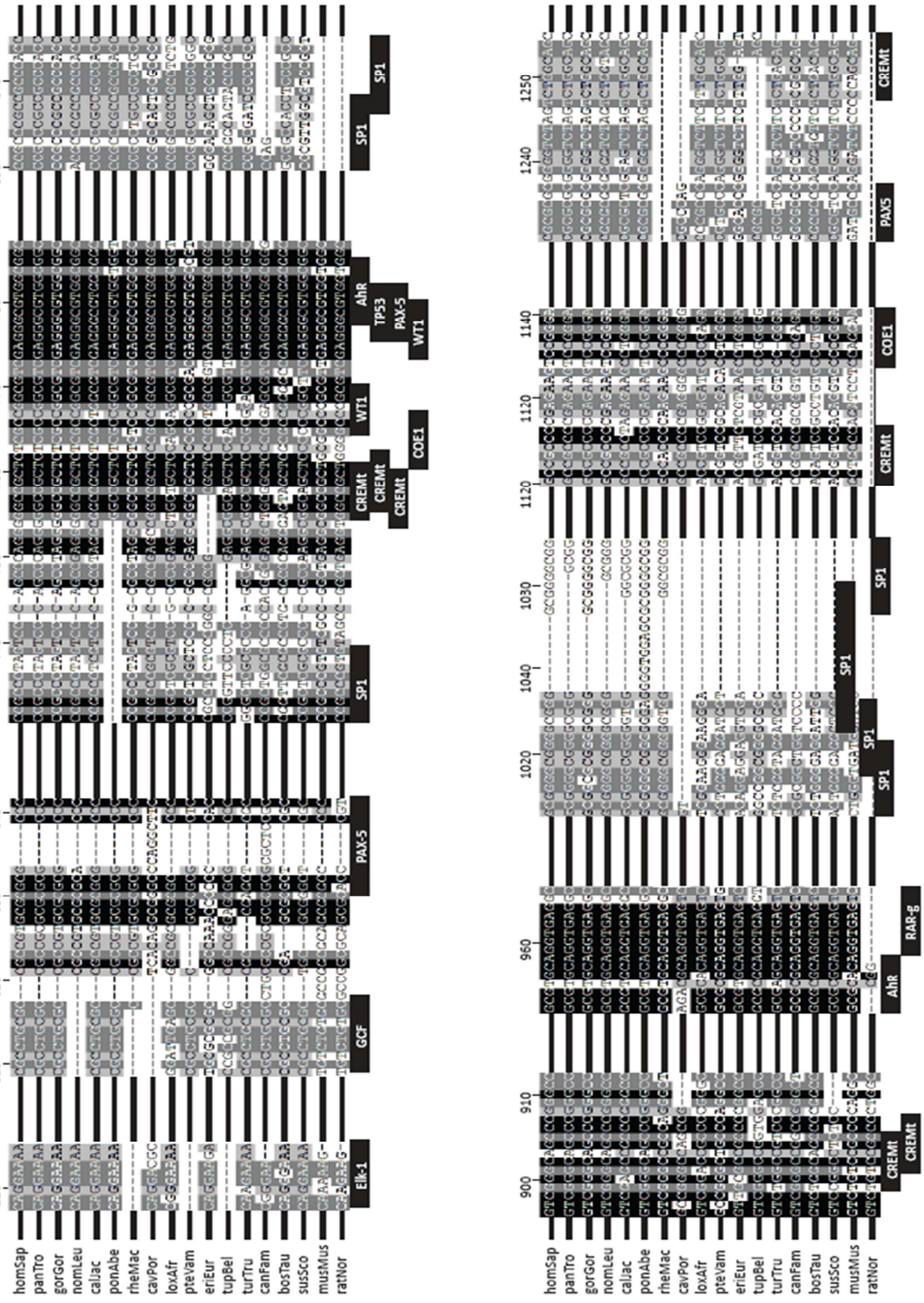
homSap
panTro
gorGor
nomLeu
calJac
ponAbe
rheMac
cavPor
loxAfr
pteVam
eriEur
tupBel
turTru
canFam
bosTau
susScr
musMus
ratNor
Elk-1
GCF
PAX-5
SP1
CREMt
CREMt
CREMt
COE1
WT1
AhR
TP53
PAX-5
WT1
SP1
SP1
CREMt
CREMt
AhR
RAR-g
SP1
SP1
SP1
CREMt
COE1
PAX5
CREMt

Figure S5. Comparative analysis of RCAN3-associated CpG island sequence conservation between mammals and in silico prediction of TFBS in this region. Alignment of 18 mammalian genomic sequences corresponding to the CpG island (based in USCS reported CpG island) associated with human RCAN3. The different TFBS conserved among most of the analyzed organisms are indicated with black boxes. Species and genome sequence versions used were as indicated in Figure S4 with the addition of *Erinaceus europaeus* (eriEur, Hedgehog; v.1 Jun 2006), *Pteropus vampyrus* (pteVam, Megabat; v.1 Jul 2008), *Nomascus leucogenys* (nomLeu, Gibbon; v.1.0 Jan 2010), and *Tupaia belangeri* (tupBel, Tree Shrew; v.1 Jun 2006). Grey intensity shade increases with sequence conservation (50, 70 and 90% of nucleotide identity). Numbers correspond to nucleotide coordinates referred to the first position of the CpG island. Exon 1 spans positions 1 to 90; exon 2a, positions 521 to 741; and exon 2, positions 521 to 774.

Table S1. Paralogous genes located in cromosome 1 (1p32-p36.3) and 6 (6p12-p21.2/q12-q22.1).

Chromosome 1				Chromosome 6			
Gene symbol	Location	Gene ID (GenBank)	Description	Gene symbol	Location	Gene ID (GenBank)	Description
EPHA8	1p36.12	2046	EPH receptor A8				
EPHB2	1p36.1-p35	2048	EPH receptor B2	EPHA7	6q16.1	2045	EPH receptor A7
EPHA10	1p34.3	284656	EPH receptor A10				
LUZP1	1p36	7798	leucine zipper protein 1	FILIP1	6q14.1	27145	filamin A interacting protein 1
HTR1D	1p36.3-p34.3	3352	5-hydroxytryptamine (serotonin) receptor 1D, G protein-coupled	HTR1B	6q13	3351	5-hydroxytryptamine (serotonin) receptor 1B, G protein-coupled
				HTR1E	6q14-q15	3354	5-hydroxytryptamine (serotonin) receptor 1E, G protein-coupled
HNRNPR	1p36.12	10236	heterogeneous nuclear ribonucleoprotein R	SYNCRIP	6q14-q15	10492	synaptotagmin binding, cytoplasmic RNA interacting protein
HMGCL	1p36.1-p35	3155	3-hydroxymethyl-3-methylglutaryl-CoA lyase	HMGCLL1	6p12.1	54511	3-hydroxymethyl-3-methylglutaryl-CoA lyase-like 1
CNR2	1p36.11	1269	cannabinoid receptor 2 (macrophage)	CNR1	6q14-q15	1268	cannabinoid receptor 1 (brain)
RCAN3	1p35.3-p33	11123	RCAN family member 3	RCAN2	6p12.3	10231	regulator of calcineurin 2
CLIC4	1p36.11	25932	chloride intracellular channel	CLIC5	6p12.3	53405	chloride intracellular channel 5
RUNX3	1p36	864	runt-related transcription factor 3	RUNX2	6p21	860	runt-related transcription factor 2
PAQR7	1p36.11	164091	progestin and adipoQ receptor family member VII	PAQR8	6p12.1	85315	progestin and adipoQ receptor family member VIII
PAFAH2	1p36	5051	platelet-activating factor acetylhydrolase 2, 40kDa	PLA2G7	6p21.2-p12	7941	phospholipase A2, group VII (platelet-activating factor acetylhydrolase, plasma)
LIN28A	1p36.11	79727	lin-28 homolog A (C. elegans)	LIN28B	6q21	389421	lin-28 homolog B (C. elegans)
GPR3	1p36.1-p35	2827	G protein-coupled receptor 3	GPR6	6q21	2830	G protein-coupled receptor 6
WASF2	1p36.11	10163	WAS protein family, member 2	WASF1	6q21	8936	WAS protein family, member 1
SESN2	1p35.3	83667	sestrin 2	SESN1	6q21	27244	sestrin 1

*EPHA2 is also a paralogous gen and it is located at 1p36. We consider that it is so far to been included into the chr1:chr6 segmental duplication.

** GJA family and GJB family are all paralogous among them. In Fig. 2 we have linked GJA famlily members and GJB family members separately.

Chromosome 1				Chromosome 6			
Gene symbol	Location	Gene ID (GenBank)	Description	Gene symbol	Location	Gene ID (GenBank)	Description
TINAGL1	1p35.2	64129	tubulointerstitial nephritis antigen-like 1	TINAG	6p12.1	27283	tubulointerstitial nephritis antigen
HCRTR1	1p33	3061	hypocretin (orexin) receptor 1	HCRTR2	6p12	3062	hypocretin (orexin) receptor 2
BAI2	1p35	576	brain-specific angiogenesis inhibitor 2	BAI3	6q12	577	brain-specific angiogenesis inhibitor 3
PTP4A2	1p35	8073	protein tyrosine phosphatase type IVA, member 2	PTP4A1	6q12	7803	protein tyrosine phosphatase type IVA, member 1
KPNA6	1p35.1	23633	karyopherin alpha 6 (importin alpha 7)	KPNA5	6q22.1	3841	karyopherin alpha 5 (importin alpha 6)
HDAC1	1p34	3065	histone deacetylase 1	HDAC2	6q21	3066	histone deacetylase 2
GJA4	1p35.1	2701	gap junction protein, alpha 4, 37kDa	GJA1	6q21-q23.2	2697	gap junction protein, alpha 1, 43kDa
GJA9	1p34	81025	gap junction protein, alpha 9, 59kDa	GJA10	6q15-q16	84694	gap junction protein, alpha 10, 62kDa
GJB5	1p35.1	2709	gap junction protein, beta 5, 31.1kDa				
GJB4	1p34.3	127534	gap junction protein, beta 4, 30.3kDa	GJB7	6q15	375519	gap junction protein, beta 7, 25kDa
GJB3	1p34	2707	gap junction protein, beta 3, 31kDa				
TRAPPC3	1p34.3	27095	trafficking protein particle complex 3	BET3L	6q22.1	10012832	BET3 like (S. cerevisiae)
GRIK3	1p34.3	2899	glutamate receptor, ionotropic, kainate 3	GRIK2	6q16.3	2898	glutamate receptor, ionotropic, kainate 2
FHL3	1p34	2275	four and a half LIM domains 3	FHL5	6q16.1-q16.3	9457	four and a half LIM domains 5
RRAGC	1p34	64121	Ras-related GTP binding C	RRAGD	6q15-q16	58528	Ras-related GTP binding D
AKIRIN1	1p34.3	79647	akirin 1	AKIRIN2	6q15	55122	akirin 2
RLF	1p32	6018	rearranged L-myc fusion	ZNF292	6q14.3	23036	zinc finger protein 292
SCMH1	1p34	22955	sex comb on midleg homolog 1 (Drosophila)	SCML4	6q21	256380	sex comb on midleg-like 4 (Drosophila)

Table S1. Paralogous genes located in cromosome 1 (1p32-p36.3) and 6 (6p12-p21.2/q12-q22.1).

exon usage		Proposed		RefSeq database*		Facchin**		Davies***	
mRNA TRANSCRIPT	PROTEIN	mRNA TRANSCRIPT	PROTEIN	mRNA TRANSCRIPT	PROTEIN	mRNA TRANSCRIPT	PROTEIN	mRNA TRANSCRIPT	PROTEIN
1,4,5,6,7 (1a,2,3,4,5)	4,5,6,7 (2,3,4,5)	RCAN3-1	RCAN3-4	transcript variant 4 (NM_001251979)	isoform 1 (NP_001238906, NP_038469, NP_001238907, NP_001238908)	RCAN3-1a,2,3,4,5	RCAN3-2,3,4,5	RCAN3-2	RCAN3-2
2,4,5,6,7 (1,2,3,4,5)		RCAN3-2		transcript variant 1 (NM_013441)		RCAN3-1,2,3,4,5		-	-
2a,4,5,6,7 (1c,2,3,4,5)		RCAN3-2a		transcript variant 2 NM_001251977		RCAN3-1c,2,3,4,5		-	-
3,4,5,6,7 (1b,2,3,4,5)		RCAN3-3		transcript variant 3 (NM_001251978)		RCAN3-1b,2,3,4,5		-	-
4,5,6a,7 (2,3,4b,5)	4,5,6a,7 (2,3,4b,5)	RCAN3-4,5,6a,7	RCAN3-4,5,6a,7	transcript variant 5 (NM_001251980)	isoform 2 (NP_001238909)	RCAN3-2,3,4b,5	RCAN3-2,3,4b,5	RCAN3-4b	RCAN3-4b (RCAN3-2,3,4b,5)
4,5,7 (2,3,5)	4,5,7 (2,3,5)	RCAN3-4,5,7	RCAN3-4,5,7	transcript variant 7 (NM_001251982)	isoform 4 (NM_001251982)	RCAN3-2,3,5	RCAN3-2,3,5	-	-
4,7 (2,5)	4,7 (2,5)	RCAN3-4,7	RCAN3-4,7	transcript variant 10 (NM_001251985)	isoform 6 (NP_001238914)	RCAN3-2,5	RCAN3-2,5	RCAN3-2,5	RCAN3-2,5
2a,4,6,7 (1c,2,4,5)	4,6,7 (2,4,5)	RCAN3-2a,4,6,7	RCAN3-4,6,7	transcript variant 6 (NM_001251981)	isoform 3 (NP_001238910)	RCAN3-1c,2,4,5	RCAN3-2,4,5	-	
2,5,6,7 (1,3,4,5)	6,7 (4,5)	RCAN3-2,5,6,7	RCAN3-6,7	transcript variant 8 (NM_001251983)	isoform 5 (NP_001238912, NP_001238913)	RCAN3-1,3,4,5	RCAN3-4,5	-	-
1,5,6,7 (1a,3,4,5)		RCAN3-1,5,6,7		transcript variant 9 (NM_001251984)		RCAN3-1a,3,4,5		-	-

* Pruitt KD, Tatusova T, Klimke W, Maglott DR (2009) NCBI Reference Sequences: current status, policy and new initiatives. Nucleic Acids Res 37: D32-36.

** Facchin F, Canaider S, Vitale L, Frabetti F, Griffoni C, et al. (2008) Identification and analysis of human RCAN3 (DSCR1L2) mRNA and protein isoforms. Gene 407: 159-168.

*** Davies KJ, Ermak G, Rothermel BA, Pritchard M, Heitman J, et al. (2007) Renaming the DSCR1/Adapt78 gene family as RCAN: regulators of calcineurin. FASEB J 21: 3023-3028.

Table S2. Different nomenclature for RCAN3 mRNA transcripts and protein isoforms used in bibliography, compared with our proposal

ANNEX TO ARTICLE

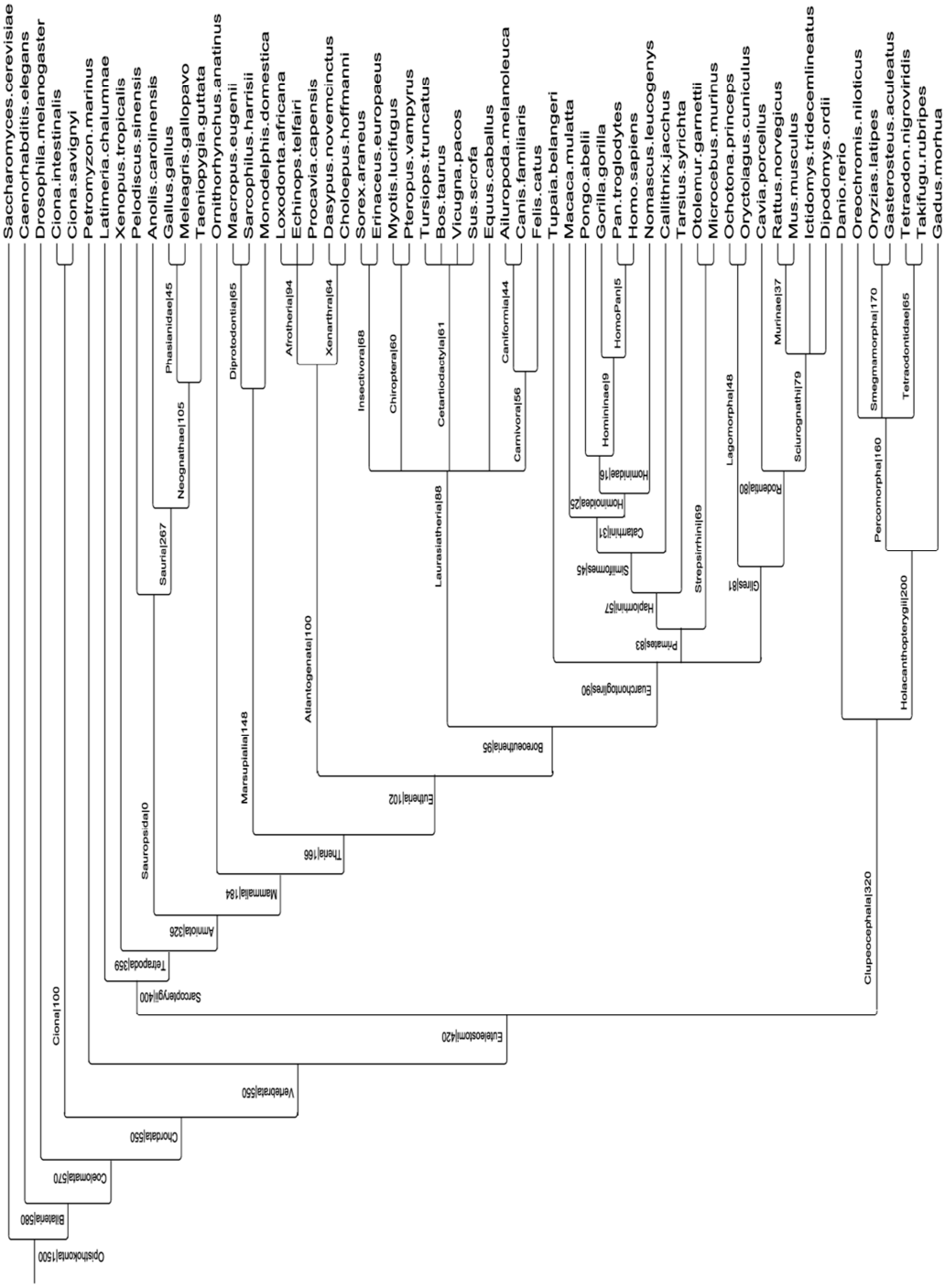

Figure A1. Species tree. Adapted from From Genomicus; http://www.dyogen.ens.fr/genomicus-68.02**;** Muffato *et al.*, 2010.

2.- RCAN PROTEINS AS MODULATORS OF CALCINEURIN-DEPENDENT PROCESSES IN T CELL DEVELOPMENT AND ACTIVATION

Eva Serrano-Candelas, German Alemán-Muench, Sergio Martínez-Høyer, Sònia Solé, Jaume Adán, Melanie Pritchard, Gloria Soldevila, Mercè Pérez-Riba

My contribution to this article has been: RNA extraction, real-time quantitative PCR, western blot, flow cytometry analysis, GST-pull down, immunoprecipitation procedures and statistical analysis. In addition, I have performed the transgenic RCAN1 mice colony maintenance and genotyping and set up bone marrow mice reconstitution experiments with retrovirally transduced BM progenitors. Finally, I contribute to the general design and conception of the experiments, figures preparation and manuscript writing.

G. Alemán contributed in the BM reconstitution experiments, cytometric analysis and manuscript writing. S. Martínez helped to set up bone marrow mice reconstitution experiments and contributed to rational discussion of the manuscript. Sònia Solé contributed to the colony maintenance. Dr. Jaume Adan developed the monoclonal antibody against RCAN1 protein. Dr. M. Pritchard kindly provided us with the TghRCAN1 model. Dr. G. Soldevila and Dr. M. Pérez contributed to the general design and conception of the experiments and manuscript writing.

RCAN proteins as modulators of T cell development and activation

Eva Serrano-Candelas[1], German Alemán-Muench[2], Sergio Martínez-Høyer[1], Sònia Solé[1], Jaume Adán[3] Melanie Pritchard[4], Gloria Soldevila[2*], Mercè Pérez-Riba[1*]

[1]Human Molecular Genetics Department, Cell Signaling Unit, Bellvitge Biomedical Research Institute – IDIBELL. 08908 L'Hospitalet de Llobregat, Barcelona, Spain.
[2]Departamento de Inmunología, Instituto de Investigaciones Biomédicas, Universidad Nacional Autónoma de México, Ciudad Universitaria, 04510 México, DF, México.
[3]LEITAT Technological Center, Biomed Divison, Parc Científic de Barcelona, 08028 Barcelona
[4]Department of Biochemistry and Molecular Biology, Monash University, Clayton, 3168 Victoria, Australia.
* These authors contributed equally to this work.

To whom correspondence should be addressed: Mercè Pérez-Riba, Human Molecular Genetics Group, Cell Signaling Unit, Bellvitge Biomedical Research Institute – IDIBELL. 08908 L'Hospitalet de Llobregat, Barcelona, Spain. Tel: +34 932607427. FAX: +34 932607414. mpr@idibell.cat.

ABSTRACT

The calcineurin (Cn)/NFATc signaling pathway is a key element in T cell mediated immune responses. In this context, Cn has been shown to regulate positive selection during thymocyte development as well as activation and survival of mature T lymphocytes. CsA and FK506 inhibit Cn activity towards all Cn substrates and are currently the main drugs used as immunosuppressants; however their life-span administration is associated to severe undesirable side-effects. The Regulators of Calcineurin (RCAN) proteins are endogenous modulators of calcineurin that play a dual role in Cn-NFAT signaling and therefore in T cell activation. To ascertain the functional role of RCAN proteins in the immune system, we first analyzed their expression in mouse lymphoid tissues and found that the different *Rcan* genes are differentially expressed in all mature and embryonic lymphoid murine organs tested. To address the function of RCANs *in vivo*, the function of *RCAN* overexpression in thymocyte development was analyzed in a transgenic murine model that overexpress *hRCAN1* and in mice reconstituted with bone marrow progenitors overexpressing *hRCAN3*. The data indicates that RCANs overexpression enhance positive selection-related markers CD3ξ and CD69 and also pERK activation on DP thymocytes. Moreover, *hRCAN1* overexpression increases the generation of nT_{regs} in thymus, and seem to influence the effector/memory T cells proportion in homeostasis. Furthermore, RCAN proteins appear to modulate other TCR signaling pathways essential for T cell function, such as JNK phosphorylation. Therefore, RCAN proteins are regulators of T cell development, differentiation and activation.

INTRODUCTION

$CD4^+$ T and $CD8^+$ T lymphocytes mediate cell-mediated adaptive immunity and play a crucial role in antigen-specific response against infections and anti-tumoral immunity. In the thymus, T cell differentiation starts with the seeding by new progenitors derived from the bone marrow (BM) in adult organisms or from fetal liver during fetal life. Four major thymocyte subpopulations can be identified based on CD4 and CD8 co-receptor expression: DN (double negative), DP (double positive), $CD4^+$ SP ($CD4^+$ single positive) and $CD8^+$ SP ($CD8^+$ single positive). Based on the expression of CD44 and CD25 cell surface markers, developing thymocytes of the most immature stage (DN) can be further subdivided into four subpopulations; DN1 ($CD44^+$ $CD25^-$), DN2 ($CD44^+$ $CD25^+$), DN3 ($CD44^-CD25^+$) and DN4 ($CD44^-$ $CD25^-$) (Ma *et al.*, 2011). The first developmental checkpoint in thymocyte development occurs at the transition from DN3 to DN4 stage and depends on pre-T Cell Receptor (pre-TCR) signaling (β-selection) which, in a cell autonomous manner, leads to the allelic exclusion of the TCR β chain, the initiation of the TCR α chain rearrangement and, after several rounds of cell division, the differentiation to $CD4^+CD8^+$ double positive cells (DP) (Yamasaki and Saito, 2007).

At the DP stage, the TCRαβ receptor complex allows the recognition of self-peptide-MHC complexes expressed on thymic stromal cells (reviewed in Labrecque *et al.*, 2011). TCR signaling sets the avidity/affinity threshold that dictates thymocyte fate, leading to cell death by negligence, rescue from apoptosis by positive selection or cell deletion by negative selection (reviewed in Starr *et al.*, 2003). In addition, another lineage of $CD4^+$ T cells, called the "naturally occurring" $CD4^+CD25^+Foxp3^+$ regulatory T cells (nT_{regs}) are generated in the thymus. The nT_{regs} have been postulated to require a higher TCR signaling threshold than conventional $CD4^+$ T cells for their selection, near to that required for negative selection (reviewed in Hsieh *et al.*, 2012).

Several studies have investigated the molecular mechanisms by which thymocytes can discriminate between positive and negative selection signals (reviewed in Sebzda *et al.*, 1999; Labrecque *et al.*, 2011). In this context, positive selecting ligands have been shown to promote phosphorylation of CD3ξ, ZAP-70 and LAT in a weaker and more sustained manner than negative selecting peptides (Daniels *et al.*, 2006). In addition, other downstream molecules are also differentially activated. For instance, upon recognition of negatively or positively selecting peptides, the RAS-RAF-ERK MAPK pathway is activated in the plasma membrane or in the Golgi, respectively (Daniels *et al.*, 2006). In particular, ERK phosphorylation is induced strongly but transiently by negative selecting peptides,

while a slow and sustained ERK activation is triggered by positive selecting peptides (McNeil *et al.*, 2005; (Daniels *et al.*, 2006). In addition, Ca^{2+} mobilization and downstream Ca^{2+}-dependent molecules are differentially activated (Daniels *et al.*, 2006). In this context, the Ca^{2+}- and calmodulin-regulated phosphatase calcineurin (Cn) and ERK have been described to be essential for positive selection, but their involvement in negative selection is not clear (Fischer *et al.*, 2005; Neilson *et al.*, 2004; Gallo *et al.*, 2007). Other molecules, such as c-Cbl, SLAP y Csk have been described to negatively modulate positive selection (Naramura *et al.*, 1998; Sosinowski *et al.*, 2001; Schmedt and Tarakhovsky, 2001), while other molecules, as the phosphatase PTEN (Suzuki *et al.*, 2001), the pro-apoptotic proteins Bim (Bouillet *et al.*, 2002) and Nur77 (Zhou *et al.*, 1996; Calnan *et al.*, 1995) and the p38 and pJNK MAPK pathways (Rincon *et al.*, 1998; Sugawara *et al.*, 1998) seem to govern the negative selection process.

Besides TCR signaling pathways triggered by self-peptide recognition, other signals including cytokines, chemokines and growth factors influence the final T cell fate of developing thymocytes (Soldevila, 2003; Takahama, 2006; Licona-Limon and Soldevila, 2007).

Cn plays a crucial role in transducing extracellular stimuli that drives intracellular calcium mobilization that leads to the activation of different transcriptional programs involved in T cell development and function (reviewed in Kiani *et al.*, 2000; Aramburu *et al.*, 2004), (Macian *et al.*, 2002). Cn is a heterodimeric protein composed by a catalytic subunit, CnA, and a regulatory B subunit, CnB. In mammals, CnA has three isoforms: α, β and γ; and CnB has two: CnB1 and CnB2. Cn shows ubiquitous expression in all mammalian tissues, but isoform CnB2 is restricted to testis and CnAγ is restricted to testis and brain (Aramburu et al., 2000; Medyouf and Ghysdael, 2008). Ca^{2+}-activated Cn dephosphorylates the cytosolic Nuclear Factor of Activated T cells 1 to 4 (NFATc1-4) transcription factors promoting their translocation to the nucleus where, in cooperation with other transcription factors, lead to gene expression (Macian *et al.*, 2001; Macian, 2005; Li *et al.*, 2011). NFATc are restricted to vertebrates and they are ubiquitously expressed, but only NFATc1 to NFATc3 are expressed in immune cell types (Macian, 2005; Wu *et al.*, 2007).

CnAβ and CnB have been reported to be essential for positive selection of thymocytes (Bueno *et al.*, 2002; Neilson *et al.*, 2004; Gallo *et al.*, 2007), while CnAα seems to be dispensable (Zhang *et al.*, 1996; Chan *et al.*, 2002). In addition, all Cn subunits are necessary for the proliferation, survival and function of mature T lymphocytes (Aramburu *et al.*, 2000; Chan *et al.*, 2002; Bueno *et al.*, 2002; Manicassamy *et al.*, 2008). Regarding NFATc proteins, NFATc1 has been reported

to enhance Th2 responses (Ranger *et al.*, 1998) while NFATc2 promotes Th1 lineage differentiation (Hodge *et al.*, 1996; Erb *et al.*, 2003; Xanthoudakis *et al.*, 1996). In turn, NFATc3 is the most relevant NFATc member in positive selection of thymocytes (Cante-Barrett *et al.*, 2007), while NFATc1 appears to be involved in the process of β-selection (Koltsova *et al.*, 2007). In addition, NFATc3$^{-/-}$ splenocytes display a hyperactivated peripheral phenotype and present increased sensitivity to apoptosis, due to an altered threshold of FasL transcription (Oukka *et al.*, 1998).

Hence, Cn-NFATc signaling is finely regulated in the immune system, depending on the cellular context. Cn is the target of the immunosuppressive drugs cyclosporine A (CsA) and FK506 (Tacrolimus), which are the basis for transplant therapy (reviewed in Martinez-Martinez and Redondo, 2004). However, the prolonged use of these drugs is associated with severe side effects, since the binding of these drugs to Cn causes the inhibition of the enzyme toward all its substrates, including the NFATc. Nowadays, a major goal of the immunosuppressive filed is to develop novel immunosuppressants that inhibit more specifically the Cn-NFATc signaling pathway. In this context, several endogenous inhibitors of Cn have been described, among them the family of Regulators of calcineurin (RCAN) (reviewed in Davies *et al.*, 2007). Among the eukaryotic RCAN proteins, vertebrate RCAN (formerly known DSCR1 or calcipressin, among others) constitute a functional subfamily (Mulero *et al.*, 2007). This subfamily includes three members in almost all vertebrates: RCAN1, RCAN2 and RCAN3, while in other eukaryotes there is only one member, with the known exception of yeast. *RCAN1* gene encodes for two major protein products, RCAN1-1 and RCAN1-4 in human, corresponding to Rcan1-1 and Rcan1-2 in mouse, respectively. Human *RCAN2* gene encodes for RCAN2-3 and RCAN2-4 isoforms, corresponding to Rcan2-2 and Rcan2-3 isoforms in mouse, respectively. Finally, one unique protein product has been detected by now from both human and mouse *RCAN3*, although numerous mRNA forms in humans have been described (Facchin *et al.*, 2011).

RCAN proteins are ubiquitously expressed but their relative abundance and distribution in the immune system remains unknown. It has been described that *RCAN1-4* transcription is promoted by intracellular calcium increase, which, in consequence, provides a negative feedback loop that inhibits Cn activity towards NFATc, in various cellular types, including T cells (Davies *et al.*, 2001; Harris *et al.*, 2005). In addition, estrogen hormone promotes *Rcan1-2* transcription in mouse, protecting female mice from ventricular hypertrophy, which suggest that expression and function of some RCAN isoforms can be functionally regulated by reproductive hormones (Pedram *et al.*, 2008; Gurgen *et al.*, 2011).

Vertebrate RCAN proteins include several highly conserved motifs in their central and carboxy-terminal regions. The RCAN FLISPP and LXXP motifs are the signature of the family as they are highly conserved in Eukarya (Mehta et al, 2009). In vertebrates, Cn signaling inhibition has been constrained to the RCAN CIC (for calcipressin (now RCAN) inhibitor of calcineurin) motif, which mammalian consensus sequence is LGPGEKYELHA[G/A]T[D/E][S/T]TPSVVVHVC[E/D]S, at the C-terminal region of the proteins (Mulero *et al.*, 2007).

In vivo functional studies have emphasized a dual role of RCAN proteins either promoting or suppressing Cn signaling, depending on the cellular context (Ryeom *et al.*, 2003; Vega *et al.*, 2003; Sanna *et al.*, 2006; Shin *et al.*, 2006; Mehta *et al.*, 2009). The RCAN protein role on thymocyte development has not yet been described.

Considering the crucial role of Cn-NFAT signaling in T cells and the relevance of the RCAN proteins as modulators of this signaling pathway, here we describe the expression pattern of the mouse *Rcan* genes in adult and embryonic lymphoid tissues and their role on T cell development *in vivo*. Remarkably, overexpression of human RCAN1 and RCAN3 proteins, by using two different animal model approaches, reveals that both proteins can act as important regulators of thymocyte development and T cell function. In particular, RCAN protein overexpression influences thymocyte positive selection process and, at the same time, modulates peripheral T cell activation.

MATERIAL AND METHODS

Mice

10 to 12 weeks old C57BL/6 mice were used and housed in the IDIBELL animal facility, officially accredited by AAALAC (unit 1255). PAC77 TgRCAN1 transgenic mice were kindly provided by Dr. Melanie Pritchard (PhD, Monash University, Australia). The 135 kb PAC genomic clone in the transgenic mice contain all the human *RCAN1* exons, and extends for approximately 35 Kb the 5' of exon 1, and 600 base pairs 3' of the *RCAN1*polyA$^+$ tract. The entire PAC insert sequence was analyzed using the NIX software from the United Kingdom Human Genome Mapping Project (UK HGMP) computing services (Bishop, 1995). From the NIX analysis, it seemed likely that *RCAN1* is the only gene present in the PAC. As expected for the larger size of the transgene, only a few copies of the *RCAN1* PAC number 77 integrated into the genome of the host mouse (between five and ten copies). All animal handling and experimental procedures were done according

with the recommendations and guidelines approved by the CCEA 86/609/CEE IDIBELL Ethics Committee.

Real time quantitative PCR analysis for mouse Rcan transcripts

Total RNA was extracted from fetal liver and thymi (E15-E16 gestation) and adult (10-12 weeks) lymphoid organs (spleen, thymus, bone marrow and maxillary, axillar and inguinal lymph nodes) and brain using TRIzol® Reagent (Invitrogen Corporation, Carlsbad, USA) according to the manufacturer's protocol. Total RNA (6 µg) was treated with DNAse™ kit (Applied Biosciences, USA) and was reversed transcribed (1.7 µg) using the Superscript II enzyme and random primers (both from Invitrogen Corporation, Carlsbad, USA) in 20 µl volume reaction according to manufacturer's instructions. Real time quantitative PCR amplification of mouse *Rcan* transcripts was performed from 0.5 µl of cDNA using specific primers (Supplementary Table 1A) (0.4 µM; Isogen Life Science, The Netherlands), Universal ProbeLibrary (UPL) probes (Roche, Switzerland; 0.2 µM) (Supplementary Table 1A) and LightCycler 480 Probes Master mix (Roche) buffer in a final volume of 10 µl. White LightCycler 480 Multiwell plates 384 and LigthCycler 480 apparatus (Roche) were used for PCR assay. Amplification conditions were an initial step of 10 min at 94°C, followed by 45 cycles of 94°C for 10 s, 55°C for 20 s, 72°C for 5 s. PCR products were resolved in a non-denaturing 12% PAGE and visualized by ethidium bromide (EtBr) staining to ensure the purity and size of the amplicons. All reactions were performed by triplicate for 6 animals. The relative quantification of gene expression was done using $2^{-\Delta\Delta CT}$ method (Livak, 2001). Amplification of *Hprt1* and *Gusb* genes were used as internal control, and results are shown normalized to *Hprt1* values.

Genotyping TghRCAN1 mice

A tail tip was denatured in 300 µl of 50 mM NaOH at 98°C, neutralized with 30 µl of 1M Tris-HCl, pH 8, and centrifuged 10 min at 13000 *g*. Supernatant was collected and DNA concentration was quantified. 300 ng of each DNA sample was PCR amplified using human RCAN and endogenous mouse DNA internal control specific primers (Supplementary Table 1B) at 62°C for 25 cycles, resolved in 1.5% agarose in Tris-buffered saline-EDTA (TBE) buffer and detected by staining with ethidium bromide (EtBr). As internal control, mouse Interleukin 2 precursor locus (*Il2p*) was amplified. The ratio between the human *RCAN1* transgene and the mouse *Il2p* locus allows us to discriminate between heterozygous and homozygous animals.

Wild type, heterozygous and homozygous TghRCAN1 mice genotypes were confirmed at the mRNA and protein level from lymphoid tissues (thymus, lymph nodes and spleen) and non-lymphoid tissues (liver, brain and kidney). For mRNA analysis, semiquantitative PCR was performed using 0.04 µl of cDNA obtained from reverse transcription of 2 µg total RNA in a final volume of 20 µl, using specific primers (0.4 µM; Isogen Life Science; Supplementary Table 1B). Samples were resolved in a 1% agarose gel and visualized by EtBr staining.

For protein expression analysis, soluble extracts were obtained by lysis in RIPA buffer (50 mM Tris-HCl, pH 7.4, 150 mM NaCl, 1 mM EDTA, 1% Triton X-100, 0.1% SDS and 0.5% sodium deoxycholate) supplemented with protease and phosphatase inhibitors cocktail tablets, incubated 4°C for 30 min, sonicated, centrifuged at 13000 *g* for 10 min and supernatants were kept at -70°C until used. Protein quantification was performed by Bicinchoninic Acid (BCA) assay kit (BioRad). Eighty micrograms of protein were resolved in reducing 12% SDS-PAGE, transferred to nitrocellulose membrane (HybondC-Extra; Amersham Biosciences, Switzerland) and analyzed with specific antibodies. Anti-hRCAN1 (1 µg/ml) antibody was incubated 4°C overnight and α-tubulin for 1 h at 4°C, both in Tris buffered saline (TBS) containing 0.1% (v/v) Tween (TBS-T) supplemented with 1% (v/v) bovine serum albumin (BSA) and 0.05% (v/v) NaN_3. Then, membranes were washed three times, incubated 1 h with rabbit anti-mouse IgG-HRP conjugated antibody (DAKO, Denmark; 1:2000) in TBS-T at room temperature (RT). Afterwards, membranes were washed several times, and protein was detected by chemiluminescence using ECL plus Western Blotting Detection System (Amersham Biosciences) in VersaDoc 5000 Imager (BioRad) apparatus and quantified with Quantity One (BioRad) software.

Antibody generation

Monoclonal antisera against the C-terminal region of RCAN1 protein was generated at the Technological Center LEITAT, Biomed Division (Barcelona, Spain), by immunizing mice with the synthetic peptide RPEYTPIHLS at the C-terminus of the protein (Figure S5, see sequence beginning at the end of TXXP motif). This sequence is shared by both human and mouse RCAN1 isoforms: RCAN1-1 (corresponding to mouse Rcan1-1) and RCAN1-4 (corresponding to mouse Rcan1-2). Peptides were purchased from Peptide 2.0 (Chantilly, VA, USA). IgG fractions were purified using protein G affinity chromatography (GE Healthcare, USA) following the manufacturer's protocol.

Generation of retroviral vectors and particles

The human full length HA-tagged RCAN3 sequence in pGEM-T Easy vector (Promega, Madison, USA) was excised by EcoRI digestion and subcloned in the retroviral vector pMIG (Addgene plasmid 9044; Van Parijs *et al.*, 1999) using the *E. Coli* HB101 strain (Promega). All DNA constructs were sequenced to ensure correct DNA sequence and reading frame. To generate retroviral particles, pMIG was cotransfected with pCL-Eco plasmid (gag/pol/env vector; Addgen plasmid 12371; Naviaux *et al.*, 1996) in HEK 293T cells by calcium phosphate method (pH 7.3). Twenty-four hours post-transfection, medium was refreshed to concentrate retrovirus in supernatant. At 48 hours post-transfection, supernatant was filtered (0.45 μm), supplemented with 8 μg/ml of polybrene (Hexadimethrine bromide (Sigma-Aldrich, USA) and used to transduce bone marrow (BM) progenitor cells and NIH 3T3 cells as control. Efficiency of retroviral transduction of progenitors was evaluated by flow cytometry measuring the percentage of GFP positive cells at 24 h post-transfection.

Isolation and transduction of bone marrow progenitor cells

To obtain BM progenitor cells, adult female C57/BL6 mice (6-8 weeks old) were injected intravenously with 5-Fluoroacil (150 mg/kg; Sigma-Aldrich) to enrich stem cell populations. After 5 days, progenitor cells were isolated from femur, tibia and iliac crest BM in DMEM-10% FBS. After lysis of erythrocytes with ammonium chloride solution (155 mM NH_4Cl, 10 mM $NaHCO_3$, 0.1 mM EDTA), cells were filtered through a 70 μm nylon mesh. $2x10^6$ cells were seeded in Retronectin® (Takara) coated 24-well flat bottom plate (NUNC; Thermo Fisher Scientific Inc., Denmark) in 2 ml of DMEM-10% FBS supplemented with 10% (v/v) of conditioned media from Baby hamster kidney/MKL (BHK) cells (as source of SCF (Tsai *et al.*, 1994) and 10% (v/v) from the myelomonocytic leukemia WEHI cell line (as source of IL-3; (Lee *et al.*, 1982)), both cell lines kindly provided by Dr. Bigas (IMIM, Barcelona, Spain). At the third day of culture, progenitor cells were transduced with pMIG-hRCAN3 or pMIG mock retrovirus supernatants in the presence of polybrene (8 μg/ml) in a ratio of retroviral supernatant/conditioned media of 80%/20% and centrifuged for 90 min at 450 *g* at 33°C. Cells were maintained in a humidified incubator with 5% CO_2 for 2 h. Then, 1 ml of media was replaced for 1 ml of fresh DMEM supplemented with FBS and WEHI and of BHK conditioned media, to a final concentration of 10% each.

Reconstitution of mice with transduced bone marrow cells

C57/BL6 female mice (8 weeks old) were reversibly intraperitoneal anaesthetized and sublethally irradiated at 900 rad following institutional guidelines. One hour later, 200 µl of 24 h transduced progenitor cells suspension in sterile phosphate-buffered saline (PBS) buffer was intravenously inoculated (1-2x10^6 cells /animal). Animals were housed for 8-10 weeks after bone marrow transplantation in specific pathogen-free (SPF) facilities.

Surface and intracellular staining

A total 3x10^6 cells from thymus, lymph nodes and spleen were stained with specific fluorescence-conjugated antibodies (see Supplementary Table 2A). After 30 min of staining at room temperature (RT), cells were washed with FACs buffer (PBS containing 5% (v/v) FBS and 0.02% (v/v) NaN_3) and subsequently fixed with 4% paraformaldehyde in PBS (PFA-PBS). For intracellular staining of phosphoproteins, thymocytes were previously stimulated in RPMI media without FBS with anti-CD3 (10 µg/ml) and anti-CD28 (10 µg/ml) antibodies, while splenocytes were stimulated with anti-CD3 (5 µg/ml) and anti-CD28 (5 µg/ml), both followed by crosslinking with anti-hamster IgG (10 µg/ml), for 3 min at 37°C (pERK, pAKT and pP38) or 15 min (pSAP/JNK). After stimulation, prewarmed 1X Lyse/Fix (Becton Dickinson (BD) Biosciences, USA) solution was added and cells were incubated at 37°C for 10 min. Subsequently, cells were washed and incubated at 4°C for 20 min with Perm Buffer II (BD Biosciences). Then, cells were blocked with 0.025 mg/ml of human IgG (Sigma-Aldrich) at 4°C for 30 min and stained for 30 min at 4°C with specific anti-phosphoprotein primary antibodies (see Supplementary Table 2B). After washing with FACs buffer, cells were stained with anti-rabbit AlexaFluor 467 (Invitrogen/Life Technologies) together with fluorescence-conjugated antibodies against surface markers (see Supplementary Table 2A) for 30 min at 4°C and fixed with 0.25% PFA-PBS. For T_{reg} cell staining, cells were previously permeabilized with Fix/Perm solution 1X (eBioscience, USA) for 3 h, washed twice with FACs buffer and stained at 4°C with for 30 min with specific fluorescence-conjugated antibodies against FoxP3 and surface markers (see Supplementary Table 2A). Dead cells were gated out based on the forward scattering (FSC) and side scattering (SSC) profile. Samples were captured in a FACSCalibur (BD Biosciences) cytometer and data was analyzed with FlowJo Tree Star software.

Pull-down and coimmunoprecipitation assays

Jurkat T cells were lysed in lysis buffer (50 mM Tris-HCl, pH 7.5, 100 mM NaCl, 2 mM $CaCl_2$, 1 mM DTT, 2 mM PMSF, 1% IGEPAL (v/v)), in presence of protease and phosphatase inhibitors cocktail (Roche). For pull-down experiments, soluble extracts were incubated with full GST-RCAN or partial RCAN regions coupled to Glutathione Sepharose beads (GE Healthcare) for 3 h at 4°C. After washing with lysis buffer, Laemmli buffer was added and samples were boiled for 10 min. For coimmunoprecipitation (coIP) assays, G protein Sepharose beads (GE Healthcare) were incubated with 2 μg of anti-BRAF (Santa Cruz) or anti-CnA (BD Pharmingen) antibodies, or unrelated IgGs as a control, for 3 h at 4°C. Then, beads were washed with lysis buffer and incubated with soluble extracts from Jurkat T cells for 2 h at 4°C. After extensive washing with lysis buffer, Laemmli buffer was added and samples were boiled as before. Samples were resolved in 10% SDS-PAGE, transferred to nitrocellulose membranes (HybondC-Extra; Amersham Biosciences) and analyzed with specific antibodies. Immunodetection was performed by using anti-CRAF (BD Biosciences; 1:1000), anti-BRAF (1:500) and anti-calcineurin A (BD Biosciences; 1:500) antibodies incubated overnight at 4°C.

RESULTS

Rcan genes are expressed in adult and embryonic lymphoid tissues

As *Rcan* gene expression pattern has not yet been described in lymphoid tissues, we performed a comparative analysis of their expression in these tissues by real-time quantitative PCR. We used brain tissue as positive control, as has been previously reported to express significant levels of Rcan (Porta *et al.*, 2007). In order to compare the relative abundance of each transcript, the amount of each *Rcan* mRNA is shown relative to *Rcan1-1* transcript level for each tissue. As shown in Figure 1A, all the Rcan transcript forms are detected in adult lymphoid tissues. In addition, *Rcan3* gene was the most transcribed gene in all adult lymphoid tissues tested. In contrast, *Rcan1-2* and *Rcan2-1* genes were expressed at lower levels compared to *Rcan1-1* and *Rcan3*, while *Rcan2-3* mRNA was almost undetectable in lymphoid tissues except in brain.

To compare the amount of each Rcan mRNA within the different lymphoid tissues, each mRNA form was relativized to its own level in thymus (Figure 1B). The differences on the level of *Rcan1-1* and *Rcan3* transcripts in lymph node, and *Rcan1-2* transcript in spleen were 2-fold at maximum. *Rcan2-1* and *Rcan2-3* transcripts forms presented higher transcription levels in spleen (around 8-fold),

lymph node (4-fold) and bone marrow (5 fold for the *Rcan2-3 form*), but to a lesser extent than in brain (Figure 1B).

In order to examine Rcan gene expression in fetal development, we analyzed E16 fetal thymi and compared it to that in adult thymi. In addition, fetal liver, which constitutes the main hematopoietic organ during fetal life, was also analyzed (Figure 1C). As a control for embryonic thymic tissue dissection we used the lymphocyte antigen 75/CD205 (Ly75/DEC-205) gene, whose expression is restricted only to thymus primordium in E14.5 and E16 embryos in fetal life, although it is expressed at high levels in many adult cell types, including adult thymic epithelial cells (Guerriero et al., 2000) (Supplementary Figure 1). We observed similar mRNA levels of Rcan1-1 and Rcan3 in fetal thymi compared to adult thymus, however, lower levels of Rcan1-1 and Rcan3 were detected in embryonic livers. These results suggest a preferential expression of both Rcan1-1 and Rcan3 in fetal thymus, which is niche for T cell progenitors, in comparison with embryonic liver, which has a different developmental function. In addition, Rcan1-2 displays preferential expression in adult thymus and Rcan2 mRNA forms showed significantly increased levels in both fetal liver and fetal thymi compared to adult thymus, suggesting a potential role in hematopoietic cell development.

Altogether, these results indicate that all mouse Rcan genes are expressed in adult and fetal lymphoid tissues, although with a different expression pattern. This suggests that Rcan forms may have differential roles instead of redundant roles in the immune system.

The human RCAN1 transgenic mice (TghRCAN1) overexpresses hRCAN1 in lymphoid tissues

Since mouse *Rcan* genes are expressed in all adult lymphoid tissues and in embryonic thymus, we wondered if Rcan proteins could play a role in T cell development and function. For this purpose, we analyzed a transgenic mouse that contains a complete copy of the human *RCAN1* gene and the 5' flanking region of the gene in a C57/BL6 background (TghRCAN1). Transgenic animals were viable, fertile at the expected Mendelian ratio and presented no macroscopic general abnormalities, but displayed reduced body weight compared to wild type animals (Figure 2A). Mice were genotyped by semiquantitative PCR analysis, as described in materials and methods (Figure 2B).

Next, *RCAN1-1* and *RCAN1-4* mRNA forms were analyzed for overexpression in the wild type (WT) and heterozygous (TghRCAN1$^{+/-}$) transgenic animals. The results indicate that both *RCAN1-1* and *RCAN1-4* mRNA form are transcribed in all

lymphoid tissues and in kidney, liver and brain from heterozygous animals, but it is not detected in WT animals (Figure 2C). At the protein level, by using a monoclonal anti-RCAN1 antibody that recognizes both RCAN1 isoforms from human and mouse, all lymphoid tissues harboring the transgene expressed both RCAN1 isoforms at higher extent than WT mouse (Figure 2D, left panel). The analysis of adult thymus, spleen and lymph nodes showed an increase in the amount of the RCAN1-1 isoform which correlated with a corresponding increase in *RCAN1* gene dosage in heterozygous (TghRCAN1$^{+/-}$) and homozygous (TghRCAN1$^{+/+}$) animals. On the other hand, the RCAN1-4 protein increase was only detected at a lower extent and unexpectedly its protein level was higher in heterozygous than in homozygous animals in thymus and lymph node. Interestingly, age-matched males did not present increased expression of the transgene (data not shown) in lymphoid tissues. Figure 2D (right panel) shows hRCAN1-1 protein amount in other TghRCAN1$^{+/-}$ non-lymphoid tissues.

In summary, RCAN1 transcripts and protein isoforms are detected in TghRCAN1$^{+/-}$ and TghRCAN1$^{+/+}$ female mice in all lymphoid tissues. In contrast to RCAN1-1, RCAN1-4 was not increased in TghRCAN1$^{+/+}$ mice compared to their TghRCAN1$^{+/-}$ littermates in thymus and lymph node, as would be expected for the increased gene dosage, suggesting that RCAN1-1 overexpression may affect *RCAN1-4* expression.

TgRCAN1 increases the proportion of positively selected thymocytes in heterozygous female animals.

To determine the effect of RCAN1 overexpression in the immune system, thymocytes, lymph node and spleen cells were isolated from WT, TghRCAN1$^{+/-}$ and TghRCAN1$^{+/+}$ mice. The total cellularity in these organs was not altered (data not shown). Subsequently, we analyzed cell populations by using specific fluorescence-conjugated monoclonal antibodies (mAb) against cell surface markers.

The analysis of thymocytes cell populations indicates that, among the CD4^{-}CD8^{-} double negative (DN) population, there is a significant accumulation of DN1 population in TghRCAN1$^{+/-}$ and TghRCAN1$^{+/+}$ female and male animals (Supplementary Figure 2 and data not shown). DN1 cells are partially committed cells that retains the capacity to become B cells, NK cells and conserve some myeloid capability to differentiate to thymic dendritic cells (Shortman and Wu, 1996). It cannot be ruled out the possibility that hRCAN1 overexpression influences commitment of cell types other than thymocytes that have not been here analyzed. Moreover, analysis for TCRβ chain expression in DN3 and DN4

populations did not show significant differences between the different genotypes (data not shown), which suggests that hRCAN1 overexpression does not alter TCRβ chain rearrangement and protein production associated with β selection process.

We also analyzed the effect of RCAN1 overexpression in thymocyte subpopulations other than DN cells. The $CD8^+CD4^+$ double positive (DP) population was decreased in all transgenic mice analyzed, while mature $CD8^+CD4^-$ and $CD4^+CD8^-$ single positive cells (SP) were increased, compared to WT mice. These effects in thymic subpopulations were only evident in females (Figure 3A). These results suggest that *RCAN1* transgene can alter thymocyte positive selection. Calcineurin/NFAT signaling pathway has been reported to be essential in positive selection of thymocytes, although their involvement in negative selection remains controversial (Wang *et al.*, 1995; Jenkins *et al.*, 1988; Neilson *et al.*, 2004). Since RCAN proteins are modulators of the Cn/NFAT pathway in mature T lymphocytes (Aubareda *et al.*, 2006; Mulero *et al.*, 2007; Mulero *et al.*, 2009) it is expected that RCAN1 overexpression could also modulate selection of thymocytes. The effect of hRCAN1 overexpression in positive selection was further analyzed by staining female thymocytes with antibodies against CD4, CD8 and either CD3ξ, TCRβ, CD5 and CD69 thymocyte development specific markers. The data reveal an increase of the $CD3\xi^{hi}$, $TCR\beta^{hi}$ and $CD69^{hi}$ populations and, to a lesser extent, of $CD5^{hi}$ population, only in heterozygous mice, when the data was relativized to WT animals (Figure 3B) in all the experiments performed, which indicates an increase of the percentage of thymocytes undergoing positive selection. $TghRCAN1^{+/+}$ mice presented more variability, showing an increase in $CD69^{hi}$ and $CD5^{hi}$ populations in some, but not all experiments. Analysis of the same positive selection markers in males suggested that positive selection is not altered in this gender (data not shown). For that reason, we performed all the following analysis only with female mice.

It has been previously described that positive selection of thymocytes depends on the ability to achieve an “ERK high competence” state, where cells are able to phosphorylate and activate ERK in response to low-avidity ligands (Gallo *et al.*, 2007). This state allows cells to undergo positive selection and has been shown to require Cn-NFATc signaling. Moreover, taking into account the interaction between RCAN1-4 and the kinase CRAF (Cho et al., 2005) we further investigated whether this protein-protein interaction might be conserved among all the RCAN and RAF proteins. Indeed, using pull-down and immunoprecipitation analysis (Figure 3C and S3) we demonstrated that both RCAN1 and RCAN3 proteins are able to interact with CRAF and BRAF, however the functional relevance of this interaction is still unknown. In addition, the binding site of RCAN to RAF appears

to be different to that on Cn (Figure S3 and Aubareda et al., 2006; Mulero et al., 2007). As a consequence, the interaction of RCAN with Cn and RAF proteins is not mutually exclusive. Therefore, we analyzed pERK activation in DP thymocytes in TghRCAN1 mice. Figure 3D shows that TghRCAN1$^{+/-}$ animals show a significant increased percentage of pERK^{hi} in DP thymocytes compared to WT mice. In contrast, lower percentage of pERK^{hi} is observed in DP thymocytes from TghRCAN1$^{+/+}$ compared to TghRCAN1$^{+/-}$ suggesting that acquisition of the "ERK competence state" is differentially regulated depending at least on the amounts of RCAN1 isoforms expressed in DP thymocytes. On the other hand, evaluation of other downstream TCR signaling kinases such as pAKT, pP38 and pJNK in DP thymocytes did not reveal significant changes between hRCAN1 transgenic mice and WT animals (data not shown).

In SP thymocytes, analysis of CD3ξ, TCRβ, CD5 and CD69 surface markers and intracellular phosphoproteins shows a trend to increase the mean fluorescence intensity (MFI) for TCRβ marker in the CD4$^+$ SP (Suppl. Figure S4).

In summary, analysis of thymocytes from TghRCAN1 mice indicates that RCAN1 overexpression causes an increase in positive selection, characterized by increased levels of CD3ξ, TCRβ and CD69 markers and increased percentage of pERK^{hi} population in DP thymocytes in TghRCAN1$^{+/-}$ females.

hRCAN1 overexpression increases peripheral CD3$^+$ cells and decreases the effector/memory peripheral T cell population in heterozygous females animals.

Once positive selected thymocytes reach their functionally maturity, these cells are exported from thymus to repopulate peripheral lymphoid organs, where they will eventually be activated by foreign antigens. To directly determine whether transgenic overexpression of hRCAN1 affects the peripheral T cell subsets under homeostatic conditions, cell suspensions from TghRCAN1 mice were stained with specific antibodies to analyze peripheral T cell subpopulations. Several differences depending on the lymphoid tissue and genotype tested (Figure 4A) were observed. For instance, CD3$^+$ T cells were increased in TghRCAN1$^{+/-}$ lymph nodes ($p=0.04$). In contrast, no differences were observed in the percentage of splenic CD3$^+$ T cells (Figure 4A).

Since the threshold of activation of Cn/NFAT pathway is determinant for an effective IL-2 production and T cell activation (Macian *et al.*, 2002), we next investigated whether the activation state of peripheral CD4$^+$ and CD8$^+$ T cells was regulated by overexpression of *RCAN1* gene. For this purpose, we analyzed the

presence of early (CD69) and late (CD44) activation markers in peripheral T cells obtained from TghRCAN1$^{+/-}$ and TghRCAN1$^{+/+}$ and wild type mice.

As shown in Figure 4B, no differences were observed in the percentages of CD8^{+}CD69^{hi} T cells in spleen and lymph nodes from transgenic mice compared to WT mice (Figure 4B). Moreover, although our data showed a high variability in CD4^{+}CD69^{hi} T cells, we observed a tendency towards a decrease in the percentage of CD69^{hi}CD4^{+} splenocytes in TghRCAN1$^{+/-}$ and TghRCAN1$^{+/+}$ mice compared WT (Figure 4B). In contrast, evaluation of CD44 surface molecules in peripheral T cells showed a significant decrease of the CD44^{hi} CD4^{+} population in TghRCAN1$^{+/-}$, and the same tendency was observed for CD8^{+} T cells. We also observed that CD44^{hi} population tends to decrease in both TghRCAN1$^{+/+}$ CD4^{+} and CD8^{+} lymph node T cells compared to WT mice. These results could be due to an impaired capacity of T cells to be activated or to an increased egression of naïve cells from the thymus in the TghRCAN1 mice.

Since alterations of surface populations are reflect of intracellular signaling pathways alteration, a more comprehensive analysis about the role of RCAN1 proteins in T cell activation was performed by evaluating the activation of ERK1/2, JNK1/2 (pJNK/SAP), p38 and AKT protein kinases after CD3-CD28 crosslinking of peripheral T cells *in vitro* (Figure 4C and data not shown). Interestingly, although ERK1/2, p38, and AKT did not shown significant differences, TCR-mediated activation of JNK1/2 was significantly increased in splenic CD3^{+} T cells of TghRCAN1$^{+/-}$ and TghRCAN1$^{+/+}$ mice compared to WT mice, in both CD4^{+} and CD8^{+} populations (Figure 4C). As both isoforms JNK1 and JNK2 play different roles in CD4^{+} and CD8^{+} lymphocytes (reviewed in Rincon and Pedraza-Alva, 2003) the functional effects of the RCAN1 overexpression through TCR-mediated JNK signaling pathway will require further experimental analysis.

Therefore, *hRCAN1* gene overexpression appears to increase the percentage of total T lymphocytes (CD3^{+}) in lymph nodes and regulates the proportions of effector/memory T cells (CD44^{hi}) in homeostasis. In addition, hRCAN1 overexpression increases SAP/JNK phosphorylation induced by TCR activation, suggesting a signaling mechanism in this pathway promoted by *RCAN1* overexpression in T cells.

Natural T_{reg} cells are increased in thymus and iT_{regs} are decreased in spleen in TgRCAN1 heterozygous female animals.

CD4^{+}Foxp3^{+} regulatory T cells (T_{reg}), are now widely regarded as the primary mediators of peripheral tolerance in the immune system, which require a key

transcription factor, known as Forkhead box P3 (FoxP3), for their development, maintenance and function (Josefowicz and Rudensky, 2009). Two types of $CD4^+FoxP3^+$ T_{regs} have been described; those generated in the thymus, known as "naturally occurring" T_{regs} (nT_{regs}), and peripherally induced T_{regs} (iT_{regs}) (Chen and Konkel, 2010; Curotto de Lafaille and Lafaille, 2009). Based exclusively on the expression of Foxp3, we cannot discriminate between nT_{regs} and iT_{regs}. However, in naïve animals, under homeostatic conditions, most of peripheral $FoxP3^+$ T_{regs} (pT_{regs}) came from the thymus (nT_{regs}) while a lower percentage of newly generated TGFβ-dependent T_{reg} (iT_{regs}) subpopulations can be found.

To investigate whether constitutive *hRCAN1* gene overexpression influences the generation and maintenance of $FoxP3^+$ T_{regs}, we analysed this subpopulation by staining of thymocytes and peripheral lymphocytes using antibodies against CD4 and FoxP3 markers. We observed that thymic $CD4^+FoxP3^+$ T cells, or natural T_{regs} (nT_{reg}), were significantly increased in $TghRCAN1^{+/-}$ compared to WT thymi (Figure 5A and 5B, upper panel). Unexpectedly, the percentages of peripheral $CD4^+Foxp3^+$ T_{regs} (pT_{regs}) present a tendency to decrease of in the spleen of $TghRCAN1^{+/-}$ and $TghRCAN1^{+/+}$ mice (Figure 5B, lower panel). These results indicate a differential role of RCAN1 protein in the generation of nT_{regs} and iT_{regs}.

In summary, *hRCAN1* gene overexpression causes an increased percentage of SP populations in thymus suggesting an enhanced positive selection process of conventional T cells and as well as of natural T_{reg} cells. In the periphery, hRCAN1 transgenic mice show an increase in $CD3^+$ T cells, a decrease percentage of effector/memory-like T cells ($CD44^{hi}$) and a decrease of peripheral T_{reg} cells. This data, together with the increased phosphorylation of SAP/JNK in response to TCR crosslinking in transgenic splenocytes, indicates that *hRCAN1* gene overexpression affects thymocyte development, differentiation and activation.

Efficient hRCAN3 overexpression in murine lymphoid organs after adoptive transfer of retrovirally transduced BM progenitors.

Since *Rcan1* and *Rcan3* genes are expressed in thymus, lymph node and spleen (Figure 1) and all mouse and human RCAN proteins share over 60% of amino acid identity at the central and C-terminal region where the Cn-binding PXIXIT site is located (Supplementary Figure 5), a conserved function among them in lymphoid tissues can be suggested. Since *Rcan3* transgenic mice are not available to explore the functional role of RCAN3 in T cell development, bone marrow (BM) reconstitution experiments were performed to overexpress human *RCAN3* with an additional haematoglutinin (HA) tag at its N-terminus. For this purpose, retroviral particles were prepared by cotransfection of the pCL-Eco plasmid and the mock

(pMIG) or HA-RCAN3 (pMIG-hRCAN3) constructs, both of them encoding hGFP (humanized Green Fluorescent Protein, from now GFP). Figure 6 shows the pMIG plasmids constructs used for retroviral transduction of progenitor cells in BM reconstitution experiments (Figure 6A) and their efficiency to express the transgen in transduced NIH 3T3 cells (Figure 6B). GFP expression correlates with HA-RCAN3 at protein levels. Also, a schematic representation of the full BM reconstitution procedure (Figure 6C) and efficient lymphoid organ reconstitution after 8 weeks, detected by GFP content analysis, are shown (Figure 6D). Animals with a percentage of BM reconstitution over 4% were analyzed for thymocytes and peripheral lymphocyte populations, always comparing GFP^+ versus GFP^- populations in each reconstituted mouse, for each construct tested, mock (pMIG) or HA-RCAN3 (pMIG-hRCAN3).

RCAN3 overexpression increases thymic positive selection and decreases $CD4^+$ and $CD8^+$ cells in peripheral lymphoid organs.

Evaluation of thymocyte development in BM reconstituted animals overexpressing HA-RCAN3 (pMIG-HA-RCAN3 retrovirus) showed no significant differences in DN subpopulations in comparison with BM reconstituted animals with pMIG retrovirus (data not shown). Mock GFP overexpression in thymi produced some, although no significant, alteration in the percentages of thymocyte subpopulations (Figure 7A, compare pMIG GFP^- with pMIG GFP^+). However, significant changes were observed when comparing GFP^+ cells versus GFP^- cells of pMIG-hRCAN3 reconstituted animals (Figure 7A). In these mice, a significant decrease of DP cells was clearly observed, together with a tendency to increase of $CD8^+CD4^-$ SP thymocytes.

In agreement with the data obtained in the analysis of TghRCAN1 adult thymi, *hRCAN3* overexpression significantly increase the $CD3\xi^{hi}$ and $CD69^{hi}$ populations, and shows a tendency to increase of $CD5^{hi}$, in the $CD4^+CD8^+$ DP population of pMIG-hRCAN3 compared with pMIG reconstituted animals (Figure 7B).

Analysis of pMIG-RCAN3 GFP^+ peripheral subsets showed some decrease of $CD3^+$ cells in both spleen and lymph nodes and a significant decrease in splenic $CD8^+$ and LN $CD4^+$ T cells compared with mock pMIG GFP^+ peripheral T cell subsets (Figure 7C). This result is opposite to that obtained in the TghRCAN1 mice, suggesting different roles of RCAN1 and RCAN3 in periphery.

Therefore, using different *in vivo* approaches to overexpress hRCAN3 and hRCAN1 proteins, our results suggest that both proteins increase positive selection in thymus, suggesting a functional overlapping role on T cell development to some

extent, although with different results in the periphery, that suggest different potential roles of these RCAN proteins in the activation, proliferation and/or survival of mature T lymphocytes.

DISCUSSION

RCAN proteins are involved in many physiological programs such as lymphocyte activation, angiogenesis, morphogenesis of the heart valves, and neural and muscle development (Davies *et al.*, 2007). However, the *in vivo* functional role of the RCAN proteins in the immune system is still unknown.

Before approaching the *in vivo* functional role of RCAN proteins in the immune system, their gene expression in lymphoid tissues was evaluated as it has not been previously reported. Here, we demonstrate that all mouse *Rcan* genes are ubiquitously expressed in adult and fetal lymphoid tissues, showing different expression patterns, which suggests a potential role for these proteins in hematopoietic cell development (Figure 1).

RCAN proteins have been described to be involved in several signaling pathways, being the most analyzed the Cn-NFATc signaling pathway (Fuentes *et al.*, 2000; Harris *et al.*, 2005; Mulero *et al.*, 2007). A dual RCAN role, either facilitative or inhibitory, towards Cn-NFAT signaling has been described in animal models depending of the RCAN expression level and the tissue or cell type analyzed (Vega *et al.*, 2003; Hilioti and Cunningham, 2003; Ryeom *et al.*, 2003; Sanna *et al.*, 2006; Shin *et al.*, 2006; Mehta *et al.*, 2009; Shin *et al.*, 2011).

In the immune system, overexpression of RCAN proteins in human T cell lines inhibits Cn-NFAT signaling (Aubareda *et al.*, 2006; Mulero *et al.*, 2007; Mulero *et al.*, 2009) and by these means inhibit NFATc-dependent cytokine gene expression and therefore T cell activation, suggesting that RCAN proteins have immunosuppressant properties in cultured cell lines. *In vivo*, *Rcan1* KO mice (Ryeom *et al.*, 2003) and double knockout mice for *Rcan1* and *Rcan2* (Sanna *et al.*, 2006), despite of having normal cell number and percentage of thymocytes and mature T cells and normal T cell activation markers, compared to WT mice, they shows less proliferation of naïve $CD4^+$ cells and a defect in Th1 response (IL-2) production, due to increased apoptosis of $CD4^+$ peripheral cells. Moreover, McKeon and colleagues (Ryeom *et al.*, 2003) found an increase in the NFAT-dependent *FasL* (CD95) gene expression in $Rcan1^{-/-}$ mice. This result agrees with the increased FasL-mediated apoptosis observed after *RCAN1-4* downregulation after partial silencing in U87MG (human glioblastoma) cells (Kim *et al.*, 2009). Ryeom *et al*. ascribed this phenotype of *Rcan1*$^{-/-}$ mice to the absence of the

inhibitory role of Rcan1 towards Cn/NFATc-dependent transcription of *FasL* gene, causing an increased cell death (Ryeom *et al.*, 2003). This idea was reinforced by the inhibition of apoptosis in $CD4^+$ lymphocytes in *Rcan1*$^{-/-}$ mice treated with CsA. However, it is known that CsA can rescue from apoptosis in a Cn-independent manner, inhibiting mitochondrial permeability transition pore formation through its binding to Cyclophilin D protein (Marchetti *et al.*, 1996; Kroemer *et al.*, 1998). To discard these additional effects of CsA, Sanna and colleagues tested apoptosis in the triple KO for *Rcan1*, *Rcan2* and *CnA*β, obtaining that the additional lack of CnAβ increased cellular apoptosis (Sanna *et al.*, 2006). To explain these results, Sanna *et al*. argued that Rcan1/2 act *in vivo* as facilitators of Cn function. It is known that CnAβ is essential in lymphocyte survival of naïve T cells (Manicassamy *et al.*, 2008). Moreover, it has been reported that NFATc3$^{-/-}$ mice presented enhanced FasL gene expression in peripheral T cells (Oukka *et al.*, 1998). All these data suggest that lack of Rcan1/2 proteins causes an insufficient activation of Cn to protect cells from apoptosis and reinforce the hypothesis of the dual role of Rcan proteins depending on cellular context and on the protein amount previously reported (Shin *et al.*, 2006).

Regarding that *Rcan* expression was found in murine lymphoid organs and taking into account their ability to modulate the activity of Cn towards NFATc and the importance of Rcan proteins in the survival of lymphocytes, it is important to determine their functional role in lymphocyte development and function. To this end, two *in vivo* approaches were used: a transgenic RCAN1 mouse model that contains the entire human *RCAN1* gene (TghRCAN1), that has been previously described to overexpress RCAN1-1 and RCAN1-4 isoforms in brain (Melanie Pritchard, personal communication), and lethally irradiated mice reconstituted with bone marrow progenitors transduced with a retrovirus encoding hRCAN3.

Analysis of overall abnormalities in the transgenic RCAN1 mice showed a reduced body weight of TghRCAN1 animals (Figure 2d). It has been reported that *Rcan1*$^{-/-}$ mice (Sanna *et al.*, 2006) also displayed body weight reduction. Interestingly, the same phenotypic trait is observed in *Rcan2*$^{-/-}$ mice due to impaired response to starvation (Sun *et al.*, 2011). Moreover, CsA treatment of rats (Lim *et al.*, 2000) and mice overexpressing a constitutively Cn active form leads to the same phenotypic effect (Jiang *et al.*, 2010). All these data suggest that Rcan proteins can be involved in body weight regulation, probably, in a Cn-dependent manner.

To investigate the consequence of RCAN3 protein overexpression in the immune system, BM reconstitution experiments were performed. To exclude any possible unspecific effects induced by the expression of the GFP reporter protein in all RCAN3 reconstituted mice, we always compared GFP^+ versus GFP^- cells of each

animal and the difference was compared to the effect of GFP expression observed in MIG reconstituted animals, which expressed the mock GFP vector.

To characterize the changes induced by *hRCAN1* and *hRCAN3* overexpression in thymocyte development and function, we first analyzed their effect on lymphocyte subpopulations. First of all, we observed a significant increase of DN1 population (Supplementary figure 2), that was not observed in hRCAN3 reconstituted animals (data not shown), probably because these BM reconstitution experiments give more heterogeneous results and as a consequence more animals need to be tested. Taking into account that the DN1 subpopulation still retains some multipotent capability to differentiate to cell lineages other than thymocytes (Shortman and Wu, 1996), the results shown that *RCAN1* overexpression can influence the early stages of progenitors development. In this context, calcineurin/NFATc inhibition by using the NFATc inhibitor VIVIT peptide (a high affinity synthetic PIXIXIT peptide derived from NFATc sequences) resulted in preferential expansion of myeloid cells versus lymphoid cells (Fric *et al.*, 2012), indicating that Cn-NFATc signaling negatively regulates myeloid lineage development. The DN1 significant increase observed in the thymocyte population suggests a possible modulatory role for RCAN1 towards Cn-NFATc signaling in the early thymic progenitors and needs further analysis to unravel their functional role in these populations.

Analysis of thymic populations of TghRCAN1 mice and hRCAN3 BM reconstituted mice revealed an increased percentage significant decrease of DP population (Figure 3A and Figure 7A). Enhanced negative selection was discarded because total thymus cellularity was unaltered and SP populations were not reduced, but incremented. One possibility to explain the results is that RCAN overexpression may favor survival of SP thymocytes or a less efficient thymus egression. A more plausible possibility is to ascribe the results to a more efficient positive selection, since an increase in $CD3^{hi}$, $TCR\beta^{hi}$, $CD69^{hi}$ and $CD5^{hi}$ populations is observed among the DP population (Figure 3B and Figure 7B). In addition, in TghRCAN1 mice the acquisition of the "ERK^{hi} competence state", essential for undertake positive selection (Gallo *et al.*, 2007), is also increased (Figure 3c). These results are difficult to explain if we considered RCAN1 and RCAN3 merely as Cn inhibitors. It has been reported that $NFATc3^{-/-}$ mice, but not $NFATc1^{-/-}$ and $NFATc2^{-/-}$ present impaired positive selection process (Ranger *et al.*, 1998; Yoshida *et al.*, 1998; Cante-Barrett *et al.*, 2007; Xanthoudakis *et al.*, 1996; Hodge *et al.*, 1996). In contrast, mice overexpressing an active form of Cn exhibit an incremented positive selection under suboptimal positive signals (Hayden-Martinez *et al.*, 2000), suggesting that Cn, specifically via NFATc3, is increasing the TCR "sensibility" to low-affinity ligands, facilitating the generation of $pERK^{hi}$

competence state and, subsequently, allowing the thymocytes to undergo positive selection process. This has been previously evidenced in *CnB*$^{-/-}$ mice, which display impaired positive selection due to the inability to acquire the pERK^{hi} competence state under low-avidity ligands stimulation (Gallo *et al.*, 2007). Altogether, these data indicate that RCAN proteins may act as positive modulators of the thymocyte positive selection process. It could be probably achieved by RCAN facilitating Cn activity, but this statement requires further analysis.

RCAN proteins can interact with BRAF and CRAF kinases (Figure 3C and S3). We also observed that RCAN interaction with RAF kinases and with Cn is not mutually exclusive (Figure S3). Therefore, these results suggest that RCAN proteins can integrate both signaling pathways that cooperate in thymocyte development (Gallo *et al.*, 2007). In this context, it has been described that Cn is able to directly link Ca^{2+} signals to ERK activity by positively regulating the KSR2 scaffold protein, which is essential for RAF to transduce its signals to MEK and ERK kinases (Dougherty *et al.*, 2009). Taking together, all these results support the hypothesis that the Cn-NFATc, RAF/ERK signaling pathways and RCAN proteins may be closely related.

Analysis of peripheral lymphocytes in TghRCAN1 mice shows an increase percentage of total T lymphocytes ($CD3^+$ cells) (Figure 4A) that is not significant detected in BM reconstituted mice (Figure 7C). These could be due to differences in the experimental approaches performed, to the presence of the non-conserved N-terminal sequences of RCAN3 and RCAN1 proteins, and/or to the fact that high amounts of hRCAN3 protein are present into the reconstituted mice, as the pMIG vector is driven by a MCMV promoter that strongly promotes constitutive gene expression, while in TghRCAN1 mice, gene expression is subjected to endogenous regulation. Therefore, the different amount on proteins might also contribute to different Cn signaling outcomes.

CD44 expression is positively dependent on TNF-α and IFN-γ cytokines (reviewed in Pure and Cuff, 2001), both being NFATc2-dependent genes. Moreover, NFATc2 is an activator of Th1 responses and a suppressor of Th2 responses *in vivo* (Xanthoudakis *et al.*, 1996). In our model, transgenic expression of hRCAN1 produces a decrease of the CD44^{hi} population and also tends to decrease CD69^{hi} in spleen (Figure 4B). This result can be ascribed to an inactivation of NFATc2 in its role to activate TNF-α and IFN-γ dependent *CD44* expression and would be in accordance to that results obtained in Jurkat T cells (Th1), where RCAN1 and RCAN3 CIC peptides inhibited Th1 cytokines production (Aubareda *et al.*, 2006; Mulero *et al.*, 2007). Conversely, NFATc2$^{-/-}$ mice presents an accumulation of peripheral lymphocytes with “pre-activated” phenotype, characterized by

increased $CD69^{hi}$ and $CD44^{hi}$ T cell activation markers. As a consequence, RCAN1 can be acting as NFATc2 activator in the regulation of T cell activation. Therefore, a more detailed analysis of RCAN proteins in the activation of NFATc2 may be performed to better understand the role of RCAN proteins in NFATc2-dependent processes involved in T cell activation.

Analysis of $FoxP3^{+}$ cells is in accordance with the notion of hRCAN1 being as positive regulator of NFATc3 and negative regulator of NFATc2 (Figure 5). $FoxP3^{+}$ cells in the thymus are selected as a population that responds to high-affinity ligands. Incremented positive selection, mainly driven by NFATc3, will also favor the selection of those cells, as was observed in TghRCAN1 mice. FoxP3 expression in the periphery depends on CD44 activation (Bollyky *et al.*, 2009), consequently, inactivation of NFATc2 by hRCAN1 would explain the reduced percentage of $FoxP3^{+}$ cells observed in the periphery of the TghRCAN1.

Interestingly, the effect of TghRCAN1 differences in thymocyte positive selection markers and peripheral lymphocyte populations were only observed in female animals. It is important to note that overexpression of both RCAN1-1 and RCAN1-4 mRNA forms were weaker in lymphoid tissues of males (data not shown). In this context, it has been reported that *RCAN1-4* gene expression is regulated by estrogen hormones (Gurgen *et al.*, 2011), therefore reproductive hormones could be also affecting *RCAN1-4* and/or *RCAN1-1* gene expression in thymocytes and lymphocytes, influencing the phenotype only in females.

Moreover, differences in thymocyte positive selection markers and peripheral lymphocyte populations were more evident in heterozygous animals. This could be explained by reduced expression of *RCAN1-4* in homozygous compared to heterozygous animals (Figure 2D). This could be due to high expression of RCAN1-1 isoform in these transgenic mice, which could inhibit NFATc-dependent *RCAN1-4* gene expression. Therefore, some of the observed phenotypes could be due to the specific balance of RCAN1-1 and/or RCAN1-4 isoforms at different gene dosage in heterozygous or homozygous animals and, as a consequence, different read out of Cn-NFATc signaling regulation.

Apart from the described interaction with Cn, RAF proteins and the TRIKA2 complex, *RCAN1* protein products have been described to interact with several proteins, such as the integrin αvβ3 (Iizuka *et al.*, 2004), the IRAK-1 inhibitor Tollip (Lee *et al.*, 2009), the NF-κB-inducing kinase (NIK) (Lee *et al.*, 2008) and the ubiquitin ligase SCFβ-TrCP (Asada *et al.*, 2008). Also, RCAN3 interaction with cardiac troponin I (TNNI3) (Canaider *et al.*, 2006) has been reported. Thus, we cannot rule out the possibility that RCAN proteins may affect other signaling

pathways involved in thymocyte development and function different of Cn-NFATc and RAF/ERK. To test this, we examined the possibility that RCAN1 overexpression may affect different phosphoproteins, other than pERK. Analysis of DP and SP thymocytes did not shown changes in the JNK1/2, AKT or p38 activation (data not shown); however, $CD3^+$ splenocytes are able to stimulate pSAP/JNK more efficiently in TghRCAN1 mice (Figure 4C). This tendency was the same for both $CD4^+$ and $CD8^+$ cells. It is known that JNK1 and JNK2 are highly expressed in DP and SP thymocytes. In the late stages of thymocyte development they are supposed to be silenced and will only be transcribed again in effector cells, as no expression was found in naïve peripheral $CD4^+$ and $CD8^+$ (reviewed in Rincon and Pedraza-Alva, 2003). It has been also shown that JNK1/2 activation depends on Cn activity (Avraham *et al.*, 1998; Werlen *et al.*, 1998) and, conversely, JNK is able to negatively regulate NFATc1, NFATc2 and NFATc3 but not NFATc4 activity (Liang *et al.*, 2003). Also, it is known that RCAN1 is able to interact with TRIKA2 complex (TAK1-TAB2/3-TAB1) (Liu *et al.*, 2009) which, in turn, regulates several signaling pathways, including the MKK4-SAP/JNK (c-Jun N-terminal kinase) cascade (Ninomiya-Tsuji *et al.*, 1999). Thus, a more detailed analysis is required to understand the crosstalk between all these signaling pathways and the possible involvement of RCANs. Interestingly, changes in pJNK phosphorylation were detected in both heterozygous and homozygous animals and it is the unique phenotypic trait that correlates with increased levels of RCAN1-1.

In summary, we have shown that the different mouse *Rcan* mRNA forms are differentially expressed during T cell development and in mature mouse lymphoid tissues, suggesting that they can play differential roles in the immune system. Moreover, by means of two different overexpression models, we have shown that RCAN1 and RCAN3 modulate T cell differentiation, promoting positive selection in the thymus and decreasing the activation state of peripheral T lymphocytes. Moreover, hRCAN1 overexpression increases nT_{regs} percentage in thymus but causes a decrease in the percentage of peripheral T_{regs}, either controlling the maintenance of nT_{regs} in periphery or *de novo* generation on iT_{regs}. Finally, JNK phosphorylation is enhanced in peripheral T lymphocytes, suggesting a RCAN regulatory role on signaling pathways other than Cn-NFAT signaling. In this context, we have also demonstrated that RCAN proteins can interact with RAF kinases and Cn at the same time. All these results point out to a crucial role of RCAN proteins in the regulation of T cell development and function by means of modulating different signaling pathways, including the Cn-NFATc pathway, in the immune system.

ACKNOWLEDGMENTS

We are grateful to Dr. J. Adan from LEITAT, Biomed Division Barcelona, Spain for raising the monoclonal anti- human RCAN1 protein. This work has been supported by grants SAF2009-08216 from MICINN and 2009SGR1490 from G.C, and Grant #79573 from CONACyT (GS). We want to thank R. Chavez and A. Aranguren for technical assistance and S. Solé for animal colony maintenance. S.M-H is a recipient of an IDIBELL PhD fellowship, G.A. is recipient of doctoral fellowship 208213 from CONACyT and E.S.-C. is supported from SAF009-08216.

FOOTNOTES

Abbreviations used were: BM; bone marrow; CIC, calcipressin (renamed as RCAN) inhibitor of calcineurin; Cn, calcineurin; CsA: Cyclosporin A; DP, double positive; DN, double negative $CD4^-$ $CD8^-$; LN, Lymph node; NFATc, cytosolic Nuclear Factor of Activated T-cells; RCAN, Regulator of Calcineurin; SP, single positive; WT, wild type.

REFERENCES

Aramburu, J., Heitman, J. and Crabtree, G.R. **Calcineurin: a central controller of signalling in eukaryotes**. (2004) *EMBO Rep* 5 pp. 343-8.

Aramburu, J., Rao, A. and Klee, C.B. **Calcineurin: from structure to function**. (2000) *Curr Top Cell Regul* 36 pp. 237-95.

Asada, S., Ikeda, A., Nagao, R., Hama, H., Sudo, T., Fukamizu, A., Kasuya, Y. and Kishi, T. **Oxidative stress-induced ubiquitination of RCAN1 mediated by SCFbeta-TrCP ubiquitin ligase**. (2008) *Int J Mol Med* 22 pp. 95-104.

Aubareda, A., Mulero, M.C. and Perez-Riba, M. **Functional characterization of the calcipressin 1 motif that suppresses calcineurin-mediated NFAT-dependent cytokine gene expression in human T cells**. (2006) *Cell Signal* 18 pp. 1430-8.

Avraham, A., Jung, S., Samuels, Y., Seger, R. and Ben-Neriah, Y. **Co-stimulation-dependent activation of a JNK-kinase in T lymphocytes**. (1998) *Eur J Immunol* 28 pp. 2320-30.

Bishop, M.J. **The United Kingdom Human Genome Mapping Project Resource Centre**. (1995) *Dis Markers* 12 pp. 85-98.

Bollyky, P.L., Falk, B.A., Long, S.A., Preisinger, A., Braun, K.R., Wu, R.P., Evanko, S.P., Buckner, J.H., Wight, T.N. and Nepom, G.T. **CD44 costimulation promotes FoxP3+ regulatory T cell persistence and function via production of IL-2, IL-10, and TGF-beta**. (2009) *J Immunol* 183 pp. 2232-41.

Bouillet, P., Purton, J.F., Godfrey, D.I., Zhang, L.C., Coultas, L., Puthalakath, H., Pellegrini, M., Cory, S., Adams, J.M. and Strasser, A. **BH3-only Bcl-2 family member Bim is required for apoptosis of autoreactive thymocytes**. (2002) *Nature* 415 pp. 922-6.

Bueno, O.F., Brandt, E.B., Rothenberg, M.E. and Molkentin, J.D. **Defective T cell development and function in calcineurin A beta -deficient mice**. (2002) *Proc Natl Acad Sci U S A* 99 pp. 9398-403.

Calnan, B.J., Szychowski, S., Chan, F.K., Cado, D. and Winoto, A. **A role for the orphan steroid receptor Nur77 in apoptosis accompanying antigen-induced negative selection**. (1995) *Immunity* 3 pp. 273-82.

Canaider, S., Facchin, F., Griffoni, C., Casadei, R., Vitale, L., Lenzi, L., Frabetti, F., D'Addabbo, P., Carinci, P., Zannotti, M. and Strippoli, P. **Proteins encoded by human Down syndrome critical region gene 1-like 2 (DSCR1L2) mRNA and by a novel DSCR1L2 mRNA isoform interact with cardiac troponin I (TNNI3)**. (2006) *Gene* 372 pp. 128-36.

Cante-Barrett, K., Winslow, M.M. and Crabtree, G.R. **Selective role of NFATc3 in positive selection of thymocytes**. (2007) *J Immunol* 179 pp. 103-10.

Curotto de Lafaille, M.A. and Lafaille, J.J. **Natural and adaptive foxp3+ regulatory T cells: more of the same or a division of labor?** (2009) *Immunity* 30 pp. 626-35.

Chan, V.S., Wong, C. and Ohashi, P.S. **Calcineurin Aalpha plays an exclusive role in TCR signaling in mature but not in immature T cells**. (2002) *Eur J Immunol* 32 pp. 1223-9.

Chen, W. and Konkel, J.E. **TGF-beta and 'adaptive' Foxp3(+) regulatory T cells**. (2010) *J Mol Cell Biol* 2 pp. 30-6.

Daniels, M.A., Teixeiro, E., Gill, J., Hausmann, B., Roubaty, D., Holmberg, K., Werlen, G., Hollander, G.A., Gascoigne, N.R. and Palmer, E. **Thymic selection threshold defined by compartmentalization of Ras/MAPK signalling**. (2006) *Nature* 444 pp. 724-9.

Davies, K.J., Ermak, G., Rothermel, B.A., Pritchard, M., Heitman, J., Ahnn, J., Henrique-Silva, F., Crawford, D., Canaider, S., Strippoli, P., Carinci, P., Min, K.T., Fox, D.S., Cunningham, K.W., Bassel-Duby, R., Olson, E.N., Zhang, Z., Williams, R.S., Gerber, H.P., Perez-Riba, M., Seo, H., Cao, X., Klee, C.B., Redondo, J.M., Maltais, L.J., Bruford, E.A., Povey, S., Molkentin, J.D., McKeon, F.D., Duh, E.J., Crabtree, G.R., Cyert, M.S., de la Luna, S. and Estivill, X. **Renaming the DSCR1/Adapt78 gene family as RCAN: regulators of calcineurin**. (2007) *FASEB J* 21 pp. 3023-8.

Davies, K.J., Harris, C.D. and Ermak, G. **The essential role of calcium in induction of the DSCR1 (ADAPT78) gene**. (2001) *Biofactors* 15 pp. 91-3.

Dougherty, M.K., Ritt, D.A., Zhou, M., Specht, S.I., Monson, D.M., Veenstra, T.D. and Morrison, D.K. **KSR2 is a calcineurin substrate that promotes ERK cascade activation in response to calcium signals**. (2009) *Mol Cell* 34 pp. 652-62.

Erb, K.J., Twardzik, T., Palmetshofer, A., Wohlleben, G., Tatsch, U. and Serfling, E. **Mice deficient in nuclear factor of activated T-cell transcription factor c2 mount increased Th2 responses after infection with Nippostrongylus brasiliensis and decreased Th1 responses after mycobacterial infection**. (2003) *Infect Immun* 71 pp. 6641-7.

Facchin, F., Vitale, L., Bianconi, E., Piva, F., Frabetti, F., Strippoli, P., Casadei, R., Pelleri, M.C., Piovesan, A. and Canaider, S. **Complexity of bidirectional transcription and alternative splicing at human RCAN3 locus**. (2011) *PLoS One* 6 p. e24508.

Fischer, A.M., Katayama, C.D., Pages, G., Pouyssegur, J. and Hedrick, S.M. **The role of erk1 and erk2 in multiple stages of T cell development**. (2005) *Immunity* 23 pp. 431-43.

Fric, J., Lim, C.X., Koh, E.G., Hofmann, B., Chen, J., Tay, H.S., Mohammad Isa, S.A., Mortellaro, A., Ruedl, C. and Ricciardi-Castagnoli, P. **Calcineurin/NFAT signalling inhibits myeloid haematopoiesis**. (2012) *EMBO Mol Med* 4 pp. 269-82.

Fuentes, J.J., Genesca, L., Kingsbury, T.J., Cunningham, K.W., Perez-Riba, M., Estivill, X. and de la Luna, S. **DSCR1, overexpressed in Down syndrome, is an inhibitor of calcineurin-mediated signaling pathways**. (2000) *Hum Mol Genet* 9 pp. 1681-90.

Gallo, E.M., Winslow, M.M., Cante-Barrett, K., Radermacher, A.N., Ho, L., McGinnis, L., Iritani, B., Neilson, J.R. and Crabtree, G.R. **Calcineurin sets the bandwidth for discrimination of signals during thymocyte development**. (2007) *Nature* 450 pp. 731-5.

Guerriero, A., Langmuir, P.B., Spain, L.M. and Scott, E.W. **PU.1 is required for myeloid-derived but not lymphoid-derived dendritic cells**. (2000) *Blood* 95 pp. 879-85.

Gurgen, D., Hegner, B., Kusch, A., Catar, R., Chaykovska, L., Hoff, U., Gross, V., Slowinski, T., da Costa Goncalves, A.C., Kintscher, U., Gustafsson, J.A., Luft, F.C. and Dragun, D. **Estrogen receptor-beta signals left ventricular hypertrophy sex differences in normotensive deoxycorticosterone acetate-salt mice**. (2011) *Hypertension* 57 pp. 648-54.

Harris, C.D., Ermak, G. and Davies, K.J. **Multiple roles of the DSCR1 (Adapt78 or RCAN1) gene and its protein product calcipressin 1 (or RCAN1) in disease**. (2005) *Cell Mol Life Sci* 62 pp. 2477-86.

Hayden-Martinez, K., Kane, L.P. and Hedrick, S.M. **Effects of a constitutively active form of calcineurin on T cell activation and thymic selection**. (2000) *J Immunol* 165 pp. 3713-21.

Hilioti, Z. and Cunningham, K.W. **The RCN family of calcineurin regulators**. (2003) *Biochem Biophys Res Commun* 311 pp. 1089-93.

Hodge, M.R., Ranger, A.M., Charles de la Brousse, F., Hoey, T., Grusby, M.J. and Glimcher, L.H. **Hyperproliferation and dysregulation of IL-4 expression in NF-ATp-deficient mice**. (1996) *Immunity* 4 pp. 397-405.

Hsieh, C.S., Lee, H.M. and Lio, C.W. **Selection of regulatory T cells in the thymus**. (2012) *Nat Rev Immunol* 12 pp. 157-67.

Iizuka, M., Abe, M., Shiiba, K., Sasaki, I. and Sato, Y. **Down syndrome candidate region 1,a downstream target of VEGF, participates in endothelial cell migration and angiogenesis**. (2004) *J Vasc Res* 41 pp. 334-44.

Jenkins, M.K., Schwartz, R.H. and Pardoll, D.M. **Effects of cyclosporine A on T cell development and clonal deletion**. (1988) *Science* 241 pp. 1655-8.

Jiang, L.Q., Garcia-Roves, P.M., de Castro Barbosa, T. and Zierath, J.R. **Constitutively active calcineurin in skeletal muscle increases endurance performance and mitochondrial respiratory capacity**. (2010) *Am J Physiol Endocrinol Metab* 298 pp. E8-E16.

Josefowicz, S.Z. and Rudensky, A. **Control of regulatory T cell lineage commitment and maintenance**. (2009) *Immunity* 30 pp. 616-25.

Kiani, A., Rao, A. and Aramburu, J. **Manipulating immune responses with immunosuppressive agents that target NFAT**. (2000) *Immunity* 12 pp. 359-72.

Kim, Y.S., Lee, H.J., Jang, C., Kim, H.S. and Cho, Y.J. **Knockdown of RCAN1.4 Increases Susceptibility to FAS-mediated and DNA-damage-induced Apoptosis by Upregulation of p53 Expression**. (2009) *Korean J Physiol Pharmacol* 13 pp. 483-9.

Koltsova, E.K., Ciofani, M., Benezra, R., Miyazaki, T., Clipstone, N., Zuniga-Pflucker, J.C. and Wiest, D.L. **Early growth response 1 and NF-ATc1 act in concert to promote thymocyte development beyond the beta-selection checkpoint**. (2007) *J Immunol* 179 pp. 4694-703.

Kroemer, G., Dallaporta, B. and Resche-Rigon, M. **The mitochondrial death/life regulator in apoptosis and necrosis**. (1998) *Annu Rev Physiol* 60 pp. 619-42.

Labrecque, N., Baldwin, T. and Lesage, S. **Molecular and genetic parameters defining T-cell clonal selection**. (2011) *Immunol Cell Biol* 89 pp. 16-26.

Lee, E.J., Seo, S.R., Um, J.W., Park, J., Oh, Y. and Chung, K.C. **NF-kappaB-inducing kinase phosphorylates and blocks the degradation of Down syndrome candidate region 1**. (2008) *J Biol Chem* 283 pp. 3392-400.

Lee, J.C., Hapel, A.J. and Ihle, J.N. **Constitutive production of a unique lymphokine (IL 3) by the WEHI-3 cell line**. (1982) *J Immunol* 128 pp. 2393-8.

Lee, J.Y., Lee, H.J., Lee, E.J., Jang, S.H., Kim, H., Yoon, J.H. and Chung, K.C. **Down syndrome candidate region-1 protein interacts with Tollip and positively modulates interleukin-1 receptor-mediated signaling**. (2009) *Biochim Biophys Acta* 1790 pp. 1673-80.

Li, H., Rao, A. and Hogan, P.G. **Interaction of calcineurin with substrates and targeting proteins**. (2011) *Trends Cell Biol* 21 pp. 91-103.

Liang, Q., Bueno, O.F., Wilkins, B.J., Kuan, C.Y., Xia, Y. and Molkentin, J.D. **c-Jun N-terminal kinases (JNK) antagonize cardiac growth through cross-talk with calcineurin-NFAT signaling**. (2003) *EMBO J* 22 pp. 5079-89.

Licona-Limon, P. and Soldevila, G. **The role of TGF-beta superfamily during T cell development: new insights**. (2007) *Immunol Lett* 109 pp. 1-12.

Lim, H.W., De Windt, L.J., Steinberg, L., Taigen, T., Witt, S.A., Kimball, T.R. and Molkentin, J.D. **Calcineurin expression, activation, and function in cardiac pressure-overload hypertrophy**. (2000) *Circulation* 101 pp. 2431-7.

Liu, Q., Busby, J.C. and Molkentin, J.D. **Interaction between TAK1-TAB1-TAB2 and RCAN1-calcineurin defines a signalling nodal control point**. (2009) *Nat Cell Biol* 11 pp. 154-61.

Ma, D., Wei, Y. and Liu, F. **Regulatory mechanisms of thymus and T cell development**. (2011) *Dev Comp Immunol*.

Macian, F. **NFAT proteins: key regulators of T-cell development and function**. (2005) *Nat Rev Immunol* 5 pp. 472-84.

Macian, F., Garcia-Cozar, F., Im, S.H., Horton, H.F., Byrne, M.C. and Rao, A. **Transcriptional mechanisms underlying lymphocyte tolerance**. (2002) *Cell* 109 pp. 719-31.

Macian, F., Lopez-Rodriguez, C. and Rao, A. **Partners in transcription: NFAT and AP-1**. (2001) *Oncogene* 20 pp. 2476-89.

Manicassamy, S., Gupta, S., Huang, Z., Molkentin, J.D., Shang, W. and Sun, Z. **Requirement of calcineurin a beta for the survival of naive T cells**. (2008) *J Immunol* 180 pp. 106-12.

Marchetti, P., Hirsch, T., Zamzami, N., Castedo, M., Decaudin, D., Susin, S.A., Masse, B. and Kroemer, G. **Mitochondrial permeability transition triggers lymphocyte apoptosis**. (1996) *J Immunol* 157 pp. 4830-6.

Martinez-Martinez, S. and Redondo, J.M. **Inhibitors of the calcineurin/NFAT pathway**. (2004) *Curr Med Chem* 11 pp. 997-1007.

McNeil, L.K., Starr, T.K. and Hogquist, K.A. **A requirement for sustained ERK signaling during thymocyte positive selection in vivo**. (2005) *Proc Natl Acad Sci U S A* 102 pp. 13574-9.

Medyouf, H. and Ghysdael, J. **The calcineurin/NFAT signaling pathway: a novel therapeutic target in leukemia and solid tumors**. (2008) *Cell Cycle* 7 pp. 297-303.

Mehta, S., Li, H., Hogan, P.G. and Cunningham, K.W. **Domain architecture of the regulators of calcineurin (RCANs) and identification of a divergent RCAN in yeast**. (2009) *Mol Cell Biol* 29 pp. 2777-93.

Mulero, M.C., Aubareda, A., Orzaez, M., Messeguer, J., Serrano-Candelas, E., Martinez-Hoyer, S., Messeguer, A., Perez-Paya, E. and Perez-Riba, M. **Inhibiting the calcineurin-NFAT (nuclear factor of activated T cells) signaling pathway with a regulator of calcineurin-derived peptide without affecting general calcineurin phosphatase activity**. (2009) *J Biol Chem* 284 pp. 9394-401.

Mulero, M.C., Aubareda, A., Schluter, A. and Perez-Riba, M. **RCAN3, a novel calcineurin inhibitor that down-regulates NFAT-dependent cytokine gene expression**. (2007) *Biochim Biophys Acta* 1773 pp. 330-41.

Naramura, M., Kole, H.K., Hu, R.J. and Gu, H. **Altered thymic positive selection and intracellular signals in Cbl-deficient mice**. (1998) *Proc Natl Acad Sci U S A* 95 pp. 15547-52.

Naviaux, R.K., Costanzi, E., Haas, M. and Verma, I.M. **The pCL vector system: rapid production of helper-free, high-titer, recombinant retroviruses**. (1996) *J Virol* 70 pp. 5701-5.

Neilson, J.R., Winslow, M.M., Hur, E.M. and Crabtree, G.R. **Calcineurin B1 is essential for positive but not negative selection during thymocyte development**. (2004) *Immunity* 20 pp. 255-66.

Ninomiya-Tsuji, J., Kishimoto, K., Hiyama, A., Inoue, J., Cao, Z. and Matsumoto, K. **The kinase TAK1 can activate the NIK-I kappaB as well as the MAP kinase cascade in the IL-1 signalling pathway**. (1999) *Nature* 398 pp. 252-6.

Oukka, M., Ho, I.C., de la Brousse, F.C., Hoey, T., Grusby, M.J. and Glimcher, L.H. **The transcription factor NFAT4 is involved in the generation and survival of T cells**. (1998) *Immunity* 9 pp. 295-304.

Pedram, A., Razandi, M., Lubahn, D., Liu, J., Vannan, M. and Levin, E.R. **Estrogen inhibits cardiac hypertrophy: role of estrogen receptor-beta to inhibit calcineurin**. (2008) *Endocrinology* 149 pp. 3361-9.

Porta, S., Marti, E., de la Luna, S. and Arbones, M.L. **Differential expression of members of the RCAN family of calcineurin regulators suggests selective functions for these proteins in the brain**. (2007) *Eur J Neurosci* 26 pp. 1213-26.

Pure, E. and Cuff, C.A. **A crucial role for CD44 in inflammation**. (2001) *Trends Mol Med* 7 pp. 213-21.

Ranger, A.M., Hodge, M.R., Gravallese, E.M., Oukka, M., Davidson, L., Alt, F.W., de la Brousse, F.C., Hoey, T., Grusby, M. and Glimcher, L.H. **Delayed lymphoid repopulation with defects in IL-4-driven responses produced by inactivation of NF-ATc**. (1998) *Immunity* 8 pp. 125-34.

Rincon, M. and Pedraza-Alva, G. **JNK and p38 MAP kinases in CD4+ and CD8+ T cells**. (2003) *Immunol Rev* 192 pp. 131-42.

Rincon, M., Whitmarsh, A., Yang, D.D., Weiss, L., Derijard, B., Jayaraj, P., Davis, R.J. and Flavell, R.A. **The JNK pathway regulates the In vivo deletion of immature CD4(+)CD8(+) thymocytes**. (1998) *J Exp Med* 188 pp. 1817-30.

Ryeom, S., Greenwald, R.J., Sharpe, A.H. and McKeon, F. **The threshold pattern of calcineurin-dependent gene expression is altered by loss of the endogenous inhibitor calcipressin**. (2003) *Nat Immunol* 4 pp. 874-81.

Sanna, B., Brandt, E.B., Kaiser, R.A., Pfluger, P., Witt, S.A., Kimball, T.R., van Rooij, E., De Windt, L.J., Rothenberg, M.E., Tschop, M.H., Benoit, S.C. and Molkentin, J.D. **Modulatory calcineurin-interacting proteins 1 and 2 function as calcineurin facilitators in vivo**. (2006) *Proc Natl Acad Sci U S A* 103 pp. 7327-32.

Schmedt, C. and Tarakhovsky, A. **Autonomous maturation of alpha/beta T lineage cells in the absence of COOH-terminal Src kinase (Csk)**. (2001) *J Exp Med* 193 pp. 815-26.

Sebzda, E., Mariathasan, S., Ohteki, T., Jones, R., Bachmann, M.F. and Ohashi, P.S. **Selection of the T cell repertoire**. (1999) *Annu Rev Immunol* 17 pp. 829-74.

Shin, S.Y., Choo, S.M., Kim, D., Baek, S.J., Wolkenhauer, O. and Cho, K.H. **Switching feedback mechanisms realize the dual role of MCIP in the regulation of calcineurin activity**. (2006) *FEBS Lett* 580 pp. 5965-73.

Shin, S.Y., Yang, H.W., Kim, J.R., Heo, W.D. and Cho, K.H. **A hidden incoherent switch regulates RCAN1 in the calcineurin-NFAT signaling network**. (2011) *J Cell Sci* 124 pp. 82-90.

Shortman, K. and Wu, L. **Early T lymphocyte progenitors**. (1996) *Annu Rev Immunol* 14 pp. 29-47.

Soldevila, G.G.-Z. **Role of Chemokines in T cell development**. (2003) *Inmunología* 22 pp. 371-384.

Sosinowski, T., Killeen, N. and Weiss, A. **The Src-like adaptor protein downregulates the T cell receptor on CD4+CD8+ thymocytes and regulates positive selection**. (2001) *Immunity* 15 pp. 457-66.

Starr, T.K., Jameson, S.C. and Hogquist, K.A. **Positive and negative selection of T cells**. (2003) *Annu Rev Immunol* 21 pp. 139-76.

Sugawara, T., Moriguchi, T., Nishida, E. and Takahama, Y. **Differential roles of ERK and p38 MAP kinase pathways in positive and negative selection of T lymphocytes**. (1998) *Immunity* 9 pp. 565-74.

Sun, X.Y., Hayashi, Y., Xu, S., Kanou, Y., Takagishi, Y., Tang, Y.P. and Murata, Y. **Inactivation of the Rcan2 gene in mice ameliorates the age- and diet-induced obesity by causing a reduction in food intake**. (2011) *PLoS One* 6 p. e14605.

Suzuki, A., Yamaguchi, M.T., Ohteki, T., Sasaki, T., Kaisho, T., Kimura, Y., Yoshida, R., Wakeham, A., Higuchi, T., Fukumoto, M., Tsubata, T., Ohashi, P.S., Koyasu, S., Penninger, J.M., Nakano, T. and Mak, T.W. **T cell-specific loss of Pten leads to defects in central and peripheral tolerance**. (2001) *Immunity* 14 pp. 523-34.

Takahama, Y. **Journey through the thymus: stromal guides for T-cell development and selection**. (2006) *Nat Rev Immunol* 6 pp. 127-35.

Tsai, S., Bartelmez, S., Sitnicka, E. and Collins, S. **Lymphohematopoietic progenitors immortalized by a retroviral vector harboring a dominant-negative retinoic acid receptor can recapitulate lymphoid, myeloid, and erythroid development**. (1994) *Genes Dev* 8 pp. 2831-41.

Van Parijs, L., Refaeli, Y., Lord, J.D., Nelson, B.H., Abbas, A.K. and Baltimore, D. **Uncoupling IL-2 signals that regulate T cell proliferation, survival, and Fas-mediated activation-induced cell death**. (1999) *Immunity* 11 pp. 281-8.

Vega, R.B., Rothermel, B.A., Weinheimer, C.J., Kovacs, A., Naseem, R.H., Bassel-Duby, R., Williams, R.S. and Olson, E.N. **Dual roles of modulatory calcineurin-interacting protein 1 in cardiac hypertrophy**. (2003) *Proc Natl Acad Sci U S A* 100 pp. 669-74.

Wang, C.R., Hashimoto, K., Kubo, S., Yokochi, T., Kubo, M., Suzuki, M., Suzuki, K., Tada, T. and Nakayama, T. **T cell receptor-mediated signaling events in CD4+CD8+ thymocytes undergoing thymic selection: requirement of calcineurin activation for thymic positive selection but not negative selection**. (1995) *J Exp Med* 181 pp. 927-41.

Werlen, G., Jacinto, E., Xia, Y. and Karin, M. **Calcineurin preferentially synergizes with PKC-theta to activate JNK and IL-2 promoter in T lymphocytes**. (1998) *EMBO J* 17 pp. 3101-11.

Wu, H., Peisley, A., Graef, I.A. and Crabtree, G.R. **NFAT signaling and the invention of vertebrates**. (2007) *Trends Cell Biol* 17 pp. 251-60.

Xanthoudakis, S., Viola, J.P., Shaw, K.T., Luo, C., Wallace, J.D., Bozza, P.T., Luk, D.C., Curran, T. and Rao, A. **An enhanced immune response in mice lacking the transcription factor NFAT1**. (1996) *Science* 272 pp. 892-5.

Yamasaki, S. and Saito, T. **Molecular basis for pre-TCR-mediated autonomous signaling**. (2007) *Trends Immunol* 28 pp. 39-43.

Yoshida, H., Nishina, H., Takimoto, H., Marengere, L.E., Wakeham, A.C., Bouchard, D., Kong, Y.Y., Ohteki, T., Shahinian, A., Bachmann, M., Ohashi, P.S., Penninger, J.M., Crabtree, G.R. and Mak, T.W. **The transcription factor NF-ATc1 regulates lymphocyte proliferation and Th2 cytokine production**. (1998) *Immunity* 8 pp. 115-24.

Zhang, B.W., Zimmer, G., Chen, J., Ladd, D., Li, E., Alt, F.W., Wiederrecht, G., Cryan, J., O'Neill, E.A., Seidman, C.E., Abbas, A.K. and Seidman, J.G. **T cell responses in calcineurin A alpha-deficient mice**. (1996) *J Exp Med* 183 pp. 413-20.

Zhou, T., Cheng, J., Yang, P., Wang, Z., Liu, C., Su, X., Bluethmann, H. and Mountz, J.D. **Inhibition of Nur77/Nurr1 leads to inefficient clonal deletion of self-reactive T cells**. (1996) *J Exp Med* 183 pp. 1879-92.

FIGURES AND TABLES

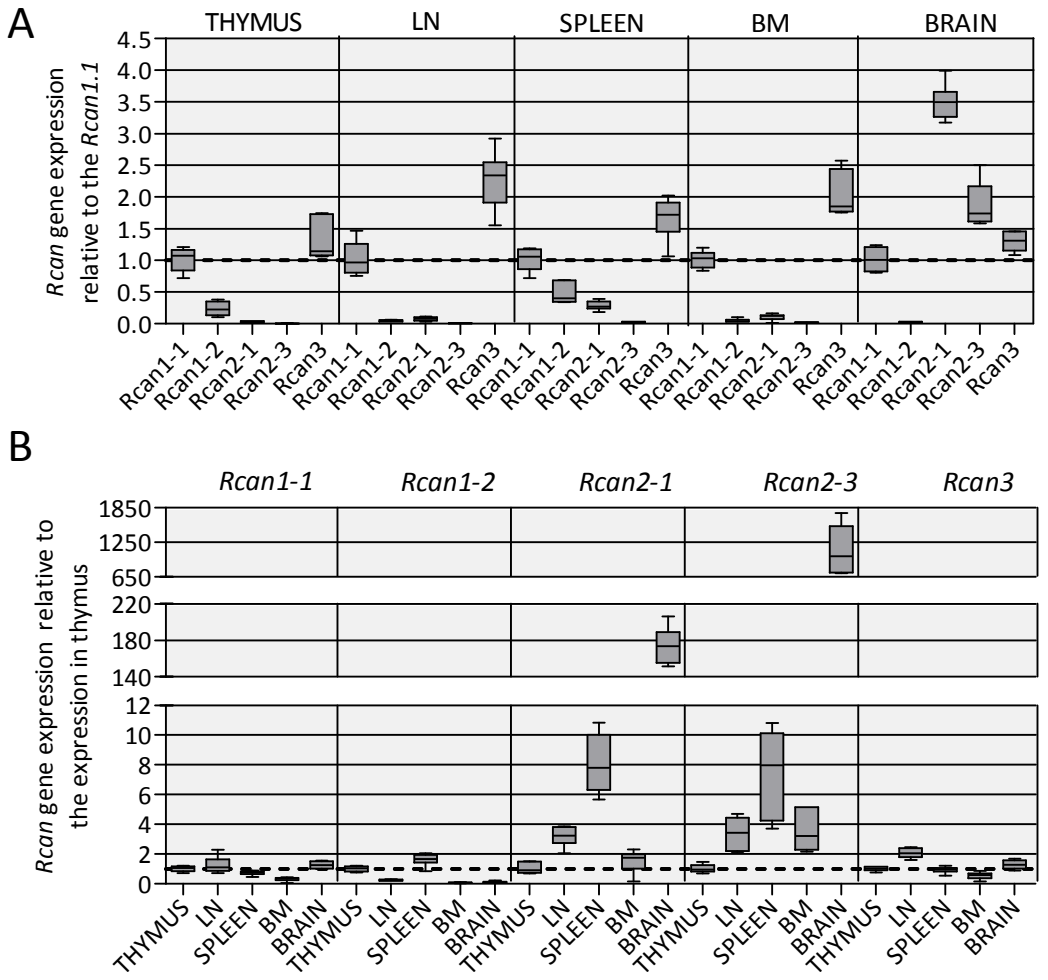

Figure 1A and B. Mouse Rcan mRNAs are expressed in adult and embryonic mouse lymphoid tissues. Quantitation of mouse *Rcan1*, *Rcan2* and *Rcan3* transcript forms was performed by real time quantitative PCR of cDNA samples obtained from adult thymus, lymph node, spleen, bone marrow and brain, as well as embryonic thymic lobes and livers at E16 maturation stage. A) Relative gene expression levels of the different *Rcan* mRNA forms in lymphoid adult tissues relative to the abundance of *Rcan1-1* mRNA in each specific tissue. B) *Rcan* mRNA levels in different adult lymphoid tissues relative to the amount of each specific transcript in thymus. Boxplot with whiskers (A and B) represents minimum to maximum values, quartiles and median value of data obtained from n ≥ 5. Brain was used as a control tissue.

C

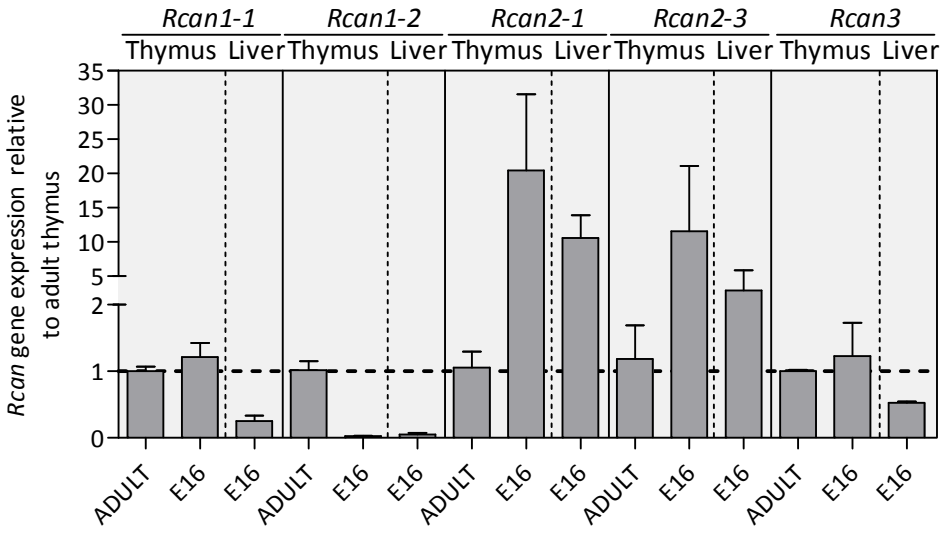

Figure 1C. Mouse Rcan mRNAs are expressed in adult and embryonic mouse lymphoid tissues. C) *Rcan* mRNA quantity in embryonic thymic lobes and liver, relative to its expression in the adult thymus. E16 refer to days of embryonic development. Bars represent the mRNA mean value ± SEM of two pools of all the fetuses from different litters collected at the same developmental stage analyzed independently. Values were normalized to *Hprt* gene and then relative to the value obtained to the mouse *Rcan* transcript or reference tissue. Horizontal dashed line corresponds to the expression value of 1.

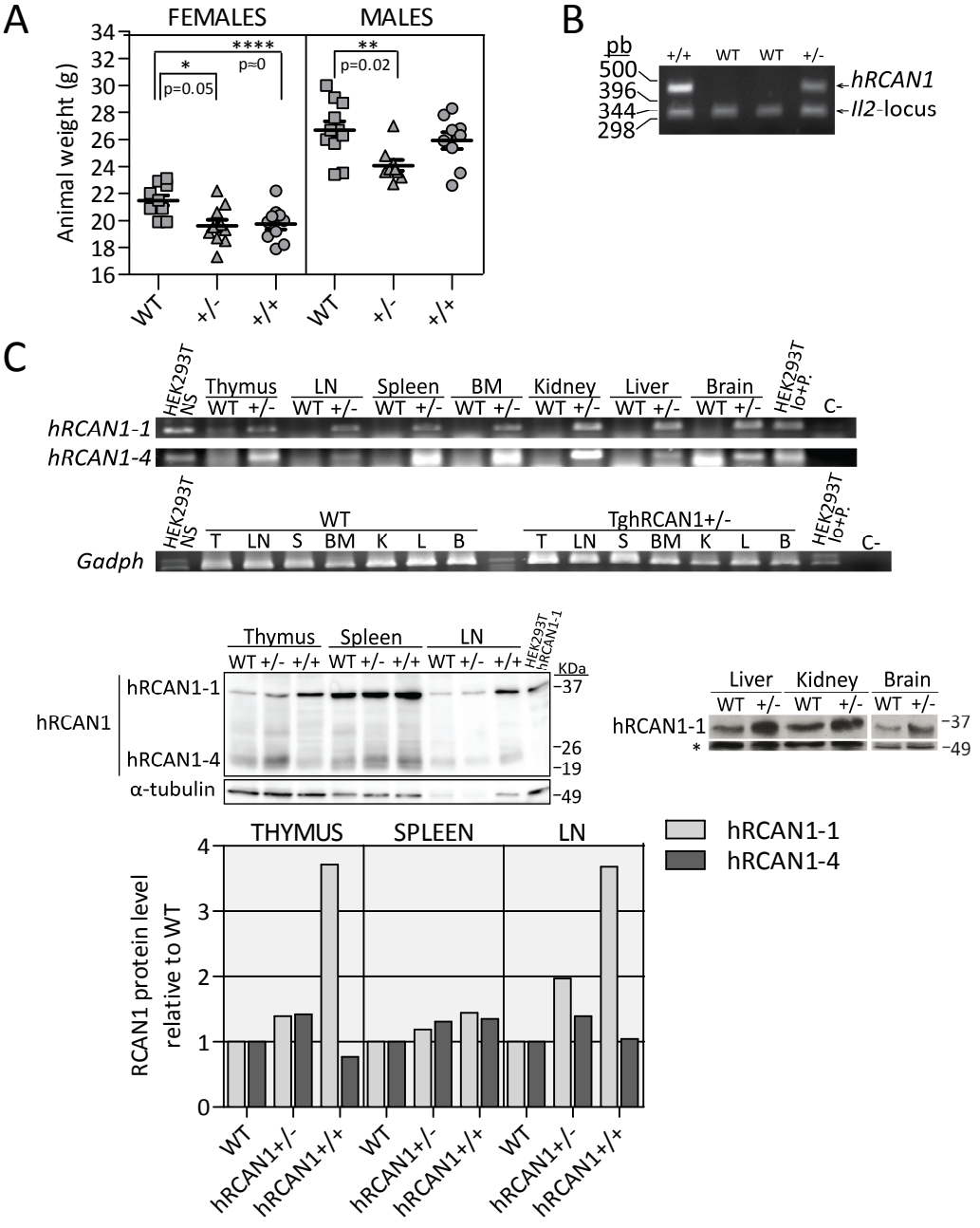
A
FEMALES
MALES
Animal weight (g)
p=0.05
p=0
p=0.02
WT
+/-
+/+
B
pb
500
396
344
298
+/+
WT
WT
+/-
hRCAN1
Il2-locus
C
HEK293T NS
Thymus
LN
Spleen
BM
Kidney
Liver
Brain
HEK293T Io+p.
C-
hRCAN1-1
hRCAN1-4
Gadph
T
LN
S
BM
K
L
B
TghRCAN1+/-
HEK293T hRCAN1-1
KDa
hRCAN1
α-tubulin
-37
-26
-19
-49
THYMUS
SPLEEN
LN
RCAN1 protein level relative to WT
hRCAN1+/-
hRCAN1+/+

Figure 2. Human RCAN1 isoforms are overexpressed in transgenic hRCAN1 mouse lymphoid tissues. A) Graph showing animal weight (g) of TghRCAN1$^{+/+}$ and TghRCAN1$^{+/-}$ animals compared to WT control littermates (n≥9). Mean values ± SEM are depicted in each plot. Mann-Whitney test: *p-value≤0.05, **p-value ≤0.01 and ****p-value. B) Genotyping of TghRCAN1 mice by semiquantitative PCR using genomic DNA isolated from tails. The lower band (about 325 bp), common in all genotypes, is located in the murine Interleukin 2 precursor locus (*Il2*-locus) and is used as genotyping control. The upper band (469 bp) corresponds to the amplification of a *hRCAN1* transgene region. C) Semiquantitative PCR amplification for *hRCAN1-1* and *hRCAN1-4* of cDNA prepared from female adult organs. PCR amplification of *Gadph* housekeeping gene was performed as internal control. Non-stimulated (NS) and ionomycin/PMA (Io+P) stimulated HEK 293T cells were used as control of *hRCAN1-4* gene expression induction. D) Detection of hRCAN1-1 and hRCAN1-4 protein levels in transgenic female mice. Soluble extracts from HEK 293T cells transfected with pHA-hRCAN1-1 were used as RCAN1 isoforms positive control. α-tubulin is used as internal loading control. In left panel, asterisks represent an unspecific electrophoretic band.

A

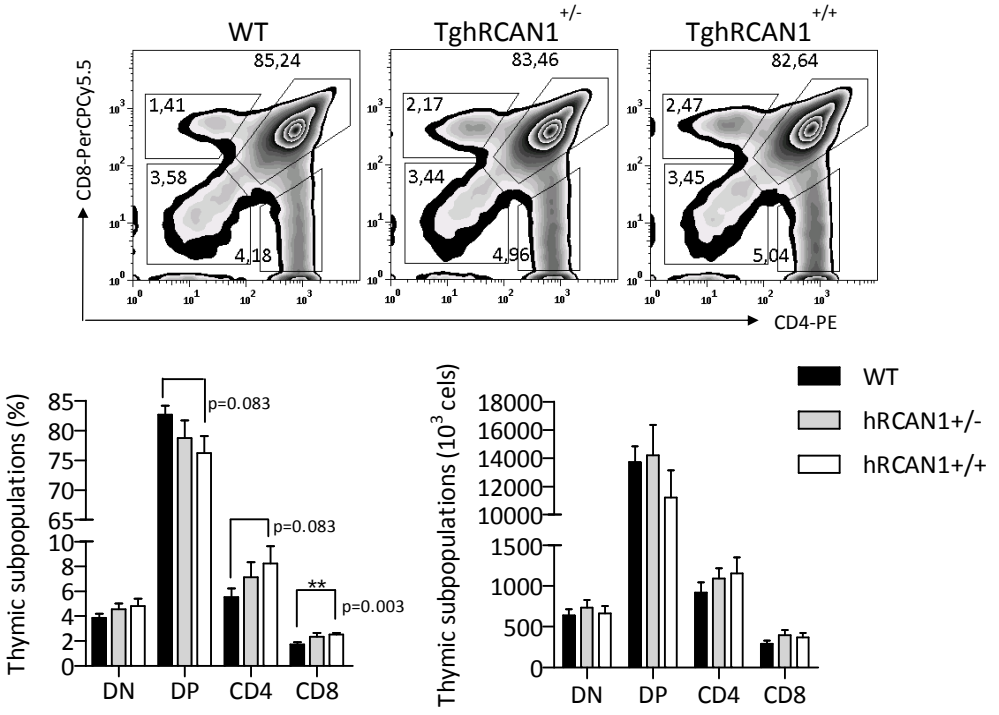
WT
TghRCAN1+/-
TghRCAN1+/+
85,24
83,46
82,64
1,41
3,58
4,18
2,17
3,44
4,96
2,47
3,45
5,04
CD8-PerCPCy5.5
CD4-PE
Thymic subpopulations (%)
p=0.083
p=0.083
**
p=0.003
DN
DP
CD4
CD8
Thymic subpopulations (10^3 cels)
WT
hRCAN1+/-
hRCAN1+/+

B

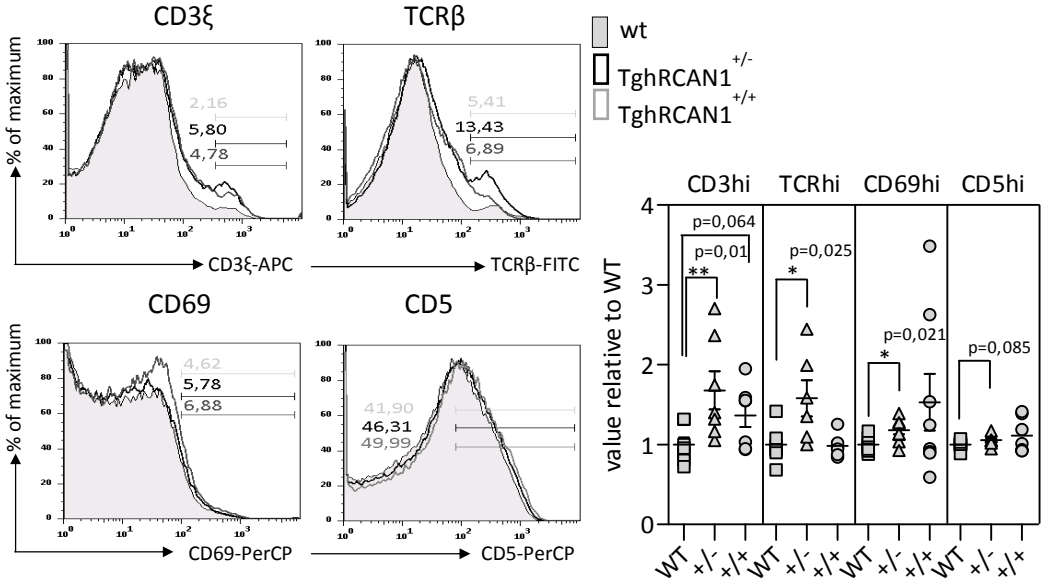
CD3ξ
TCRβ
wt
TghRCAN1+/-
TghRCAN1+/+
% of maximum
2,16
5,80
4,78
5,41
13,43
6,89
CD3ξ-APC
TCRβ-FITC
CD69
CD5
4,62
5,78
6,88
41,90
46,31
49,99
CD69-PerCP
CD5-PerCP
CD3hi
TCRhi
CD69hi
CD5hi
value relative to WT
p=0,064
p=0,01
**
p=0,025
*
p=0,021
*
p=0,085
WT
+/-
+/+

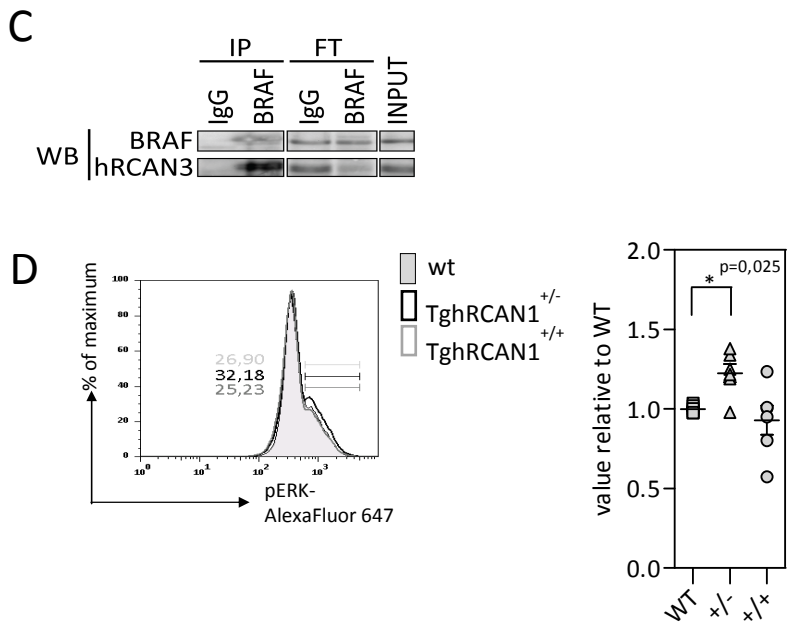

Figure 3A. Overexpression hRCAN1 gene increases positive selection and pERK signaling of thymocytes in TghRCAN1 female animals. Flow cytometric analysis of thymocyte development in TghRCAN1 mice. (A) Upper panel, representative CD4 versus CD8 staining dot plots from female wild-type, TghRCAN1$^{+/+}$ and TghRCAN1$^{+/-}$ mice. Lower panel, graphs represent the percentage and total cells of each thymocyte subsets from female wild-type, TghRCAN1$^{+/+}$ and TghRCAN1$^{+/-}$ mice. Bars represent the mean value ± SEM and are the summary from at least two independent experiments, n≥7. Mann-Whitney test: **p-value≤0,01. p-values≤0,1 are also indicated. DN, double negative; DP, double positive populations. B) Left panel, representative histograms showing CD3ξ, TCRβ, CD69 and CD5 in gated DP thymocytes from female mice. Percentages are shown within histogram. Right panel, graph shows the percentage of CD3ξ^{hi}, TCRβ^{hi}, CD69^{hi} and CD5^{hi} subpopulations in gated DP thymocytes from female wild-type, TghRCAN1$^{+/+}$ and TghRCAN1$^{+/-}$ mice. Data represents the summary of at least two independent experiments, relative to the mean of the value in WT animals within each experiment; n≥6. Mean values ± SEM ***are*** depicted in each plot. Mann-Whitney test: *p-value≤0.05, **p-value≤0.01. p-values≤0.1 are also indicated. C) Immunoprecipitation assay using anti-BRAF, anti-CnA and anti-RCAN3 antibodies, and unrelated mouse IgG as a control. Soluble extracts from Jurkat T cells were used as a source of RCAN3.D) Left panel, representative histogram of pERK levels in gated DP thymocytes previously stimulated *in vitro* by TCR crosslinking with anti-CD3 and anti-CD28 antibodies. Percentages are shown within histogram. Right panel, graph shows the analysis of the percentage of pERK^{hi} subpopulation in DP thymocytes from female WT, TghRCAN1$^{+/+}$ and TghRCAN1$^{+/-}$ mice. Data represents the summary of at least two independent experiments, relative to the mean of the value in WT animals within each experiment; n≥6. Mean values ± SEM are depicted in each plot. Mann-Whitney test: *p-value≤0.05.

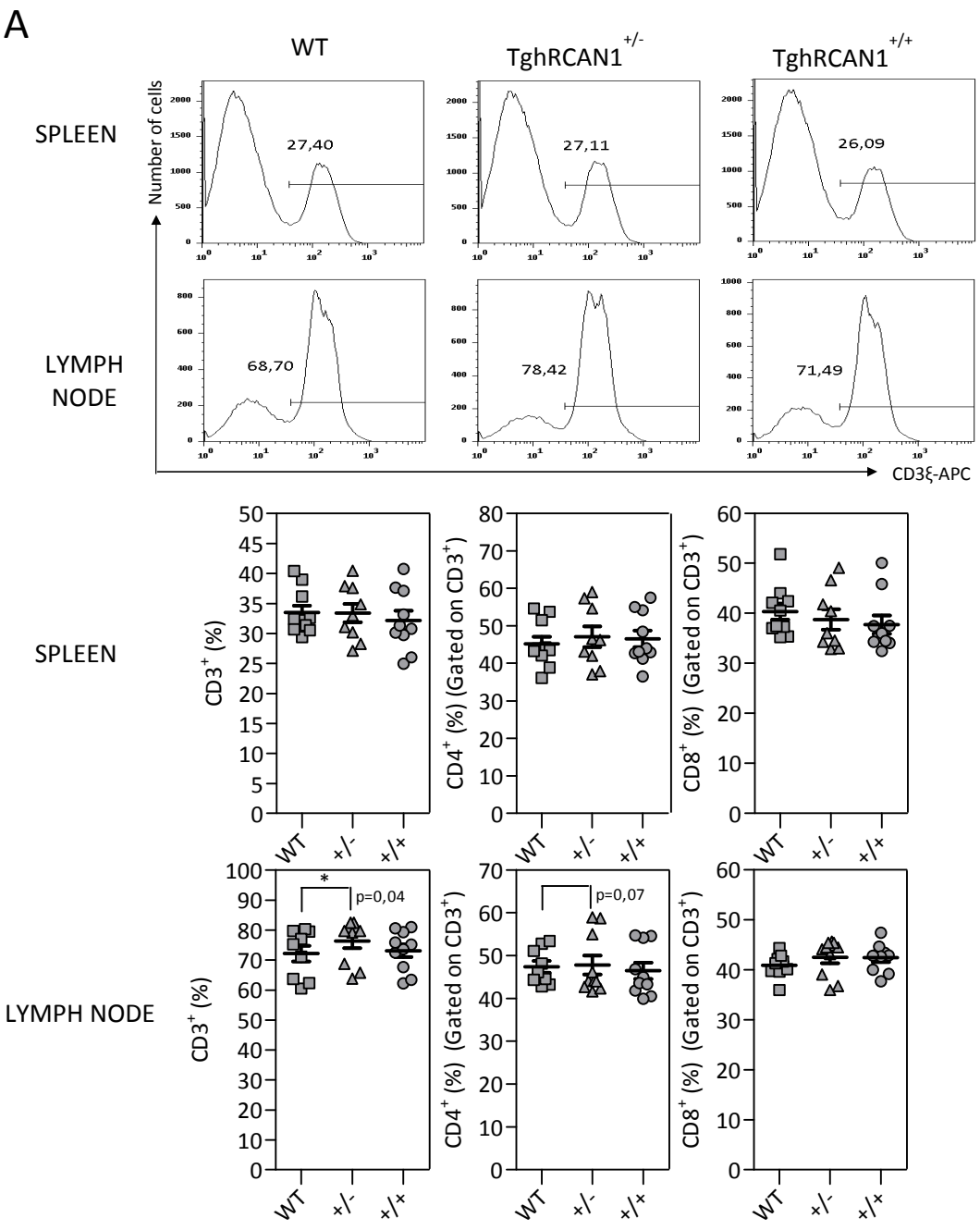
A
WT
TghRCAN1 +/-
TghRCAN1 +/+
SPLEEN
LYMPH NODE
Number of cells
27,40
27,11
26,09
68,70
78,42
71,49
CD3ξ-APC
SPLEEN
LYMPH NODE
CD3+ (%)
CD4+ (%) (Gated on CD3+)
CD8+ (%) (Gated on CD3+)
WT
+/-
+/+
*
p=0,04
p=0,07

Figure 4A. Overexpression of hRCAN1 increases the proportion of peripheral T cells with a reduced activation state phenotype. A) Upper panel, representative histograms show CD3 staining for splenocytes and lymph node cells from TghRCAN1$^{+/+}$ and TghRCAN1$^{+/-}$ and WT mice. Lower panel, graphs show the analysis of the percentages of CD3^{+}, CD4^{+} and CD8^{+} cells in both spleen and lymph node tissues. Data is the summary of three independent experiments, n≥9. Mean values ± SEM are depicted in each plot. Mann-Whitney test: *p-value≤0.05. p-values≤0.1 are also indicated.

B

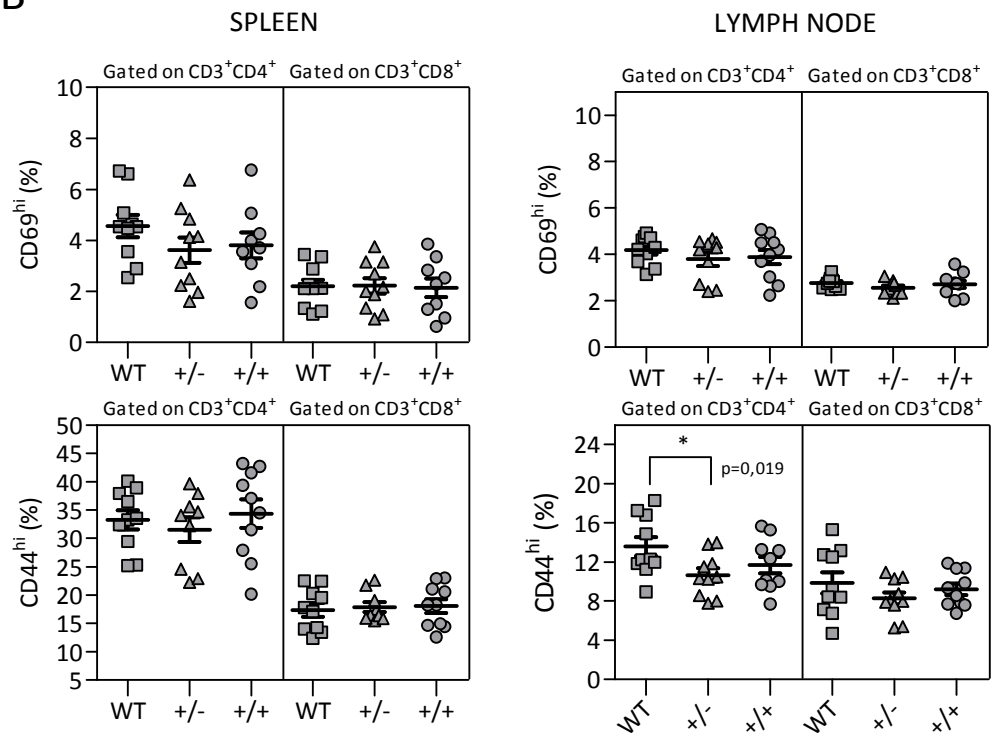
SPLEEN
LYMPH NODE
Gated on CD3+CD4+
Gated on CD3+CD8+
CD69hi (%)
CD44hi (%)
WT
+/-
+/+
p=0,019
*

C

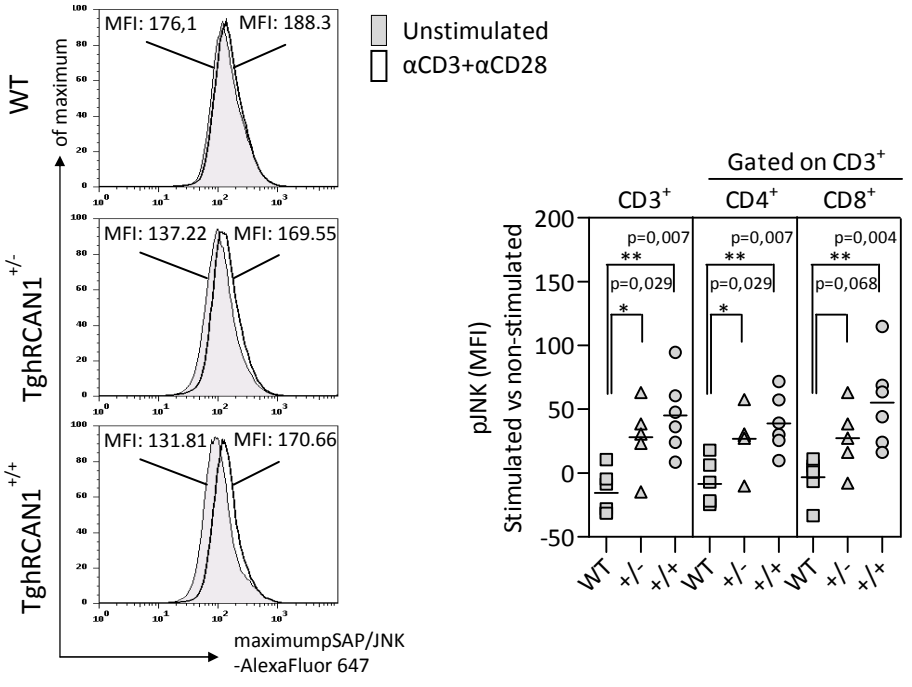
WT
TghRCAN1+/-
TghRCAN1+/+
MFI: 176,1
MFI: 188.3
MFI: 137.22
MFI: 169.55
MFI: 131.81
MFI: 170.66
of maximum
maximumpSAP/JNK
-AlexaFluor 647
Unstimulated
αCD3+αCD28
Gated on CD3+
CD3+
CD4+
CD8+
pJNK (MFI)
Stimulated vs non-stimulated
p=0,007
p=0,029
p=0,007
p=0,029
p=0,004
p=0,068
**
*

Figure 4B and C. Overexpression of hRCAN1 increases the proportion of peripheral T cells with a reduced activation state phenotype. B) Lymph node cells and splenocytes were stained with antibodies against CD4, CD8, CD3, CD44 and CD69. Graphs show the analysis of the percentages $CD44^{hi}$ and $CD69^{hi}$ populations in gated $CD4^{+}$ and $CD8^{+}$ T cells of spleen and lymph nodes from $TghRCAN1^{+/+}$ and $TghRCAN1^{+/-}$ and WT mice. Data represents the summary of three independent experiments, n ≥9. Mean values ± SEM are depicted in each plot. Mann-Whitney test: *p-value≤0.05. C) Splenocytes were stimulated *in* vitro with anti-CD3 plus anti-CD28 and stained with antibodies to CD4, CD8 and pJNK/SAP proteins. Left panel, representative histograms show the activation state of pSAP/JNK in unstimulated and stimulated condition in gated T cells ($CD3^{+}$) and in T cell subpopulations ($CD4^{+}$ and $CD8^{+}$). Right panel, graphs show the difference of MFI in pJNK between non-stimulated and stimulated conditions. Data represents the summary of three independent experiments, n ≥9. Mean values ± SEM are depicted in each plot. Mann-Whitney test: *p-value≤0.05, **p-value≤0.01. p-values≤0.1 are also indicated.

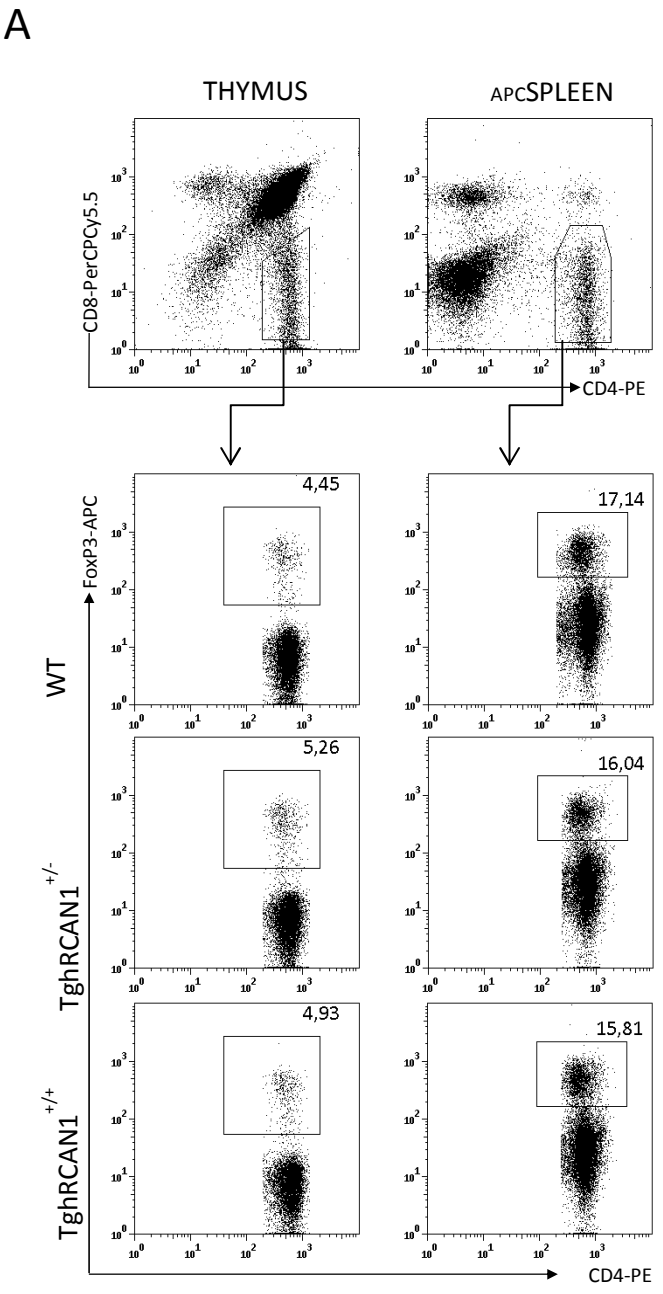
A
THYMUS
APCSPLEEN
CD8-PerCPCy5.5
CD4-PE
4,45
17,14
5,26
16,04
4,93
15,81
FoxP3-APC
WT
TghRCAN1+/-
TghRCAN1+/+
CD4-PE

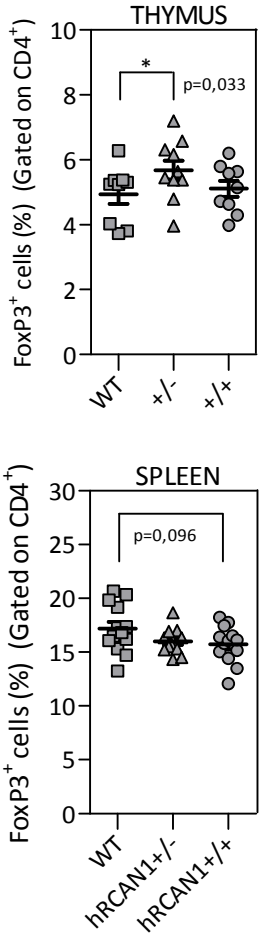
B
THYMUS
FoxP3+ cells (%) (Gated on CD4+)
*
p=0,033
WT
+/-
+/+
SPLEEN
FoxP3+ cells (%) (Gated on CD4+)
p=0,096
WT
hRCAN1+/-
hRCAN1+/+

Figure 5. FoxP3+ (Tregs) cell population increases in thymus (nTreg), but decreases in spleen (pTreg) of the TghRCAN1 transgenic mice. Thymocytes and splenocytes were permeabilized and stained for CD4-PE, CD8-PerCPCy5.5 and intracellular FoxP3-APC. (A) Upper panel, dotplots show CD4 versus CD8 staining in thymocytes and splenocytes. Lower panel, dot plots showing CD4 versus Foxp3 staining in gated $CD4^+$ cells. (B) Quantification of the percentages of $CD4^+FoxP3^+$ cells in in thymus and spleen from $TghRCAN1^{+/+}$ and $TghRCAN1^{+/-}$ and WT mice**.** Data represents the summary of three independent experiments, n ≥9. Mean values ± SEM are depicted in each plot. Mann-Whitney test: *p-value≤0.05. p-values≤0.1 are also indicated.

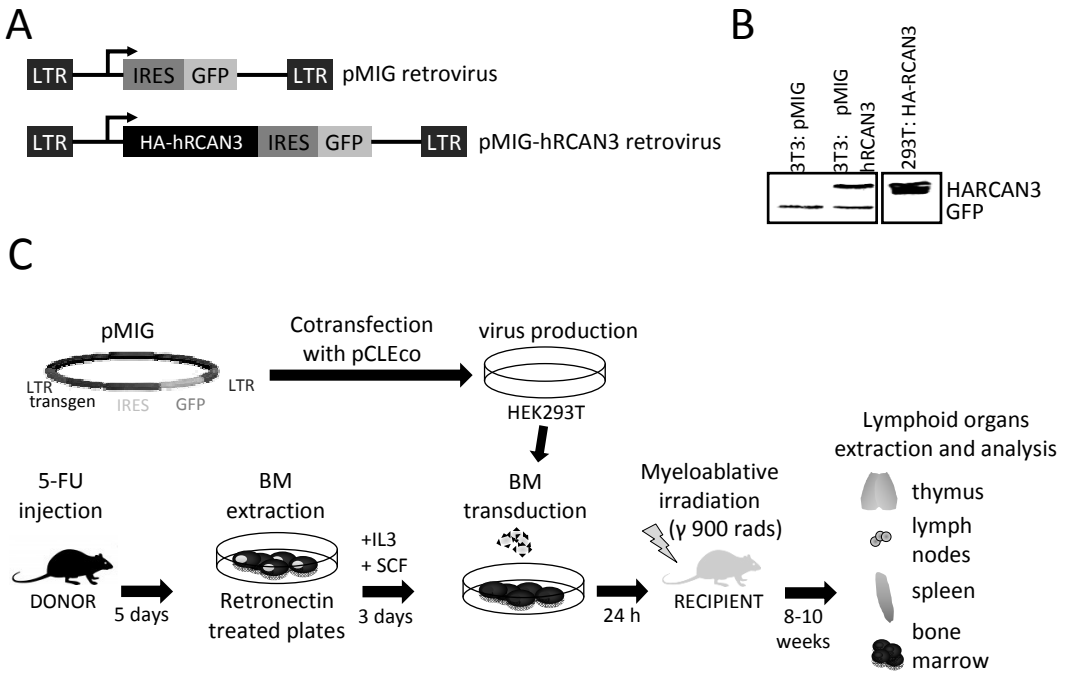

Figure 6A, B and C. Bone marrow reconstitution with hematopoietic progenitor cells overexpressing HA-hRCAN3 protein. A) Representation of retroviral constructions used to transduce bone marrow progenitors. LTR: Long Terminal Repeat; IRES: Internal Ribosomal Entry Site; HA-hRCAN3: human RCAN3 protein containing an N-terminal HA (Hemagglutinin) tag; GFP: Green Fluorescent Protein. Mock vector (pMIG) was used as control. B) GFP and HA-RCAN3 proteins are immunodetected in pMIG-hRCAN3 transduced NIH 3T3 cells by western blot analysis. HEK 293T cells overexpressing HA-RCAN3 were used as a positive control. C) Schematic representation of the bone marrow reconstitution protocol. Briefly, progenitor enriched bone marrow cells from donor mice were cultured in retronectin treated plates in the presence of SCF and IL3 cytokines for 3 days to induce stem cell proliferation. Subsequently, cells were transduced with retrovirus and, after 24 hours, they were inoculated in irradiated recipient mice and left for 8 to 10 weeks to reconstitute lymphoid organs.

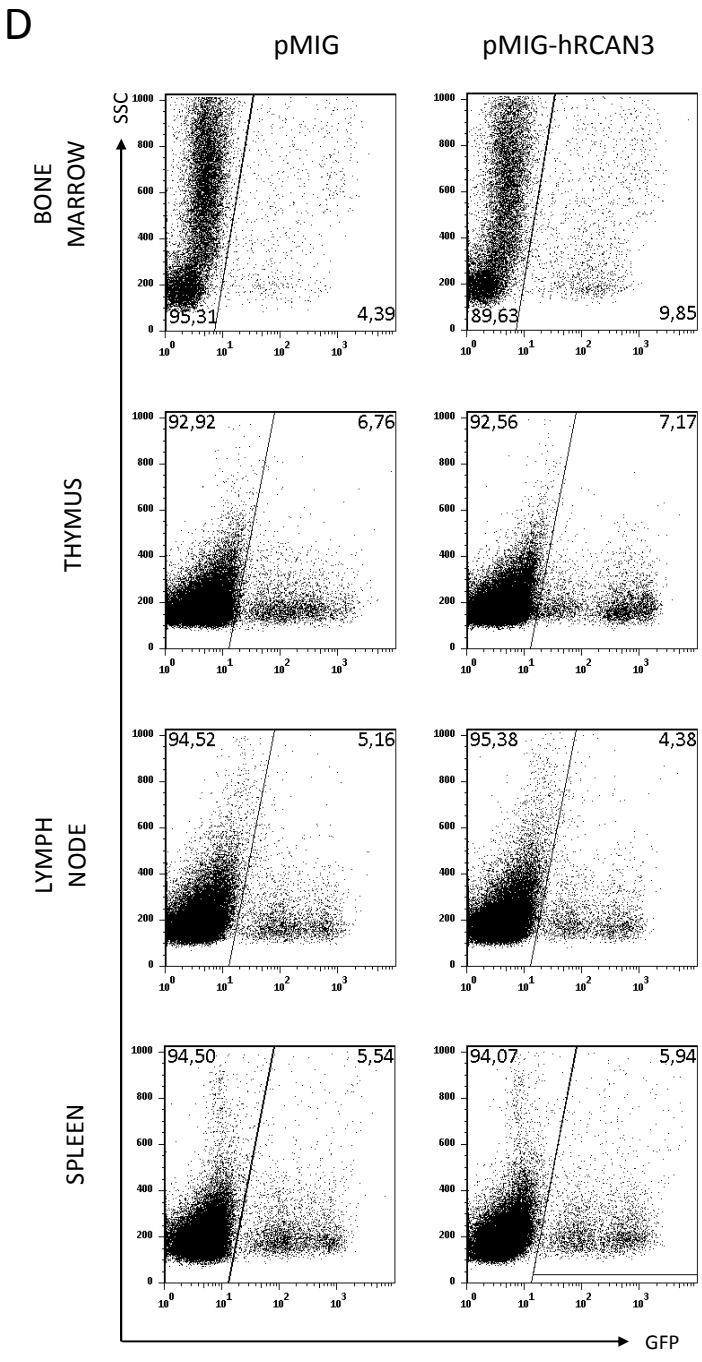

Figure 6D. Bone marrow reconstitution with hematopoietic progenitor cells overexpressing HA-hRCAN3 protein. D) Representative dot plots of GFP^+ cells in lymphoid tissues at 8 weeks of low bone marrow reconstitution.

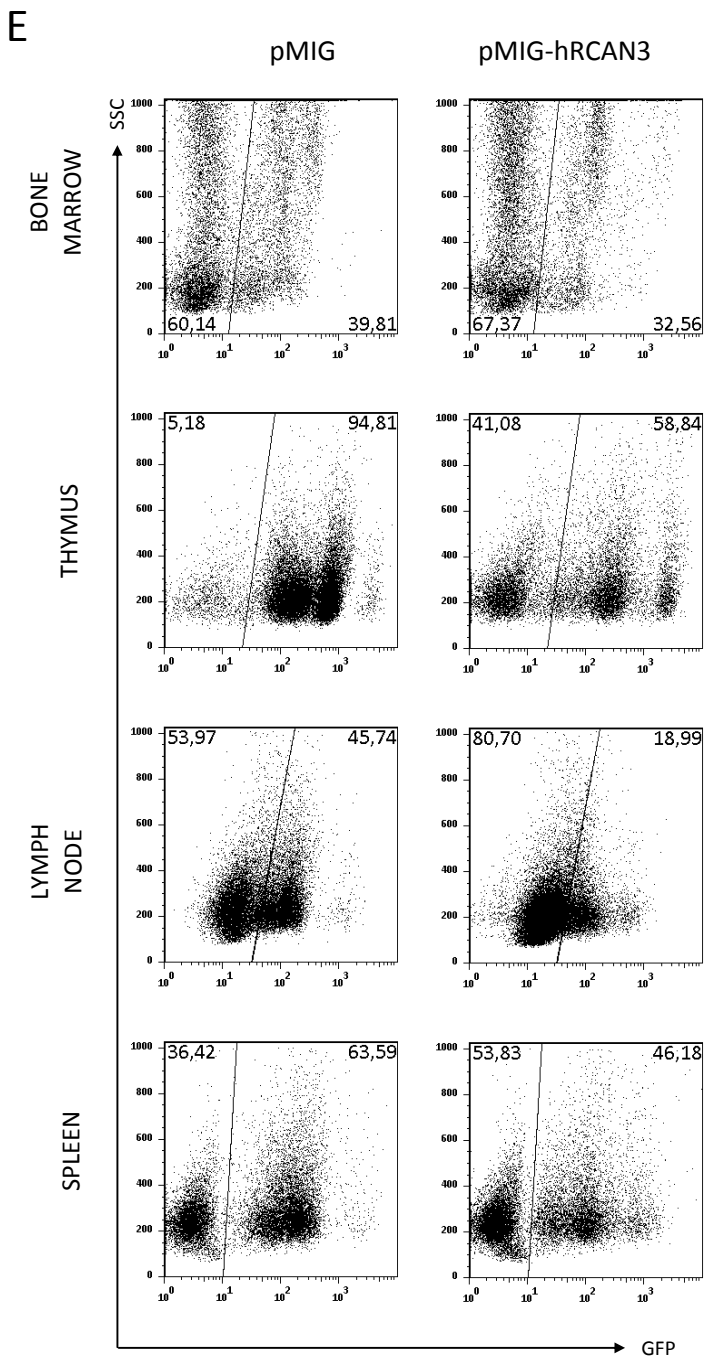

Figure 6E. Bone marrow reconstitution with hematopoietic progenitor cells overexpressing HA-hRCAN3 protein. E) Representative dot plots of GFP^+ cells in lymphoid tissues at 8 weeks of high bone marrow reconstitution.

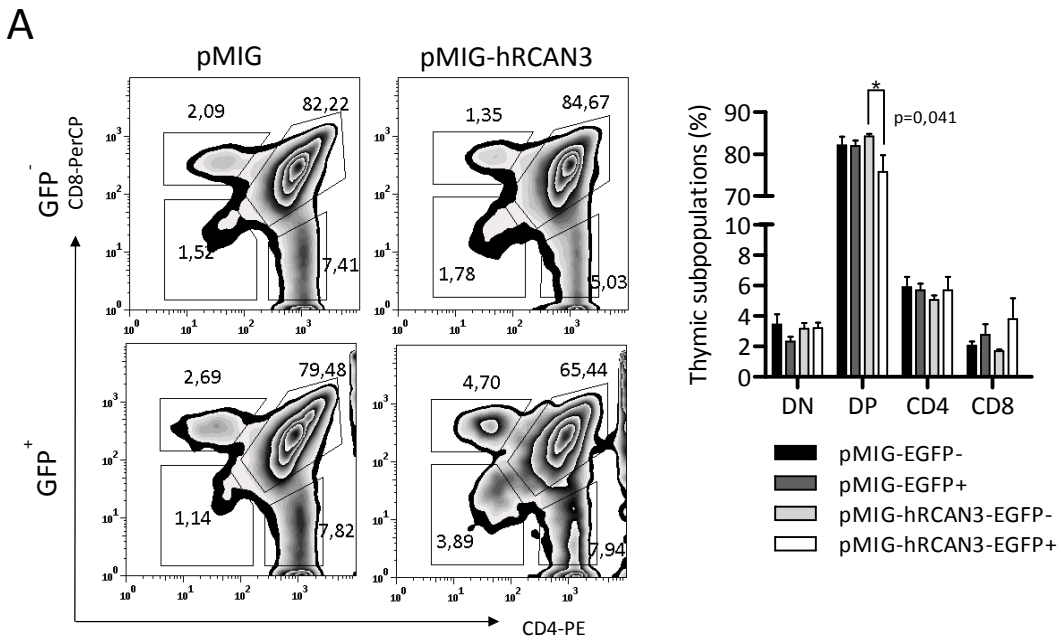

Figure 7A. hRCAN3 overexpression increases positive-selection in the thymus and decreases CD4+ and CD8+ cells in peripheral lymphoid organs. A) Left panel, representative dot plots of CD4 versus CD8 staining showing the percentages of developing thymocytes in both endogenous GFP^- and reconstituted GFP^+ cells. pMIG control cells are shown to comparison. Right panel, analysis of the percentages of endogenous GFP^- and reconstituted GFP^+ cells is shown for pMIG and pMIG-RCAN3 reconstitution. Bars represents mean values ± SEM. Data represents the summary of four independent experiments, n≥6. Mann-Whitney test: *p-value≤0.05.

B

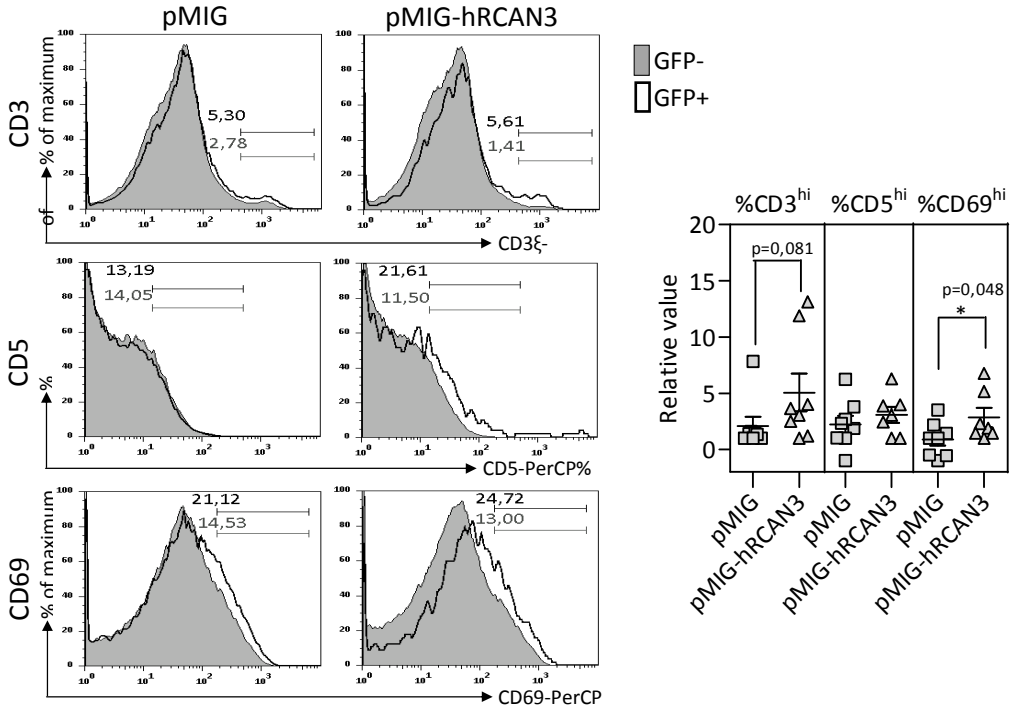
pMIG
pMIG-hRCAN3
GFP-
GFP+
CD3
% of maximum
5,30
2,78
5,61
1,41
CD3ξ-
CD5
%
13,19
14,05
21,61
11,50
CD5-PerCP%
CD69
% of maximum
21,12
14,53
24,72
13,00
CD69-PerCP
%CD3hi
%CD5hi
%CD69hi
Relative value
p=0,081
p=0,048
*
pMIG
pMIG-hRCAN3

C

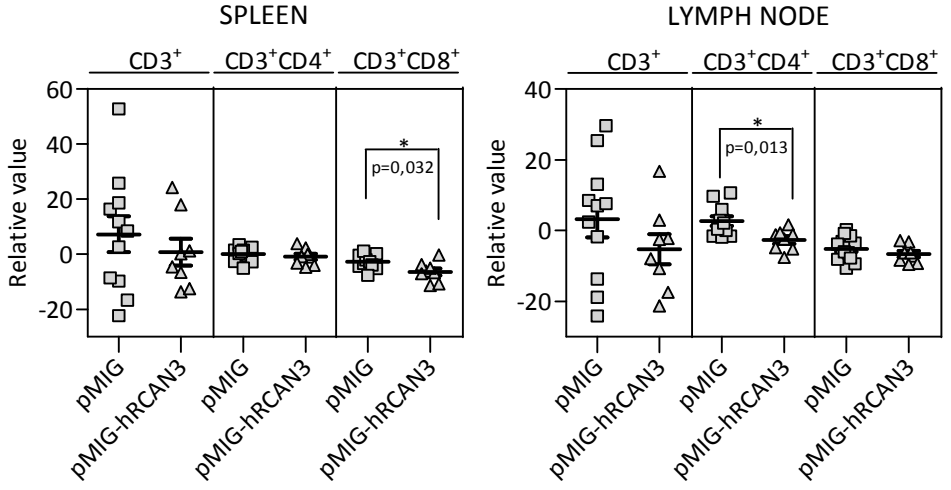
SPLEEN
LYMPH NODE
CD3+
CD3+CD4+
CD3+CD8+
Relative value
p=0,032
p=0,013
*
pMIG
pMIG-hRCAN3

Figure 7B and C. hRCAN3 overexpression increases positive-selection in the thymus and decreases CD4+ and CD8+ cells in peripheral lymphoid organs. B) Reconstituted thymocytes were stained with antibodies to CD4, CD8, CD3ξ, CD69 and CD5. Left panel, representative histograms showing CD3ξ, CD69 and CD5 staining in gated DP thymocytes from pMIG and pMIG-hRCAN3 reconstitutions. In right panel, analysis of $CD3\xi^{hi}$, $CD5^{hi}$ and $CD69^{hi}$ in gated DP subset. Values in gated GFP^+ cells are showed as a relative to respective GFP^- cells and normalized to the lowest value for each experiment. Data represents the summary of four independent experiments, n≥6. Mean values ± SEM are depicted in each plot. Mann-Whitney test: *p-value≤0.05. p-values≤0.1 are also indicated. C) Peripheral lymphocytes from lymph node and spleen were stained with antibodies to CD4, CD8 and CD3. Graphs show the analysis of CD3+, CD3+CD4+ and CD3+CD8+ T cells in gated GFP+ cells. Values of GFP+ population are showed as a relative to its own GFP- population values for each specific surface marker. Data represents the summary of four independent experiments, n≥8. Mean values ± SEM are also indicated. Mann-Whitney test: *p-value≤0.05.

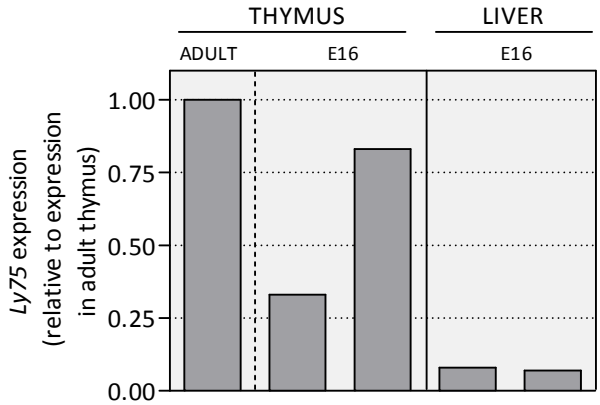

Figure S1. Ly75 expression in embryonic samples. cDNA was prepared from total RNA from two different pools of fetal livers and thymi collected at the same embryonic stage (E16). Both pools were analyzed independently by real time quantitative PCR using UPL probes (Roche) and specific primers for mouse *Ly75* transcript. Adult thymus was included as a positive control. Values normalized to *Hprt* gene and normalized to the value in adult thymus are shown.

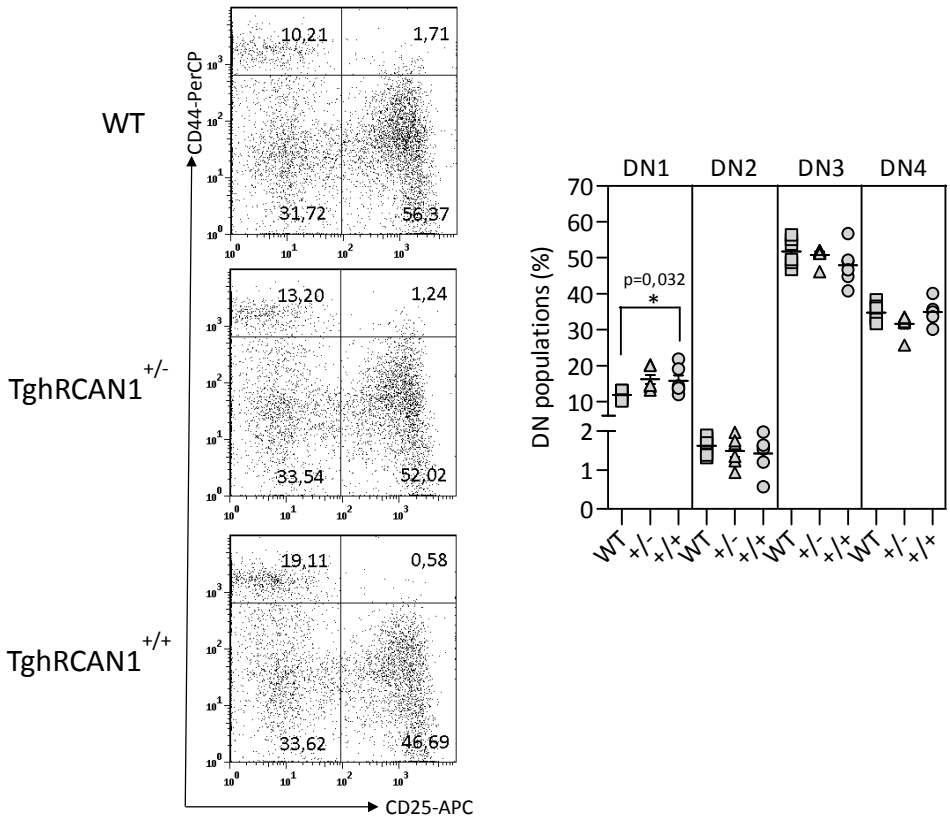

Figure S2. Analysis of DN immature subsets in hRCAN1 transgenic mice. Thymocytes were isolated and stained with a combination of CD4-PE, CD8-PE, CD25-APC and CD44-PerCP antibodies. Representative dot plots of CD44 and CD25 staining in gated DN ($CD4^-CD8^-$) cells from $TghRCAN1^{+/+}$ and $TghRCAN1^{+/-}$ and WT mice. Data represents the summary of two independent experiments, n=6. Mean values ± SEM are depicted in each plot. Mann-Whitney test: *p-value≤0.05.

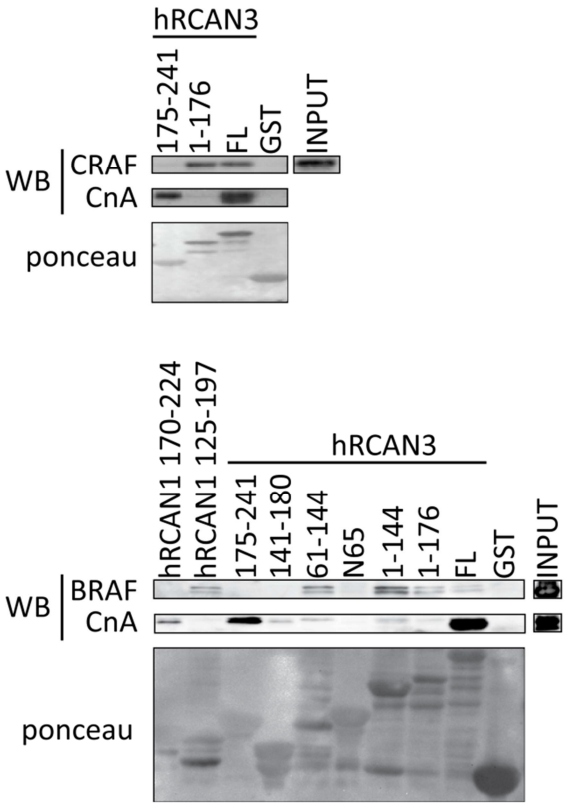

Figure. S3. RCAN interacts with CRAF and Cn in a non-mutually exclusive manner. Pull down experiments using GST-RCAN3 fusion proteins and deletion mutants as a bait and soluble protein extract from Jurkat T cells as source of CnA and RAF proteins. Samples were resolved by SDS 10% reducing PAGE, and visualized by Western blotting with anti-BRAF and anti-CnAα antibody.

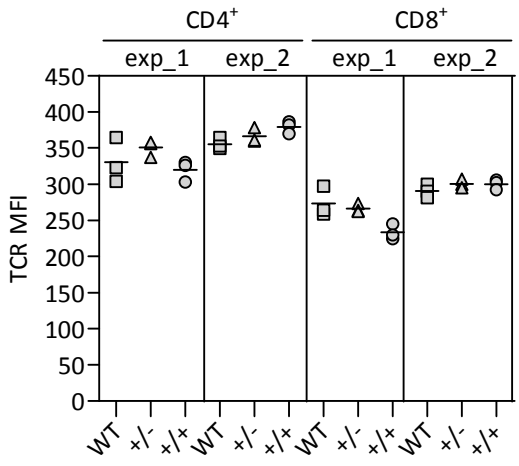

Figure. S4. Overexpression of hRCAN1 increased the TCR expression in SP thymocytes. Graph shows the MFI of TCR expression in SP thymic subpopulations from TghRCAN1$^{+/+}$ and TghRCAN1$^{+/-}$ and WT mice from two independent experiments.

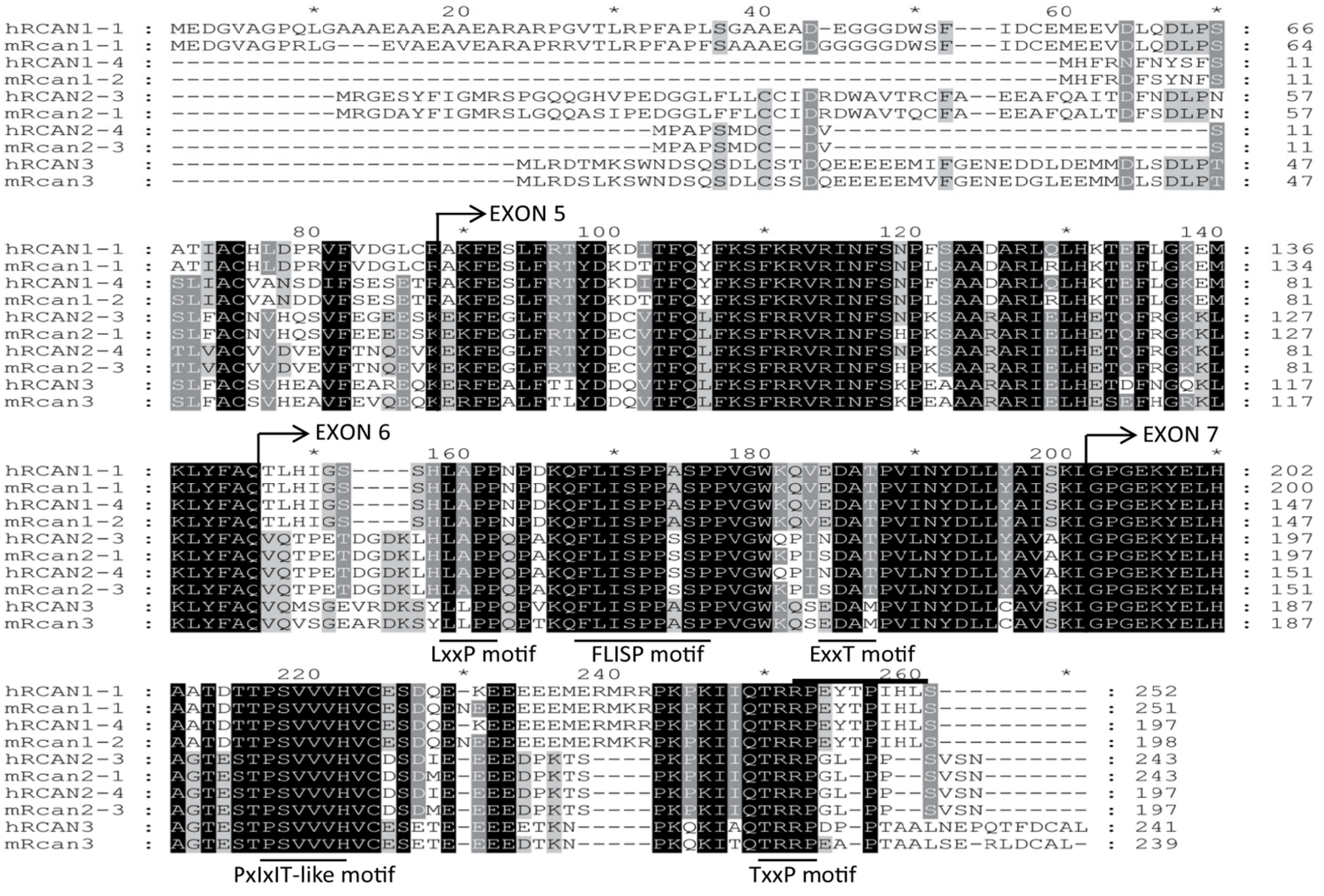
EXON 5
EXON 6
EXON 7
LxxP motif
FLISP motif
ExxT motif
PxIxIT-like motif
TxxP motif

Figure. S5. Alignment of human RCAN and mouse Rcan proteins. Protein sequence identity among the different protein isoforms encoded by human *RCAN* genes [protein RefSeq acc. number: RCAN1-1, NP_004405.3 (252 aa); RCAN1-2, NP_981962.1 (117 aa); RCAN1-4, NP_981963.1 (197 aa); RCAN2α, NP_005813.2 (197 aa); RCAN2β, NP_001238902.1 / NP_001238903.1 (243 aa); RCAN3-4, NP_038469.1 / NP_001238906.1 / NP_001238907.1 / NP_001238908.1 (241 aa)] and mouse Rcan genes [protein Refseq acc. number: Rcan1-1, NP_001075018.1 (251 aa); Rcan1-2, NP_062339 (198 aa); Rcan2-1, NP_997532 (243 aa); Rcan2-3, NP_085101 (197 aa); Rcan3, NP_075356 (239 aa)]. Grey intensity shade increases with sequence conservation (50, 80 or 100% of amino acid conservation). Numbers correspond to protein amino acid number. Conserved motifs and peptide sequence used to generation of RCAN1 antibody (RPEYTPIHLS) are indicated.

Supplementary Table 1A- PRIMERS AND PROBES FOR REAL TIME QUANTITATIVE PCR ANALYSIS OF MOUSE mRNA FORMS

TRANSCIPT (RefSeq)	PRIMER NAME	PRIMER SEQUENCE (5'->3')	LOCATION*	Tm (°C)	nt	UPL probe
m*Rcan1-1* (NM_001081549)	mRcan1-1 Fw	AGCTTCATCGACTGCGAGAT	210-229	60	137	#10
	mRcan1-1 Rv	TCATATGTTCTGAAGAGGGATTCA	323-346	59		
m*Rcan1-2* (NM_019466)	mRcan1-2 Fw	CGATGATGTCTTCAGCGAAA	152-171	59	74	#81
	mRcan1-2 Rv	TGGTGTCCTTGTCATATGTTCTG	203-225	59		
m*Rcan2-1* (NM_207649)	mRcan2-1 Fw	CATTGTTTGCCTGCAATGTT	421-440	59	75	#91
	mRcan2.1 Rv	GGAACAGTCCCTCGAATTTTT	475-495	59		
m*Rcan2-2* (NM_030598)	mRcan2-2 Fw	TAGGCTCAGCTCGCTCTCTT	127-146	59	71	#6
	mRcan2-2 Rv	TCAGGATGGATACTGTCCTGTACT	174-197	59		
m*Rcan2-2* (NM_030598)	mRcan2-2_b Fw**	GCCGGGTCCTTCTTTACTCT	48-67	59	87	#32
	mRcan2-2_b Rv**	TGAGCCTAGGGAGACTCAGG	115-134	59		
m*Rcan3* (NM_022980)	mRcan3 Fw	GATGCCAGTGATCAACTATGACC	720-742	60	76	#20
	mRcan3 Rv	CGCGTGCAGTTCGTATTTC	777-795	60		
m*Gusb* (NM_010368)	mGusb Fw	CTCTGGTGGCCTTACCTGAT	868-887	59	73	#42
	mGusb Rv	CAGTTGTTGTCACCTTCACCTC	919-940	59		
m*Hprt1* (NM_013556)	mHprt1 Fw	TCCTCCTCAGACCGCTTTT	104-122	59	90	#95
	mHprt1 Rv	CCTGGTTCATCATCGCTAATC	173-193	59		
m*Actb* (NM_007393)	mActb is Fw	CTAAGGCCAACCGTGAAAAG	414-433	59	104	#64
	mActb is Rv	ACCAGAGGCATACAGGGACA	498-517	60		
m*Ly75* (NM_013825)	mLy75 Fw	CGGACTCTCCAGTCAAGATGA	3492 - 3512	60	105	#26
	mLy75 Rv	ACGCAGTCATCAAGTTGCTC	3577 - 3596	59		
m*Gapdh* (NM_008084)	mGapdh Fw	TGTCCGTCGTGGATCTGAC	763-781	60	75	#80
	mGapdh Rv	CCTGCTTCACCACCTTCTTG	818-837	60		

Supplementary Table 1A- DNA primers and probes for real time quantitative PCR analysis of mouse Rcan mRNA forms

Supplementary Table 1B- PRIMERS FOR TRANSGENE GENOTYPING AND mRNA QUANTIFICATION in TghRCAN1 mice					
GENE /TRANSCRIPT (RefSeq)	**PRIMER NAME**	**PRIMER SEQUENCE (5'->3')**	**LOCATION***	**Tm (°C)**	**nt**
human *RCAN1* (NT_011512)	hRCAN1.ex3 Fw***	GCACAAGGACATTTGGGACTG	N/A****	54	469
	hRCAN1.ex4 Rv***	GTTGGGGATGCTGAGTGAATG	N/A****	54	
mouse *Il2 precursor locus* (NT_162143.4)	mIl2P Fw***	CTAGGCCACGAATTGAAAGATCT	N/A****	53	325
	mIl2P Rv***	GTAGGTGGAAATTCTAGCATCATCC	N/A****	54	
human *RCAN1-1* (NM_004414)	hRCAN1.ex1 Fw	GAGGAGGTGGACCTGCAG	241-258	51	219
	hRCAN1.ex5 Rv	AGTCTTATGCAGCTGGAGC	459-441	51	
human *RCAN1-4* (NM_203418)	hRCAN1.ex4 Fw	TCCCTGATTGCCTGTGTGG	248-266	54	189
	hRCAN1.ex5 Rv	AGTCTTATGCAGCTGGAGC	436-418	52	
mouse *Gapdh* (NM_008084)	mGapdh Fw	CCCATCACCATCTTCCAGGA	277-296	53	446
	mGapdh Rv	ATGACCTTGCCCACAGCCT	722-704	56	

LOCATION*: Location referred to RefSeq ID

***: primers used for hRCAN1 transgene genotyping

m*Rcan2-2*-b**: primers used to *Rcan2-2* detection in embryonic samples

N/A****: Not applicable

Supplementary Table 1B- Primers for genotyping and mRNA quantification in TghRCAN1 mice

Supplementary Table 2A - FLOW CYTOMETRY ANTIBODIES				
ANTIBODY	**SOURCE**	**CLONE**	**REFERENCE - MANUFACTURER**	**DILUTION**
mCD4-PE	Rat	H129.19	553652 - BD Pharmigen TM	1/300
mCD4-APC	Rat	GK1.5	100411 - BioLegend	1/300
mCD8a-PE	Rat	53-6.7	100707 - Biolegend	1/300
mCD8a-PerCP	Rat	53-6.7	553036 - BD Pharmigen ™	1/50
mCD8a-PerCPCy5.5	Rat	53-6.7	100733 - Biolegend	1/300
mCD3ξ-FITC	Armenian Hamster	145-2C11	553061 - BD Pharmigen ™	1/200
mCD5-PerCP	Rat	53-7.3	100615 - Biolegend	1/300
mCD69-PerCP	Armenian Hamster	H1.2F3	104520 - Biolegend	1/300
mCD44-PerCPCy5.5	Rat	IM7	560570 - BD Pharmigen ™	1/200
mCD25-FITC	Rat	PC61.5.3	22150253 - Immunotools	1/100
mCD25-APC	Rat	PC61	557192 - BD Pharmigen ™	1/300
mTCRβ-FITC	Hamster	H57-597	562081 - BD Pharmigen ™	1/150
mFoxP3-APC	Rat	FJK-16s	17-5773-82 - eBioscience	1/200
pERK1/2 (Thr202/Tyr204)	Rabbit	polyclonal	9101 - Cell Signaling	1/100
pP38 (Thr180/Tyr182)	Rabbit	polyclonal	9211 - Cell Signaling	1/100
pAkt (Ser473)	Rabbit	193H12	4058 - Cell Signaling	1/100
p-SAP/JNK (Thr183/Tyr185)	Rabbit	polyclonal	9251 - Cell Signaling	1/100
anti-Rabbit IgG-AlexaFluor-647	Donkey	polyclonal	A-31573 - Life Technologies	1/400

Supplementary Table 2B - T CELL STIMULATION ANTIBODIES				
ANTIBODY	**SOURCE**	**CLONE**	**REFERENCE - MANUFACTURER**	**STIMULATING CONDITIONS***
mCD3	Syrian Hamster	145-2C11	22150031 - Immunotools	T- 10 µg/mlS-5 µg/ml
mCD28	Syrian Hamster	37.51	553295 - BD Pharmigen ™	T- 10 µg/mlS-5 µg/ml
anti-syriam Hamster IgG	Goat	polyclonal	31115 - Pierce ® Thermo scientific	T- 20 µg/mlS-10 µg/ml

* STIMULATING CONDITIONS: Time of stimulation was 3 min for pERK, pAKT and pP38 and 15 min for pSAP/JNK. T, thymus; S, spleen.

Supplementary Table 2A – Antibodies used for flow cytometry analysis and for T cell stimulation.

ANNEX TO ARTICLE

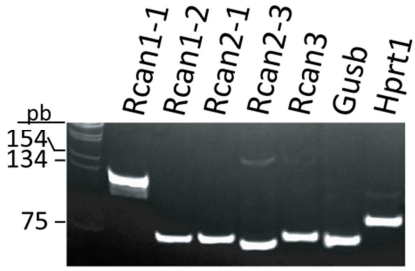

Figure A1. Correct length of amplicons in the real time quantitative PCR analysis of mouse Rcan mRNA forms. PCR products were resolved by electrophoresis on a continuous polyacrylamide gel (12%) and stained in ethidium bromide (EtBr) solution.

CONCLUDING REMARKS

The members of the RCAN family are endogenous modulators of the phosphatase Calineurin (Cn). Cn protein is the only serine/threonine phosphatase regulated by calcium and calmodulin and is highly conserved from yeast to humans. Cn dephosphorylates *in vivo* many substrates, among them NFATc, TAU protein, the enzyme NO synthase 2 (NOS2), BAD, and by these means play a crucial role in many cellular processes. In lower eukaryotes, Cn is essential in processes such as salt stress adaptation and cell cycle progression (reviewed in Rusnak and Mertz, 2000). With the advent of vertebrates, NFATc transcription factors emerged as a multigenic family, probably originated by recombination of an ancient precursor with Rel domain. Cn and NFATc proteins function as molecular integrators of Ca^{2+} signals together with other signaling pathways, and they are essential in the orchestration of the complex cellular interactions crucial for vertebrate systems (reviewed in Rusnak and Mertz, 2000; Aramburu et al., 2004). NFATc dephosphorylation by Cn promotes their translocation from the cytoplasm to the nucleus where, in cooperation with other transcription factors, regulates different transcriptional programs important in morphogenesis, organogenesis and lymphocyte development and function (Wu *et al.*, 2007).

The appearance of NFATc proteins in vertebrates coincides with the generation of three RCAN proteins, which contribute for the tightly regulated complex network of cellular processes needed in vertebrate organisms. Moreover, the regulation of RCAN proteins over Cn activity specifically towards NFATc highlights the importance of RCAN proteins in this signaling pathway in vertebrates.

The first part of this Thesis has focused on analyzing the *RCAN* family origin as a multigenic family, deepening in their gene structure and exploring mechanisms that could be involved in the regulation of *RCAN3* gene expression. Moreover, given the importance of the Ca^{2+}-Cn-NFATc pathway in T lymphocyte development and function, and also the interaction of RCAN proteins with other molecules involved in TCR-dependent signaling pathways, the second part of this Thesis has focused on examining the *in vivo* effect of *RCAN* overexpression in T cell development and function.

EVOLUTION, GENE STRUCTURE AND REGULATION OF *RCAN* GENE EXPRESSION

Three *RCAN* genes have been described in almost all jawed vertebrates, while in invertebrates and lower eukaryotes only one gene has been described. However, by a comparative genomic analysis, we have found several exceptions to this rule. In jawed vertebrates there are some organisms that have lost or gain some *RCAN* gene. For instance, all fish genomes lack *Rcan2* gene, except *Dario rerio* (zebrafish)

and *Latimeria chalumnae* (coelacanth). *Rcan2* gene probably was lost in a reorganization event posterior to zebrafish divergence. *Rcan2* gene was also lost in *Anolis carolinensis* (anole lizard). Regarding the *RCAN1* gene, in vertebrates such as *Sorex araneus* (common shrew), *Taeniopygia guttata* (zebra finch) *Procavia capensis* (hyrax), *Felis catus* (cat) and *Vicugna pacos* (alpaca), *RCAN1* gene is not yet annotated, however, *RCAN1* sequence can be found in contigs that have not been yet assembled into the genome. Instead, other organims present additional *RCAN* genes, as zebrafish and *Callithrix jacchus* (marmoset), likely originated by an individual gene duplication event.

RCAN genes from jawed vertebrates are located in the called ACD clusters, together with *RUNX* and *CLIC* genes (Results chapter, Article 1, Fig. 1). Concretely in humans, these gene clusters are located in chromosome 21 (ACD21), chromosome 6 (ACD6) and chromosome 1 (ACD1) (Strippoli *et al.*, 2002). Our analysis of *CLIC*, *RUNX* and *RCAN* paralogous genes in Urochordata and Cephalochordata, as representative of invertebrate organisms within chordates, but also in agnathans, as representative "living fossils" of early vertebrates (jawless vertebrates), revealed that these genes are independently located in these organisms. This fact suggests that ACD clustering formation took place after agnathans-gnasthostomes split in vertebrates, and may be important in jawed vertebrate organims. The maintenance of this clustered distribution among evolution suggests a possible cooperation of ACD clustered genes, *RUNX*, *CLIC* and *RCAN*. Actually, we have observed that this functional cooperation seems plausible. For instance, a possible cooperation among ACD clustered genes could be inferred from their role in immune responses and skeletogenesis. Concerning the immune response, the role of CLIC (Honda and Taniguchi, 2006; He *et al.*, 2011) and RCAN (Hesser *et al.*, 2004; Minami *et al.*, 2009; Lee *et al.*, 2009; Narayan *et al.*, 2005) proteins in innate immunity has been extensively studied. Both genes are involved in TLR signaling and inflammation. Moreover, the role of RUNX proteins in innate immune responses can be concluded by their involvement in macrophage differentiation, monocyte migration and DC maturation (Estecha *et al.*, 2012). Likewise, RUNX (Levanon and Groner, 2004; Puig-Kroger and Corbi, 2006; Djuretic *et al.*, 2009) and RCAN (Ryeom *et al.*, 2003; Sanna *et al.*, 2006) has been described to participate in adaptive immunity. On the other hand, the most important evidence of cooperation between these three family of proteins is their participation in osteoblast differentiation and/or function and, subsequently, in bone formation (Lian and Stein, 2003; Lian *et al.*, 2004; Bassett *et al.*, 2012; Yang *et al.*, 2009a). Interestingly, the presence of two functional copies of *Runx* genes in both living representative organims of jawless vertebrates reinforces the importance of *Runx* genes in skeletogenesis. Thus, the

three genes in ACD clusters seem to play essential roles in several processes of vertebrates and, probably, suggest that their clustered organization and further maintenance along evolution is due to functional purposes.

In order to deepen in the human *RCAN* gene structure and possible mechanisms involved in *RCAN* gene expression regulation, we performed a detailed bioinformatic comparative analysis among the three human members (Results chapter, Article 1, Fig. 3). All of them present a conserved complex structure characterized by the presence of different transcripts generated by alternative splicing. Due to this conserved structure among all human *RCAN* genes and the recent description of several novel *RCAN3* exons (Facchin *et al.*, 2011), we have proposed a novel nomenclature for *RCAN3* known exons and mRNA forms, that can be also used for future exons and transcripts if discovered (Results chapter, Article 1, Fig. 4 and table S2) This nomenclature is based on exons being used in each transcript and also to give the same number to common exon in all the *RCAN* genes, which encode for the highly conserved amino acid sequences at RCAN central and C-terminal protein regions. According to this novel nomenclature for *RCAN3* gene, all *RCAN* genes present seven exons. Exons 5 to 7 are common to all transcript forms of each gene, and the different transcripts arise from alternative combination of the first exons. The transcription of these different *RCAN* mRNA forms can be regulated at different levels.

All *RCAN* transcripts bear 5' untranslated regions (UTR) and 3'UTR. It has been described that these regions in mRNAs may work as post-transcriptional and translational regulators by different mechanisms (reviewed in Pesole *et al.*, 2000). Therefore both UTR regions probably constitute important regulatory regions of *RCAN* gene expression and post-transcriptional and translational regulation. However, the role of these UTR sequences should be analyzed to understand their regulatory role in *RCAN* genes.

Concerning *RCAN* gene structure, all *RCAN* genes present alternative and mutually exclusive first exons that give rise to alternative transcripts. The presence of alternative transcripts is characteristic, but not exclusive, of vertebrate genes. They confer the possibility to generate multiple isoforms of proteins and, by this means, they contribute to expand the proteome of the organisms. The presence of different alternative transcripts from one single gene requires a specific and fine-tuned gene expression regulation in response to specific stimulus or/and a specific tissue which is driven by the use of different promoters. Regarding *RCAN* gene expression regulation, promoters regions that regulates the expression of some *RCAN* transcripts are regulated by a TATA box, while other bear CpG islands. In particular, exon 1 and exon 2 of *RCAN1* and *RCAN3* genes, and also exon 2 of

RCAN2 gene are located in a CpG island, while exon 4 of *RCAN1* gene and exon 3 of *RCAN3* gene include a putative TATA box (Fuentes *et al.*, 1997; Facchin *et al.*, 2011), which is supposed to direct its transcription initiation. TATA-containing promoters are very common in inducible promoters and are often associated with tight regulation of genes (Muller *et al.*, 2007; Bai and Morozov, 2010), whereas CpG island are present in housekeeping genes and in about half of the tissue-specific genes (reviewed in Antequera, 2003; Roider *et al.*, 2009). This fact is in accordance with *RCAN1-1* (constitutive) and *RCAN1-4* (inducible) transcript regulation and it is likely that the regulation of *RCAN2* and *RCAN3* transcripts takes place in the same direction. Therefore, it is expected that the three *RCAN* genes would give rise to several constitutively and inducible transcripts, regulated by different promoters.

It is known that the transcriptional activation regulated by CpG-containing promoters requires a non-methylated status of CpG island in order to acquire an opened chromatin conformation (reviewed in Antequera, 2003; Fan *et al.*, 2008). By means of a human genome methylation array analysis, we found that *RCAN1*- and *RCAN3*-associated CpG islands seem to be in an unmethylated status, suggesting that these regions may be transcriptionally active. Moreover, our results indicate that at least the CpG island associated to *RCAN3* is transcriptionally active by using luciferase gene reporter assays under the control of putative *RCAN3* promoter regions including the *RCAN3* CpG island (-281 to +550 nt, where +1 nt correspond to the TSS of exon 2, following the novel nomenclature) (Results chapter, Article 1, Fig. 6). Therefore, this particular region of *RCAN3* is likely part of the *RCAN3* proximal promoter that regulates gene expression of transcripts harboring the *RCAN3-2/2a* exons as first exons.

Our analysis also indicates that all human *RCAN* genes include associated natural antisense transcripts (NAT) located in the complementary DNA strand (Results chapter, Article 1, Fig. 3 and S2). The presence of NATs associated to *RCAN3* (*RCAN3AS*; Facchin *et al.*, 2011) and the reported here for *RCAN1* (*RCAN1AS*) and *RCAN2* (*RCAN2AS*) may also play a role in *RCAN* gene regulation. It has been reported that NAT-gene pairs that partially overlaps in the *5'* gene region (overlapping tails; *cis*-encoded), as would be the case of *RCAN2*- and *RCAN3*-associated NATs, present usually a co-regulated expression driven by a bidirectional promoter (Ho *et al.*, 2012). These *cis*-encoded NATs can regulate the associated gene at transcriptional level by different mechanisms, including modification of local chromatin structure, modification of histones (imprinting) or transcriptional interference (Prescott and Proudfoot, 2002; Pauler *et al.*, 2007; and reviewed in Wei *et al.*, 2011), and also can regulate the splicing of the associated gene (Munroe and Lazar, 1991). In contrast, *RCAN1*-associated NAT

seems to be a *trans*-encoded NAT because it is not overlapping with *RCAN1* gene; however, by their structural homology with *RCAN2AS* and *RCAN3AS*, it is expected to present an additional exon neighboring *RCAN1* gene, but it has not yet been described. *Trans*-encoded NATs regulate the associated gene at different levels than the *cis*-encoded NATs, including transcription, maturation, transport, stability and translation (Vanhee-Brossollet and Vaquero, 1998). Thus, irrespective of the mechanism, these NATs may constitute an additional way to regulate *RCAN* genes at different levels and further experiments should be performed to understand their functional role in *RCAN* genes. Moreover, we determined that the genomic sequence that would codify for these NATs is conserved among different mammals (Results chapter, Article 1, Fig. S4) and, given the presence of several retrotransposon sequences, at least in *RCAN2AS* and *RCAN3AS*, we could postulate that their origin would be a retrotransposition event.

We also found the presence of a Tigger DNA-retrotransposon sequence in the intron 3 of all three human *RCAN* genes (Results chapter, Article 1, Fig. 3). This sequence is located just before the TSS of some transcripts forms (*RCAN1-4*, *RCAN2-4* and *RCAN3* mRNA forms that use exon 4 as the first exon (Facchin *et al.*, 2011). Interestingly, these Tigger are highly degenerated in *RCAN1.* In addition, *RCAN2* and *RCAN3*-associated Tigger sequences are only present in primates (data not shown). It is likely that this retrotransposon sequence could be a reminiscence of an ancient event without actual function or that has been maintained to contribute to regulate transcription of precise mRNA forms in primates, by conferring additional TFBS or a specific DNA structure.

In summary, here we have hypothesized on how *RCAN* evolution took place, finding evidences for a segmental duplication that would have been the origin of the current *Rcan2* and *Rcan3* genes in jawed vertebrates (Results chapter, Article 1, Fig. 2), and on ACD clustering evolution and cooperative function (Results chapter, Article 1, Fig. 1). In addition, we have analyzed *RCAN* gene structure and rename *RCAN3* exons for a better functional understanding of *RCAN* genes. Therefore, the knowledge of *RCAN* genome evolution and the characterization of the different elements present in *RCAN* genes that play a role on gene expression regulation, post-transcriptional modification and translation will provide us with novel clues to better understand the functional relevance of RCAN proteins. In addition, the knowledge of the molecular mechanisms involved in RCAN protein production may provide the possibility to modify the amount of protein needed to modulate a particular cellular function depending on the desired outcome.

IN VIVO FUNCTIONAL ROLE OF RCAN PROTEINS IN THE IMMUNE SYSTEM

Taking into account the regulation of RCAN proteins in Cn signaling towards NFATc transcription factors and the essential role of Cn-NFATc signaling in the development and function of T lymphocytes, it is likely that RCAN proteins play an important role in the immune system. In this context, overexpression of *RCAN* genes has demonstrated their capacity as negative modulators of Cn-NFATc dependent gene expression of cytokines in Jurkat T cells (Aubareda *et al.*, 2006; Mulero *et al.*, 2007). However, depending on the cellular context and RCAN protein levels, a dual role of these proteins in different cellular processes has been proposed (reviewed in Shin *et al.*, 2006; Shin *et al.*, 2011). Concretely in the immune system, Rcan1$^{-/-}$ and Rcan1$^{-/-}$/Rcan2$^{-/-}$ mice show alterations in Th1 responses due to increased CD4^{+} cell death (Ryeom *et al.*, 2003; Sanna *et al.*, 2006), but the particular underlying mechanism still remains controversial.

To explore the role of the *RCANs* in the immune system, we previously analyzed the expression pattern of the different mouse *Rcan* genes in embryonic thymus and adult lymphoid organs (Results chapter, Article 2, Fig. 1). This analysis was performed by real-time quantitative PCR (qPCR) analysis using the Universal ProbeLibrary (UPL) probes (Roche). These probes confer specificity when combined with a specific pair of primers of the transcript to be amplified. This qPCR amplification system is easy to perform, cheaper than using Taqman probes, and more specific than PCR amplification with SyBrGreen since UPL probes present one unique fluorescent label per probe. In our hands, real time qPCR analysis using UPL probes has been a suitable technique to study *RCAN* mRNA levels. As a result of this analysis, we show for the first time that mouse *Rcans* genes are broadly expressed in adult immune tissues but also in E16 thymi embryonic tissue. *Rcan* genes seem to present different patterns of expression, suggesting that they may play different roles in the lymphoid tissues analyzed.

As a control for the real time qPCR analysis performed to evaluate *RCAN* gene expression, we used brain tissue, where the expression pattern of RCAN genes has been already described (Porta *et al.*, 2007a). Our *RCAN* gene expression values obtained from brain tissue is in accordance with previously reported data, except for *Rcan1-2*. This discrepancy can be due to different amplification techniques (SyBrGreen versus UPL probes) and/or the primers used on PCR amplification for transcript detection. Nevertheless, western blot analysis showed that the Rcan1-1 isoform seems to be more abundant Rcan1 isoform in brain (Porta *et al.*, 2007a). Other studies at mRNA and protein level reported that *Rcan1-1* and *Rcan2-3* transcription and mRNA expression occurs predominantly in brain, compared with other tissues including thymus, while similar levels of Rcan3 protein in both

tissues has been reported (Mizuno *et al.*, 2004; Sanna *et al.*, 2006), both in agreement with our results.

To determine the role of RCAN proteins in immune system, we analyzed the functional consequence of human *RCAN1* and *RCAN3* gene overexpression by using two different *in vivo* approaches, a transgenic animal that contains the human *RCAN1* gene (TghRCAN1) and bone marrow (BM) reconstituted animals with BM progenitors retrovirally transduced with *hRCAN3*.

TghRCAN1 mouse and animals reconstituted with BM progenitors that overexpress *RCAN3* gene as models to study T cell development and function

The transgenic TghRCAN1 mouse include several copies (from 5 to 10) of the human *RCAN1* gene (TghRCAN1), including 35 Kb upstream of *RCAN1* exon 1 and, therefore, containing the endogenous human *RCAN1* promoter. Gene and mRNA expression analysis indicated that both RCAN1 isoforms, RCAN1-1 and RCAN1-4, are detected in lymphoid tissues and also in liver, kidney and brain (Results chapter, Article 2, Fig. 2C and 2D). Therefore, the endogenous promoter of the *RCAN1* transgene seems to drive its gene expression in many tissues, including lymphoid tissues. This appears to be consistent with the described ubiquitous expression for this gene, when expressed either constitutively (*RCAN1-1*) or induced (*RCAN1-4*) form. In addition, our results show that both RCAN1-1 and RCAN1-4 isoforms have a differential expression pattern in TgRCAN1 mice probably due to differences in their promoter regulation. In this context, there are increased levels of RCAN1-1 isoform according with the *RCAN1* gene dosage in females, but not in male animals, what suggest a gender hormone dependent regulation of this transcript. In this context, it has been reported that murine *Rcan1-4* transcription can be induced by estrogen hormones (Gurgen *et al.*, 2011). It is possible that human *RCAN1-1* can also be regulated in the same way. For that reason further experiments were only performed in female animals. Regarding the TghRCAN1 mice, the RCAN1-4 isoform was detected in increased amounts in thymus, spleen and lymph node of heterozygous female animals compared to WT animals. However, the RCAN1-4 protein levels in the spleen of homozygous animals, but not in thymus and lymph node, were similar to that of heterozygous female animals. It can be hypothesized that highly RCAN1-1 overexpression in homozygous animals, possibly by inhibition of Cn-NFATc signaling, down-regulates NFAT-dependent *RCAN1-4* gene expression in these animals, probably in a tissue specific manner, and by these means the RCAN1-4 levels seems reduced.

Concerning the phenotypic traits of the TghRCAN1 mice, these animals show a significant reduced body weight that was evident in both heterozygous and

homozygous female animals (Results chapter, Article 2, Fig. 2A). In males, it was evident in heterozygous animals and less acute in homozygous animals. It has been previously described that Rcan proteins levels correlates with body weight alteration (Sanna *et al.*, 2006; Sun *et al.*, 2011b). This could be due to *RCAN1* gene overexpression affecting a cellular program involved in nutrition or related pathways in one or more of the tissues where *RCAN1* is overexpressed.

As a second approach to analyze the functional relevance of *RCAN* gene overexpression, an animal BM reconstitution model with retrovirally transduced BM progenitors that overexpress human *RCAN3* was used. The retrovirus chosen for progenitors transduction was the pMIG vector, which is a bicistronic vector that encodes for the GFP protein, as a reporter fluorescent gene, and for the transgen, in our case HA-fused *hRCAN3*, both of them under the regulation of a single promoter, the MCMV (Murine Stem Cell Virus). pMIG codifies for humanized GFP protein (hGFP), which is adapted for high levels of expression in mammalian cells, mainly in human cells (Zolotukhin *et al.*, 1996). Both proteins are expressed individually, not as a fusion protein. As there are no good commercial antibodies against human RCAN3 protein and HA epitope for flow cytometric analysis, we were forced to evaluate the effects of RCAN3 overexpression indirectly by the evaluation of GFP protein content using cytometric analysis.

The use of retroviral or lentiviral vectors encoding GFP as a reporter protein is a common technique to easily track the percentage and the distribution of transduced cells. However, overexpression of GFP protein in mammalian cells, especially in the study of immune responses, bears some troubles. It has been reported that GFP protein is able to induce cytotoxic and antibody responses that can provoke the depletion of GFP^+ cells. This effect was shown to be evident in Balb/C mice (Stripecke *et al.*, 1999) and monkeys (Rosenzweig *et al.*, 2001), however, GFP protein presented minimal immunogenicity in C57/BL6 strain (Skelton *et al.*, 2001), which is the strain used in this Thesis work. Thus, the use of GFP proteins in BM reconstitution experiments must always take into account a possible effect due to the GFP expression *per se* and, importantly, in the application of GFP protein with therapeutic purposes. To this end, we always analyzed de GFP^+ population versus the GFP^- population of each individual animal and compared the results obtained with the mock vector (empty vector that express GFP protein) versus the ones obtained with the RCAN3 vector.

The use of bicistronic vectors also presents several limitations that must be taken into consideration. It has been reported that the second gene in bicistronic vectors is expressed at lower levels than the first gene (Mizuguchi *et al.*, 2000). In

pMIG vectors, GFP coding sequence is located downstream, in order to ensure that GFP^+ cells express the transgen; however, it is not possible to estimate directly the amount of exogenous protein by the evaluation of GFP protein level. To avoid this issue, vectors containing the 2A sequence, that triggers ribosome skipping, have demonstrated to present more homogenous expression of both transgenes (Chinnasamy *et al.*, 2006).

Lymphoid organs from animals reconstituted with BM progenitors overexpressing *hRCAN3* present a highly heterogeneous degree of BM reconstitution, from 2% up to 95 % of GFP^+ cells (Results chapter, Article 2, Fig. 6D and 6E). In addition, the use of retronectin coated culture dishes in some experiments highly increased the efficiency of transduction of BM progenitor cells (50 to 90% of GFP^+ cells). Additionally to this heterogeneous expression of the transgen, it has been reported that exogenous protein can be silenced by several mechanisms and this seems to be independent of the initial exogenous protein level (Klug *et al.*, 2000). In our case, we found GFP silencing when thymocytes from reconstituted mice were cultured *ex vivo*. At day 3 of culture, all the cells were GFP^-, but after stimulation they became again GFP^+ cells.

As both the transgenic TghRCAN1 and the BM overexpressing *hRCAN3* models expressed RCAN proteins in lymphoid tissues, both approaches were used to investigate the functional role of *RCAN* overexpression in thymocyte development, differentiation and peripheral T lymphocytes populations.

Effects of overexpression of *hRCAN1* and *hRCAN3* in murine lymphoid organs

Effects of *RCAN* overexpression in thymus

Analysis of TghRCAN1 female thymi revealed an alteration in the proportion of DN subpopulations. In particular, increased proportions of DN1 subpopulation are observed, but this effect was only significant in homozygous animals (Results chapter, Article 2, Fig. S2). DN1 subpopulation is considered as progenitor cells, with capacity to differentiate to cell lineages other than T cells (Shortman and Wu, 1996). It is in the DN1 transition to DN2 subpopulation when cells are committed to T cell lineage, partially driven by Notch signaling pathway (Yuan *et al.*, 2010). It has been reported that *Rcan1-1* form is negatively regulated by this signaling pathway but neither its relevance in T cell lineage commitment nor if *RCAN*s genes are expressed at this DN1 stage are known (Mammucari *et al.*, 2005). In addition, both Cn and NFATc proteins have been involved in progenitors differentiation into T cell lineage versus myeloid lineage and DN differentiation (Fric *et al.*, 2012; Yoshida *et al.*, 1998). Given the importance of the Cn-NFAT signaling pathway in progenitor commitment, it is likely that RCANs proteins, as tightly related

modulators of this signaling pathway, could play a role also in progenitors commitment, but this hypothesis still needs to be approached at the experimental level to be confirmed.

The analysis of TghRCAN1 thymi also showed reduced percentage of DP and increased percentage of SP thymocytes (Results chapter, Article 2, Fig. 3A). This result suggested an increase on thymocyte positive selection that was reinforced by the observed significant increase of the positive selection-related markers CD3ξ, TCRβ, CD69 and a trend of CD5 in DP thymocytes of heterozygous female animals (Results chapter, Article 2, Fig. 3B). Moreover, this increase on positive selection surface markers correlates with an enhancement of the phosphorylation state of pERK, as observed by an increase of the $pERK^{hi}$ subpopulation in female heterozygous animals (Results chapter, Article 2, Fig. 3D). This $pERK^{hi}$ subpopulation has been described to be Cn-dependent and essential to accomplish positive selection, as was demonstrated in the $CnB^{-/-}$ mice (Gallo *et al.*, 2007). In this context, due to the differential pattern of expression of hRCAN1-1 and RCAN1-4 isoforms in heterozygous versus homozygous animals described above, we can speculate that positive selection may be affected by the incremented levels of both RCAN1 isoforms or by the predominant amount of hRCAN1-4 isoform in the heterozygous mice. Concerning the BM reconstitution model, a similar significant increase in CD3ξ, CD69 and CD5 positive selection related markers was observed in DP thymocytes from animals reconstituted with BM progenitors transduced with pMIG-hRCAN3, compared with those transduced with pMIG alone as a control, strongly suggesting a common role of RCAN proteins in positive selection of thymocytes. However, to fully understand the function of RCAN proteins in positive selection process, additional experiments need to be performed. One such a possibility is to perform experiments with animals that overexpress *RCAN* genes in lymphoid tissues using clonotypic TCR with high and low avidity specifically against antigens exposed by MHC I and II, in order to study the positive selection process (low avidity) of $CD4^+$ (MHCII) and $CD8^+$ (MHCI) cells and to fully discard their role in the negative selection process (high avidity). Another possibility is to perform experiments of Fetal Thymic Organ Culture (FTOC) from animals that overexpress *RCAN* genes under positive and negative selecting conditions and determine the proliferation rate and level of apoptosis of immature thymocytes.

The enhancement on thymocyte positive selection by *RCAN* overexpression is similar to that reported for a transgenic mouse overexpressing a constitutively active form of CnB (Hayden-Martinez *et al.*, 2000). This model suggests an essential role of CnB in thymocyte positive selection. Indeed, $CnB^{-/-}$ mice, but not $CnA\alpha^{-/-}$ and $CnA\beta^{-/-}$, presented an evident defect on positive selection (Zhang *et*

al., 1996; Bueno *et al.*, 2002; Gallo *et al.*, 2007; Manicassamy *et al.*, 2008). Regarding NFATc proteins, NFATc1 and NFATc2 seem to be involved in mature T lymphocyte function (Yoshida *et al.*, 1998; Ranger *et al.*, 1998a; Viola *et al.*, 1998; Schuh *et al.*, 1998; Erb *et al.*, 2003), while NFATc3 seems to play a preferential role in thymocyte development, but the particular mechanism is unknown (Oukka *et al.*, 1998; Cante-Barrett *et al.*, 2007). This scenario suggests a particular role for RCAN proteins in thymocyte positive selection, besides CnB, that could be mediated specifically by NFATc3 protein. In this context, we could not evaluate the effect of RCAN proteins on NFATc signaling in our animal models for technical reasons.

We were also able to detect an incremented percentage of $FoxP3^+$ (intracellular marker of T regulatory cells, T_{regs}) cells in thymus (natural T_{regs}, nT_{regs}) (Results chapter, Article 2, Fig. 5B). T_{regs} are known to be essential in maintaining immune tolerance and homeostasis (Sakaguchi *et al.*, 2008). Reduced numbers of T_{regs} are related with autoimmune diseases, including multiple sclerosis and rheumatoid arthritis, while increased numbers of these cells have been involved in many malignant disorders, including several types of cancer (Beyer and Schultze, 2006). In this context, NFATc and SMAD transcription factors cooperation is involved in *FoxP3* gene expression (Mantel *et al.*, 2006; Tone *et al.*, 2008) and cooperation of NFATc with FoxP3 is essential to activate the expression of several genes essential for T_{reg} function (Bettelli *et al.*, 2005; Rudensky *et al.*, 2006). Since thymic nT_{regs} generation is partially dependent on TCR strength (Hsieh *et al.*, 2012), any alteration of TCR-triggered signaling pathways, including the Cn-NFATc signaling pathway, will impact in T_{regs} generation at thymus.

All these data point out that *hRCAN1* and *hRCAN3* overexpression may affect Cn-NFATc-dependent events involved in positive selection and in the generation of nT_{regs}. However, we cannot discard other Cn-independent mechanisms. Due to the known cooperation and requirement of Cn and RAF proteins in T cell development and, concretely, in thymocyte positive selection (Gallo *et al.*, 2007), it could be hypothesized that RCAN proteins can influence RAF signaling. It was reported previously the interaction of RCAN1-4 with CRAF kinase (Cho *et al.*, 2005). Here, we show that RCAN1-1 and RCAN3 interact with CRAF and BRAF proteins (Results chapter, Article 2, Fig. 3C and S3). Interestingly, by pull down assays, we show that full length RCAN3 protein is able to interact with Cn and RAF protein, in an independent and non-exclusive manner. In addition, we demonstrate that RCAN proteins interact with Cn and RAF proteins trough different RCAN regions. Therefore, it could be hypothesized that RCAN proteins function as scaffold proteins for both closely related pathways in a particular intracellular network, although this hypothesis still needs to be analyzed to be confirmed.

Effects of *RCAN* overexpression in peripheral lymphoid organs

In the analysis of peripheral lymphoid organs (lymph node and spleen), we obtained different results in both *hRCAN1* and *hRCAN3* overexpression models. TghRCAN1 peripheral lymphoid organs shows a significant increase of $CD3^+$ cells percentage in lymph node of heterozygous animals, while not significant changes could be found in spleen (Results chapter, Article 2, Fig. 4A). Once again, this fact may be influenced by the increased amounts of both RCAN1 isoforms or by the prevalence of hRCAN1-4 isoform in the heterozygous mice. In contrast, *hRCAN3* overexpression does not show any significant change in $CD3^+$ population (Results chapter, Article 2, Fig. 7C). This could be due to technical limitations of this experimental approach that give more heterogeneous results than the transgenic animal approach. To confirm that issue, further functional studies on peripheral T cells must be performed, including analysis of cell proliferation and apoptosis. Moreover, it could be interesting to analyze the effect of *RCAN* overexpression on $CD3^-$ populations, as B cells subpopulations, because RCAN could alter the balance between T and B cells and, consequently, modify the balance of cytokines, chemokines and growth factors relevant in the immune system function.

$CD44^{hi}$ are cells that have been exposed to an antigen (antigen-experienced cell) and include two subpopulations: the effector memory cell population (T_{EM}; $CD62L^-$) that are cells that present an activated phenotype and immediate effector functions, and the central memory T cell population (T_{CM}; $CD62L^+$) that are resting cells that have been maintained as memory cells. CD69 molecule is also used to analyze the activation status of T cells (Biselli *et al.*, 1992). CD69 is considered an early activation marker, because it is rapidly induced after antigen recognition. Interestingly, the involvement of NFATc2 (Schuh *et al.*, 1998) and NFATc3 (Oukka *et al.*, 1998) in the generation of an activated phenotype ($CD44^{hi}$, $CD69^{hi}$ and/or $CD62L^-$) of peripheral T cells has been reported previously. Moreover, $CnA\beta^{-/-}$ mice showed increased proportions of $CD44^{hi}CD62L^-$ cells in spleen (Doetschman *et al.*, 2011). In an attempt to analyze the activation state of peripheral T lymphocytes ($CD3^+$) in TghRCAN1 model in homeostasis, the expression of CD44, but not CD62L marker, and also the CD69 activation marker were evaluated (Fig. 4B article 2 of results chapter). We did not found significant changes in $CD69^{hi}$ population, in either $CD4^+$ or $CD8^+$ cells from lymph nodes or spleen. Conversely, we found a significant reduction in the proportion of $CD44^{hi}$ cells within $CD4^+$ cells from lymph nodes, and a similar tendency was observed in $CD8^+$ cells. However, spleen cells did not show these apparent changes in $CD44^{hi}$ subpopulation. The decrease in $CD44^{hi}$ subpopulation (the effector/memory cell population), as was found in TghRCAN1 mice, implies an increase in the proportion of naïve T cells ($CD44^{lo}$). This phenotype could be due to an impaired capacity of naïve cells to respond to

antigens and to be activated, or to an increased velocity of naïve cells to egress from the thymus to lymph nodes. To differentiate among these possibilities, several *in vitro* experiments with peripheral T lymphocytes upon antigen stimulation can be performed, such as evaluation of cell proliferation, analysis of expression of surface activating markers (CD25, CD69 and CD44) or measurement of secreted cytokines. Moreover, it could be interesting to differentiate among the different $CD44^{hi}$ subpopulations, T_{CM} and T_{EM}. Regarding all these data, in the case that peripheral T cells of TghRCAN1 mice present an impaired response to antigen, novel therapeutic possibilities in transplantation therapy could arise.

RCAN proteins involvement in survival and T cell lineage commitment has been reported previously. $Rcan1^{-/-}$ mice present increased FasL-mediated apoptosis and subsequent impaired Th1 response (Ryeom *et al.*, 2003). In another context, increased FasL-mediated apoptosis was also evident when RCAN1-4 was downregulated in U87MG astrocytoma cells (Kim *et al.*, 2009). Regarding Cn-NFATc signaling, survival of peripheral cells could be mainly mediated by CnAβ isoform (Bueno *et al.*, 2002; Manicassamy *et al.*, 2008) and NFATc3 (Oukka *et al.*, 1998; Cante-Barrett *et al.*, 2007). Concretely, $NFATc3^{-/-}$ mice presented increased levels of FasL and a hyperactivated phenotype in peripheral T cells (Oukka *et al.*, 1998). This idea suggest that CnAβ, NFATc3 and also RCAN1 would be essential in survival of T cells, indicating that RCAN1 could be acting as facilitator of Cn and NFATc3-mediated signaling in the survival of T cells. Regarding other NFATc members, NFATc1 and NFATc2 proteins seems to play a role in the balance of Th1 and Th2-like responses (Yoshida *et al.*, 1998; Ranger *et al.*, 1998a; Viola *et al.*, 1998; Erb *et al.*, 2003). Concretely, $NFATc2^{-/-}$ presented reduced Th1 response (Yoshida *et al.*, 1998; Ranger *et al.*, 1998a), similar to that present in $Rcan1^{-/-}$ mice (Ryeom *et al.*, 2003). The analysis of RCAN proteins *in vivo* in Th1 and Th2 responses could also contribute to better understand the role of RCAN proteins in NFATc1 and NFATc2-mediated responses in the immune system.

In order to explore the role of RCAN proteins toward other signaling pathways involved in peripheral lymphoid function, we analyzed the phosphorylation status of several MAPK (ERK, AKT, P38, JNK) that have been shown to be relevant in the immune system. Among them, JNK phosphorylation was enhanced in heterozygous and homozygous splenocytes of TghRCAN1 mice (Fig. 4C article 2 of results chapter). This effect correlates with increased levels of RCAN1-1 in heterozygous and homozygous animals. It is known that JNK and Cn-NFATc signaling cooperate at different levels, including the immune system, and both pathways seems to be reciprocally regulated (Avraham *et al.*, 1998; Werlen *et al.*, 1998; Liang *et al.*, 2003). Moreover, it has been reported that RCAN1 protein is able to interact with several upstream molecules involved in JNK activation, such

as TAB2 and Tollip proteins (Lee *et al.*, 2009; Liu *et al.*, 2009). Hence, the involvement of RCAN proteins in signaling pathways other than Cn-NFATc is important to evaluate in order to determine the physiological relevance of the RCAN family members in cellular processes, including the immune system.

Additionally to the peripheral subpopulations changes already described, peripheral T_{regs} were reduced in TghRCAN1 mice (Fig. 5B lower panel article 2 of results chapter). Among the peripheral T_{reg} subpopulation, there are nT_{reg} cells ($CD25^{+}$), originated in the thymus, and iT_{reg} cells ($CD25^{-}$), generated in periphery. iT_{regs} generation is dependent on TGFβ and CD44 activation (Bollyky *et al.*, 2009; Chen and Konkel, 2010). It could be interesting to analyze the putative role of RCAN1 in the generation of the different T_{regs} subpopulations in periphery, to determine if RCANs play a role in this process, either through regulation of NFATc or independently of this pathway.

Finally, given the presence of several NFATc proteins in vertebrates and their non-overlapping functions, it could be hypothesized that this could be also the case for RCAN proteins. In this context, RCAN proteins could also have a relevant role in the immune system as NFATc have. Moreover, it could be interesting to analyze the differential affinity of RCAN proteins for binding to Cn, their expression in the different thymic subpopulations and their relevance in positive selection of thymocytes using transgenic animals or null mice for each specific *RCAN* gene to determine their involvement in this cell developmental process. Also, using the same animal models, it would be interesting to analyze their effect on peripheral lymphoid tissues and on T cell activation. In addition, a lot of work should be performed to determine which other proteins bind to RCANs and the signaling pathways that cross-talk with RCAN proteins in order to unravel their functional relevance in the immune system and other biological processes. The underlying mechanisms involved in RCAN signaling should give some clues to improve some therapeutic agents for immuno-related diseases.

CONCLUSIONS

1. The emergence of RCAN gene family in vertebrates as multigenic family seems to be the result of two rounds of whole genome duplication followed by a segmental duplication. This segmental duplication is inferred from the presence of many paralogous genes between human chromosome 1 (HSA1) and 6 (HSA6). The *RCAN* genes have evolved in parallel with the *RUNX* and *CLIC* genes within the known ACD clusters and they seem to keep clustered for functional purposes.
2. Three genes are found in jawed vertebrates and only one gene can be found in most of the rest of Eukarya. Several exceptions to this rule in several eukaryotes has been found and annotated.
3. Since all human *RCAN* genes share a similar genomic structure organization a novel nomenclature of *RCAN3* exons and introns have been proposed based on the *RCAN1* and *RCAN2* gene structure. Based in this novel nomenclature, all *RCAN* genes have seven exons being exons 5, 6 and 7 common to all transcripts of each gene. In addition, *RCAN* genes harbor a DNA-retrotransposon sequence in intron 3.
4. A comparative genomic analysis of the *RCAN* gene family shows a highly DNA sequence conservation not only in primates but in mammals among the coding region. In addition, phylogenetic analysis of the *RCAN3* gene exons shows a parallel evolution of coding and non-coding exons. Moreover, 5'UTR and 3'UTR exons analysis reveals that these regions in rodents are more divergent than the rest of mammals.
5. All three *RCAN* gene putative promoter regions include CpG islands that extend at least one of their first exons. The CpG islands associated with *RCAN1* and *RCAN3* seems to present an unmethylated status in several normal and cancer human cell lines, suggesting that these regions may be transcriptionally active. At least the CpG island associated to *RCAN3* gene is functionally active. A multispecies prediction of TFBS in this CpG island show several TFBS highly conserved along evolution.
6. It is proposed the existence of Natural Antisense Transcripts (NATs) associated with all *RCAN* genes, regulated by a bidirectional promoter at least in *RCAN2* and *RCAN3*. The presence of conserved retrotransposon sequences in these regions suggests an ancient retrotransposon origin.
7. All murine *Rcan* genes are expressed in embryonic thymus and adult lymphoid tissues.

8. Overexpression of the human *RCAN1* gene in the transgenic TghRCAN1 mice reduces animal weight.
9. Concerning the TgRCAN1 mice model, human RCAN1-1 and RCAN1-4 isoforms are expressed in all lymphoid tissues tested. A differential expression pattern of RCAN1-1 and RCAN1-4 protein isoforms is observed, depending on *RCAN1* gene dosage and on gender.
10. Regarding the model of bone marrow (BM) reconstitution with mouse bone marrow progenitor cells transduced with retroviral particles, it constitutes an efficient method to overexpress exogenous proteins such us *RCAN* genes in murine lymphoid organs to study their effect in the immune system.
11. Overexpression of human *RCAN1* in TghRCAN1 mice and of *RCAN3* after adoptive transfer of retrovirally transduced BM progenitors increases the proportion of positive selected thymocytes. This sentence is supported by the observed significant increase of $CD3\xi^{hi}$, $CD69^{hi}$ and, in a lesser extent, of $CD5^{hi}$ subpopulations among DP cells in thymus. This was also reinforced by an increase of the $pERK^{hi}$ intracellular population what correlates with an increased activation of this kinase.
12. Overexpression of RCAN proteins affects differentially the proportion of peripheral mature T lymphocytes in the TgRCAN1 and in BM reconstituted mice.
13. TghRCAN1 mice present an altered proportion of DN subpopulations in the thymus, with an increase of DN1 subpopulation that could be related with a role in progenitor cells commitment. *RCAN1* overexpression seems to not affect TCR expression as no changes are observed in DN3 and DN4 subpopulations.
14. Overexpression of human *RCAN1* in the TghRCAN1 causes a decrease in $CD44^{hi}$ subpopulation mainly in $CD4^{+}$ peripheral T cells, therefore affecting the generation of effector/memory T cells.
15. Overexpression of *RCAN1* increases the ability of SAP/JNK kinase to be phosphorylated in peripheral T cells. The precise role of this phosphorylation increase is still unknown.
16. Overexpression of human *RCAN1* in TghRCAN1 promotes the generation of natural regulatory T cells (nT_{regs}) in the thymus but negatively affects the population of induced regulatory T (iT_{regs}) cells.

17. RCAN proteins seem to cross-talk with signaling pathways other than Cn. In this context, RCAN1 and RCAN3 interact with BRAF and CRAF kinases. The RCAN interaction with RAF and Cn takes place in a non-exclusive manner, suggesting that Cn, RAF kinases and RCAN proteins may cooperate to regulate specific steps of different cellular processes, including T cell development, and function.
18. It can be concluded that *RCAN* gene overexpression *in vivo* influences T cell development, differentiation, and may influence T cell activation in peripheral lymphoid tissues.

MATERIAL AND METHODS

The methods used for bioinformatic analysis are fully detailed in the article entitled “RCAN genes: evolution, structure and regulation” in the results chapter. Therefore they are not included here in the Material and Methods chapter.

I.- GENERAL PROTOCOLS IN DNA MANIPULATION AND ANALYSIS

I.1.- Polymerase chain reaction (PCR)

Polymerase chain reaction (PCR) is a process where the template is exponentially amplified and abundant copies can be obtained. The final amount of the product will be proportional to the template.

General PCR reaction mix is prepared as follows:

- Template DNA
- 1X Taq DNA polymerase Buffer 10X (Roche)
- 0.2 µM Forward Primer
- 0.2 µM Reverse Primer
- 0.2 µM (each) dNTP
- 1.25 units Taq DNA polymerase (Roche)
- Distilled water up to 25 µl

PCR reaction always consist in a first step of denaturing template (at 94-95°C), followed by several cycles (25-40) that contain a denaturing step (at 94-95°C), an annealing step (that depends on the melting temperature of your specific primers, (referred here as X°C) and an amplification step (usually 72°C, but can vary depending on the polymerase used). It is assumed that polymerase enzyme amplifies 1 kb in 1 min, but it can vary for specific polymerases. Finally, a larger elongation step allows amplification of incomplete fragments.

Amplification is carried out in a thermocycler with the following program:

- 94°C 1.5 min
- 94°C 30 s
- X°C 30 s
- 72°C 1min/kb

  ] 25-40 cycles
- 72°C 4.5 min
- 15°C ∞

It is recommended not to exceed of 30-35 cycles to avoid errors in the DNA fragments. In case to perform a semiquantitative PCR to compare the amount of template among different samples, it is important to decrease the number of amplification cycles to avoid saturated and non-quantitative bands.

When PCR is performed from cDNA template, it is important to design the primers that spans over an intron, in order to avoid detection of contaminant DNA that could lead to obtain erroneous results. It is very important in semiquantitative and real-time quantitative PCR. Previous treatment of RNA samples with DNAse (Section VIII.2) also will reduce background contamination.

PCR products are resolved by gel electrophoresis (see Section I.2) or used directly in other applications.

I.1.a.- PCR amplification for cloning

For cloning, specific primers must be designed to specifically amplify the region to be cloned. As a cloning strategy, sequence for specific sites for restriction enzymes can be added in the primers.

DNA amplification is performed with 10-50 ng of plasmid DNA as template by using a standard PCR protocol.

To clone the regions with very high content of C and G nucleotides (as in the luciferase assays performed in the study of the RCAN3 promoter), some enhancing reagents, as betaine or DMSO, can be added to the PCR mix. In our case, a specific kit (GC-RICH PCR System; Roche, #12140306001) was used to amplify these rich GC regions.

I.1.b- PCR screening

PCR screening is a very rapid way to find positive clones after cloning (see Section IV).

- Perform a PCR reaction with 35 cycles by using:
    - 2 µl of a 2 h bacterial culture (see Section IV.7)
    - 1.25 µl of Taq DNA polymerase Buffer 10x (Roche)
    - 0.5 µl of 2.5 mM dNTPs mix
    - 0.5 µl of 10 mM Forward Primer
    - 0.5 µl of 10 mM Reverse Primer
    - 1 unit of Taq DNA polymerase (Roche)
    - Adjust the volume with distilled water to a final volume of 12.5 µl

Forward and reverse primers must be designed to anneal one with the inserted fragment and the other one with the plasmid backbone, in order to ensure amplification only of the correctly oriented DNA insert.

I.1.c- PCR Sequencing

The PCR-sequencing protocol was performed as follows:

- 100 ng/ kb of plasmid DNA
- 1 µl Big Dye Buffer
- 1 µl Big Dye 3 DNA polymerase
- 0.5 µl of 10 mM sequencing primer
- Adjust the volume with distilled water to a final volume of 10 µl

Sequencing PCR program does not need the last larger elongation step because the incorporation of fluorescent dNTPs stops the reaction and it constitutes the basis of the method:

- 96°C 1 min
- 94°C 10 s
- 50°C 5 s
- 60°C 1 min/kb

] 25 cycles

- 4°C ∞

PCR product needs to be purified by Sephadex G-50, lyophilized or precipitated prior to sequencing, depending of the sequencing platform being used.

I.1.d.- PCR for mycoplasma detection

Used to detect the presence of mycoplasma in a cell culture (see how to obtain the media sample in Section VI.3).

Perform a PCR with 35 cycles by using specific primers (see table IV). Perform the reaction with 2 µl of direct sample and one replicate with 2 µl of a dilution 1:10 of the sample. Ensure the presence of negative and positive controls.

Positive samples for mycoplasma detection will amplify a 0.5 kb electrophoresis mobility band.

Table I.1.- PRIMERS USED FOR MYCOPLASMA DETECTION

PRIMER NAME	SEQUENCE	Tm (°C)
Mycoplasma_Fw	GGCGAATGGGTGAGTAACACG	62
Mycoplasma_Rv	CGGATAACGCTTGCGACTATG	59

Table I.1. Primers used for mycoplasma detection

To determine the genotype of TghRCAN1 animals, genomic DNA from tail tip was extracted as indicate in Section X.1 and multiplex semiquantitative PCR was performed by using the mix:

- 300 ng of genomic DNA
- 2.5 µl of Taq DNA polymerase Buffer 10x (Roche)
- 2 µl of 2.5 mM dNTPs mix
- 0.4 µl of a 25 mM mix of all the primers (hRCAN1.ex3 Fw, hRCAN1.ex4 Rv, mIl2P Fw and mIl2P Rv primers; see supplementary table 1B in article 2 in results chapter)
- 1 µl of Taq DNA polymerase (Roche)

Amplification was carried out in a thermocycler with the following program:

- 95°C 2 min
- [95°C 30 s
- 62°C 30 s
- 72°C 30 s] 25 cycles
- 72°C 10 min
- 15°C ∞

I.1.f.- Semiquantitative PCR for determination of mRNA levels

This technique has been used to detect the expression of human RCAN1 transgen in the TghRCAN1 mice. To this end, cDNA from several mice tissues was obtained as described in section VIII and a standard PCR reaction with 25 amplification cycles was performed by using specific primers designed to hybridize with human RCAN1-1 and RCAN1-4 transcript forms but not with the mouse corresponding forms (see supplementary table 1B of article 2 in results chapter).

To perform a PCR reaction from cDNA samples, it is important to dilute the samples in order to avoid inhibition of DNA polymerase by the dNTPs used in retrotranscriptase reaction.

I.1.g.- Real-time quantitative PCR for determination of mRNA levels

Real-time quantitative PCR was performed by using Universal ProbeLibrary System (UPL, Roche). This system offers 165 short (8 nt) fluorescent probes (FAM-labelled short oligonucleotides) that cover the totally of the genome. The specificity of the reaction is achieved by combining specific primers for your gene of interest with the unspecific probe. Table 1B of article 2 in results chapter summarizes the different combination of primers and probes used for the study of mRNA expression of mouse Rcan in lymphoid tissues.

Designing of primers was performed by using the online application provided by Roche (http://www.roche-applied-science.com/sis/rtpcr/upl) selecting, when possible, intron-spanning primers. Among the suggested options, we check the specificity of the primers by using primer-BLAST tool (Ye *et al.*, 2012; http://www.ncbi.nlm.nih.gov/tools/primer-blast).

PCR reaction was performed as follows:

- Prepare a common mix for all the samples with the same primer probe combination as follows (10 µl final volume):
    - 5 µl of LightCycler 480 Probes Master mix 5x (Roche; #04707494001)
    - 0.4 µl of a mix of 10 mM primers (each) (Table 1B of article 2 in results chapter)
    - 0.2 µl of 10 µM probe solution (Roche) (Table 1B of article 2 in results chapter)
    - 3.4 µl of PCR grade water (supplied with the Probes Master kit)
- Distribute the reaction mix (9 µl) to each well in White LightCycler 480 Multiwell Plates 384 (Roche, #04729692001).
- Spin, if necessary to avoid presence of the PCR mix in the top of the well
- Dispense carefully 1 µl of cDNA sample (at desired dilution*)
- Seal the plate with a sealing foil (Roche, #04729757001) and spin the plate at 1500 *g* for 5 min

* DNA sample correct dilution must be determined previously by a standard curve, called calibration curve, to determine the quantitative range of concentration. In our case, a ½ dilution of 1 µl of cDNA obtained from a 1.7 µg of total RNA reversed transcribed in a 20 µl reaction (see section VIII).

Amplification was carried out in a LigthCycler 480 thermocycler (Roche) thermocycler with the following program:

Table I.2.- AMPLIFICATION PROGRAM FOR REAL-TIME QUANTITATIVE PCR					
PROGRAM NAME	**NUMBER OF CYCLES**	**TEMPERATURE (°C)**	**ACQUISITION MODE**	**HOLD**	**RAMP RATE (°C/s)**
Denaturalization	1	95	-	10 m	4.8
Amplification	45	95	-	10 s	4.8
		60	-	30 s	2.5
		72	Single	1 s	4.8
Melting	1	95	-	10 s	4.8
		55	-	20 s	2.5
		70	Continuous	5 s	0.11
Cooling	1	40	-	30 s	2.5

Table I.2. Amplification program used for real-time quantitative PCR

Standard curve also allowed us to quantify the efficiency of the reaction for each pair of primers. In our case, efficiency was similar for all the pair primers used, 1.95 to 2.06 and quantification of gene expression was performed by using $2^{-\Delta\Delta CT}$ method (Livak and Schmittgen, 2001). As reference genes, we used *Hprt* and *Gusb*, obtaining similar results for all the conditions tested. The data is presented relative to *Hprt* gene values. Previously, besides the *Hprt* and *Gusb* genes, we checked the gene expression levels of several reference gens such as *Gadph* and *Actb* among all the samples by using Qbase (http://www.biogazelle.com; Hellemans *et al.*, 2007) and NormFinder (http://www.mdl.dk; Andersen *et al.*, 2004) software. *Hprt* and *Gusb* were the most regularly expressed in the different conditions being used in our experiments and, therefore, the more suitable genes for gene expression quantification.

Finally, in other real-time quantitative techniques (e.g. SybrGreen), the correct length of the amplicon and the presence of unspecific products can be checked in the melting step, when the melting temperature (Tm) of the final product can be calculated. However, using this method for calculate length of the amplicon by measuring the Tm is not possible when using UPL probes, because the fluorescence is carried by the probe and all UPL probes have the same length. In this case, correct length of the amplicon and specificity of the reaction was checked by electrophoresis on a 12% polyacrylamide gel (Section I.2.b).

I.2.- DNA gel electrophoresis

DNA electrophoresis allows to separate linear DNA fragments by size. DNA will migrate to the positive pole, as it is negatively charged. DNA electrophoresis is

usually performed in agarose gels (section I.2.a). Alternatively, for very small fragments of DNA, polyacrylamide gels can be used (I.2.b).

In both cases, DNA loading buffer (see 6X recipe) is added to the samples to ensure density and visualize the migration.

I.2.a.- DNA electrophoresis in agarose gels

To prepare agarose solution, powered agarose is dissolved in TBE 0.5X (see 10X recipe) by boiling. The percentage (w/v) of agarose will be determined by the length of the DNA (kb) to be resolved (>5 kb: 0.8%; 1- 5 kb: 1%; 0.5- 1 kb: 1.5%; <0.5 kb: 2%). The electrophoresis agarose gel is run in TBE 0.5X buffer.

The current intensity (amperage) will determine the velocity of migration. Usually, all running electrophoresis procedures are performed at 120 V (equivalent to 35 mA), but, depending on the agarose percentage used, the running conditions can vary.

For DNA detection by UV lighting, gel can be stained with 5 µg/ml ethidium bromide (EtBr) solution in TBE for 15 min or, alternatively, SYBR® Safe reagent (Invitrogen; # S33102) (1:10000 in TBE) can be added to agarose solution.

I.2.b.- DNA electrophoresis in polyacrylamide gels

This technique was used to visualize small PCR products (less than 150 bp) of real-time quantitative PCR (Section I.1.g) reactions to ensure the correct length of the amplicon being amplified, because agarose gels are not enough resolutive.

Continuous 12% (v/v) polyacrylamide gel is prepared as following, and run in TBE 1X (see 10X recipe):

- 6 ml of 30% acrylamide/bisacrylamide Solution 29:1 ratio (Biorad; #161-0156)
- 3 ml of TBE 5X
- 6 ml of distilled water
- 100 µl of APS 10% (w/v) solution
- 10 µl of N, N, N', N'- Tetramethylethylenediamine (TEMED) solution
- Mix and use immediately

For DNA detection by UV light, gel is stained with 0.5 µg/ml EtBr solution in TBE for 20 min.

I.3.- DNA quantification

In solution, nucleic acids (DNA and RNA) absorb UV light with a maximum peak of absorbance at 260 nm. Direct determination of nucleic acids concentration in solution can be performed by spectrophotometry at 260 nm. In our case, we used a Nanodrop spectrophotometer (Thermo Fisher Scientific Inc.) that allows measurement of highly concentrated samples and using little amount of sample.

Concentration of nucleic acids can be determined directly by using the Beer-Lambert law ($A= \varepsilon \cdot c \cdot l$), being A=absorbance at 260nm; ε the molar extinction coefficient; c=concentration of protein and l=cuvette length. By using this equation, it has been calculated that 1 OD is, approximately, 50 µg/ml for double strand DNA (dsDNA) samples, 40 µg/ml for RNA or single strand DNA (ssDNA) samples and 33 µg/ml for oligonucleotides.

To obtain an estimation of the quality of nucleic acid samples, it is performed a range of measurement over the wavelength range 220 to 350 nm. The value of the ratio of absorbance at 260 and 280 nm (260/280) and at 260 and 230 nm (260/230) is an indicator of the purity of the nucleic acid sample. A 260/280 value of 1.8 and 2 is accepted for pure DNA and RNA, respectively. Lower values indicate the presence of proteins or aromatic molecules in the sample. A 260/230 value of 1.8-2.2 is accepted for pure DNA and RNA samples. Lower value indicates the presence of aromatic molecules or other contaminants. It is important to note that TRIzol® reagent can absorb at 230 nm and at about 260 nm.

I.4.- Plasmids

pGEM®-T Easy (Promega; #A1360), used to subclone DNA fragments.

pcDNA3.1-HA: pcDNA™3.1 (Invitrogen; #V790-20), with three N-terminal hemagglutinin (HA) tags, used to overexpression of proteins in mammalian cells.

pGEX-5X (GE Healthcare; #28-9545), used to overexpress recombinant proteins in prokaryotes. Protein can be excised from GST by cleavage with Factor X enzyme.

pGL3-Basic (Promega; #E1751), used to subclone RCAN3 promoter and perform luciferase reporter gene assays.

pRL-null (Promega; #E2271); from Dr. Carmen Marín (University of León, Spain). Encodes for Renilla luciferase and is used as transfection control in luciferase reporter gene assays. This vector does not contain any TK, CMV or SV40 promoter, to reduce background signal.

pMIG (Addgen; #9044); from Dr. G. Soldevila (UNAM, Mexico). It is a bicistronic retroviral vector that contains a MSCV promoter.

pCLEco (Addgen; #12371); from Dr. G. Soldevila (UNAM, Mexico). It is ectotropic (only infects mouse and rat cells) retroviral vector plasmid that codifies for the gag, env and pol proteins needed for packaging retroviral particles.

II.- GENERAL PROTOCOLS IN PROTEIN ANALYSIS

II.1.- Preparation of total soluble protein lysates

To avoid protein degradation, all the steps must be performed on ice. To obtain protein extract from bacterial cells, see section V.3.

II.1.a.- Preparation of soluble protein cell lysates from mammalian cells

- Wash cells with ice-cold PBS 1X. For adherent cells, washing can be performed directly in the plate, with PBS supplemented with 0.1 mg/ml $CaCl_2$ and 0.1 mg/ml $MgCl_2$ (to prevent cell detaching). For non-adherent cells, pellet the cells previously by centrifugation at 500 *g* at 4°C for 5 min.
- Add 1 ml of ice-cold PBS 1X and transfer cells to a 1.5 ml tube. For adherent cells, detach cells with a cell scraper.
- Centrifuge cells at 500 *g* at 4°C for 5 min.
- Discard supernatant and add the adequate volume* of the desired lysis buffer**.
- Incubate in an orbital shaker at 4°C.
- To reduce viscosity of the sample due to the presence of DNA, sonicate the sample on ice in short bursts (to avoid overheating the samples) or pass the cell lysate several times through a 30G needle.
- Centrifuge cell lysate at 13000 *g* at 4°C for 5 min.
- Collect the supernatant that contain soluble proteins and transfer to a clean tube and keep on ice.
- Quantify protein concentration (Section II.2).
- For protein separation and analysis by polyacrylamide gel electrophoresis, add Laemmli buffer (see 6X recipe) and incubate the sample for 10 min at 98°C.

* The volume of lysis buffer will be adjusted depending of the sample amount. To lysate a confluent 100 mm diameter culture dish of HEK 293T cells, use 1 ml of lysis buffer. To lysate a pellet of $25x10^6$ of Jurkat cells, use 750 µl of lysis buffer.

** The choice of the lysis buffer (pH, salts, additives...) will depend on the nature and the protein localization being analysed (nucleus, plasma membrane, cytosol...) and the assay to be performed (immunoprecipitation, western blot, crystallography...). In our case, we have used RIPA-like lysis buffer (see recipe) to obtain total extracts to be separated and analysed by protein electrophoresis, and IGEPAL-based lysis buffer (see recipe) for analysis of protein-protein interactions (immunoprecipitation and GST-pull down; see section VII).

II.1.a.- Preparation of soluble protein cell lysates from mammalian tissue

To obtain protein extracts from mammalian tissues, fresh or cooled samples must be previously homogenized on ice, for avoiding overheating the sample, in presence of the desired lysis buffer. Big tissues (brain, liver or kidney) can be homogenized by using a polytron homogenizer. In our case, we used 500 µl of lysis buffer for 0.25 mg of tissue, except for brain samples, for which we used 1 ml for 0.25 mg of tissue. For very small samples (lymph node, thymus or spleen) a tissue grinder can be used instead. In our case we used 200 µl of lysis buffer in these cases.

II.2.- Protein quantification

Direct spectrophotometric determination of protein concentration (Section II.2.a) can only be performed for a solution of a single protein with a known extinction coefficient (ε) or by using standard solutions. In other cases, for instance for a soluble cell extract from a cell, colorimetric assay must be used (Section II.2.b).

II.2.a.- Quantification of proteins by spectrophotometry

In solution, proteins absorb UV light with a maximum peak of absorbance at 280 nm. Direct determination of protein concentration in solution can be performed by spectrophotometry at 280 nm (Nanodrop spectrophotometer; Thermo Fisher Scientific Inc.).

In the case of purified proteins, concentration of protein can be determined directly by using the Beer-Lambert law (described in section I.3). For GST-fused proteins from bacteria (Section V), it can be calculated by using the ε of GST of 2 $\mu M^{-1}\ cm^{-1}$.

II.2.b.- Bicinchoninic Acid Assaycolorimetric assay for protein quantification

Total protein concentration from soluble cell extracts from mammalian cells or tissues (Section II.1) are mainly measured by colorimetric techniques. We used in our assays the Bicinchoninic Acid Assay (BCA) Kit (Pierce; #23227) for protein concentration quantification, following manufacturer's instructions. The reaction has a peak of absorbance at 470-490 nm and a peak of emission at 562 nm, which can be read in a microplate spectrometer. For this technique, the same buffer used for lysate the cells must be used for the standard curve. Before the assay, it should be checked that the components of the buffer would not interfere in the BCA assay.

II.3.- Discontinuos polyacrilamide gel electrophoresis (SDS-PAGE) of proteins

Protein extracts or purified proteins can be separated in an electric field by denaturing the proteins and resolving them by their molecular mass, SDS-PAGE (Sodium dodecyl sulfate – Polyacrylamide gel electrophoresis) technique. The SDS of the protein Loading Buffer (Laemmli buffer; see 6X recipe) denature the proteins and confers a negative charge to the samples, that will migrate to the positive pole in the electrophoresis. Moreover, reduced agents as DDT o β-mercaptoethanol will eliminate disulphide bonds to allow migration of individual subunits from a covalent protein complex.

Discontinuous Tris-Glycine polyacrylamide minigels were prepared as follows:

- A resolving lower part of variable percentage of acrylamide/bisacrylamide, depending on the molecular mass of the protein or proteins being analyzed (usually 10% or 12%). Recipe for 2 gels (1.5 mm thick):
- 5.25 ml (for 10% gels) and 6.3 ml (for 12% gels) of a 30% acrylamide/bisacrylamide solution (37.5:1 ratio) (BioRad; # 161-0158)
- 4 ml of 4xTris-HCl/SDS, pH 8.8 solution (see recipe)
- 200 µl 10% ammonium persulfate solution in water
- 13 µl of TEMED
- Adjust with distilled water to a final volume of 16 ml
- Mix vigorously and use immediately
- A stacking upper gel containing 4% of acrylamide/bisacrylamide. Recipe for 2 gel (1.5 mm thick):
    - 0.65 ml of 30% acrylamide/bisacrylamide solution (37.5:1) (BioRad; # 161-0158)
    - 1.66 ml of 4xTris-HCl/SDS, pH 6.8 solution (see recipe)

- 50 µl of 10% ammonium persulfate solution in water
- 5 µl of TEMED
- Adjust with distilled water to a final volume of 6.5 ml
- Mix vigorously and use immediately

Between 10 and 80 µg of total protein was loaded in each well of the gel.

Gel was run using a Mini-Protean III cuvette at 30 mA per gel submerged in 1X running buffer (see recipe) until the front dye reaches the end of the gel (approximately 1 hour). The gel was directly stained by Coomassie Blue (Section II.4) or transferred to a nitrocellulose membrane (II.5).

II.4.- Detection of proteins in polyacrylamide gels by Coomassie Blue staining

Direct staining with Coomassie Brilliant Blue R-250 was performed to stain proteins directly in polyacrylamide gels. The sensibility of this technique is in the micromolar range (0.3 to 1 µg/band).

Gels are stained with 0.025% (w/v) Coomassie Blue staining solution (see recipe) 2 h at room temperature (RT). Subsequently, the gel is destained by washing with Coomassie Blue destaining Solution (see recipe) until protein bands appear in blue, while the gel remains transparent.

II.5.- Protein transfer of gel proteins to membranes (Western blot - electroblotting)

Alternatively to direct staining of polyacrylamide gels, proteins can be transferred (blotted) to a membrane (PVDF or nitrocellulose) for subsequent detection by Ponceau-S staining (Section II.6.a) or by immunodetection (Section II.6.b).

Transference into nitrocellulose membranes was performed by electroblotting in transfer buffer (see 10X recipe) by using the Mini Trans-Blot Electrophoretic Transfer Cell (Bio-Rad; #170-3930), following the manufacturer's protocol. It is important to ensure the correct position of the membrane and the gel. The transference was performed at 100 V for 1h. Longer transferences must be performed at 4°C to avoid overheating the sample.

II.6.- Detection of proteins in a membrane

II.6.a.- Detection of proteins by Ponceau-S staining

Ponceau-S staining of total proteins in a membrane shows the correct transference of proteins. This technique has a low sensitivity of protein detection (about 500 ng per lane) (Yonan *et al.*, 2005) but is a reversible staining.

Membranes are soaked in Ponceau-S Staining Solution (see recipe) and subsequently the excess of staining is removed by washing in distilled water still protein bands appear in red. Complete destaining of Ponceau-S is achieved by washing the membrane with TBS-T 0.1% (see recipe).

II.6.b- Immunodetection of proteins

Immunodetection ensure the detection of a specific protein among the total of proteins present in the membrane by using specific antibodies.

For this end, the immunodetection was performed as follows:

- Block the nitrocellulose membranes for 1 h at RT with 1% BSA in blocking solution (see recipe) under shaking.
- Incubate membranes with the specific primary antibody (Section II.7) diluted in blocking solution.
- Wash three times the membranes with TBS-T 0.1% (see recipe) for 10 min.
- Incubate membranes with HRP-conjugated secondary antibody (Section II.7) diluted in TBS-T 0.1%.
- Wash the membranes three times with TBS-T 0.1% for 10 min.
- Develop membranes by chemiluminescence reaction by incubating with 1 ml of either Luminol Solution (see recipe) or ECL Plus reagent (GE Healthcare; #RPN2132) following manufacturer's protocol. Detect the signals by film exposure (CL-Xposure film, Pierce; #34090) of by using VersaDoc 5000 Imager (Bio-Rad) and posterior analysis by Quantity One software (Bio-Rad).

It is important not to overexpose the reaction, in order to avoid saturated non-quantitative bands.

II.7.- Antibodies for immunodetection of proteins in a membrane and anti-RCAN1 Monoclonal antibody generation

All antibodies were diluted in TBS-T 0.1% at desired concentration (see table II.1) and incubated overnight at 4°C in an orbital shaker.

Table II.1.- MONOCLONAL ANTIBODIES USED FOR PROTEIN IMMUNODETECTION IN MEMBRANES

ANTIBODY	SOURCE	CLONE	REFERENCE - MANUFACTURER	DILUTION
BRAF	Mouse	F-7	sc-5284 - Santa Cruz	1:500
CRAF	Mouse	53/c-Raf-1	610152 - BD Biosciences	1:1000
CnA	Mouse	G182-1847	556350 - BD Biosciences	1:500
HA	Mouse	12CA5	11583816001 - Sigma Aldrich	1:1000
hRCAN1	Mouse	C8	N/A*	1 µg/ml
anti-mouse-HPRT conjugated	Rat	polyclonal	P0260 - Dako	1:5000

N/A*: Not applicable

Table II.1. Monoclonal antibodies used for protein immunodetection in membranes

Anti-hRCAN1 monoclonal antibody (mAb; clone C8) was generated my immunizing mice with the synthetic peptide RPEYTPIHLS (from Peptide 2.0 company). This peptide is located in the C-terminal region of the human RCAN1 protein, which sequence is common to human and mouse RCAN1 isoforms: RCAN1-1 (corresponding to mouse Rcan1-1) and RCAN1-4 (corresponding to mouse Rcan1-2). Mice immunization and hybridomas generation and amplification were performed by LEITAT Biomed Division (Barcelona, Spain).

To reduce the background, the IgG fractions were purified and concentrated by using protein G coupled resin (HiTrap protein G, GE Healthcare; #17-0404-01) following the manufacturer's protocol.

Anti-hRCAN1 mAb test for western blot, immunoprecipitation and immunocytochemistry analysis was performed in our lab against endogenous and overexpressed RCAN1 isoforms. By western blot analysis, it was found that the antibody properly recognizes endogenous RCAN1-1 and RCAN1-4 in human cell lines and mouse tissues as well as both HA-tagged hRCAN1 isoforms proteins overexpressed in HEK 293T cells (Sergio Martínez, personal communication). Moreover, the mAb was able to immunoprecipitate overexpressed GFP-tagged hRCAN1-1 protein and to recognize overexpressed GFP-hRCAN1-1 by immunocytochemistry.

III.- GENERAL PROTOCOLS IN BACTERIA MANIPULATION

III.1.- Bacterial Strains

Information about bacterial genotypes can be obtained from http://openwetware.org/wiki/E._coli_genotypes or in the manufacturer's website.

XL1-Blue

This strain is used for general plasmid propagation.

Genotype: *endA1 gyrA96(nal^R) thi-1 recA1 relA1 lac glnV44 F'[::Tn10 proAB$^+$ lacI^q Δ(lacZ)M15] hsdR17(r_K^- m_K^+)*
Tetracyclin resistant

DH10B (Invitrogen; #18290-015)

These cells are very suitable for propagation of big plasmids (> 20 kb). To avoid any chance of recombination, it is recommended to growth transformed cells at 30°C.

Genotype: *F- mcrA Δ(mrr-hsdRMS-mcrBC) φ80lacZΔM15 ΔlacX74 recA1 endA1 araD139 Δ(ara, leu)7697 galU galK λ- rpsL nupG*
Streptomycin resistant

Rosetta (Rosetta2(DE3)pLysS) (Novagen; # 71403)

Rosetta strain is a BL21 based strain, suitable for expression of heterologous proteins because it is deficient in OmpT and Lon proteases and have been manipulated to contain pRARE plasmids that codify for codons rarely used in *E. Coli*. The Rosetta2 strain is also modified to contain the plasmid pLysS (T7 phage lysocyme) and the T7 polymerase gen (λDE3 lysogen). Both, pLys and λDE3 form a system to repress the basal expression of heterologous protein that will be only activated upon IPTG stimulation.

Genotype: *F$^-$ ompT hsdS$_B$(R_B^- m_B^-) gal dcm λ(DE3 [lacI lacUV5-T7 gene 1 ind1 sam7 nin5]) pLysSRARE*
Chloramphenicol resistant

III.2.- Preparation of Competent Bacteria

The precise protocol may vary depending on the strain.

III.2.a.- Preparation of XL1-Blue Chemi-competent (Heat-shock) cells

Based on Current protocols in Molecular Biology, 2001. Unit 1.8(DOI: 10.1002/0471142727.mb0108s37)

It is important to keep cells and all material and solutions always on ice and under sterile conditions.

- Growth cells in 4 ml of LB medium (see recipe) with tetracycline (see table XII.1) overnight under shaking 37°C and 250 rpm.
- Inoculate 4 ml of overnight culture in 400 ml of fresh LB with tetracycline and shake at 37°C and 250 rpm still optical density (OD) at 600 nm reaches 0.38 units (no more than 0.4 units).
- Transfer cells to prechilled 50 ml sterile tubes and incubate for 5 to 10 min on ice.
- Centrifuge cells 15 min at 1600 *g* at 4°C, without brake.
- Discard supernatant and resuspend each pellet with 10 ml of ice-cold $CaCl_2$ Solution (see recipe) on ice.
- Centrifuge cells 10 min at 1600 *g* at 4°C, without brake.
- Discard supernatant and resuspend each pellet with 10 ml of ice-cold $CaCl_2$ solution in ice.
- Incubate for 30 min on ice.
- Centrifuge cells 10 min at 1600 *g* at 4°C, without brake.
- Discard supernatant and resuspend each pellet with 2 ml of ice-cold $CaCl_2$ solution always in ice.
- Dispense cells in ready-to-use aliquots in prechilled 1.5 ml tubes and freeze in dry ice and store at -80°C.

III.2.b.- Preparation of Rosetta Chemi-competent (Heat-shock) cells

- Growth cells in 4 ml of SOB medium (see recipe) with chloramphenicol (see table XII.1) under shaking 37°C and 250 rpm overnight.
- Inoculate 1 ml of overnight culture in fresh 100 ml SOB with chloramphenicol and shake at 37°C and 250 rpm still OD at 600 nm reaches 0.45-0.55 units
- Transfer cells to prechilled 50 ml sterile tubes and incubate for 10 min on ice.
- Centrifuge cells 10 min at 1600 *g* at 4°C, without brake.

- Discard supernatant and resuspend each pellet with 20 ml of ice-cold FSB buffer (see recipe) on ice.
- Incubate 10 min on ice.
- Centrifuge cells 10 min at 1600 *g* at 4°C, without brake.
- Discard supernatant and resuspend each pellet with 4 ml of ice-cold FSB solution in ice.
- Add 140 µl of ice-cold DMSO and mix gently.
- Incubate for 15 min on ice.
- Add additional 140 µl of ice-cold DMSO and mix gently.
- Incubate for 15 min on ice.
- Dispense cells in ready-to-use aliquots in prechilled 1.5 ml tubes and freeze in dry ice and store at -80°C

III.3.- Transformation of Competent Bacterial Cells

The bacterial cell transformation protocol varies depending on the strain used. In the case of Rosetta2, we indicate the protocol to transform home-made competent cells. When commercial bacterial competent cells were used (DH10B in our case), the manufacturer's protocol was followed.

III.3.a.-Transformation of XL1-Blue and Rosetta Chemi-Competent (Heat-shock) cells

Based on Current protocols in Molecular Biology, 2001. Unit 1.8(DOI: 10.1002/0471142727.mb0108s37)

In this protocol, the time of cells heat-shock and to keep the cells below 4°C are the critical steps in the transformation process and vary depending on the strain. The transformation protocol is as follows:

- Thaw bacterial cells on ice and mix with DNA in an 1.5 ml sterile tube:
    - 100 µl of XL1-Blue or 50 µl of Rosetta2 competent cells
    - Transforming DNA:
        - 10 ng of plasmid DNA; or
        - 5 µl of DNA ligation reaction
- Mix gently and incubate 10 min at 4°C (45 min in the case of Rosetta2 cells).
- Heat-shock cells by placing tubes into a 42°C water bath for 1.5 min (45 s in the case of Rosetta2 cells).
- Incubate on ice for 2 min (30-60 min in the case of Rosetta2 cells).
- Add 900 µl of LB medium (see recipe) (500 µl of SOC medium (see recipe) in the case of Rosetta2 cells).

- Shake cells for 1h at 37°C and 250 rpm.
- Spread transformed cells in LB-agar plates with the antibiotic required for the plasmid and the bacterial strain selection (see table XII.1)
    - 50 µl of transformed cells suspension; or,
    - in the case of DNA ligation: spin previously cell suspension, discard supernatant, resuspend in 50 µl of LB and spread all the transformed bacteria.
- Incubate plates overnight at 37°C.

III.3.b.- Transformation of DH10B Electro-competent Cells (commercial)

- Thaw bacterial cells on ice and mix in an 1.5 ml sterile tube:
    - 3 µl of competent cells (unused cells can be frozen in a dry ice/ethanol bath for 5 min and refreeze them at -80°C)
    - 36 µl of sterile water
    - Transforming DNA:
        - 1 ng of plasmid DNA; or
        - 2-3 µl of DNA ligation
- Transfer cell-DNA mix into a prechilled 0.1 cm cuvette.
- Electroporate cells: BTX electroporator ECM-630 at 1505 V, 50 µF, 125 Ω.
- Recover cells in 900 µl of 2xYP medium (see recipe).
- Shake cells (250 rpm) for 1h at 30°C, to avoid recombination of big plasmids.
- Spread transformed cells in LB-agar plates with the antibiotic required for the plasmid and the bacterial strain selection (see table XII.1):
    - 50 µl of transformed cells suspension; or,
    - in the case of DNA ligation: spin all cell suspension, discard supernatant, resuspend in 50 µl of 2xYP and spread the half of the transformed bacteria.
- Incubate plates overnight at 30°C to avoid recombination of big plasmids.

III.4.- Glycerol stocks from bacterial transformed cells.

Transformed cells can be stored (up to a year) at -80°C in a glycerol stock, by adding 800 µl of sterile 80% (v/v) glycerol in LB to 400 µl of liquid cultured bacterial cells. Some DNA rearrangements can occur, so it is recommended to test the quality and refresh long-term stored glycerol stocks.

IV.- RECOMBINANT DNA TECHNOLOGY (DNA CLONING)

DNA cloning technology has been used to generate pMIG-HA-hRCAN3 plasmid, pGST-RCAN3 plasmids encoding GST-fused proteins used in pull-down experiments and to clone different 5' flanking DNA regions of human RCAN3 promoters into the pGL3 plasmid (Promega) that codifies for a luciferase gene expression under the control of promoters being cloned (luciferase activity assays).

A brief schema of the general cloning protocol used is as follows:

1. Amplification of the DNA insert to be cloned by polymerase chain reaction (PCR) (Section I.1.a).
2. DNA Ligation (Section IV.1.a) in pGEM®-T vector, transformation in XL1-Blue cells (see Section III.3.a).
3. Selection of positive clones by white/blue screening in LB-agar plates (Section IV.2) and by PCR screening (Section IV.7 and Section I.1.b).
4. Amplification and purification of plasmid DNA (Section IV.3) from the DNA positive clones.
5. Restriction enzyme digestion (Section IV.4) of DNA fragment insert and subcloning into a destination vector.
6. Dephosphorylation of destination vector by Shrimp Alkaline Phosphatase (SAP) treatment (Section IV.5).
7. In-gel purification of DNA (Section IV.6) to purify the DNA fragment and the destination vector.
8. DNA Ligation (Section IV.1.b) of purified DNA fragment with the plasmid of destination.
9. Transformation in XL1-Blue or other suitable strain (see Section III.3).
10. Selection of positive clones by PCR screening (Section IV.7 and Section I.1.b).
11. Amplification and purification of plasmid DNA (Section IV.3) from the positive clones by DNA mini- or maxi-preparation kit (Qiagen).
12. Verification of positive clones by restriction enzyme digestion (Section IV.4).
13. Sequence verification of the selected clones by sequencing PCR (Section I.1.c) and DNA sequencing in the Genomic Service at the University of Barcelona.

Alternatively, if the DNA fragment of interest in inserted into another vector and flanked sites for restriction enzyme are appropriate for subcloning in our vector of interest, steps 1 to 4 are not necessary.

IV.1.- DNA Ligation

DNA ligation reaction creates covalent bonds between 3'-OH of one nucleotide and 5'-phosphate of other nucleotide. This procedure is used to introduce DNA fragments into DNA vectors or to recircularize digested vectors.

IV.1.a.- DNA Ligation in pGEM®-T vector

DNA insert fragment ligation in pGEM®-T and pGEM®-T easy vectors (Promega; #TM042) can be done directly, without necessity of previously purify the PCR amplified DNA fragment or dephosphorylate it (see Section II.6), because the pGEM®-T easy backbone is open and contain an additional 3' terminal T nucleotide in both extremes. This T nucleotide binds to the 5' terminal A nucleotide of the DNA fragment to be subcloned that is added by the majority of DNA polymerases.

Ligation in pGEM®-T easy was performed following the manufacturer's protocol.

IV.1.b.- DNA ligation of purified DNA fragment and the plasmid of destination

The general DNA ligation reaction was performed as follows:

- Mix in a 0.5 ml tube:
  - 20 ng vector DNA
  - X ng of insert DNA (see below)*
  - 1.5 µl 10X Roche ligation buffer** (Roche)
  - 1 µl of T4 DNA ligase (Roche)
  - Adjust the volume with distilled water to a final volume of 15 µl
- Incubate overnight at 4°C for sticky ends ligation or at RT for blunt ligation.

*The amount of insert was calculated with the following formula by using a ratio insert/vector of 6:1:

$$\text{ng of insert} = \frac{\text{ng of vector x size of insert (kb)}}{\text{size of vector (kb)}} \text{ x ratio insert/vector}$$

*Ligation buffer must be dispensed in single ready-to-use aliquots after the first use. The aliquots cannot be rethawed after use.

Several controls should be included:

- The digestion control: a reaction containing vector but without neither insert nor ligase enzyme, to the test the efficiency of the digestion of the destination vector.
- Plasmid dephosphorylation control: a reaction containing the dephosphorylated vector but without insert, to check the efficiency of the SAP phosphatase treatment.

IV.2.- White/blue colony screening for insert cloning

pGEM®-T vectors encode for the enzyme β-galactosidase. Those colonies that insert the DNA fragment disrupt the β-galactosidase coding sequence (white), while those colonies that do not contain the DNA insert will produce the enzyme (blue colonies).

Transformed colonies are seeded in a plate where previously 100 µl of 100 mM IPTG (see recipe) and 20 µl of 50 mg/ml X-Gal (see recipe) have been spread over the surface. White colonies will contain an inserted DNA fragment.

IV.3.- Amplification and purification of plasmid DNA

To recover the DNA of interest, the positive clones are inoculated in 5 ml of LB medium (see recipe) containing the antibiotic appropriate for the plasmid (table XII.1) and growth overnight under shaking (250 rpm) at 37°C (or 30°C in the case of big plasmids, to avoid recombination).

The next day, plasmid DNA purification can be performed manually (Current Protocols in Molecular Biology, 2001. Unit 1.6 (DOI: 10.1002/ 0471142727.mb0106s15) or using commercial kits (Spin Miniprep Kit (Qiagen; #27104). Manual protocol is highly recommended to purify vectors with very high molecular weight, as BACs or PACs.

Alternatively, when higher amounts or high purity grade plasmid DNA are needed, alternative commercial kits can be used Plasmid Maxi Kit (Qiagen; #12163) or PureLink HiPure Plasmid Purification Kit (Invitrogen; #K2100-06).

DNA quality and amount is quantified as indicated in section I.3.

IV.4.- Restriction enzyme digestion

Restriction enzyme digestion is used to excise the DNA fragment of interest from pGEM®-T vectors or other carrier vector and to subclone in the destination vector of interest. Also, vector used as destination vector must be digested with the

appropriate restriction enzyme. Enzyme digestion is also used to ensure the presence of a specific DNA insert in a vector.

Restriction enzyme activity is measured in units (U) of activity: 1 unit (U) digests 1 µg on DNA in 1 hour at 37°C. Thus, quantity of restriction enzyme and incubation time must be adjusted for our conditions.

The standard protocol of restriction enzyme digestion is performed as following; however, a specific enzyme may require other conditions:

- Mix in a 1.5 ml tube:
    - Substrate DNA (1 to 6 µg of a purified plasmid DNA)
    - Enzyme buffer 10X
    - BSA (final concentration of 0.1 mg/ml) (if needed)
    - Restriction enzyme of interest
    - Distilled water up to 20-50 µl
- Incubate in a water bath at 37°C the time necessary
- Inactivate the enzyme by incubating the reaction at 65°C for 20 min

IV.5.- Shrimp Alkaline Phosphatase (SAP) Treatment

Dephosphorylation of DNA vector must be done in order to avoid the recircularization of the plasmid of destination in the ligation step (see section IV.1.b).

To dephosphorylate plasmid DNA:

- Add 1 µl of Shrimp Alkaline Phosphatase (SAP) to the digestion reaction (Fermentas; #EF0511)
- Mix thoroughly and spin down
- Incubate in a water bath at 37°C for 2 h
- Inactivate the enzyme by incubating the reaction at 65°C for 20 min

IV.6.- In-gel purification of DNA

Both, dephosphorylated destination vector and DNA fragment of interest are resolved in an agarose gel (see Section I.2.a) at slow electrophoresis voltage to avoid contamination of heavier fragments. It is recommended to load into the gel the sample to be purified far from other samples and DNA ladder to avoid cross-contamination.

By illuminating the gel under UV light, locate the specific electrophoretic bands and, rapidly, to avoid cross-linking of thymidine nucleotides, excise them from the agarose gel using a clean scalpel and deposit them into a clean 1.5 ml tube.

DNA extraction is performed using commercial kit QIAquick Gel Extraction kit (Qiagen; #28704) following manufacturer's protocol. Alternatively, it can be extracted manually following protocol in Current Protocols in Molecular Biology, 2001. Unit 2.6. (DOI: 10.1002/0471142727.mb0206s59).

DNA quality and quantity is checked as indicated in section I.3.

Long storage of plasmid DNA in aqueous solution must be performed at -20°C to avoid DNA degradation and in rubber sealed tubes to avoid evaporation.

IV.7.- Bacterial culture to perform PCR screening

A quick method to find positive bacterial clones after a DNA ligation is:

- Inoculate one single colony in 100 µl of LB medium (see recipe) supplemented with antibiotic (see table XII.1) in a 96-well V-Bottom plate.
- Incubate sealed plate at 37°C (or 30°C for big plasmids) for 2h.
- Perform PCR-screening (see section I.1.b).
- Positive clones can be grown directly from the 96-well culture.

V. PRODUCTION OF HETEROLOGOUS PROTEINS IN BACTERIAL CELLS

We used the pGEX system to express GST-fused human RCAN3 protein and deletion mutants in bacteria, to perform pull down experiments (Section VII.1). For additional information, consult pGEX system manufacturer's protocols.

For protein expression in bacteria, it is important to use recipients at least 4 times higher than the culture volume to be used in order to ensure adequate culture aeration.

The general protocol to produce heterologous proteins in bacteria is as follows:

- Transformation of bacteria (Section III.3) with the chosen expression plasmid (pGEX). To this end, choose a bacterial strain adequate to express proteins (in our case, Rosetta2 (Section III.1).
- Perform a small-scale of screening of protein expression clones (Section V.1) to find a clone able to produce high amounts of soluble protein.
- Once we have chosen the best clone expression conditions, perform a high-scale production of protein (Section V.2).
- Purification of GST-fused protein (Section V.3).

V.1.- Screening of clones for protein expression

- Inoculate a single colony in 2 ml of LB medium (see recipe) chloramphenicol (for bacteria selection) and ampicillin (for plasmid selection) (see table XII.1).
- Incubate culture under shaking (250 rpm) at 37°C until OD at 600 nm reaches 0.7 units (no more than 0.8 units) (3-5 h).
- Collect 0.5 ml of the culture, spin cells at maximum speed, discard supernatant and froze the pellet. This sample is the non-induced sample (NI) for SDS-PAGE analysis of the protein expression protocol.
- Collect 0.5 ml of the culture and keep at 4°C. This sample will serve to re-inoculate LB medium for high-scale production of proteins.
- Induce the production of proteins in the remaining liquid culture by adding 0.5 mM of IPTG (see 100 mM recipe).
- Incubate under shaking (250 rpm) at 37°C for 2 h.
- Collect 0.5 ml of the culture, spin cells at maximum speed and discard supernatant. This sample is the Induced Sample (IS) for SDS-PAGE analysis of the protein expression protocol.
- Resuspend bacterial pellet with 1 volume of 2X Laemmli buffer (see 6X recipe) and boil de samples for 20 min.
- Resolve NI and the IS samples onto a SDS-PAGE (II.3) and detect the proteins in the gel by Coomassie Blue staining (II.4). Induced proteins can be distinguished among the total of proteins in the gel when comparing NI and I pattern.

Once we have selected an efficient-producing colony, we can generate a culture glycerol stock (Section III.4).

V.2.- High-scale production of recombinant proteins

This protocol describes the protein expression protocol from a 250 ml of bacterial culture. For higher or lower amounts, scale-up or scale-down directly the proportions:

- Growth cells by inoculating 250 µl from a liquid culture or directly from a glycerol in 4 ml of LB with chloramphenicol (for bacteria selection) and ampicillin (for plasmid selection) (see table XII.1) and incubate overnight under shaking (250 rpm) at 37°C.
- Inoculate 4 ml of overnight culture in 250 ml of fresh LB containing chloramphenicol and ampicillin and shake at 37°C and 250 rpm until OD at 600 nm reaches 0.6-0.7 units (no more than 0.8 units).

- Collect 0.5 ml of the culture, spin cells at maximum speed, discard supernatant and froze the pellet. This sample is the non-induced sample (NI) for SDS-PAGE analysis of the protein expression protocol.
- Induce the production of proteins in the remaining liquid culture by adding 0.5 mM of IPTG (see 100 mM recipe).
- Incubate under shaking (250 rpm) at 25-37°C* for 2-5 h*.
- Pellet cells by centrifugation at 5000 *g* at 4°C for 10 min.
- Discard the supernatant.
- Proceed with purification of GST-fused proteins (Section V.3). If desired, pellet can be frozen prior to continue with the purification step. To this end, resuspend the pellet in 12.5 ml of ice-cold PBS 1X (see 10X recipe) and transfer to a 50 ml tube, centrifuge at 1600 *g* at 4°C for 10 min and discard all the supernatant. Froze the tubes in dry ice and store at -80°C.

*The time and the temperature used in the protein induction step may vary between proteins to be expressed. Excessive time or temperature can form protein aggregates, which difficult the recovery of soluble proteins. It is recommended to test different temperature and time conditions and check the presence of our protein of interest in the bacterial protein soluble and insoluble extracts.

V.3.- Purification of GST-fusion proteins

To generate soluble protein extract:

- Resuspend completely each pelleted cells from a 250 ml of culture in 25 ml of bacterial lysis buffer (see recipe). Resuspension must be performed carefully and avoiding the formation of foam, that indicates protein degradation.
- Incubate 30 min under soft shaking at RT.
- Sonicate cells on ice (to avoid overheating the sample) to reduce viscosity produced by DNA.
- Add Triton X-100 (Sigma; #X100) to a final concentration of 1%.
- Incubate 30 min under soft shaking at 4°C.
- Centrifuge at 13000 *g* at 4°C for 30 min and collect the supernatant that will contain soluble proteins. Pellet can be resuspended in 2 ml of PBS 1X (see 10X recipe) containing 0.5 mM of DTT to analyze for the presence of protein aggregates.

To purify GST-fused proteins:

- Prepare Glutathione Sepharose 4B beads (GE Healthcare; #17-0756-01) following the manufacturer's protocol to remove ethanol that inhibits the purification of GST-containing proteins at 50% density (50% beads and 50% bacterial lysis buffer).
- Add 250 µl of Glutathione Sepharose 4B beads at 50% density to the soluble cell extract.
- Incubate 30 min under soft shaking at 4°C.
- Wash the beads several times with bacterial lysis buffer.

The beads bound to GST-fused protein can be used directly for pull down experiments (VII.1) or to purify GST-fused proteins by elution from the Glutathione Sepharose beads by adding reduced glutathione. Elution of the purified protein can be followed by spectrophotometric analysis at 280 nm (Nanodrop, Thermo Fisher Scientific Inc.). Alternatively, pGEX vectors encode for a specific protease cleavage sequence, between the GST and the protein fused to it, such as thrombin (in pGEX-1T, 2T and 4T), Factor Xa (in pGEX-3X and 5X) or PreScission (in pGEX-6P), that allows to purify protein alone from the GST-protein fusion.

VI. GENERAL PROTOCOLS IN MAMMALIAN CELLS MANIPULATION

The work with mammalian cells must be always be performed in sterile conditions and using sterile material. Work always in a flow hood.

VI.1.- Mammalian cell lines

- HEK 293T cells, human embryonic kidney cells, were purchased from ECACC.
- NIH 3T3 cells, mouse embryonic fibroblast cell line, were purchased from ATCC.
- Jurkat T cells E6.1 clone, acute leukemia human T cells, obtained from ECACC.
- WEHI, myelomonocytic leukemia, kindly given from Anna Bigas.
- BHK/MKL (Baby hamster kidney/MKL), kindly given from Anna Bigas.

VI.2.- Maintenance of mammalian cells

- HEK 293T, NIH 3T3 and BHK/MKL cells were cultured in DMEM with Glutamax high glucose (Invitrogen; # 61965-026) supplemented with heat inactivated 10% fetal bovine serum (FBS, Invitrogen; #10270-106).

- Jurkat and WEHI cells were cultured in RPMI with Glutamax (Invitrogen; #61870-010) supplemented with heat inactivated 10% FBS.
- To avoid contamination, all cells were cultured in presence 100 U/ml penicillin and 100 µg/ml streptomycin solutions (Invitrogen; #15070-063).
- The cells were growth in a humidifier incubator at 37°C, 5% CO_2 and high relative humidity (95%).

VI.3.- Mycoplasma test

Cell contamination with mycoplasma is frequent in cell line cultures and modifies the normal physiology of the cell and lead to erroneous and heterogeneous results.

Mycoplasma test must be performed routinely to test cell lines been used and when changes in the normal fate or growing rate of the cells are detected. Also, it is recommendable to perform the test when a new cell line is going to be used.

To perform a mycoplasma test, be very careful with all the products and material used for the test to avoid mycoplasma or bacterial contamination.

To obtain the sample:

- Seed cells of the cell line to be tested in fresh medium without antibiotics.
- Let cells to growth until overconfluence and then maintain the culture growing for 2 more days.
- Collect 200 µl of the culture supernatant and perform a PCR assay for mycoplasma detection (Section I.1.d).

For additional information, see Drexler and Uphoff, 2002.

VI.4.- Mammalian cell DNA transfection

Several methods can be used to introduce plasmid DNA in mammalian cells. In our case, we used calcium phosphate method (section VI.4.a) for obtain retroviral particles in HEK 293T cells and PEI-mediated transfection method (section VI.4.b) for transfect pGL3 plasmids used for luciferase assays in the study of RCAN3 promoter (section IX).

In all cases, cells need be exponentially growing (approx. 40% of confluence) in the moment of DNA transfection.

VI.4.a.- Mammalian cell DNA transfection by calcium phosphate method

Based in Current Protocols in Molecular Biology, 2003. Unit 9.1 (DOI: 10.1002/0471142727.mb0901s63)).

- Seed cells to be transfected at 30% of confluence
- The next day, prepare solutions A and B separately in sterile 1.5 ml tubes, following the conditions indicated in table XI.1. Here, it is indicated the transfection method used to transfect a P60 dish.
    - Solution A:
        - 5.6 µg of high pure pMIG plasmid
        - 5.6 µg of high pure pCLEco plasmid

        ] 11.2 µg of total DNA
        - 3.92 µl (10% (v/v)) of sterile $CaCl_2$ 2.5 M solution
        - Sterile water up to 392 µl
    - Solution B:
        - 392 µl of HEPES-buffered saline (HeBBs) solution (see recipe) at desired pH*
- Helped by a mechanical pipettor with a Pasteur pipet, bubble the solution B and add solution A drop-wise.
- Vortex for 5 s and incubate the transfection mix solution at RT for 20 min. A fine precipitate suspension (calcium phosphate-DNA aggregates) can be seen after incubation.
- Add transfection mix drop-wise to the cells while swirling the plate carefully. To reduce toxicity, increment volume of culture with fresh media to a final volume equal to 10 times the volume of transfection mix (7.84 ml).

*Transfection efficiency is critically dependent of a correct drop-wise and vigorous bubbling of solution B in A and the pH of HeBBS solution used for transfection which is dependent of the cell line to be transfected. It is recommended to test a range of different pH (increasing pH of 0.02 from 6.95 to 7.12) for each different cell line.

Calcium phosphate-DNA aggregates are very toxic for the cells. Thus, it is important to refresh the medium 16 h post-transfection to avoid excessive cell death. In order to concentrate viral supernatant, we reduced the volume of medium used for refreshing.

VI.4.b.- Mammalian cell DNA transfection by PEI method

Polyethylenimine MAX (PEI, Polysciences Inc., #24765) is a linear polymer of 25.000 kDa that forms a complex with DNA that can be internalized by mammalian cells.

The standard protocol of transfection mediated by PEI was performed as follows:

- Prepare solutions A and B separately in sterile 1.5 ml tubes. The typical amount of DNA used is 200 ng/cm^2, but it can be optimized for the conditions of the experiment. Here, it is indicated the transfection method used to transfect a P100 dish, and may be scale-up or scale-down for other specific conditions.
    - Solution A:
        - 8 µg DNA in 500 µl of sterile 150 mM NaCl.
    - Solution B:
        - 15 µl of PEI (stock prepared at 1mg/ml) in 500 µl of sterile 150 mM NaCl.
- Solution B should be added to solution A, avoiding direct contact of solution A with the tube.
- Vortex briefly and incubate at RT for 20 min.
- Add transfection mix drop-wise to the cells.

Although PEI polymer has relative low toxicity to the cells, it is recommended to refresh the medium 16 h post-transfection.

VI.5.- Cryopreservation of Mammalian Cells

Mammalian cells can be long time stored in liquid nitrogen. To avoid cell death, the cells are processed as follows:

- Collect the cells and pellet by centrifugation at 500 *g*.
- Resuspend the cells in a mix that contains 40% of culture media, 50% of FBS and 10% of sterile DMSO (cell culture grade Sigma; #D8418).
- Incubate in a freezing container that decreases 1°C per minute until reaching -80°C (around 3 h).
- Store frozen cells in liquid nitrogen.

To recover cells, thaw frozen cells rapidly (< 1 minute) in a 37°C bath. Dilute cell suspension with pre-warmed growth medium and centrifuge at 400 *g* for 5 min. Discard the supernatant and resuspend the pellet with the appropriate media for cell culture.

VI.6- Production of IL-3 from WEHI cells

- Growth cells in a T75 flask with 30 ml of RPMI supplemented with 10% FBS until cells form a multilayer.

- Eliminate supernatant but keep 6 ml. Detach cells with a cell scraper and distribute cells in five T-150 flask with 100 ml of RPMI supplemented with 5% FBS.
- After 3 days, detach cells from each flask with a cell scraper, centrifuge at 700 *g* for 10 min and collect the supernatant, leaving 6 ml. Filter supernatant with a 0.22 µm filter and store at 4°C (conditioned media 1). Seed cells in the same flask with 100 ml of RPMI supplemented with 5% FBS.
- After 3 days, detach cells with a cell scraper, centrifuge 700 *g* for 10 min and collect the supernatant. Filter supernatant with a 0.22 µm filter and store at 4°C (conditioned media 2)
- Put together conditioned media 1 and 2, dispense in ready-to-use aliquots and store at -80°C.

VI.7- Production of SCF from BHK/MKL cells

- Growth cells in a T75 flask with 50 ml of DMEM supplemented with 5% FBS until reaching 80% of cell confluence.
- Detach cells with a cell scraper and distribute cells in four T75 flask with 50 ml of DMEM supplemented with 5% FBS.
- After 2 days, detach cells with a cell scraper, centrifuge at 700 *g* for 10 min and collect the supernatant. Filter supernatant with a 0.22 µm filter and store at 4°C (conditioned media 1). Seed cells in the same flask with 60 ml of DMEM supplemented with 5% FBS and 100 U/ml penicillin and 100 µg/ml streptomycin.
- After 2 days, detach cells with a cell scraper, centrifuge 700 at *g* for 10 min and collect the supernatant. Filter supernatant with a 0.22 µm filter and store at 4°C (conditioned media 2).
- Put together conditioned media 1 and 2, dispense in ready-to-use aliquots and store at -80°C.

VII.- PROTOCOLS FOR ANALYSIS OF PROTEIN-PROTEIN INTERACTION

VII.1.- GST Pull down

GST pull down technique is used to analyze the interaction of an endogenous protein present in mammalian cells (RAF kinases in our case) with a protein expressed in bacteria fused to GST (GST-RCAN3 and deletion mutants in our case).

To this end,

- Generate GST-protein coupled to Glutathione Sepharose beads (Section V) (from 100 ml of bacterial culture/per assay in our case).
- Lyse the cells used as source of interactor proteins (Section II.1.a) ($25x10^6$ Jurkat T cells/per assay in our case) with IGEPAL-based lysis buffer (see recipe).
- Incubate soluble extracts with bait beads for 3 h at 4°C under soft shaking or in an orbital shaker.
- After washing extensively with IGEPAL-based lysis buffer, add Laemmli buffer (see 6X recipe) and boil samples at 98°C for 10 min.
- Resolve samples in 10% SDS-PAGE (Section II.3), transfer to nitrocellulose membranes (Section II.5) and immunodetect the protein of interest with specific antibodies (II.6.b and II.7).

VII.2.- Immunoprecipitation

Immunoprecipitation technique is used to detect interaction between cell endogenous proteins (RAF and RCAN proteins in our case). One of the proteins is bound to a specific antibody and is able to co-precipitate the interactor protein.

To that end:

- Incubate Protein G Sepharose 4 Fast Flow beads (prepared following the manufacturer's protocol; GE Healthcare; #17-0618) with 2 µg of the antibody used for protein immunoprecipitation at 4°C for 2 h in an orbital shaker.
- Lyse the cells used as source of interactor proteins (Section II.1.a) ($25x10^6$ Jurkat T cells/per assay in our case) with IGEPAL-based lysis buffer (see recipe).
- Incubate soluble extracts with Protein G Sepharose beads for 3 h at 4°C in an orbital shaker.
- After washing extensively with IGEPAL-based lysis buffer, add Laemmli buffer (see 6X recipe) and boil samples at 98°C for 10 min.
- Resolve samples in 10% SDS-PAGE (Section II.3), transfer to nitrocellulose membranes (Section II.5) and immunodetect the protein of interest with specific antibodies (II.6.b and II.7).

VIII.- DETERMINATION OF mRNA LEVELS IN MAMMALIAN CELLS AND TISSUES

To determine cells mRNA levels, total RNA is extracted (Section VIII.1), and treated with DNAse (Section VIII.2) and reversed transcribed to cDNA (Section VIII.2). The resulting cDNA is amplified by semiquantitative PCR (Section I.1.f.) or real-time quantitative PCR (Section I.1.g).

RNA manipulation must be always performed at 4°C and using RNAse- DNA-free material. Long storage of samples must be performed at -80°C.

VIII.1.- RNA extraction

For extraction of total RNA from tissues, frozen samples were homogenized with a polytron homogenizer (or with a 30G needle in case of very little samples) in presence of TRIzol® reagent (Invitrogen; #15596-018), following the manufacturer's protocol. Extraction of total RNA from pelleted frozen cells was performed by using RNeasy Mini Kit (Qiagen; #74104).

Quality and amount of RNA samples was quantified as described for DNA in section I.3. Additionally, 250 ng of the sample was analyzed by electrophoresis in a 1.5% agarose gel (Section I.2.1) and stained with EtBr for qualitative evaluation of RNA integrity by the presence of 18s and 28s rRNA bands.

VIII.2.- DNAse treatment of RNA samples

RNA samples were treated with DNA- RNAse-free to avoid any contamination of DNA. DNAse treatment was performed with DNA-free™ (Invitrogen; #AM1906), following the manufacturer's protocol.

After DNAse treatment, quality and amount of RNA samples was quantified again as described for DNA in section I.3.

VIII.3.- Reverse transcription of total RNA: cDNA synthesis

Reverse transcription of RNA samples to cDNA was performed using SuperScript™ II Reverse Transcriptase (Invitrogen; #18064) in a 20 µl final volume as follows:

- For each reaction, mix in a clean RNAse- DNA-free PCR tube:
  - 1 µl of 250 ng/µl random primers (Invitrogen; #48190-011)
  - X µg of DNAse treated RNA*
  - 1 µl of 10 mM (each) dNTPs mix
  - Add RNAse-free or distilled water to a final volume of 12 µl

- Incubate samples in a thermocycler at 65°C for 5 min and place immediately on ice.
- Prepare a mix as follows:
    - 4 µl of First-Strand buffer 5X (supplied in the kit)
    - 2 µl of DTT (supplied in the kit)
    - 1 µl of RNAse-free or distilled water (alternatively, 1 µl of the ribonuclease inhibitor RNAse™ out (Invitrogen; #10777-019) can be added)
- Add the mix (7 µl) to each reaction tube.
- Incubate samples in a thermocycler at 25°C for 2 min.
- Without removing the tubes from the thermocycler, add carefully 1 µl of SuperScript II retrotranscriptase enzyme. Change the tip between samples to avoid RNA contamination.
- Incubate samples in a thermocycler at 25°C for 10 min.
- Incubate at 42°C for 50 min.
- Incubate at 70°C for 15 min.
- Place on ice for immediate use or at -80°C for long storage.

*The quantity of sample used in the reaction can vary from 0.7 µg to 5 µg of total RNA. In our case, the amount of total DNAse treated RNA that was reversed transcribed was 2 µg for semiquantitative PCR analysis and 1.7 µg for real-time quantitative PCR.

An additional negative control reaction must be performed by using a pool of all the used RNAs (containing the same amount of total RNA than the samples) but without retrotranscriptase enzyme. Also, the same pool can be used in a reaction with retrotranscriptase and will serve as calibrator sample for real time quantitative PCR (See section I.1.g).

IX.- LUCIFERASE REPORTER GENE ASSAY

Luciferase reporter gene assays are used to assess the transcriptional activity of a putative gene promoter. These experiments were performed by Álvaro Aranguren to anlyse the transcriptional activity of *RCAN3-2/2a* transcript promoter.

In luciferase experiments, *RCAN3* promoter regions were amplified by PCR (section I.1.a) from the BAC clone RP4-633K13 (Children's Hospital Oakland Research Institute (CHORI); (http://www.chori.org)) using specific primers (table IX.1) and subsequently cloned into a pGL3-basic vector (section IV) or other suitable reporter vector, which codifies for firefly beetle (*Photinus pyralis*) luciferase, and transfected into HEK 293T cells. Luciferase protein catalyses the oxidation of luciferin substrate, in a reaction that requires ATP, oxygen and Mg2+

and emits light. It can be measured to quantify the transcriptional activity of the putative promoter. Luciferase units must be normalized to an internal control of transfection in order to compare between diferent wells. To this end, cells are co-transfected with pRL-null vector, a promoterless vector that codifies for sea pansy (*Renilla reniformis*) luciferase. This enzyme catalyses the oxidation of coelenterate-luciferin (coelenterazine) substrate, in a reaction that emits light.

Table IX.1.- PRIMERS FOR RCAN3 5' FLANKING REGIONS CONTRUCTS			
PRIMER NAME	**SEQUENCE**	**LOCATION (from RCAN3-2 TSS)**	**Tm (°C)**
-5Kb_TSS_hR3	CCAACTGATCCACCCACCTTGG	-4775	63
-2Kb_TSS_hR3	CCACTTGTATCATTTTCATA	-1999	48
-700pb_TSS_hR3	ATCTCATTTGATGTGAAAACTC	-699	53
-300pb_TSS_hR3	GGAGTAAGAGGAGGAGGGAG	-281	58
+550pb_TSS_hR3	CGCCAGAGGTCCTGTTTTC	+550	59

Table IX.1. Primers used for *RCAN3* 5' flanking regions contructs

HEK 293T cells were seeded at 50000 cells per well in 24-well plates and co-transfected by PEI-mediated transfection (section VI.4.b) with 30 fmol of each pGL3-RCAN3 constructs, 1 ng of pRL-null vector and pCDNA3.1 vector, to maintain constant proportions of plasmid DNA.

48 h after transfection, luciferase assays were perfomred by using the Dual Luciferase Reporter Assay System (Promega; #1910) following manufacturer's instructions on a multiplate luminometer (FLUOstar Optima, BMG). Briefly, cells of each well were lysed with 50 µl of Passive Lysis Buffer (PLB) and 10 µl of the lysate were plated into a white opaque 96-well plate (PerkinElmer; #6005299). Firefly luciferase reporter was measured first by adding 50 µl of Luciferase Assay Reagent II (LAR II) to each well followed by a 10-seconds measurement lecture. After quantifying the firefly luminescence, this reaction is quenched, and the Renilla luciferase reaction is initiated by adding Stop & Glo® Reagent to the same well, followed by another 10-seconds measurement lecture. Firefly luciferase units were normalized to Renilla luciferase values and relativized to the activity of the empty vector.

X.- GENERAL PROTOCOLS IN ANIMAL MANIPULATION

In our experiments, animals were housed in specific-pathogen free (SPF) conditions at the IDIBELL animal facility, officially accredited by AAALAC (unit 1255), and cared for in compliance with the regulation approved by the CCEA 86/609/CEE IDIBELL Ethics Committee. The number of animals utilized for each study was the minimum necessary to obtain scientifically valid data.

For general protocols and normative in animal manipulation, http://www.aaalac.org and Festing and Altman, 2002.

X.1- DNA purification from animal tail for genotyping

- Cut a 0.2 - 0.5 mm of animal tail and place in a 1.5 ml clean tube
- Add 300 µl of 50 mM NaOH
- Incubate at 98°C while vortexing until tail is completely dissolved
- Add 30 µl of 1 M Tris-HCl, pH 8
- Incubate on ice for 10 min
- Centrifuge at 13000 *g* for 10 min at 4°C
- Transfer the supernatant containing genomic DNA to a clean tube
- DNA quality and amount was quantified as described in section I.3

XI.- BONE MARROW RECONSTITUTION WITH RETROVIRAL TRANSDUCED HEMATOPOIETIC PROGENITORS

For additional information: Klug *et al.*, 2000; Jordan, 2006; Cornetta *et al.*, 2008 and Current Protocols in Immunology, 2001, Unit 10.17C (DOI: 10.1002/0471142735.im1017cs31).

For animal irradiation additional information: http://www.bu.edu/orccommittees/iacuc/policies-and-guidelines/irradiation-of-rodents/ and Cui *et al.*, 2002

For generation of BHK/MKL and WEHI supernatants see Section VI.6 and VI.7.

The protocol for bone marrow (BM) reconstitution followed was:

Day 1

- Inject to each donor mouse intraperitoneally 150 mg/kg of 5-Fluoroacil (5-FU; Sigma Aldrich #F6627) in a proportion of 30% of 5-FU (60 µl of a stock solution of 50 mg/ml in DMSO) to 70% (140 µl) of sterile physiological saline solution or PBS pH 7.3 in a maximum volume of 200 µl.

Day 5

- Prepare RetroNectin coated plates for BM culture in 24-well tissue culture flat bottom plates as follows:

    - Add RetroNectin solution (TAKARA; #T100A) from a stock solution at 48 µg/ml in PBS (Invitrogen; #14190-169) to cover the bottom well.
    - Incubate 2h at RT under shaking.
    - Collect the RetroNectin solution (it can be used up to 5 times) and cover the wells with 1 ml of sterile PBS containing 2% BSA.
    - Incubate 30 min at RT.
    - Just before use, aspire PBS containing 2% BSA solution and wash twice with sterile PBS.

  RetroNectin coated plates can be prepared and kept at 4°C for a week:

- BM progenitor cells isolation – All steps must be performed under sterile conditions at 4°C to reduce cell death and using appropriate surgical sterilized material.

    - Sacrifice donor animals by cervical dislocation or overdose of CO_2. Approximately $4x10^6$ cells will be recovered from each animal and, after transduction, the yield will be of approximately $2x10^6$ progenitors cells from each animal.
    - Femur, tibia and iliac crest are dissected and cleaned from muscle and hair and maintained in DMEM containing 10% FBS (also Iscove's medium can be used) at 4°C.
    - Femur and tibia BM is recovered by breaking the extreme of the bone and flushing out the BM by forcing media through the bone cavity with a 30 G needle until bones appear white. BM must have a suspension consistence, not a compacted one, because it indicates an insufficient 5-Fluoruacil administration. For BM recovery from Iliac crest, place all iliac crests in a mortar (Afora, C181/125) with 2 ml of media and crushed using a sterile pestle (Afora, C182/30).
    - Filter the cells through a 70 µm nylon cell strainer (BD; #352350), centrifuge at 400 *g* for 5 min at 4°C and wash them with PBS.
    - Add 1-2 ml of erythrocytes lysis buffer (see recipe) and resuspend cells carefully with a P1000 pipette. Incubate 10 min at RT and add 3 volumes of PBS.
    - Centrifuge at 400 *g* at 4°C for 5 min and wash with PBS.

- Resuspend cells in PBS (approximately 2 ml per donor animal) and count live cells with Trypan Blue Solution (at 1:1 ratio) (Biochrom AG; #L-6323).
- Centrifuge at 400 *g* for 5 min at 4°C and resuspend cells in the volume needed to seed $2x10^6$ cells in DMEM supplemented with 10% FBS, 10% of WEHI and 10% of BHK/MKL supernatant in a final volume of 2 ml.
- Seed cells in 24-well RetroNectin coated plates.
- Incubate cells in an incubator at 37°C, 5% CO_2 in a humidified atmosphere (95%).

- Seeding of HEK 293T cells for production of retroviral supernatant:

  - Seed the quantity of HEK 293T cell needed (table XI.1) assuming that 1.6 ml of retroviral supernatant will be needed to transduce each well of BM culture. In day 7, NIH 3T3 cells will be seeded and in day 8 will be transduced with 0.5 ml of retroviral supernatant per well.

Table XI.1.- TRANSFECTION CONDITIONS USED FOR PRODUCTION OF RETROVIRAL PARTICLES IN HEK 293T CELLS

CULTURE PLATE	SEEDING DENSITY	µg DNA [pMIG/pCLEco 1:1]	FINAL VOLUME OF TRANSFECTION MIX (µl)	VOLUME OF MEDIUM FOR TRANSFECTION (ml)	VOLUME OF MEDIUM FOR REFRESHING (ml)
P60	$1x10^6$	11.2	784	7.84	3
p100	$2.5x10^6$	30.9	2100	21	8.3

Final volume of transfection mix will be obtained by mixing the half of the final volume of the solution A with the half of the final volume of the solution B.
See section VI.4.a for detailed transfection protocol.

Table XI. Transfection conditions used for production of retroviral particles in HEK 293T cells

Day 6

- Transfection of HEK 293T cells for production of retroviral supernatant:
  - Transfect cells with equal amount of pCLEco and pMIG vectors, following the indications indicated in table XI.1 by calcium phosphate transfection method (Section VI.4.a).

Day 7

- Refresh and concentration of retroviral supernatant:
    - After 16 h post-transfection (do not overload this time to avoid excessive cell dead), replace HEK 293T cells medium by fresh medium (see table XI.1 to calculate the volume of medium needed).

- NIH 3T3 cells seeding:
    - Plate approximately $6x10^5$ cells (30% of confluence) in a 24-well culture tissue flat bottom plates in a final volume of 1 ml.

Day 8

- BM progenitors and NIH 3T3 cells retroviral transduction:
    - Collect retroviral supernatant of HEK 293T cells, filter through a 0.45 µm filter and separate 0.5 ml to transduce each well of NIH 3T3 cells.
    - For BM transduction replace 1.4 ml of BM media with 1.6 ml of retroviral supernatant supplemented with polybrene (hexadimethrine bromide; Sigma-Aldrich; #H9268) to a final concentration of 8 µg/ml. Only 1.4 ml of BM media is eliminated instead of 1.6 ml due to its usual evaporation. Final ratio of retroviral supernatant/conditioned media will be 80%/20%.
    - For NIH 3T3 cells, replace 0.5 ml of cells media with 0.5 ml of retroviral supernatant supplemented with polybrene to a final concentration of 8 µg/ml.
    - Centrifuge plates at 400 *g* at 33°C for 90 min (not seconds) to spin down the viruses.
    - Incubate cells in a humidifier incubator, 5% CO_2 at 37°C for two hours.
    - Eliminate 1 ml of supernatant and replace with 1 ml of fresh DMEM media supplemented with 20% FBS and 20% of WEHI and 20% of BHK/MKL supernatants.

Day 9

- Mouse irradiation:
  - Anaesthetize recipient animals with intraperitoneal injection of ketamine (75 mg/kg) and medetomidine (1 mg/kg).
  - Sublethally gamma-irradiate animals. Conditions: 900 rad administering 450 rad in bottom y-axis and 450 rad in top y-axis (1 Gy = 100 rad = 82.67 MU (monitor units); Dose rate: 240 MU/min; Collimator 35x35 in isocentric position).
  - Inject intraperitoneally 5 mg/kg of atipamezol and set animals near a heat source until recovered from anaesthesia.

- BM transduced cells recovery for mice injection
  - Recover BM supernatant in a 50 ml tube at 4°C.
  - Wash each well twice with sterile PBS 1X at 37°C collecting it in a 50 ml tube.
  - Add 1ml to each well of Cell Dissociation Buffer (Gibco #13151-014) or sterile PBS without and Ca^{2+} and Mg^{2+} and incubate cells 10 min 37°C.
  - Recover cells from all the previous steps in the 50 ml tube. Repeat cell dissociation step or/and use a cell scraper if necessary, in order to recover the majority of cells, and wash wells with sterile PBS.
  - Centrifuge cells at 400 *g* for 5 min at 4°C and resuspend cells in sterile PBS.
  - Count cells with Trypan Blue solution (at 1:1 ratio).
  - Centrifuge cells at 400 *g* for 5 min at 4°C and resuspend them in sterile physiologic saline solution in a suitable volume to inject intraperitoneally $7.5x10^5$ to $2x10^6$ cells per animal in a maximum volume of 200 µl.
  - Keep approximately 20 µl of cell suspension at 4°C to analyze transduction efficiency.

- NIH 3T3 cells recovery:
  - Eliminate supernatant of NIH 3T3 cells and collect cells by using a cell scraper.
  - Centrifuge cells at 400 *g* for 5 min at 4°C and resuspend cells in 100 µl of PBS 1X.

- Transduction efficiency assay: of NIH 3T3 and BM progenitor cells
  - Add 100 µl of 4% PFA solution (see recipe) to NIH 3T3 cells and 20 µl to BM cells.

- Evaluate cell transduction efficiency by analyzing GFP^+ cells percentage by cytometric analysis in a cytometer.

XI.- CYTOMETRIC ANALYSIS OF CELLULAR LYMPHOID SUBPOPULATIONS

Cytometric analysis constitutes a rapid and accurate technique to analyze different cellular populations by the presence of a specific surface or intracellular protein or to semi-quantitatively analyze the amount of a protein into the cells. With that purpose, cells must be isolated from tissues as single-cell suspension (Section XI.1) and stained with fluorochrome-conjugated antibody against surface or intracellular proteins (Sections XI.2, XI.3 and XI.4). Subsequently, the analysis must be performed by using a cytometer. In our case, all cytometric FACs analysis were performed in a FACSCalibur (BD Biosciences) using CellQuest software (Becton Dickinson) for data acquisition and FlowJo software (Tree Star Inc.) for data analysis.

It is very important to add all the appropriate controls to the analysis in order to obtain reliable results. These controls include non-stained controls (to discriminate the background of each cell type), the compensation controls (to allow the discrimination of the signal given by the single fluorochromes used) and the isotype controls (to discriminate the specific and the non-specific signal of the antibody).

XI.1.- Isolation of lymphocytes cells from lymphoid tissues

Sacrifice animals by cervical dislocation or overdose of CO2 and isolate thymus, lymph nodes (maxillary, axillar and inguinal) and spleen organs (see figure XI.1A) from adult mice (8-12 weeks) using appropriate surgical sterilized material. For isolation of fetal thymus and liver, place embryos in a P100 plate with PBS and decapitate them. Open the chest of the embryo by using forceps and collect the fetal thymus and liver (see figure XI.1B). Collect the organs in a 1.5 ml tube containing RPMI supplemented with 10% FBS and keep on ice.

To isolate lymphoid cells, force the lymphoid organs through a 70 µm nylon mesh and collect the suspension in RPMI supplemented with 10% FBS. Perform all centrifugations at 700 *g* at 4°C for 5 min and keep cells on ice to reduce cell death. Splenocytes are incubated in 1 ml of erythrocytes lysis buffer (see recipe) for 10 min at RT, dilute with 3 ml of PBS and wash them twice by centrifugation with PBS supplemented with 5% of FBS. In case of using peripheral blood, lyse erythrocytes in 5 ml and do not dilute sample before centrifugation. Dilute cells in RPMI supplemented with 10% FBS to a final volume of 1 ml in case lymph node cells and to a final volume of 6 ml in case of thymocytes and splenocytes. Count cells with

Trypan Blue Solution (at 1:1 ratio). Cells are then ready for surface and intracellular protein staining (Section XI.2) or for stimulation and intracellular phosphomolecules staining (Section XI.3). Subsequently, perform the cytometric analysis.

A

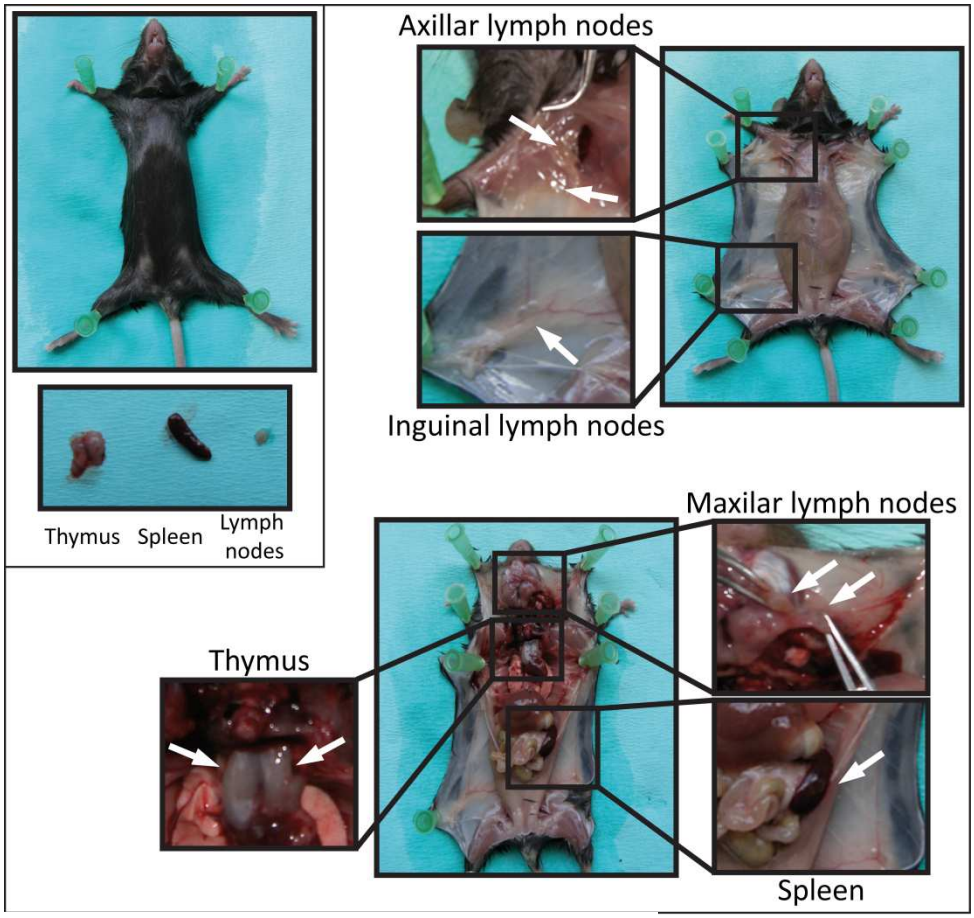

B

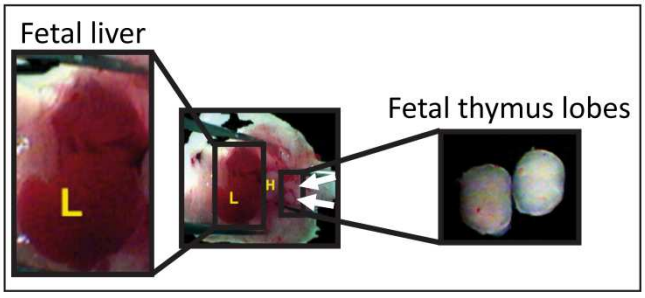

Figure XI.1. Mouse lymphoid organs dissection. A) Extraction of lymphoid organs from adult mice. B) Extraction of lymphoid organ from mice embryos. L, liver; H, heart. Figure B adapted from Anderson and Jenkinson, 2007.

XI.2.- Analysis of lymphocyte populations by surface and intracelular markers staining

For staining of surface molecules, seed $3x10^6$ lymphoid cells in a 96-well V-Bottom plate, wash with FACS buffer (see recipe) and centrifuge at 700 *g* for 5 min at 4°C. Resuspend cells in specific fluorescence-conjugated antibodies (see supplementary table 2A in article 2 in results chapter) diluted in FACS buffer and incubate for 30 min at RT, protected from light. Wash cells twice with FACS buffer and resuspend cells with 4% PFA solution (see recipe). Keep at 4°C and protected from light until cytometric analysis.

For staining of intracellular FoxP3 protein, permeabilize previously $3x10^6$ lymphoid cells with freshly prepared Fix/Perm solution 1X (eBiosciences; #00-5521-00) for 3 h in the dark (manufacturer's protocol indicate that incubation can be performed from 30 min up to 18h). Wash twice with FACS buffer by centrifugation and stain with fluorescence-conjugated antibodies against surface and FoxP3 molecules as described above.

XI.4.- Stimulation of cells and analysis of intracellular phosphoproteins

For stimulation of cells and intracellular staining of phosphomolecules, distribute $3x10^6$ cells per each staining to be performed in cytometry tubes. Temperate cells to RT and stimulate cells in RPMI media without FBS at 37°C, following the conditions indicated in supplementary table 2A in article 2 in results chapter.

After stimulation, add 1 volume of pre-warmed freshly prepared 1X Lyse/Fix solution (BD Biosciences; #558049) to the cells and incubate 10 min at 37°C. Wash cells with PBS 1X (see 10X recipe) by centrifugation and permeabilize for 20 min at 4°C with ice cold PermBuffer II (BD Biosciences; #558052). Wash twice with FACS buffer (see recipe), seed cells in a 96-well V-Bottom plate and block with 0.025 mg/ml of human IgG (Sigma Aldrich; #I-4506) diluted in FACS buffer at 4°C for 30 min. Wash twice with FACS buffer and resuspend with specific unconjugated anti-phospho-primary antibodies (see supplementary table 2A in article 2 in results chapter) diluted in FACS buffer and incubate for 30 min at 4°C. Wash twice with FACS buffer and resuspend with fluorescence-conjugated antibodies against surface markers (see supplementary table 2A in article 2 in results chapter) and secondary anti-rabbit AlexaFluor 467 (Life Technologies; #A-21245) diluted in FACS buffer. Incubate for 30 min at 4°C protected from light. After washing with PBS 1X by centrifugation, resuspend with 0.25% PFA solution (see recipe). Keep at 4°C and protected from light until cytometric analysis.

XII.- COMMON LABORATORY SOLUTIONS AND BUFFERS

XII.1- General buffers

PBS (Phosphate Buffered Saline) (10X)

8% (w/v) NaCl
0.2% (w/v) KCl
1.15% (w/v) $Na_2HPO_4 \cdot 7H_2O$
0.2% (w/v) KH_2PO_4
Dissolve in distilled water

When diluted to 1X or 2X, adjust pH to 7.4 by adding 1 N HCl if necessary

TBS (Tris Buffered Saline) (10X)

1 M Tris-HCl, pH 7.5
1.5 M NaCl
Adjust with distilled water

Store at RT

XII.2.- Solutions for bacterial manipulation

LB (Luria Bertani) medium and LB-agar plates

1% (w/v) tryptone
0.5% (w/v) yeast extract
1% (w/v) NaCl
0.1% (v/v) 1N NaOH
Adjust with distilled water
Autoclave and store at RT or 4°C if containing antibiotics

To prepare agar plates: add 1.5% (w/v) agar to LB medium prior to autoclaving

SOB (Super Optimal Broth) medium

2% (w/v) Bacto Tryptone
0.5% (w/v) yeast extract
10 mM NaCl
2.5 mM KCl
Adjust with distilled water
Autoclave and cool down to RT

Add $MgCl_2$ from a 1 M filtered stock solution (prepared in water) to a final concentration of 10 mM just before use

Store at 4°C

SOC medium

Add to SOB medium (see recipe above) glucose from a 1 M filtered stock-solution (prepared in water) to a final concentration of 20 mM before use.

Store sterile at 4°C

2xYP medium

2% (w/v) Yeast extract
4% (w/v) Peptone
Dissolve in distilled water
Autoclave and cool down to RT
Add glucose from a 20% (w/v) filtered stock solution (prepared in distilled water) to a final concentration of 2% (v/v)

Store at 4°C

$CaCl_2$ solution for preparation of XL1-Blue competent bacteria

10 mM PIPES
60 mM $CaCl_2$
15% (v/v) Glycerol
Adjust with Milli-Q water
Sterilize by filtration at 0.22 µm

Store at 4°C

FSB (Frozen Storage Buffer) solution for preparation of Rosetta2 competent bacteria

0.89% (w/v) $MnCl_2 \cdot 4H_2O$
0.15% (w/v) $CaCl_2 \cdot 2H_2O$
0.74% (w/v) KCl
0.08% (w/v) $HACoCl_3$ (Hexammine cobalt chloride)
10% (v/v) glycerol
1% (v/v) from a 1 M potassium acetate solution (see recipe below)

Dissolve in Milli-Q water
Adjust pH to 6.4 with 0.1 N HCl
Adjust with Milli-Q water
Sterilize by filtration at 0.22 µm

Store at 4°C

Potassium acetate solution (1 M; 100 ml)

Dissolve 9.8 g of KCH_3CO_2 (potassium acetate) in 90 ml of distilled water
Adjust pH to 7.5 with 2 M acetic acid
Adjust with Milli-Q water to a final volume of 100 ml
Dispense in 10 ml aliquots and store at -20°C

IPTG solution (100 mM; 50 ml)

Dissolve 1.2 g of IPTG (Isopropil-β-D-1-tiogalactopiranósido, Sigma; # I5502) in a 50 ml of distilled water
Sterilize by filtration at 0.22 µm

Store at -20°C

X-Gal

Dissolve X-gal (Sigma; #B4252) in N,N´-dimethylformamide to a final concentration of 50 mg/ml

Store at -20°C and protect from light
When spread over LB-agar plates, allowed to absorb for 10 minutes at RT prior to use.

Antibiotics

Store at -20°C

Table XII.1.- ANTIBIOTICS FOR BACTERIAL CELL CULTURE

ANTIBIOTIC	STOCK CONCENTRATION	DILUENT	WORKING CONCENTRATION
Ampicillin	100 µg/ml	H_2O	100 ng/ml
Chloramphenicol	170 µg/ml	100% EtOH	170 ng/ml
Kanamycin	50 µg/ml	Water	50 ng/ml
Tetracycline	50 µg/ml	100% EtOH	50 ng/ml

Table XII.2. Antibiotics used for bacterial cell culture

When antibiotics are added to liquid bacterial growth medium, add after the medium has been autoclaved and cooled at least to 50°C.
When spread over LB-agar plates, allowed to absorb for 10 minutes at RT prior to plate use.

XII.3.- Solutions for mammalian cells manipulation

Erythrocytes Lysis Buffer

155 mM NH_4Cl
10 mM $NaHCO_3$
0.1 mM EDTA
Adjust with Milli-Q water

Store at RT

HeBBS buffer for mammalian cells transfection (2x)

0.28 M NaCl
0.05 M HEPES (Sigma; #H3375)
1.5 mM Na_2HPO_4
Adjust with Milli-Q water
Adjust pH to a range between 6.95 and 7.12 with 1 N NaOH, increasing pH of 0.02
Filter through a 0.22 µm

Store at 4°C for short-term storage and at -20°C for long-term storage
Test different pH for optimal transfection efficiency

4% PFA (Paraformaldehid) solution [500 ml]

Paraformaldehyde fumes are very toxic. Heating must be performed in a fume hood.

Add 20 g of paraformaldehyde to 300 ml PBS 1X (see recipe above)
Heat to 55° - 60°C
Slowly add 1 N NaOH drop-wise until the solution becomes clear (approximately 1 ml)
Cool down to RT
Adjust to pH 7.2 with 1 N NaOH
Adjust with PBS 1X

Adjust (if necessary) to pH 7.2 with 1 N NaOH

Store at 4°C for short-term storage and at -20°C for long-term storage
To obtain 0.25% or other desired concentration, dilute 4% PFA solution stock in ice cold PBS 1X (see recipe above).

FACs buffer

5% (v/v) FBS (fetal bovine serum)
0.02% (v/v) from a 1M sodium azide (NaN_3) solution prepared in distilled water
Adjust with PBS 1X (see recipe above)

Store at 4°C
NaN_3 is very toxic and must be handled with gloves. NaN_3 serves as preservative and also impedes the coating of antibodies, reducing the background.

XII.4.- Solutions for DNA analysis

DNA loading buffer (6X)

0.25% (w/v) bromophenol blue
0.25% (w/v) xylene cyanol FF
30% (v/v) glycerol
Adjust with distilled water

Store at 4°C

TBE (Tris/Boric Acid/EDTA) Buffer (10x)

890 mM Tris base
890 mM Boric Acid
4% (v/v) of 0.5 M of EDTA solution, pH 8.0
Adjust with distilled water

Store at 4°C

XII.5.-Solutions for protein analysis

Bacterial Lysis Buffer

5 mM DTT
2 mM $MgCl_2$

1 mM EGTA
2 µg/ml Aprotinin
2 µg/ml Leupeptin
2 mM of phenylmethylsulfonyl fluoride (PMSF)
10 µg/ml DNAase I
1 mg/ml Lysozime
Adjust with PBS 2X

Prepare just before use and keep on ice

RIPA-like lysis buffer for mammalian cells

50 mM Tris-HCl pH 7.5
150 mM NaCl
2 mM EGTA
1% Triton X-100
0.5% (w/v) sodium deoxycholate
0.1% (v/v) SDS (From a 20% (w/v) stock-solution)
1 mM PMSF
Adjust with Milli-Q water

Prepare just before use and keep on ice

IGEPAL-based lysis buffer for mammalian cells

50 mM Tris-HCl, pH 7.5
100 mM NaCl
2 mM $CaCl_2$
1 mM DTT
2 mM PMSF
1 mM Sodium Orthovanadate
1% (v/v) NP-40 (IGEPAL® CA-630. Sigma; # I3021)
Protease and phosphatase inhibitor cocktails (Roche)
Adjust with Milli-Q water

Prepare just before use and keep on ice

Protein loading buffer – Laemmli buffer (6X)

70% (v/v) 4xTris-HCl/SDS pH 6.8 solution (see recipe below)
30% (v/v) glycerol
10% (w/v) SDS

9.3% (w/v) DTT
0.012% (w/v) bromophenol blue
Adjust with Milli-Q water

Store in 0.5 ml aliquots at -20°C

4xTris-HCl/SDS, pH 6.8 solution (0.5 M Tris-HCl containing 0.4% SDS) [500ml]

Dissolve 30.3 g Tris base in 300 ml distilled water
Adjust to pH 6.8 with 1 N HCl
Adjust with distilled water
Add 2 g SDS

Store at RT

4xTris-HCl/SDS, pH 8.8 solution (1.5 M Tris-HCl containing 0.4% SDS) [500ml]

Dissolve 91 g Tris base in 300 ml distilled water
Adjust to pH 8.8 with 1 N HCl
Adjust with distilled water
Add 2 g SDS

Store at RT

Electrophoresis running buffer (5X)

125 mM Tris base
960 mM glycine
17 mM SDS (it is recommended to add SDS from a 20% (w/v) solution in a final concentration of 0.5% (v/v))
Adjust with distilled water

Store at RT
Use at 1X in distilled water

Transfer buffer (10X)

250 mM Tris base
1.92 M glycine
Adjust with distilled water

Store at RT
Use at 1X in 20% (v/v) EtOH solution. For PVDF membranes, use 20% (v/v) MeOH solution.

Coomassie Blue Staining Solution

0.025% (w/v) Coomassie Brilliant Blue R-250 (BioRad; #161-0400)
40% (v/v) MeOH
7% (v/v) acetic acid
Adjust with distilled water

Store at RT

Coomassie Blue Destaining Solution

40% (v/v) MeOH
10% (v/v) acetic acid
Adjust with distilled water

Store at RT

Ponceau-S Staining Solution

0.5% (w/v) Ponceau-S Red (Sigma; #P3504)
1% (v/v) **glacial** acetic acid
Adjust with distilled water

Store at RT.

TBS-T (Tris Buffered Saline-Tween) 0.1%

Add 0.1% (v/v) Tween 20 (Sigma; #P1379) to TBS 1X (see recipe above)

Store at 4°C

Blocking Solution

1% (w/v) Bovine Albumin Fraction V (Sigma; # A7906)
0.05% (v/v) from a 1M sodium azide (NaN_3) solution prepared in distilled water
Dilute in TBS 1X (see recipe)

NaN_3 it is very toxic and must be handled with gloves. NaN_3 serves as preservative and also impedes the coating of antibodies, reducing the

background; however, it can inhibit HRP (horse rabbit peroxidase) present on some secondary antibodies.

Luminol solution

Luminol solution should be prepared immediately before use by mixing Luminol Stock Solution and Enhancer Solution at 1X.

Luminol Stock-Solution [500 ml]

32.25 ml of 1.5 M Tris-HCl, pH 8.8
125 mg Luminol sodium salt (Sigma; #A4685)
155 µl of 30% H_2O_2 solution
Adjust with Milli-Q water
Store at 4°C and protect from light

Enhancer Solution [100X; 50 ml]

27.5 mg p-coumaric acid (Sigma; #C9008)
25 ml DMSO
Adjust with Milli-Q water
Store at RT and protect from light

AUXILIARY BIBLIOGRAPHY

Abbasi, S., Lee, J.D., Su, B., Chen, X., Alcon, J.L., Yang, J., Kellems, R.E. and Xia, Y. **Protein kinase-mediated regulation of calcineurin through the phosphorylation of modulatory calcineurin-interacting protein 1**. (2006) *J Biol Chem* 281 pp. 7717-26.

Abbasi, S., Su, B., Kellems, R.E., Yang, J. and Xia, Y. **The essential role of MEKK3 signaling in angiotensin II-induced calcineurin/nuclear factor of activated T-cells activation**. (2005) *J Biol Chem* 280 pp. 36737-46.

Abraham, S.N. and St John, A.L. **Mast cell-orchestrated immunity to pathogens**. (2010) *Nat Rev Immunol* 10 pp. 440-52.

Adachi, S. and Iwata, M. **Duration of calcineurin and Erk signals regulates CD4/CD8 lineage commitment of thymocytes**. (2002) *Cell Immunol* 215 pp. 45-53.

Alberola-Ila, J., Forbush, K.A., Seger, R., Krebs, E.G. and Perlmutter, R.M. **Selective requirement for MAP kinase activation in thymocyte differentiation**. (1995) *Nature* 373 pp. 620-3.

Amasaki, Y., Adachi, S., Ishida, Y., Iwata, M., Arai, N., Arai, K. and Miyatake, S. **A constitutively nuclear form of NFATx shows efficient transactivation activity and induces differentiation of CD4(+)CD8(+) T cells**. (2002) *J Biol Chem* 277 pp. 25640-8.

Amasaki, Y., Miyatake, S., Arai, N. and Arai, K. **Regulation of nuclear factor of activated T-cell family transcription factors during T-cell development in the thymus**. (2000) *J Allergy Clin Immunol* 106 pp. S1-9.

Andersen, C.L., Jensen, J.L. and Orntoft, T.F. **Normalization of real-time quantitative reverse transcription-PCR data: a model-based variance estimation approach to identify genes suited for normalization, applied to bladder and colon cancer data sets**. (2004) *Cancer Res* 64 pp. 5245-50.

Anderson, G. and Jenkinson, E.J. **Lymphostromal interactions in thymic development and function**. (2001) *Nat Rev Immunol* 1 pp. 31-40.

Anderson, G. and Jenkinson, E.J. **Fetal thymus organ culture**. (2007) *CSH Protoc* 2007 p. pdb prot4808.

Anderton, S.M. and Wraith, D.C. **Selection and fine-tuning of the autoimmune T-cell repertoire**. (2002) *Nat Rev Immunol* 2 pp. 487-98.

Antequera, F. **Structure, function and evolution of CpG island promoters**. (2003) *Cell Mol Life Sci* 60 pp. 1647-58.

Aramburu, J., Garcia-Cozar, F., Raghavan, A., Okamura, H., Rao, A. and Hogan, P.G. **Selective inhibition of NFAT activation by a peptide spanning the calcineurin targeting site of NFAT**. (1998) *Mol Cell* 1 pp. 627-37.

Aramburu, J., Heitman, J. and Crabtree, G.R. **Calcineurin: a central controller of signalling in eukaryotes**. (2004) *EMBO Rep* 5 pp. 343-8.

Aramburu, J., Rao, A. and Klee, C.B. **Calcineurin: from structure to function**. (2000) *Curr Top Cell Regul* 36 pp. 237-95.

Aramburu, J., Yaffe, M.B., Lopez-Rodriguez, C., Cantley, L.C., Hogan, P.G. and Rao, A. **Affinity-driven peptide selection of an NFAT inhibitor more selective than cyclosporin A**. (1999) *Science* 285 pp. 2129-33.

Asada, S., Ikeda, A., Nagao, R., Hama, H., Sudo, T., Fukamizu, A., Kasuya, Y. and Kishi, T. **Oxidative stress-induced ubiquitination of RCAN1 mediated by SCFbeta-TrCP ubiquitin ligase**. (2008) *Int J Mol Med* 22 pp. 95-104.

Ashton-Rickardt, P.G. and Tonegawa, S. **A differential-avidity model for T-cell selection**. (1994) *Immunol Today* 15 pp. 362-6.

Aubareda, A., Mulero, M.C. and Perez-Riba, M. **Functional characterization of the calcipressin 1 motif that suppresses calcineurin-mediated NFAT-dependent cytokine gene expression in human T cells**. (2006) *Cell Signal* 18 pp. 1430-8.

Avraham, A., Jung, S., Samuels, Y., Seger, R. and Ben-Neriah, Y. **Co-stimulation-dependent activation of a JNK-kinase in T lymphocytes**. (1998) *Eur J Immunol* 28 pp. 2320-30.

Azzam, H.S., DeJarnette, J.B., Huang, K., Emmons, R., Park, C.S., Sommers, C.L., El-Khoury, D., Shores, E.W. and Love, P.E. **Fine tuning of TCR signaling by CD5**. (2001) *J Immunol* 166 pp. 5464-72.

Baek, K.H., Zaslavsky, A., Lynch, R.C., Britt, C., Okada, Y., Siarey, R.J., Lensch, M.W., Park, I.H., Yoon, S.S., Minami, T., Korenberg, J.R., Folkman, J., Daley, G.Q., Aird, W.C., Galdzicki, Z. and Ryeom, S. **Down's syndrome suppression of tumour growth and the role of the calcineurin inhibitor DSCR1**. (2009) *Nature* 459 pp. 1126-30.

Bai, L. and Morozov, A.V. **Gene regulation by nucleosome positioning**. (2010) *Trends Genet* 26 pp. 476-83.

Barker, K.S., Liu, T. and Rogers, P.D. **Coculture of THP-1 human mononuclear cells with Candida albicans results in pronounced changes in host gene expression**. (2005) *J Infect Dis* 192 pp. 901-12.

Barton, K., Muthusamy, N., Chanyangam, M., Fischer, C., Clendenin, C. and Leiden, J.M. **Defective thymocyte proliferation and IL-2 production in transgenic mice expressing a dominant-negative form of CREB**. (1996) *Nature* 379 pp. 81-5.

Bassett, J.H., Logan, J.G., Boyde, A., Cheung, M.S., Evans, H., Croucher, P., Sun, X.Y., Xu, S., Murata, Y. and Williams, G.R. **Mice lacking the calcineurin inhibitor Rcan2 have an isolated defect of osteoblast function**. (2012) *Endocrinology* 153 pp. 3537-48.

Bauerfeind, R., Takei, K. and De Camilli, P. **Amphiphysin I is associated with coated endocytic intermediates and undergoes stimulation-dependent dephosphorylation in nerve terminals**. (1997) *J Biol Chem* 272 pp. 30984-92.

Bell, J.J. and Bhandoola, A. **The earliest thymic progenitors for T cells possess myeloid lineage potential**. (2008) *Nature* 452 pp. 764-7.

Beschorner, W.E., Namnoum, J.D., Hess, A.D., Shinn, C.A. and Santos, G.W. **Cyclosporin A and the thymus. Immunopathology**. (1987) *Am J Pathol* 126 pp. 487-96.

Bettelli, E., Dastrange, M. and Oukka, M. **Foxp3 interacts with nuclear factor of activated T cells and NF-kappa B to repress cytokine gene expression and effector functions of T helper cells**. (2005) *Proc Natl Acad Sci U S A* 102 pp. 5138-43.

Beyer, M. and Schultze, J.L. **Regulatory T cells in cancer**. (2006) *Blood* 108 pp. 804-11.

Bhoiwala, D.L., Kannabiran, V., Hushmendy, S.F., Hahn, A., Heuring, J.M. and Crawford, D.R. **The calcineurin inhibitor RCAN1 is involved in cultured macrophage and in vivo immune response**. (2011) *FEMS Immunol Med Microbiol* 61 pp. 103-13.

Biron, C.A. and Brossay, L. **NK cells and NKT cells in innate defense against viral infections**. (2001) *Curr Opin Immunol* 13 pp. 458-64.

Biselli, R., Matricardi, P.M., D'Amelio, R. and Fattorossi, A. **Multiparametric flow cytometric analysis of the kinetics of surface molecule expression after polyclonal activation of human peripheral blood T lymphocytes**. (1992) *Scand J Immunol* 35 pp. 439-47.

Biswas, G., Anandatheerthavarada, H.K., Zaidi, M. and Avadhani, N.G. **Mitochondria to nucleus stress signaling: a distinctive mechanism of NFkappaB/Rel activation through calcineurin-mediated inactivation of IkappaBbeta**. (2003) *J Cell Biol* 161 pp. 507-19.

Blackburn, C.C. and Manley, N.R. **Developing a new paradigm for thymus organogenesis**. (2004) *Nat Rev Immunol* 4 pp. 278-89.

Bluestone, J.A., Khattri, R., Sciammas, R. and Sperling, A.I. **TCR gamma delta cells: a specialized T-cell subset in the immune system**. (1995) *Annu Rev Cell Dev Biol* 11 pp. 307-53.

Bollyky, P.L., Falk, B.A., Long, S.A., Preisinger, A., Braun, K.R., Wu, R.P., Evanko, S.P., Buckner, J.H., Wight, T.N. and Nepom, G.T. **CD44 costimulation promotes FoxP3+ regulatory T cell persistence and function via production of IL-2, IL-10, and TGF-beta**. (2009) *J Immunol* 183 pp. 2232-41.

Bopp, T., Palmetshofer, A., Serfling, E., Heib, V., Schmitt, S., Richter, C., Klein, M., Schild, H., Schmitt, E. and Stassen, M. **NFATc2 and NFATc3 transcription factors play a crucial role in suppression of CD4+ T lymphocytes by CD4+ CD25+ regulatory T cells**. (2005) *J Exp Med* 201 pp. 181-7.

Bouillet, P., Purton, J.F., Godfrey, D.I., Zhang, L.C., Coultas, L., Puthalakath, H., Pellegrini, M., Cory, S., Adams, J.M. and Strasser, A. **BH3-only Bcl-2 family member Bim is required for apoptosis of autoreactive thymocytes**. (2002) *Nature* 415 pp. 922-6.

Bromley, S.K., Burack, W.R., Johnson, K.G., Somersalo, K., Sims, T.N., Sumen, C., Davis, M.M., Shaw, A.S., Allen, P.M. and Dustin, M.L. **The immunological synapse**. (2001) *Annu Rev Immunol* 19 pp. 375-96.

Budd, R.C., Cerottini, J.C., Horvath, C., Bron, C., Pedrazzini, T., Howe, R.C. and MacDonald, H.R. **Distinction of virgin and memory T lymphocytes. Stable acquisition of the Pgp-1 glycoprotein concomitant with antigenic stimulation**. (1987) *J Immunol* 138 pp. 3120-9.

Bueno, O.F., Brandt, E.B., Rothenberg, M.E. and Molkentin, J.D. **Defective T cell development and function in calcineurin A beta -deficient mice**. (2002) *Proc Natl Acad Sci U S A* 99 pp. 9398-403.

Calnan, B.J., Szychowski, S., Chan, F.K., Cado, D. and Winoto, A. **A role for the orphan steroid receptor Nur77 in apoptosis accompanying antigen-induced negative selection**. (1995) *Immunity* 3 pp. 273-82.

Cameron, A.M., Steiner, J.P., Roskams, A.J., Ali, S.M., Ronnett, G.V. and Snyder, S.H. **Calcineurin associated with the inositol 1,4,5-trisphosphate receptor-FKBP12 complex modulates Ca2+ flux**. (1995) *Cell* 83 pp. 463-72.

Canaider, S., Facchin, F., Griffoni, C., Casadei, R., Vitale, L., Lenzi, L., Frabetti, F., D'Addabbo, P., Carinci, P., Zannotti, M. and Strippoli, P. **Proteins encoded by**

human Down syndrome critical region gene 1-like 2 (DSCR1L2) mRNA and by a novel DSCR1L2 mRNA isoform interact with cardiac troponin I (TNNI3). (2006) *Gene* 372 pp. 128-36.

Cante-Barrett, K., Gallo, E.M., Winslow, M.M. and Crabtree, G.R. **Thymocyte negative selection is mediated by protein kinase C- and Ca2+-dependent transcriptional induction of bim [corrected]**. (2006) *J Immunol* 176 pp. 2299-306.

Cante-Barrett, K., Winslow, M.M. and Crabtree, G.R. **Selective role of NFATc3 in positive selection of thymocytes**. (2007) *J Immunol* 179 pp. 103-10.

Cantrell, D.A. **T-cell antigen receptor signal transduction**. (2002) *Immunology* 105 pp. 369-74.

Cao, X., Kambe, F., Miyazaki, T., Sarkar, D., Ohmori, S. and Seo, H. **Novel human ZAKI-4 isoforms: hormonal and tissue-specific regulation and function as calcineurin inhibitors**. (2002) *Biochem J* 367 pp. 459-66.

Cao, X., Kambe, F., Moeller, L.C., Refetoff, S. and Seo, H. **Thyroid hormone induces rapid activation of Akt/protein kinase B-mammalian target of rapamycin-p70S6K cascade through phosphatidylinositol 3-kinase in human fibroblasts**. (2005) *Mol Endocrinol* 19 pp. 102-12.

Casas, C., Martinez, S., Pritchard, M.A., Fuentes, J.J., Nadal, M., Guimera, J., Arbones, M., Florez, J., Soriano, E., Estivill, X. and Alcantara, S. **Dscr1, a novel endogenous inhibitor of calcineurin signaling, is expressed in the primitive ventricle of the heart and during neurogenesis**. (2001) *Mech Dev* 101 pp. 289-92.

Cornetta, K., Pollok, K.E. and Miller, A.D. **Retroviral vectors for gene transfer**. (2008) *CSH Protoc* 2008 p. pdb top29.

Cousin, M.A. and Robinson, P.J. **The dephosphins: dephosphorylation by calcineurin triggers synaptic vesicle endocytosis**. (2001) *Trends Neurosci* 24 pp. 659-65.

Crabtree, G.R. and Clipstone, N.A. **Signal transmission between the plasma membrane and nucleus of T lymphocytes**. (1994) *Annu Rev Biochem* 63 pp. 1045-83.

Crabtree, G.R. and Olson, E.N. **NFAT signaling: choreographing the social lives of cells**. (2002) *Cell* 109 Suppl pp. S67-79.

Crawford, D.R., Leahy, K.P., Abramova, N., Lan, L., Wang, Y. and Davies, K.J. **Hamster adapt78 mRNA is a Down syndrome critical region homologue that is inducible by oxidative stress**. (1997) *Arch Biochem Biophys* 342 pp. 6-12.

Cui, Y.Z., Hisha, H., Yang, G.X., Fan, T.X., Jin, T., Li, Q., Lian, Z. and Ikehara, S. **Optimal protocol for total body irradiation for allogeneic bone marrow transplantation in mice**. (2002) *Bone Marrow Transplant* 30 pp. 843-9.

Cummins, P. and Perry, S.V. **Troponin I from human skeletal and cardiac muscles**. (1978) *Biochem J* 171 pp. 251-9.

Chan, B., Greenan, G., McKeon, F. and Ellenberger, T. **Identification of a peptide fragment of DSCR1 that competitively inhibits calcineurin activity in vitro and in vivo**. (2005) *Proc Natl Acad Sci U S A* 102 pp. 13075-80.

Chandok, M.R. and Farber, D.L. **Signaling control of memory T cell generation and function**. (2004) *Semin Immunol* 16 pp. 285-93.

Chao, D.L., Davenport, M.P., Forrest, S. and Perelson, A.S. **The effects of thymic selection on the range of T cell cross-reactivity**. (2005) *Eur J Immunol* 35 pp. 3452-9.

Chen, W., Jin, W., Hardegen, N., Lei, K.J., Li, L., Marinos, N., McGrady, G. and Wahl, S.M. **Conversion of peripheral CD4+CD25- naive T cells to CD4+CD25+ regulatory T cells by TGF-beta induction of transcription factor Foxp3**. (2003) *J Exp Med* 198 pp. 1875-86.

Chen, W. and Konkel, J.E. **TGF-beta and 'adaptive' Foxp3(+) regulatory T cells**. (2010) *J Mol Cell Biol* 2 pp. 30-6.

Chinnasamy, D., Milsom, M.D., Shaffer, J., Neuenfeldt, J., Shaaban, A.F., Margison, G.P., Fairbairn, L.J. and Chinnasamy, N. **Multicistronic lentiviral vectors containing the FMDV 2A cleavage factor demonstrate robust expression of encoded genes at limiting MOI**. (2006) *Virol J* 3 p. 14.

Cho, K.O., Kim, Y.S., Cho, Y.J. and Kim, S.Y. **Upregulation of DSCR1 (RCAN1 or Adapt78) in the peri-infarct cortex after experimental stroke**. (2008) *Exp Neurol* 212 pp. 85-92.

Cho, Y.J., Abe, M., Kim, S.Y. and Sato, Y. **Raf-1 is a binding partner of DSCR1**. (2005) *Arch Biochem Biophys* 439 pp. 121-8.

Choi, J.M., Sohn, J.H., Park, T.Y., Park, J.W. and Lee, S.K. **Cell permeable NFAT inhibitory peptide Sim-2-VIVIT inhibits T-cell activation and alleviates allergic airway inflammation and hyper-responsiveness**. (2012) *Immunol Lett* 143 pp. 170-6.

Dahl, S.C., Handler, J.S. and Kwon, H.M. **Hypertonicity-induced phosphorylation and nuclear localization of the transcription factor TonEBP**. (2001) *Am J Physiol Cell Physiol* 280 pp. C248-53.

Dai, Y., Walker, S.A., de Vet, E., Cook, S., Welch, H.C. and Lockyer, P.J. **Ca2+-dependent monomer and dimer formation switches CAPRI Protein between Ras GTPase-activating protein (GAP) and RapGAP activities**. (2011) *J Biol Chem* 286 pp. 19905-16.

Daniels, M.A., Teixeiro, E., Gill, J., Hausmann, B., Roubaty, D., Holmberg, K., Werlen, G., Hollander, G.A., Gascoigne, N.R. and Palmer, E. **Thymic selection threshold defined by compartmentalization of Ras/MAPK signalling**. (2006) *Nature* 444 pp. 724-9.

Davies, K.J., Ermak, G., Rothermel, B.A., Pritchard, M., Heitman, J., Ahnn, J., Henrique-Silva, F., Crawford, D., Canaider, S., Strippoli, P., Carinci, P., Min, K.T., Fox, D.S., Cunningham, K.W., Bassel-Duby, R., Olson, E.N., Zhang, Z., Williams, R.S., Gerber, H.P., Perez-Riba, M., Seo, H., Cao, X., Klee, C.B., Redondo, J.M., Maltais, L.J., Bruford, E.A., Povey, S., Molkentin, J.D., McKeon, F.D., Duh, E.J., Crabtree, G.R., Cyert, M.S., de la Luna, S. and Estivill, X. **Renaming the DSCR1/Adapt78 gene family as RCAN: regulators of calcineurin**. (2007) *FASEB J* 21 pp. 3023-8.

Davis, A.P., King, B.L., Mockus, S., Murphy, C.G., Saraceni-Richards, C., Rosenstein, M., Wiegers, T. and Mattingly, C.J. **The Comparative Toxicogenomics Database: update 2011**. (2011) *Nucleic Acids Res* 39 pp. D1067-72.

Dawson, T.M., Steiner, J.P., Dawson, V.L., Dinerman, J.L., Uhl, G.R. and Snyder, S.H. **Immunosuppressant FK506 enhances phosphorylation of nitric oxide synthase and protects against glutamate neurotoxicity**. (1993) *Proc Natl Acad Sci U S A* 90 pp. 9808-12.

de la Luna, S. and Estivill, X. **Cooperation to amplify gene-dosage-imbalance effects**. (2006) *Trends Mol Med* 12 pp. 451-4.

Dierssen, M., Arque, G., McDonald, J., Andreu, N., Martinez-Cue, C., Florez, J. and Fillat, C. **Behavioral characterization of a mouse model overexpressing DSCR1/ RCAN1**. (2011) *PLoS One* 6 p. e17010.

Djuretic, I.M., Cruz-Guilloty, F. and Rao, A. **Regulation of gene expression in peripheral T cells by Runx transcription factors**. (2009) *Adv Immunol* 104 pp. 1-23.

Doetschman, T., Sholl, A., Chen, H., Gard, C., Hildeman, D.A. and Bommireddy, R. **Divergent effects of calcineurin Abeta on regulatory and conventional T-cell homeostasis**. (2011) *Clin Immunol* 138 pp. 321-30.

Dong, C., Yang, D.D., Wysk, M., Whitmarsh, A.J., Davis, R.J. and Flavell, R.A. **Defective T cell differentiation in the absence of Jnk1**. (1998) *Science* 282 pp. 2092-5.

Dougherty, M.K., Ritt, D.A., Zhou, M., Specht, S.I., Monson, D.M., Veenstra, T.D. and Morrison, D.K. **KSR2 is a calcineurin substrate that promotes ERK cascade activation in response to calcium signals**. (2009) *Mol Cell* 34 pp. 652-62.

Drexler, H.G. and Uphoff, C.C. **Mycoplasma contamination of cell cultures: Incidence, sources, effects, detection, elimination, prevention**. (2002) *Cytotechnology* 39 pp. 75-90.

Dykstra, M., Cherukuri, A., Sohn, H.W., Tzeng, S.J. and Pierce, S.K. **Location is everything: lipid rafts and immune cell signaling**. (2003) *Annu Rev Immunol* 21 pp. 457-81.

Dzierzak, E. **The emergence of definitive hematopoietic stem cells in the mammal**. (2005) *Curr Opin Hematol* 12 pp. 197-202.

Erb, K.J., Twardzik, T., Palmetshofer, A., Wohlleben, G., Tatsch, U. and Serfling, E. **Mice deficient in nuclear factor of activated T-cell transcription factor c2 mount increased Th2 responses after infection with Nippostrongylus brasiliensis and decreased Th1 responses after mycobacterial infection**. (2003) *Infect Immun* 71 pp. 6641-7.

Ermak, G., Harris, C.D. and Davies, K.J. **The DSCR1 (Adapt78) isoform 1 protein calcipressin 1 inhibits calcineurin and protects against acute calcium-mediated stress damage, including transient oxidative stress**. (2002) *Faseb J* 16 pp. 814-24.

Ermak, G., Hench, K.J., Chang, K.T., Sachdev, S. and Davies, K.J. **Regulator of calcineurin (RCAN1-1L) is deficient in Huntington disease and protective against mutant huntingtin toxicity in vitro**. (2009) *J Biol Chem* 284 pp. 11845-53.

Ermak, G., Morgan, T.E. and Davies, K.J. **Chronic overexpression of the calcineurin inhibitory gene DSCR1 (Adapt78) is associated with Alzheimer's disease**. (2001) *J Biol Chem* 276 pp. 38787-94.

Ermak, G., Pritchard, M.A., Dronjak, S., Niu, B. and Davies, K.J. **Do RCAN1 proteins link chronic stress with neurodegeneration?** (2011) *FASEB J* 25 pp. 3306-11.

Esteban, V., Mendez-Barbero, N., Jimenez-Borreguero, L.J., Roque, M., Novensa, L., Garcia-Redondo, A.B., Salaices, M., Vila, L., Arbones, M.L., Campanero, M.R. and Redondo, J.M. **Regulator of calcineurin 1 mediates pathological vascular wall remodeling**. (2011) *J Exp Med* 208 pp. 2125-39.

Estecha, A., Aguilera-Montilla, N., Sanchez-Mateos, P. and Puig-Kroger, A. **RUNX3 regulates intercellular adhesion molecule 3 (ICAM-3) expression during**

macrophage differentiation and monocyte extravasation. (2012) *PLoS One* 7 p. e33313.

Facchin, F., Canaider, S., Vitale, L., Frabetti, F., Griffoni, C., Lenzi, L., Casadei, R. and Strippoli, P. **Identification and analysis of human RCAN3 (DSCR1L2) mRNA and protein isoforms**. (2008) *Gene* 407 pp. 159-68.

Facchin, F., Vitale, L., Bianconi, E., Piva, F., Frabetti, F., Strippoli, P., Casadei, R., Pelleri, M.C., Piovesan, A. and Canaider, S. **Complexity of bidirectional transcription and alternative splicing at human RCAN3 locus**. (2011) *PLoS One* 6 p. e24508.

Fan, S., Zhang, M.Q. and Zhang, X. **Histone methylation marks play important roles in predicting the methylation status of CpG islands**. (2008) *Biochem Biophys Res Commun* 374 pp. 559-64.

Fehervari, Z. and Sakaguchi, S. **Development and function of CD25+CD4+ regulatory T cells**. (2004) *Curr Opin Immunol* 16 pp. 203-8.

Feng, B. and Stemmer, P.M. **Interactions of calcineurin A, calcineurin B, and Ca2+**. (1999) *Biochemistry* 38 pp. 12481-9.

Festing, M.F. and Altman, D.G. **Guidelines for the design and statistical analysis of experiments using laboratory animals**. (2002) *ILAR J* 43 pp. 244-58.

Finger, J.H., Smith, C.M., Hayamizu, T.F., McCright, I.J., Eppig, J.T., Kadin, J.A., Richardson, J.E. and Ringwald, M. **The mouse Gene Expression Database (GXD): 2011 update**. (2011) *Nucleic Acids Res* 39 pp. D835-41.

Fischer, A.M., Katayama, C.D., Pages, G., Pouyssegur, J. and Hedrick, S.M. **The role of erk1 and erk2 in multiple stages of T cell development**. (2005) *Immunity* 23 pp. 431-43.

Fischer, K.D., Zmuldzinas, A., Gardner, S., Barbacid, M., Bernstein, A. and Guidos, C. **Defective T-cell receptor signalling and positive selection of Vav-deficient CD4+ CD8+ thymocytes**. (1995) *Nature* 374 pp. 474-7.

Fric, J., Lim, C.X., Koh, E.G., Hofmann, B., Chen, J., Tay, H.S., Mohammad Isa, S.A., Mortellaro, A., Ruedl, C. and Ricciardi-Castagnoli, P. **Calcineurin/NFAT signalling inhibits myeloid haematopoiesis**. (2012) *EMBO Mol Med* 4 pp. 269-82.

Fu, G., Vallee, S., Rybakin, V., McGuire, M.V., Ampudia, J., Brockmeyer, C., Salek, M., Fallen, P.R., Hoerter, J.A., Munshi, A., Huang, Y.H., Hu, J., Fox, H.S., Sauer, K., Acuto, O. and Gascoigne, N.R. **Themis controls thymocyte selection through regulation of T cell antigen receptor-mediated signaling**. (2009) *Nat Immunol* 10 pp. 848-56.

Fuentes, J.J., Genesca, L., Kingsbury, T.J., Cunningham, K.W., Perez-Riba, M., Estivill, X. and de la Luna, S. **DSCR1, overexpressed in Down syndrome, is an inhibitor of calcineurin-mediated signaling pathways**. (2000) *Hum Mol Genet* 9 pp. 1681-90.

Fuentes, J.J., Pritchard, M.A. and Estivill, X. **Genomic organization, alternative splicing, and expression patterns of the DSCR1 (Down syndrome candidate region 1) gene**. (1997) *Genomics* 44 pp. 358-61.

Fuentes, J.J., Pritchard, M.A., Planas, A.M., Bosch, A., Ferrer, I. and Estivill, X. **A new human gene from the Down syndrome critical region encodes a proline-rich protein highly expressed in fetal brain and heart**. (1995) *Hum Mol Genet* 4 pp. 1935-44.

Gaestel, M., Benndorf, R., Hayess, K., Priemer, E. and Engel, K. **Dephosphorylation of the small heat shock protein hsp25 by calcium/calmodulin-dependent (type 2B) protein phosphatase**. (1992) *J Biol Chem* 267 pp. 21607-11.

Galy, A., Verma, S., Barcena, A. and Spits, H. **Precursors of CD3+CD4+CD8+ cells in the human thymus are defined by expression of CD34. Delineation of early events in human thymic development**. (1993) *J Exp Med* 178 pp. 391-401.

Gallegos, A.M. and Bevan, M.J. **Central tolerance to tissue-specific antigens mediated by direct and indirect antigen presentation**. (2004) *J Exp Med* 200 pp. 1039-49.

Gallo, E.M., Winslow, M.M., Cante-Barrett, K., Radermacher, A.N., Ho, L., McGinnis, L., Iritani, B., Neilson, J.R. and Crabtree, G.R. **Calcineurin sets the bandwidth for discrimination of signals during thymocyte development**. (2007) *Nature* 450 pp. 731-5.

Gao, E.K., Lo, D., Cheney, R., Kanagawa, O. and Sprent, J. **Abnormal differentiation of thymocytes in mice treated with cyclosporin A**. (1988) *Nature* 336 pp. 176-9.

Garcia-Pavia, P., Vazquez, M.E., Segovia, J., Salas, C., Avellana, P., Gomez-Bueno, M., Vilches, C., Gallardo, M.E., Garesse, R., Molano, J., Bornstein, B. and Alonso-Pulpon, L. **Genetic basis of end-stage hypertrophic cardiomyopathy**. (2011) *Eur J Heart Fail* 13 pp. 1193-201.

Genesca, L., Aubareda, A., Fuentes, J.J., Estivill, X., De La Luna, S. and Perez-Riba, M. **Phosphorylation of calcipressin 1 increases its ability to inhibit calcineurin and decreases calcipressin half-life**. (2003) *Biochem J* 374 pp. 567-75.

Genolet, R., Stevenson, B.J., Farinelli, L., Osteras, M. and Luescher, I.F. **Highly diverse TCRalpha chain repertoire of pre-immune CD8(+) T cells reveals new insights in gene recombination**. (2012) *EMBO J* 31 pp. 1666-78.

Gollogly, L.K., Ryeom, S.W. and Yoon, S.S. **Down syndrome candidate region 1-like 1 (DSCR1-L1) mimics the inhibitory effects of DSCR1 on calcineurin signaling in endothelial cells and inhibits angiogenesis**. (2007) *J Surg Res* 142 pp. 129-36.

Gong, Q., Cheng, A.M., Akk, A.M., Alberola-Ila, J., Gong, G., Pawson, T. and Chan, A.C. **Disruption of T cell signaling networks and development by Grb2 haploid insufficiency**. (2001) *Nat Immunol* 2 pp. 29-36.

Goto, S., Yamamoto, H., Fukunaga, K., Iwasa, T., Matsukado, Y. and Miyamoto, E. **Dephosphorylation of microtubule-associated protein 2, tau factor, and tubulin by calcineurin**. (1985) *J Neurochem* 45 pp. 276-83.

Gringhuis, S.I., de Leij, L.F., Coffer, P.J. and Vellenga, E. **Signaling through CD5 activates a pathway involving phosphatidylinositol 3-kinase, Vav, and Rac1 in human mature T lymphocytes**. (1998) *Mol Cell Biol* 18 pp. 1725-35.

Gurgen, D., Hegner, B., Kusch, A., Catar, R., Chaykovska, L., Hoff, U., Gross, V., Slowinski, T., da Costa Goncalves, A.C., Kintscher, U., Gustafsson, J.A., Luft, F.C. and Dragun, D. **Estrogen receptor-beta signals left ventricular hypertrophy sex differences in normotensive deoxycorticosterone acetate-salt mice**. (2011) *Hypertension* 57 pp. 648-54.

Gurney, K.B. and Uittenbogaart, C.H. **Human immunodeficiency virus persistence and production in T-cell development**. (2006) *Clin Vaccine Immunol* 13 pp. 1237-45.

Hamann, D., Baars, P.A., Rep, M.H., Hooibrink, B., Kerkhof-Garde, S.R., Klein, M.R. and van Lier, R.A. **Phenotypic and functional separation of memory and effector human CD8+ T cells**. (1997) *J Exp Med* 186 pp. 1407-18.

Hayden-Martinez, K., Kane, L.P. and Hedrick, S.M. **Effects of a constitutively active form of calcineurin on T cell activation and thymic selection**. (2000) *J Immunol* 165 pp. 3713-21.

He, G., Ma, Y., Chou, S.Y., Li, H., Yang, C., Chuang, J.Z., Sung, C.H. and Ding, A. **Role of CLIC4 in the host innate responses to bacterial lipopolysaccharide**. (2011) *Eur J Immunol* 41 pp. 1221-30.

Hellemans, J., Mortier, G., De Paepe, A., Speleman, F. and Vandesompele, J. **qBase relative quantification framework and software for management and automated analysis of real-time quantitative PCR data**. (2007) *Genome Biol* 8 p. R19.

Hesser, B.A., Liang, X.H., Camenisch, G., Yang, S., Lewin, D.A., Scheller, R., Ferrara, N. and Gerber, H.P. **Down syndrome critical region protein 1 (DSCR1), a novel VEGF target gene that regulates expression of inflammatory markers on activated endothelial cells**. (2004) *Blood* 104 pp. 149-58.

Hilioti, Z., Gallagher, D.A., Low-Nam, S.T., Ramaswamy, P., Gajer, P., Kingsbury, T.J., Birchwood, C.J., Levchenko, A. and Cunningham, K.W. **GSK-3 kinases enhance calcineurin signaling by phosphorylation of RCNs**. (2004) *Genes Dev* 18 pp. 35-47.

Hill, J.A., Rothermel, B., Yoo, K.D., Cabuay, B., Demetroulis, E., Weiss, R.M., Kutschke, W., Bassel-Duby, R. and Williams, R.S. **Targeted inhibition of calcineurin in pressure-overload cardiac hypertrophy. Preservation of systolic function**. (2002) *J Biol Chem* 277 pp. 10251-5.

Hirakawa, Y., Nary, L.J. and Medh, R.D. **Glucocorticoid evoked upregulation of RCAN1-1 in human leukemic CEM cells susceptible to apoptosis**. (2009) *J Mol Signal* 4 p. 6.

Ho, M.R., Tsai, K.W. and Lin, W.C. **A unified framework of overlapping genes: Towards the origination and endogenic regulation**. (2012) *Genomics* 100 pp. 231-9.

Hoeffer, C.A., Dey, A., Sachan, N., Wong, H., Patterson, R.J., Shelton, J.M., Richardson, J.A., Klann, E. and Rothermel, B.A. **The Down syndrome critical region protein RCAN1 regulates long-term potentiation and memory via inhibition of phosphatase signaling**. (2007) *J Neurosci* 27 pp. 13161-72.

Hogan, P.G., Chen, L., Nardone, J. and Rao, A. **Transcriptional regulation by calcium, calcineurin, and NFAT**. (2003) *Genes Dev* 17 pp. 2205-32.

Hogquist, K.A., Jameson, S.C., Heath, W.R., Howard, J.L., Bevan, M.J. and Carbone, F.R. **T cell receptor antagonist peptides induce positive selection**. (1994) *Cell* 76 pp. 17-27.

Holmes, K., Chapman, E., See, V. and Cross, M.J. **VEGF stimulates RCAN1.4 expression in endothelial cells via a pathway requiring Ca2+/calcineurin and protein kinase C-delta**. (2010) *PLoS One* 5 p. e11435.

Honda, K. and Taniguchi, T. **IRFs: master regulators of signalling by Toll-like receptors and cytosolic pattern-recognition receptors**. (2006) *Nat Rev Immunol* 6 pp. 644-58.

Hsieh, C.S., Lee, H.M. and Lio, C.W. **Selection of regulatory T cells in the thymus**. (2012) *Nat Rev Immunol* 12 pp. 157-67.

Hsu, S.C., Wu, C.C., Han, J. and Lai, M.Z. **Involvement of p38 mitogen-activated protein kinase in different stages of thymocyte development**. (2003) *Blood* 101 pp. 970-6.

Iizuka, M., Abe, M., Shiiba, K., Sasaki, I. and Sato, Y. **Down syndrome candidate region 1,a downstream target of VEGF, participates in endothelial cell migration and angiogenesis**. (2004) *J Vasc Res* 41 pp. 334-44.

Irving, B.A., Chan, A.C. and Weiss, A. **Functional characterization of a signal transducing motif present in the T cell antigen receptor zeta chain**. (1993) *J Exp Med* 177 pp. 1093-103.

Jameson, S.C., Hogquist, K.A. and Bevan, M.J. **Positive selection of thymocytes**. (1995) *Annu Rev Immunol* 13 pp. 93-126.

Jang, C., Lim, J.H., Park, C.W. and Cho, Y.J. **Regulator of Calcineurin 1 Isoform 4 (RCAN1.4) Is Overexpressed in the Glomeruli of Diabetic Mice**. (2011) *Korean J Physiol Pharmacol* 15 pp. 299-305.

Jang, I.K., Zhang, J., Chiang, Y.J., Kole, H.K., Cronshaw, D.G., Zou, Y. and Gu, H. **Grb2 functions at the top of the T-cell antigen receptor-induced tyrosine kinase cascade to control thymic selection**. (2010) *Proc Natl Acad Sci U S A* 107 pp. 10620-5.

Jenkins, M.K., Schwartz, R.H. and Pardoll, D.M. **Effects of cyclosporine A on T cell development and clonal deletion**. (1988) *Science* 241 pp. 1655-8.

Johnson, A.L., Aravind, L., Shulzhenko, N., Morgun, A., Choi, S.Y., Crockford, T.L., Lambe, T., Domaschenz, H., Kucharska, E.M., Zheng, L., Vinuesa, C.G., Lenardo, M.J., Goodnow, C.C., Cornall, R.J. and Schwartz, R.H. **Themis is a member of a new metazoan gene family and is required for the completion of thymocyte positive selection**. (2009) *Nat Immunol* 10 pp. 831-9.

Jordan, M.S. **Genetic reconstitution of bone marrow for the study of signal transduction ex vivo**. (2006) *Methods Mol Biol* 332 pp. 331-42.

Josefowicz, S.Z., Lu, L.F. and Rudensky, A.Y. **Regulatory T cells: mechanisms of differentiation and function**. (2012) *Annu Rev Immunol* 30 pp. 531-64.

June, C.H., Rabinovitch, P.S. and Ledbetter, J.A. **CD5 antibodies increase intracellular ionized calcium concentration in T cells**. (1987) *J Immunol* 138 pp. 2782-92.

Kanariou, M., Huby, R., Ladyman, H., Colic, M., Sivolapenko, G., Lampert, I. and Ritter, M. **Immunosuppression with cyclosporin A alters the thymic microenvironment**. (1989) *Clin Exp Immunol* 78 pp. 263-70.

Kang, S., Li, H., Rao, A. and Hogan, P.G. **Inhibition of the calcineurin-NFAT interaction by small organic molecules reflects binding at an allosteric site**. (2005) *J Biol Chem* 280 pp. 37698-706.

Ke, H. and Huai, Q. **Structures of calcineurin and its complexes with immunophilins-immunosuppressants**. (2003) *Biochem Biophys Res Commun* 311 pp. 1095-102.

Keating, D.J., Chen, C. and Pritchard, M.A. **Alzheimer's disease and endocytic dysfunction: clues from the Down syndrome-related proteins, DSCR1 and ITSN1**. (2006) *Ageing Res Rev* 5 pp. 388-401.

Keating, D.J., Dubach, D., Zanin, M.P., Yu, Y., Martin, K., Zhao, Y.F., Chen, C., Porta, S., Arbones, M.L., Mittaz, L. and Pritchard, M.A. **DSCR1/RCAN1 regulates vesicle exocytosis and fusion pore kinetics: implications for Down syndrome and Alzheimer's disease**. (2008) *Hum Mol Genet* 17 pp. 1020-30.

Khaled, A.R. and Durum, S.K. **Lymphocide: cytokines and the control of lymphoid homeostasis**. (2002) *Nat Rev Immunol* 2 pp. 817-30.

Kim, S.S., Oh, Y., Chung, K.C. and Seo, S.R. **Protein kinase A phosphorylates Down syndrome critical region 1 (RCAN1)**. (2012) *Biochem Biophys Res Commun* 418 pp. 657-61.

Kim, Y.S., Cho, K.O., Lee, H.J., Kim, S.Y., Sato, Y. and Cho, Y.J. **Down syndrome candidate region 1 increases the stability of the IkappaBalpha protein: implications for its anti-inflammatory effects**. (2006) *J Biol Chem* 281 pp. 39051-61.

Kim, Y.S., Lee, H.J., Jang, C., Kim, H.S. and Cho, Y.J. **Knockdown of RCAN1.4 Increases Susceptibility to FAS-mediated and DNA-damage-induced Apoptosis by Upregulation of p53 Expression**. (2009) *Korean J Physiol Pharmacol* 13 pp. 483-9.

Kishi, T., Ikeda, A., Nagao, R. and Koyama, N. **The SCFCdc4 ubiquitin ligase regulates calcineurin signaling through degradation of phosphorylated Rcn1, an inhibitor of calcineurin**. (2007) *Proc Natl Acad Sci U S A* 104 pp. 17418-23.

Klug, C.A., Cheshier, S. and Weissman, I.L. **Inactivation of a GFP retrovirus occurs at multiple levels in long-term repopulating stem cells and their differentiated progeny**. (2000) *Blood* 96 pp. 894-901.

Kondo, M., Wagers, A.J., Manz, M.G., Prohaska, S.S., Scherer, D.C., Beilhack, G.F., Shizuru, J.A. and Weissman, I.L. **Biology of hematopoietic stem cells and progenitors: implications for clinical application**. (2003) *Annu Rev Immunol* 21 pp. 759-806.

Kostareva, A., Gudkova, A., Sjoberg, G., Morner, S., Semernin, E., Krutikov, A., Shlyakhto, E. and Sejersen, T. **Deletion in TNNI3 gene is associated with restrictive cardiomyopathy**. (2009) *Int J Cardiol* 131 pp. 410-2.

Labrecque, N., Baldwin, T. and Lesage, S. **Molecular and genetic parameters defining T-cell clonal selection**. (2011) *Immunol Cell Biol* 89 pp. 16-26.

Laouar, Y. and Crispe, I.N. **Functional flexibility in T cells: independent regulation of CD4+ T cell proliferation and effector function in vivo**. (2000) *Immunity* 13 pp. 291-301.

Leahy, K.P., Davies, K.J., Dull, M., Kort, J.J., Lawrence, K.W. and Crawford, D.R. **adapt78, a stress-inducible mRNA, is related to the glucose-regulated protein family of genes**. (1999) *Arch Biochem Biophys* 368 pp. 67-74.

Lee, E.J., Seo, S.R., Um, J.W., Park, J., Oh, Y. and Chung, K.C. **NF-kappaB-inducing kinase phosphorylates and blocks the degradation of Down syndrome candidate region 1**. (2008) *J Biol Chem* 283 pp. 3392-400.

Lee, J.W., Kang, H.S., Lee, J.Y., Lee, E.J., Rhim, H., Yoon, J.H., Seo, S.R. and Chung, K.C. **The transcription factor STAT2 enhances proteasomal degradation of RCAN1 through the ubiquitin E3 ligase FBW7**. (2012) *Biochem Biophys Res Commun* 420 pp. 404-10.

Lee, J.Y., Lee, H.J., Lee, E.J., Jang, S.H., Kim, H., Yoon, J.H. and Chung, K.C. **Down syndrome candidate region-1 protein interacts with Tollip and positively modulates**

interleukin-1 receptor-mediated signaling. (2009) *Biochim Biophys Acta* 1790 pp. 1673-80.

Levanon, D. and Groner, Y. **Structure and regulated expression of mammalian RUNX genes**. (2004) *Oncogene* 23 pp. 4211-9.

Lewis, S.M. and Wu, G.E. **The origins of V(D)J recombination**. (1997) *Cell* 88 pp. 159-62.

Li, H., Rao, A. and Hogan, P.G. **Interaction of calcineurin with substrates and targeting proteins**. (2011) *Trends Cell Biol* 21 pp. 91-103.

Lian, J.B., Javed, A., Zaidi, S.K., Lengner, C., Montecino, M., van Wijnen, A.J., Stein, J.L. and Stein, G.S. **Regulatory controls for osteoblast growth and differentiation: role of Runx/Cbfa/AML factors**. (2004) *Crit Rev Eukaryot Gene Expr* 14 pp. 1-41.

Lian, J.B. and Stein, G.S. **Runx2/Cbfa1: a multifunctional regulator of bone formation**. (2003) *Curr Pharm Des* 9 pp. 2677-85.

Liang, Q., Bueno, O.F., Wilkins, B.J., Kuan, C.Y., Xia, Y. and Molkentin, J.D. **c-Jun N-terminal kinases (JNK) antagonize cardiac growth through cross-talk with calcineurin-NFAT signaling**. (2003) *EMBO J* 22 pp. 5079-89.

Lin, H.Y., Michtalik, H.J., Zhang, S., Andersen, T.T., Van Riper, D.A., Davies, K.K., Ermak, G., Petti, L.M., Nachod, S., Narayan, A.V., Bhatt, N. and Crawford, D.R. **Oxidative and calcium stress regulate DSCR1 (Adapt78/MCIP1) protein**. (2003) *Free Radic Biol Med* 35 pp. 528-39.

Lin, K.G., Tang, M., Guo, Y.B., Han, H.Y. and Lin, Y.H. **Two polymorphisms of RCAN1 gene associated with Alzheimer's disease in the Chinese Han population**. (2011) *East Asian Arch Psychiatry* 21 pp. 79-84.

Liu, Q., Busby, J.C. and Molkentin, J.D. **Interaction between TAK1-TAB1-TAB2 and RCAN1-calcineurin defines a signalling nodal control point**. (2009) *Nat Cell Biol* 11 pp. 154-61.

Livak, K.J. and Schmittgen, T.D. **Analysis of relative gene expression data using real-time quantitative PCR and the 2(-Delta Delta C(T)) Method**. (2001) *Methods* 25 pp. 402-8.

Lockyer, P.J., Kupzig, S. and Cullen, P.J. **CAPRI regulates Ca(2+)-dependent inactivation of the Ras-MAPK pathway**. (2001) *Curr Biol* 11 pp. 981-6.

Ma, D., Wei, Y. and Liu, F. **Regulatory mechanisms of thymus and T cell development**. (2011) *Dev Comp Immunol*.

Ma, L., Tang, H., Ren, Y., Deng, H., Wu, J. and Wang, Z. **p38alpha MAP kinase phosphorylates RCAN1 and regulates its interaction with calcineurin**. (2012) *Sci China Life Sci* 55 pp. 559-66.

Macian, F. **NFAT proteins: key regulators of T-cell development and function**. (2005) *Nat Rev Immunol* 5 pp. 472-84.

Macian, F., Lopez-Rodriguez, C. and Rao, A. **Partners in transcription: NFAT and AP-1**. (2001) *Oncogene* 20 pp. 2476-89.

Mammucari, C., Tommasi di Vignano, A., Sharov, A.A., Neilson, J., Havrda, M.C., Roop, D.R., Botchkarev, V.A., Crabtree, G.R. and Dotto, G.P. **Integration of Notch 1 and calcineurin/NFAT signaling pathways in keratinocyte growth and differentiation control**. (2005) *Dev Cell* 8 pp. 665-76.

Manicassamy, S., Gupta, S., Huang, Z., Molkentin, J.D., Shang, W. and Sun, Z. **Requirement of calcineurin a beta for the survival of naive T cells**. (2008) *J Immunol* 180 pp. 106-12.

Mantel, P.Y., Ouaked, N., Ruckert, B., Karagiannidis, C., Welz, R., Blaser, K. and Schmidt-Weber, C.B. **Molecular mechanisms underlying FOXP3 induction in human T cells**. (2006) *J Immunol* 176 pp. 3593-602.

Martin, K.R., Corlett, A., Dubach, D., Mustafa, T., Coleman, H.A., Parkington, H.C., Merson, T.D., Bourne, J.A., Porta, S., Arbones, M.L., Finkelstein, D.I. and Pritchard, M.A. **Over-expression of RCAN1 causes Down syndrome-like hippocampal deficits that alter learning and memory**. (2012) *Hum Mol Genet* 21 pp. 3025-41.

Martinez-Martinez, S., Genesca, L., Rodriguez, A., Raya, A., Salichs, E., Were, F., Lopez-Maderuelo, M.D., Redondo, J.M. and de la Luna, S. **The RCAN carboxyl end mediates calcineurin docking-dependent inhibition via a site that dictates binding to substrates and regulators**. (2009) *Proc Natl Acad Sci U S A* 106 pp. 6117-22.

Martinez-Martinez, S. and Redondo, J.M. **Inhibitors of the calcineurin/NFAT pathway**. (2004) *Curr Med Chem* 11 pp. 997-1007.

Martinez-Martinez, S., Rodriguez, A., Lopez-Maderuelo, M.D., Ortega-Perez, I., Vazquez, J. and Redondo, J.M. **Blockade of NFAT activation by the second calcineurin binding site**. (2006) *J Biol Chem* 281 pp. 6227-35.

Matallanas, D., Birtwistle, M., Romano, D., Zebisch, A., Rauch, J., von Kriegsheim, A. and Kolch, W. **Raf family kinases: old dogs have learned new tricks**. (2011) *Genes Cancer* 2 pp. 232-60.

McCarty, N., Paust, S., Ikizawa, K., Dan, I., Li, X. and Cantor, H. **Signaling by the kinase MINK is essential in the negative selection of autoreactive thymocytes**. (2005) *Nat Immunol* 6 pp. 65-72.

McGargill, M.A., Ch'en, I.L., Katayama, C.D., Pages, G., Pouyssegur, J. and Hedrick, S.M. **Cutting edge: Extracellular signal-related kinase is not required for negative selection of developing T cells**. (2009) *J Immunol* 183 pp. 4838-42.

McNeil, L.K., Starr, T.K. and Hogquist, K.A. **A requirement for sustained ERK signaling during thymocyte positive selection in vivo**. (2005) *Proc Natl Acad Sci U S A* 102 pp. 13574-9.

Medyouf, H. and Ghysdael, J. **The calcineurin/NFAT signaling pathway: a novel therapeutic target in leukemia and solid tumors**. (2008) *Cell Cycle* 7 pp. 297-303.

Mehta, S., Li, H., Hogan, P.G. and Cunningham, K.W. **Domain architecture of the regulators of calcineurin (RCANs) and identification of a divergent RCAN in yeast**. (2009) *Mol Cell Biol* 29 pp. 2777-93.

Michie, A.M. and Zuniga-Pflucker, J.C. **Regulation of thymocyte differentiation: pre-TCR signals and beta-selection**. (2002) *Semin Immunol* 14 pp. 311-23.

Michtalik, H.J., Narayan, A.V., Bhatt, N., Lin, H.Y., Mulligan, M.T., Zhang, S.L. and Crawford, D.R. **Multiple oxidative stress-response members of the Adapt78 family**. (2004) *Free Radic Biol Med* 37 pp. 454-62.

Minami, T., Horiuchi, K., Miura, M., Abid, M.R., Takabe, W., Noguchi, N., Kohro, T., Ge, X., Aburatani, H., Hamakubo, T., Kodama, T. and Aird, W.C. **Vascular endothelial**

growth factor- and thrombin-induced termination factor, Down syndrome critical region-1, attenuates endothelial cell proliferation and angiogenesis. (2004) *J Biol Chem* 279 pp. 50537-54.

Minami, T., Yano, K., Miura, M., Kobayashi, M., Suehiro, J., Reid, P.C., Hamakubo, T., Ryeom, S., Aird, W.C. and Kodama, T. **The Down syndrome critical region gene 1 short variant promoters direct vascular bed-specific gene expression during inflammation in mice**. (2009) *J Clin Invest* 119 pp. 2257-70.

Miyazaki, T., Kanou, Y., Murata, Y., Ohmori, S., Niwa, T., Maeda, K., Yamamura, H. and Seo, H. **Molecular cloning of a novel thyroid hormone-responsive gene, ZAKI-4, in human skin fibroblasts**. (1996) *J Biol Chem* 271 pp. 14567-71.

Mizuguchi, H., Xu, Z., Ishii-Watabe, A., Uchida, E. and Hayakawa, T. **IRES-dependent second gene expression is significantly lower than cap-dependent first gene expression in a bicistronic vector**. (2000) *Mol Ther* 1 pp. 376-82.

Mizuno, Y., Kanou, Y., Rogatcheva, M., Imai, T., Refetoff, S., Seo, H. and Murata, Y. **Genomic organization of mouse ZAKI-4 gene that encodes ZAKI-4 alpha and beta isoforms, endogenous calcineurin inhibitors, and changes in the expression of these isoforms by thyroid hormone in adult mouse brain and heart**. (2004) *Eur J Endocrinol* 150 pp. 371-80.

Molfetta, R., Peruzzi, G., Santoni, A. and Paolini, R. **Negative signals from FcepsilonRI engagement attenuate mast cell functions**. (2007) *Arch Immunol Ther Exp (Warsz)* 55 pp. 219-29.

Muffato, M., Louis, A., Poisnel, C.E. and Roest Crollius, H. **Genomicus: a database and a browser to study gene synteny in modern and ancestral genomes**. (2010) *Bioinformatics* 26 pp. 1119-21.

Mulero, M., Orzaez, M., Messeguer, J., Messeguer, A., Perez-Paya, E. and Perez-Riba, M. **A fluorescent polarization-based assay for the identification of disruptors of the RCAN1-calcineurin A protein complex**. (2010) *Anal Biochem* 398 pp. 99-103.

Mulero, M.C., Aubareda, A., Orzaez, M., Messeguer, J., Serrano-Candelas, E., Martinez-Hoyer, S., Messeguer, A., Perez-Paya, E. and Perez-Riba, M. **Inhibiting the calcineurin-NFAT (nuclear factor of activated T cells) signaling pathway with a regulator of calcineurin-derived peptide without affecting general calcineurin phosphatase activity**. (2009) *J Biol Chem* 284 pp. 9394-401.

Mulero, M.C., Aubareda, A., Schluter, A. and Perez-Riba, M. **RCAN3, a novel calcineurin inhibitor that down-regulates NFAT-dependent cytokine gene expression**. (2007) *Biochim Biophys Acta* 1773 pp. 330-41.

Muller, F., Demeny, M.A. and Tora, L. **New problems in RNA polymerase II transcription initiation: matching the diversity of core promoters with a variety of promoter recognition factors**. (2007) *J Biol Chem* 282 pp. 14685-9.

Muller, M.R. and Rao, A. **NFAT, immunity and cancer: a transcription factor comes of age**. (2010) *Nat Rev Immunol* 10 pp. 645-56.

Munroe, S.H. and Lazar, M.A. **Inhibition of c-erbA mRNA splicing by a naturally occurring antisense RNA**. (1991) *J Biol Chem* 266 pp. 22083-6.

Murthy, A.S., Bramblett, G.T. and Flavin, M. **The sites at which brain microtubule-associated protein 2 is phosphorylated in vivo differ from those accessible to cAMP-dependent kinase in vitro**. (1985) *J Biol Chem* 260 pp. 4364-70.

Nalesnik, M.A., Todo, S., Murase, N., Gryzan, S., Lee, P.H., Makowka, L. and Starzl, T.E. **Toxicology of FK-506 in the Lewis rat**. (1987) *Transplant Proc* 19 pp. 89-92.

Naramura, M., Kole, H.K., Hu, R.J. and Gu, H. **Altered thymic positive selection and intracellular signals in Cbl-deficient mice**. (1998) *Proc Natl Acad Sci U S A* 95 pp. 15547-52.

Narayan, A.V., Stadel, R., Hahn, A.B., Bhoiwala, D.L., Cornielle, G., Sarazin, E., Koleilat, I. and Crawford, D.R. **Redox response of the endogenous calcineurin inhibitor Adapt 78**. (2005) *Free Radic Biol Med* 39 pp. 719-27.

Neilson, J.R., Winslow, M.M., Hur, E.M. and Crabtree, G.R. **Calcineurin B1 is essential for positive but not negative selection during thymocyte development**. (2004) *Immunity* 20 pp. 255-66.

Niemeyer, M., Darmoise, A., Mollenkopf, H.J., Hahnke, K., Hurwitz, R., Besra, G.S., Schaible, U.E. and Kaufmann, S.H. **Natural killer T-cell characterization through gene expression profiling: an account of versatility bridging T helper type 1 (Th1), Th2 and Th17 immune responses**. (2008) *Immunology* 123 pp. 45-56.

Ninomiya-Tsuji, J., Kishimoto, K., Hiyama, A., Inoue, J., Cao, Z. and Matsumoto, K. **The kinase TAK1 can activate the NIK-I kappaB as well as the MAP kinase cascade in the IL-1 signalling pathway**. (1999) *Nature* 398 pp. 252-6.

Noble, A., Thomas, M.J. and Kemeny, D.M. **Early Th1/Th2 cell polarization in the absence of IL-4 and IL-12: T cell receptor signaling regulates the response to cytokines in CD4 and CD8 T cells**. (2001) *Eur J Immunol* 31 pp. 2227-35.

Noble, A., Truman, J.P., Vyas, B., Vukmanovic-Stejic, M., Hirst, W.J. and Kemeny, D.M. **The balance of protein kinase C and calcium signaling directs T cell subset development**. (2000) *J Immunol* 164 pp. 1807-13.

Oeschger, F.M., Wang, W.Z., Lee, S., Garcia-Moreno, F., Goffinet, A.M., Arbones, M.L., Rakic, S. and Molnar, Z. **Gene expression analysis of the embryonic subplate**. (2012) *Cereb Cortex* 22 pp. 1343-59.

Oh-hora, M. **Calcium signaling in the development and function of T-lineage cells**. (2009) *Immunol Rev* 231 pp. 210-24.

Osman, N., Turner, H., Lucas, S., Reif, K. and Cantrell, D.A. **The protein interactions of the immunoglobulin receptor family tyrosine-based activation motifs present in the T cell receptor zeta subunits and the CD3 gamma, delta and epsilon chains**. (1996) *Eur J Immunol* 26 pp. 1063-8.

Oukka, M., Ho, I.C., de la Brousse, F.C., Hoey, T., Grusby, M.J. and Glimcher, L.H. **The transcription factor NFAT4 is involved in the generation and survival of T cells**. (1998) *Immunity* 9 pp. 295-304.

Page, D.M., Alexander, J., Snoke, K., Appella, E., Sette, A., Hedrick, S.M. and Grey, H.M. **Negative selection of CD4+ CD8+ thymocytes by T-cell receptor peptide antagonists**. (1994) *Proc Natl Acad Sci U S A* 91 pp. 4057-61.

Park, J., Oh, Y. and Chung, K.C. **Two key genes closely implicated with the neuropathological characteristics in Down syndrome: DYRK1A and RCAN1**. (2009) *BMB Rep* 42 pp. 6-15.

Pauler, F.M., Koerner, M.V. and Barlow, D.P. **Silencing by imprinted noncoding RNAs: is transcription the answer?** (2007) *Trends Genet* 23 pp. 284-92.

Pedram, A., Razandi, M., Lubahn, D., Liu, J., Vannan, M. and Levin, E.R. **Estrogen inhibits cardiac hypertrophy: role of estrogen receptor-beta to inhibit calcineurin**. (2008) *Endocrinology* 149 pp. 3361-9.

Peiris, H., Raghupathi, R., Jessup, C.F., Zanin, M.P., Mohanasundaram, D., Mackenzie, K.D., Chataway, T., Clarke, J.N., Brealey, J., Coates, P.T., Pritchard, M.A. and Keating, D.J. **Increased Expression of the Glucose-Responsive Gene, RCAN1, Causes Hypoinsulinemia, beta-Cell Dysfunction, and Diabetes**. (2012) *Endocrinology*.

Peng, S.L., Gerth, A.J., Ranger, A.M. and Glimcher, L.H. **NFATc1 and NFATc2 together control both T and B cell activation and differentiation**. (2001) *Immunity* 14 pp. 13-20.

Pesole, G., Grillo, G., Larizza, A. and Liuni, S. **The untranslated regions of eukaryotic mRNAs: structure, function, evolution and bioinformatic tools for their analysis**. (2000) *Brief Bioinform* 1 pp. 236-49.

Porta, S., Marti, E., de la Luna, S. and Arbones, M.L. **Differential expression of members of the RCAN family of calcineurin regulators suggests selective functions for these proteins in the brain**. (2007a) *Eur J Neurosci* 26 pp. 1213-26.

Porta, S., Serra, S.A., Huch, M., Valverde, M.A., Llorens, F., Estivill, X., Arbones, M.L. and Marti, E. **RCAN1 (DSCR1) increases neuronal susceptibility to oxidative stress: a potential pathogenic process in neurodegeneration**. (2007b) *Hum Mol Genet* 16 pp. 1039-50.

Prescott, E.M. and Proudfoot, N.J. **Transcriptional collision between convergent genes in budding yeast**. (2002) *Proc Natl Acad Sci U S A* 99 pp. 8796-801.

Pugh-Humphreys, R.G., Ross, C.S. and Thomson, A.W. **The influence of FK-506 on the thymus: an immunophenotypic and structural analysis**. (1990) *Immunology* 70 pp. 398-404.

Puig-Kroger, A. and Corbi, A. **RUNX3: a new player in myeloid gene expression and immune response**. (2006) *J Cell Biochem* 98 pp. 744-56.

Purtic, B., Pitcher, L.A., van Oers, N.S. and Wulfing, C. **T cell receptor (TCR) clustering in the immunological synapse integrates TCR and costimulatory signaling in selected T cells**. (2005) *Proc Natl Acad Sci U S A* 102 pp. 2904-9.

Qin, L., Zhao, D., Liu, X., Nagy, J.A., Hoang, M.V., Brown, L.F., Dvorak, H.F. and Zeng, H. **Down syndrome candidate region 1 isoform 1 mediates angiogenesis through the calcineurin-NFAT pathway**. (2006) *Mol Cancer Res* 4 pp. 811-20.

Quesenberry, P. and Levitt, L. **Hematopoietic stem cells**. (1979) *N Engl J Med* 301 pp. 755-61.

Quilliam, L.A., Rebhun, J.F. and Castro, A.F. **A growing family of guanine nucleotide exchange factors is responsible for activation of Ras-family GTPases**. (2002) *Prog Nucleic Acid Res Mol Biol* 71 pp. 391-444.

Ramsden, D.A., Weed, B.D. and Reddy, Y.V. **V(D)J recombination: Born to be wild**. (2010) *Semin Cancer Biol* 20 pp. 254-60.

Ranger, A.M., Hodge, M.R., Gravallese, E.M., Oukka, M., Davidson, L., Alt, F.W., de la Brousse, F.C., Hoey, T., Grusby, M. and Glimcher, L.H. **Delayed lymphoid repopulation with defects in IL-4-driven responses produced by inactivation of NF-ATc**. (1998a) *Immunity* 8 pp. 125-34.

Ranger, A.M., Oukka, M., Rengarajan, J. and Glimcher, L.H. **Inhibitory function of two NFAT family members in lymphoid homeostasis and Th2 development**. (1998b) *Immunity* 9 pp. 627-35.

Rao, A., Luo, C. and Hogan, P.G. **Transcription factors of the NFAT family: regulation and function**. (1997) *Annu Rev Immunol* 15 pp. 707-47.

Rasooly, R., Schuster, G.U., Gregg, J.P., Xiao, J.H., Chandraratna, R.A. and Stephensen, C.B. **Retinoid x receptor agonists increase bcl2a1 expression and decrease apoptosis of naive T lymphocytes**. (2005) *J Immunol* 175 pp. 7916-29.

Refaeli, Y., Van Parijs, L., London, C.A., Tschopp, J. and Abbas, A.K. **Biochemical mechanisms of IL-2-regulated Fas-mediated T cell apoptosis**. (1998) *Immunity* 8 pp. 615-23.

Reiser, J.B., Gregoire, C., Darnault, C., Mosser, T., Guimezanes, A., Schmitt-Verhulst, A.M., Fontecilla-Camps, J.C., Mazza, G., Malissen, B. and Housset, D. **A T cell receptor CDR3beta loop undergoes conformational changes of unprecedented magnitude upon binding to a peptide/MHC class I complex**. (2002) *Immunity* 16 pp. 345-54.

Richardson, L., Venkataraman, S., Stevenson, P., Yang, Y., Burton, N., Rao, J., Fisher, M., Baldock, R.A., Davidson, D.R. and Christiansen, J.H. **EMAGE mouse embryo spatial gene expression database: 2010 update**. (2010) *Nucleic Acids Res* 38 pp. D703-9.

Rincon, M., Conze, D., Weiss, L., Diehl, N.L., Fortner, K.A., Yang, D., Flavell, R.A., Enslen, H., Whitmarsh, A. and Davis, R.J. **Conference highlight: do T cells care about the mitogen-activated protein kinase signalling pathways?** (2000a) *Immunol Cell Biol* 78 pp. 166-75.

Rincon, M., Enslen, H., Raingeaud, J., Recht, M., Zapton, T., Su, M.S., Penix, L.A., Davis, R.J. and Flavell, R.A. **Interferon-gamma expression by Th1 effector T cells mediated by the p38 MAP kinase signaling pathway**. (1998a) *EMBO J* 17 pp. 2817-29.

Rincon, M., Flavell, R.A. and Davis, R.A. **The JNK and P38 MAP kinase signaling pathways in T cell-mediated immune responses**. (2000b) *Free Radic Biol Med* 28 pp. 1328-37.

Rincon, M. and Pedraza-Alva, G. **JNK and p38 MAP kinases in CD4+ and CD8+ T cells**. (2003) *Immunol Rev* 192 pp. 131-42.

Rincon, M., Whitmarsh, A., Yang, D.D., Weiss, L., Derijard, B., Jayaraj, P., Davis, R.J. and Flavell, R.A. **The JNK pathway regulates the In vivo deletion of immature CD4(+)CD8(+) thymocytes**. (1998b) *J Exp Med* 188 pp. 1817-30.

Ritter, M.A. and Boyd, R.L. **Development in the thymus: it takes two to tango**. (1993) *Immunol Today* 14 pp. 462-9.

Rodriguez, A., Roy, J., Martinez-Martinez, S., Lopez-Maderuelo, M.D., Nino-Moreno, P., Orti, L., Pantoja-Uceda, D., Pineda-Lucena, A., Cyert, M.S. and Redondo, J.M. **A conserved docking surface on calcineurin mediates interaction with substrates and immunosuppressants**. (2009) *Mol Cell* 33 pp. 616-26.

Roehrl, M.H., Kang, S., Aramburu, J., Wagner, G., Rao, A. and Hogan, P.G. **Selective inhibition of calcineurin-NFAT signaling by blocking protein-protein interaction with small organic molecules**. (2004) *Proc Natl Acad Sci U S A* 101 pp. 7554-9.

Roider, H.G., Lenhard, B., Kanhere, A., Haas, S.A. and Vingron, M. **CpG-depleted promoters harbor tissue-specific transcription factor binding signals--implications for motif overrepresentation analyses**. (2009) *Nucleic Acids Res* 37 pp. 6305-15.

Rosenzweig, M., Connole, M., Glickman, R., Yue, S.P., Noren, B., DeMaria, M. and Johnson, R.P. **Induction of cytotoxic T lymphocyte and antibody responses to enhanced green fluorescent protein following transplantation of transduced CD34(+) hematopoietic cells**. (2001) *Blood* 97 pp. 1951-9.

Roskoski, R., Jr. **RAF protein-serine/threonine kinases: structure and regulation**. (2010) *Biochem Biophys Res Commun* 399 pp. 313-7.

Rothermel, B., Vega, R.B., Yang, J., Wu, H., Bassel-Duby, R. and Williams, R.S. **A protein encoded within the Down syndrome critical region is enriched in striated muscles and inhibits calcineurin signaling**. (2000) *J Biol Chem* 275 pp. 8719-25.

Rothermel, B.A., McKinsey, T.A., Vega, R.B., Nicol, R.L., Mammen, P., Yang, J., Antos, C.L., Shelton, J.M., Bassel-Duby, R., Olson, E.N. and Williams, R.S. **Myocyte-enriched calcineurin-interacting protein, MCIP1, inhibits cardiac hypertrophy in vivo**. (2001) *Proc Natl Acad Sci U S A* 98 pp. 3328-33.

Rudd, C.E. **Adaptors and molecular scaffolds in immune cell signaling**. (1999) *Cell* 96 pp. 5-8.

Rudensky, A.Y., Gavin, M. and Zheng, Y. **FOXP3 and NFAT: partners in tolerance**. (2006) *Cell* 126 pp. 253-6.

Rusnak, F. and Mertz, P. **Calcineurin: form and function**. (2000) *Physiol Rev* 80 pp. 1483-521.

Ryeom, S., Baek, K.H., Rioth, M.J., Lynch, R.C., Zaslavsky, A., Birsner, A., Yoon, S.S. and McKeon, F. **Targeted deletion of the calcineurin inhibitor DSCR1 suppresses tumor growth**. (2008) *Cancer Cell* 13 pp. 420-31.

Ryeom, S., Greenwald, R.J., Sharpe, A.H. and McKeon, F. **The threshold pattern of calcineurin-dependent gene expression is altered by loss of the endogenous inhibitor calcipressin**. (2003) *Nat Immunol* 4 pp. 874-81.

Sakaguchi, S., Yamaguchi, T., Nomura, T. and Ono, M. **Regulatory T cells and immune tolerance**. (2008) *Cell* 133 pp. 775-87.

Sakano, H., Huppi, K., Heinrich, G. and Tonegawa, S. **Sequences at the somatic recombination sites of immunoglobulin light-chain genes**. (1979) *Nature* 280 pp. 288-94.

Sallusto, F., Geginat, J. and Lanzavecchia, A. **Central memory and effector memory T cell subsets: function, generation, and maintenance**. (2004) *Annu Rev Immunol* 22 pp. 745-63.

Samelson, L.E. **Signal transduction mediated by the T cell antigen receptor: the role of adapter proteins**. (2002) *Annu Rev Immunol* 20 pp. 371-94.

Sanna, B., Brandt, E.B., Kaiser, R.A., Pfluger, P., Witt, S.A., Kimball, T.R., van Rooij, E., De Windt, L.J., Rothenberg, M.E., Tschop, M.H., Benoit, S.C. and Molkentin, J.D. **Modulatory calcineurin-interacting proteins 1 and 2 function as calcineurin facilitators in vivo**. (2006) *Proc Natl Acad Sci U S A* 103 pp. 7327-32.

Schmedt, C. and Tarakhovsky, A. **Autonomous maturation of alpha/beta T lineage cells in the absence of COOH-terminal Src kinase (Csk)**. (2001) *J Exp Med* 193 pp. 815-26.

Schuh, K., Kneitz, B., Heyer, J., Bommhardt, U., Jankevics, E., Berberich-Siebelt, F., Pfeffer, K., Muller-Hermelink, H.K., Schimpl, A. and Serfling, E. **Retarded thymic involution and massive germinal center formation in NF-ATp-deficient mice**. (1998) *Eur J Immunol* 28 pp. 2456-66.

Sebzda, E., Mariathasan, S., Ohteki, T., Jones, R., Bachmann, M.F. and Ohashi, P.S. **Selection of the T cell repertoire**. (1999) *Annu Rev Immunol* 17 pp. 829-74.

Seo, S.R. and Chung, K.C. **CREB activates proteasomal degradation of DSCR1/RCAN1**. (2008) *FEBS Lett* 582 pp. 1889-93.

Shin, S.Y., Choo, S.M., Kim, D., Baek, S.J., Wolkenhauer, O. and Cho, K.H. **Switching feedback mechanisms realize the dual role of MCIP in the regulation of calcineurin activity**. (2006) *FEBS Lett* 580 pp. 5965-73.

Shin, S.Y., Yang, H.W., Kim, J.R., Heo, W.D. and Cho, K.H. **A hidden incoherent switch regulates RCAN1 in the calcineurin-NFAT signaling network**. (2011) *J Cell Sci* 124 pp. 82-90.

Shortman, K. and Wu, L. **Early T lymphocyte progenitors**. (1996) *Annu Rev Immunol* 14 pp. 29-47.

Skelton, D., Satake, N. and Kohn, D.B. **The enhanced green fluorescent protein (eGFP) is minimally immunogenic in C57BL/6 mice**. (2001) *Gene Ther* 8 pp. 1813-4.

Smith-Garvin, J.E., Koretzky, G.A. and Jordan, M.S. **T cell activation**. (2009) *Annu Rev Immunol* 27 pp. 591-619.

Soldevila, G.G.-Z. **Role of Chemokines in T cell development**. (2003) *Inmunología* 22 pp. 371-384.

Sosinowski, T., Killeen, N. and Weiss, A. **The Src-like adaptor protein downregulates the T cell receptor on CD4+CD8+ thymocytes and regulates positive selection**. (2001) *Immunity* 15 pp. 457-66.

Sprent, J. and Surh, C.D. **T cell memory**. (2002) *Annu Rev Immunol* 20 pp. 551-79.

Starr, T.K., Jameson, S.C. and Hogquist, K.A. **Positive and negative selection of T cells**. (2003) *Annu Rev Immunol* 21 pp. 139-76.

Stathatos, N., Bourdeau, I., Espinosa, A.V., Saji, M., Vasko, V.V., Burman, K.D., Stratakis, C.A. and Ringel, M.D. **KiSS-1/G protein-coupled receptor 54 metastasis suppressor pathway increases myocyte-enriched calcineurin interacting protein 1 expression and chronically inhibits calcineurin activity**. (2005) *J Clin Endocrinol Metab* 90 pp. 5432-40.

Stripecke, R., Carmen Villacres, M., Skelton, D., Satake, N., Halene, S. and Kohn, D. **Immune response to green fluorescent protein: implications for gene therapy**. (1999) *Gene Ther* 6 pp. 1305-12.

Strippoli, P., D'Addabbo, P., Lenzi, L., Giannone, S., Canaider, S., Casadei, R., Vitale, L., Carinci, P. and Zannotti, M. **Segmental paralogy in the human genome: a large-scale triplication on 1p, 6p, and 21q**. (2002) *Mamm Genome* 13 pp. 456-62.

Strippoli, P., Lenzi, L., Petrini, M., Carinci, P. and Zannotti, M. **A new gene family including DSCR1 (Down Syndrome Candidate Region 1) and ZAKI-4: characterization from yeast to human and identification of DSCR1-like 2, a novel human member (DSCR1L2)**. (2000) *Genomics* 64 pp. 252-63.

Sugawara, T., Moriguchi, T., Nishida, E. and Takahama, Y. **Differential roles of ERK and p38 MAP kinase pathways in positive and negative selection of T lymphocytes**. (1998) *Immunity* 9 pp. 565-74.

Sun, L., Deng, L., Ea, C.K., Xia, Z.P. and Chen, Z.J. **The TRAF6 ubiquitin ligase and TAK1 kinase mediate IKK activation by BCL10 and MALT1 in T lymphocytes**. (2004) *Mol Cell* 14 pp. 289-301.

Sun, X., Wu, Y., Chen, B., Zhang, Z., Zhou, W., Tong, Y., Yuan, J., Xia, K., Gronemeyer, H., Flavell, R.A. and Song, W. **Regulator of calcineurin 1 (RCAN1) facilitates neuronal apoptosis through caspase-3 activation**. (2011a) *J Biol Chem* 286 pp. 9049-62.

Sun, X.Y., Hayashi, Y., Xu, S., Kanou, Y., Takagishi, Y., Tang, Y.P. and Murata, Y. **Inactivation of the Rcan2 gene in mice ameliorates the age- and diet-induced obesity by causing a reduction in food intake**. (2011b) *PLoS One* 6 p. e14605.

Suzuki, A., Yamaguchi, M.T., Ohteki, T., Sasaki, T., Kaisho, T., Kimura, Y., Yoshida, R., Wakeham, A., Higuchi, T., Fukumoto, M., Tsubata, T., Ohashi, P.S., Koyasu, S., Penninger, J.M., Nakano, T. and Mak, T.W. **T cell-specific loss of Pten leads to defects in central and peripheral tolerance**. (2001) *Immunity* 14 pp. 523-34.

Takahama, Y. **Journey through the thymus: stromal guides for T-cell development and selection**. (2006) *Nat Rev Immunol* 6 pp. 127-35.

Takeo, S., Swanson, S.K., Nandanan, K., Nakai, Y., Aigaki, T., Washburn, M.P., Florens, L. and Hawley, R.S. **Shaggy/glycogen synthase kinase 3beta and phosphorylation of Sarah/regulator of calcineurin are essential for completion of Drosophila female meiosis**. (2012) *Proc Natl Acad Sci U S A* 109 pp. 6382-9.

Tang, Y., Yu, J. and Field, J. **Signals from the Ras, Rac, and Rho GTPases converge on the Pak protein kinase in Rat-1 fibroblasts**. (1999) *Mol Cell Biol* 19 pp. 1881-91.

Thome, M. and Weil, R. **Post-translational modifications regulate distinct functions of CARMA1 and BCL10**. (2007) *Trends Immunol* 28 pp. 281-8.

Thomson, A.W., Pugh-Humphreys, R.G. and Woo, J. **The influence of FK 506 on the thymus: implications of drug-induced injury to thymic epithelial cells**. (1991) *Transplant Proc* 23 pp. 947-8.

Tian, J. and Karin, M. **Stimulation of Elk1 transcriptional activity by mitogen-activated protein kinases is negatively regulated by protein phosphatase 2B (calcineurin)**. (1999) *J Biol Chem* 274 pp. 15173-80.

Tone, Y., Furuuchi, K., Kojima, Y., Tykocinski, M.L., Greene, M.I. and Tone, M. **Smad3 and NFAT cooperate to induce Foxp3 expression through its enhancer**. (2008) *Nat Immunol* 9 pp. 194-202.

Trama, J., Lu, Q., Hawley, R.G. and Ho, S.N. **The NFAT-related protein NFATL1 (TonEBP/NFAT5) is induced upon T cell activation in a calcineurin-dependent manner**. (2000) *J Immunol* 165 pp. 4884-94.

U, M., Shen, L., Oshida, T., Miyauchi, J., Yamada, M. and Miyashita, T. **Identification of novel direct transcriptional targets of glucocorticoid receptor**. (2004) *Leukemia* 18 pp. 1850-6.

van den Wijngaard, A., Volders, P., Van Tintelen, J.P., Jongbloed, J.D., van den Berg, M.P., Lekanne Deprez, R.H., Mannens, M.M., Hofmann, N., Slegtenhorst, M., Dooijes, D., Michels, M., Arens, Y., Jongbloed, R. and Smeets, B.J. **Recurrent and founder mutations in the Netherlands: cardiac Troponin I (TNNI3) gene mutations as a cause of severe forms of hypertrophic and restrictive cardiomyopathy**. (2011) *Neth Heart J* 19 pp. 344-51.

Vanhee-Brossollet, C. and Vaquero, C. **Do natural antisense transcripts make sense in eukaryotes?** (1998) *Gene* 211 pp. 1-9.

Vega, R.B., Rothermel, B.A., Weinheimer, C.J., Kovacs, A., Naseem, R.H., Bassel-Duby, R., Williams, R.S. and Olson, E.N. **Dual roles of modulatory calcineurin-interacting protein 1 in cardiac hypertrophy**. (2003) *Proc Natl Acad Sci U S A* 100 pp. 669-74.

Vega, R.B., Yang, J., Rothermel, B.A., Bassel-Duby, R. and Williams, R.S. **Multiple domains of MCIP1 contribute to inhibition of calcineurin activity**. (2002) *J Biol Chem* 277 pp. 30401-7.

Veillette, A., Latour, S. and Davidson, D. **Negative regulation of immunoreceptor signaling**. (2002) *Annu Rev Immunol* 20 pp. 669-707.

Viola, J.P., Kiani, A., Bozza, P.T. and Rao, A. **Regulation of allergic inflammation and eosinophil recruitment in mice lacking the transcription factor NFAT1: role of interleukin-4 (IL-4) and IL-5**. (1998) *Blood* 91 pp. 2223-30.

Wada, H., Masuda, K., Satoh, R., Kakugawa, K., Ikawa, T., Katsura, Y. and Kawamoto, H. **Adult T-cell progenitors retain myeloid potential**. (2008) *Nature* 452 pp. 768-72.

Wan, Y.Y., Chi, H., Xie, M., Schneider, M.D. and Flavell, R.A. **The kinase TAK1 integrates antigen and cytokine receptor signaling for T cell development, survival and function**. (2006) *Nat Immunol* 7 pp. 851-8.

Wang, C., Deng, L., Hong, M., Akkaraju, G.R., Inoue, J. and Chen, Z.J. **TAK1 is a ubiquitin-dependent kinase of MKK and IKK**. (2001) *Nature* 412 pp. 346-51.

Wang, C.R., Hashimoto, K., Kubo, S., Yokochi, T., Kubo, M., Suzuki, M., Suzuki, K., Tada, T. and Nakayama, T. **T cell receptor-mediated signaling events in CD4+CD8+ thymocytes undergoing thymic selection: requirement of calcineurin activation for thymic positive selection but not negative selection**. (1995) *J Exp Med* 181 pp. 927-41.

Wang, H.G., Pathan, N., Ethell, I.M., Krajewski, S., Yamaguchi, Y., Shibasaki, F., McKeon, F., Bobo, T., Franke, T.F. and Reed, J.C. **Ca2+-induced apoptosis through calcineurin dephosphorylation of BAD**. (1999) *Science* 284 pp. 339-43.

Wang, W., Zhu, J.Z., Chang, K.T. and Min, K.T. **DSCR1 interacts with FMRP and is required for spine morphogenesis and local protein synthesis**. (2012) *EMBO J* 31 pp. 3655-66.

Wang, Z., Hong, J., Sun, W., Xu, G., Li, N., Chen, X., Liu, A., Xu, L., Sun, B. and Zhang, J.Z. **Role of IFN-gamma in induction of Foxp3 and conversion of CD4+ CD25- T cells to CD4+ Tregs**. (2006) *J Clin Invest* 116 pp. 2434-41.

Weerkamp, F. **Molecular Regulation of Early T-Cell Development in the Thymus** (2005), Erasmus Universiteit Rotterdam, Rotterdam, The Netherlands

Wei, W., Pelechano, V., Jarvelin, A.I. and Steinmetz, L.M. **Functional consequences of bidirectional promoters**. (2011) *Trends Genet* 27 pp. 267-76.

Werlen, G., Hausmann, B. and Palmer, E. **A motif in the alphabeta T-cell receptor controls positive selection by modulating ERK activity**. (2000) *Nature* 406 pp. 422-6.

Werlen, G., Jacinto, E., Xia, Y. and Karin, M. **Calcineurin preferentially synergizes with PKC-theta to activate JNK and IL-2 promoter in T lymphocytes**. (1998) *EMBO J* 17 pp. 3101-11.

Weyrich, A.S., Denis, M.M., Kuhlmann-Eyre, J.R., Spencer, E.D., Dixon, D.A., Marathe, G.K., McIntyre, T.M., Zimmerman, G.A. and Prescott, S.M. **Dipyridamole selectively inhibits inflammatory gene expression in platelet-monocyte aggregates**. (2005) *Circulation* 111 pp. 633-42.

Williams, C.J., Naito, T., Arco, P.G., Seavitt, J.R., Cashman, S.M., De Souza, B., Qi, X., Keables, P., Von Andrian, U.H. and Georgopoulos, K. **The chromatin remodeler Mi-2beta is required for CD4 expression and T cell development**. (2004) *Immunity* 20 pp. 719-33.

Woodland, D.L. and Dutton, R.W. **Heterogeneity of CD4(+) and CD8(+) T cells**. (2003) *Curr Opin Immunol* 15 pp. 336-42.

Wu, H., Peisley, A., Graef, I.A. and Crabtree, G.R. **NFAT signaling and the invention of vertebrates**. (2007) *Trends Cell Biol* 17 pp. 251-60.

Wu, H., Rothermel, B., Kanatous, S., Rosenberg, P., Naya, F.J., Shelton, J.M., Hutcheson, K.A., DiMaio, J.M., Olson, E.N., Bassel-Duby, R. and Williams, R.S. **Activation of MEF2 by muscle activity is mediated through a calcineurin-dependent pathway**. (2001) *Embo J* 20 pp. 6414-23.

Yamasaki, S. and Saito, T. **Molecular basis for pre-TCR-mediated autonomous signaling**. (2007) *Trends Immunol* 28 pp. 39-43.

Yang, J., Rothermel, B., Vega, R.B., Frey, N., McKinsey, T.A., Olson, E.N., Bassel-Duby, R. and Williams, R.S. **Independent signals control expression of the calcineurin inhibitory proteins MCIP1 and MCIP2 in striated muscles**. (2000) *Circ Res* 87 pp. E61-8.

Yang, J.Y., Jung, J.Y., Cho, S.W., Choi, H.J., Kim, S.W., Kim, S.Y., Kim, H.J., Jang, C.H., Lee, M.G., Han, J. and Shin, C.S. **Chloride intracellular channel 1 regulates osteoblast differentiation**. (2009a) *Bone* 45 pp. 1175-85.

Yang, S.A. and Klee, C.B. **Low affinity Ca2+-binding sites of calcineurin B mediate conformational changes in calcineurin A**. (2000) *Biochemistry* 39 pp. 16147-54.

Yang, Y.J., Chen, W., Edgar, A., Li, B., Molkentin, J.D., Berman, J.N. and Lin, T.J. **Rcan1 negatively regulates Fc epsilonRI-mediated signaling and mast cell function**. (2009b) *J Exp Med* 206 pp. 195-207.

Ye, J., Coulouris, G., Zaretskaya, I., Cutcutache, I., Rozen, S. and Madden, T.L. **Primer-BLAST: A tool to design target-specific primers for polymerase chain reaction**. (2012) *BMC Bioinformatics* 13 p. 134.

Yonan, C.R., Duong, P.T. and Chang, F.N. **High-efficiency staining of proteins on different blot membranes**. (2005) *Anal Biochem* 338 pp. 159-61.

Yoshida, H., Nishina, H., Takimoto, H., Marengere, L.E., Wakeham, A.C., Bouchard, D., Kong, Y.Y., Ohteki, T., Shahinian, A., Bachmann, M., Ohashi, P.S., Penninger, J.M., Crabtree, G.R. and Mak, T.W. **The transcription factor NF-ATc1 regulates lymphocyte proliferation and Th2 cytokine production**. (1998) *Immunity* 8 pp. 115-24.

Yu, D.Y., Tong, L., Song, G.J., Lin, W.L., Zhang, L.Q., Bai, W., Gong, H., Yin, Y.X. and Wei, Q. **Tau binds both subunits of calcineurin, and binding is impaired by calmodulin**. (2008) *Biochim Biophys Acta* 1783 pp. 2255-61.

Yuan, J.S., Kousis, P.C., Suliman, S., Visan, I. and Guidos, C.J. **Functions of notch signaling in the immune system: consensus and controversies**. (2010) *Annu Rev Immunol* 28 pp. 343-65.

Zhang, B.W., Zimmer, G., Chen, J., Ladd, D., Li, E., Alt, F.W., Wiederrecht, G., Cryan, J., O'Neill, E.A., Seidman, C.E., Abbas, A.K. and Seidman, J.G. **T cell responses in calcineurin A alpha-deficient mice**. (1996) *J Exp Med* 183 pp. 413-20.

Zhang, W., Sloan-Lancaster, J., Kitchen, J., Trible, R.P. and Samelson, L.E. **LAT: the ZAP-70 tyrosine kinase substrate that links T cell receptor to cellular activation**. (1998) *Cell* 92 pp. 83-92.

Zhou, T., Cheng, J., Yang, P., Wang, Z., Liu, C., Su, X., Bluethmann, H. and Mountz, J.D. **Inhibition of Nur77/Nurr1 leads to inefficient clonal deletion of self-reactive T cells**. (1996) *J Exp Med* 183 pp. 1879-92.

Zolotukhin, S., Potter, M., Hauswirth, W.W., Guy, J. and Muzyczka, N. **A "humanized" green fluorescent protein cDNA adapted for high-level expression in mammalian cells**. (1996) *J Virol* 70 pp. 4646-54.

Zorn, E., Nelson, E.A., Mohseni, M., Porcheray, F., Kim, H., Litsa, D., Bellucci, R., Raderschall, E., Canning, C., Soiffer, R.J., Frank, D.A. and Ritz, J. **IL-2 regulates FOXP3 expression in human CD4+CD25+ regulatory T cells through a STAT-dependent mechanism and induces the expansion of these cells in vivo**. (2006) *Blood* 108 pp. 1571-9.

Annex

Table A1 - SURFACE AND INTRACELULAR T LYMPHOCYTE MARKERS			
Antigen Name	**Others names**	**Distribution**	**Function**
CD2	LFA-2, Ly-37, SRBC-R, T11	thymocytes, T, NK, B, pre-B, myeloid, erythrocytes	adhesion, T activation, CD48 receptor
CD3ξ	T3ξ, CD3ξ, CD3 ξ chain, CD3	Thymocyte subset, T cells, NKT	TCR subunit, TCR expression & signal transduction
CD4	Ly-4, L3T4	Thymocyte subset, T subset, DC , NK	TCR coreceptor, thymic differentiation, T activation, MHC class II receptor
CD5	Ly-1 Lyt-1, Ly-12, Ly-A	Thymocytes, T cells, B subset (B1)	T activation, T-B interaction, CD72 receptor
CD8	Ly-2, Lyt-2, Ly-B, Ly-35	Thymocyte subset, T subset , DC subset, not fresh NK	TCR coreceptor, MHC class I receptor, T differentiation, homodimer or heterodimer with CD8b
CD9	p24, MRP-1, DRAP-27	myeloid, platelets, activated T cells, B subset, stromal cells, mesenchimal stem cells	cell adhesion, migration, T costimulation, platelets activation
CD25	Ly-43, p55, IL2Ralpha	Pre-B, Pre-T, activated T and B cells, DC subset, monocytes, macrophages	Low affinity IL-2 binding, with IL-2Rbeta & gamma forms IL-2 receptor high affinity, also soluble form
CD28	Tp44, T44	T, thymocytes, NK	CD80 & CD86 receptor, T costimulation
CD44	Pgp-1, Ly-24, HERMES	Broad, memory T cells, not platelets, or hepatocytes	Receptor for hyaluronate, adhesion, homing, metastasis, T cell activation, marker for memory T cells
CD45	LCA, Ly-5, Ptprc, T200	leukocytes, not mature erythrocytes	tyrosine phosphatase, leukocyte differentiation / activation, pan-leukocyte marker
CD62L	L-selectin, LECAM-1, sell, LAM-1, MEL-14, Ly-22	B, T, monocytes, granulocytes, NK, thymocytes	CD34, GlyCAM, & MAdCAM-1 receptor, lymphocyte homing, leukocyte tethering & rolling
CD69	Activation Inducer Molecule, VEA, Leu 23, AIM, EA-1, MLR-3	Activated T, B, NK and granulocytes, thymocytes, platelets	Lymphocyte activation, early activation marker
CD80	B7, B7-1, BB1, Ly-53	activated B and T cells, monocytes, macrophages, DC, pancreatic β cells	CD28 & CD152 receptor, costimulation, T-B interaction
CD95	Apo-1, Fas	thymocytes, activated lymphocytes, monocytes, neutrophil, fibroblasts	CD95L (FasL) receptor, apoptosis induction, immune system regulation, lpr mutation
FoxP3	Forkhead box P3, SCURFIN	T cells ($CD4^+/CD25^+$ subset and $CD8^+$ subset)	Transcription factor, may be upregulated in Tregs
NK1.1	CD161c, NKR-P1c, Ly-55	NK, T subset	NK cell-mediated cytotoxicity
TCRβ	TCR subunit β	T subset	Antigen recognition

Table A1. Surface and intracelular T lymphocyte markers.